Synaptic frailty and mitochondrial dysfunction in familial amyotrophic lateral sclerosis

Xavier Ramon Gallart Palau

Xavier Ramon Gallart Palau

Synaptic frailty and mitochondrial dysfunction in familial amyotrophic lateral sclerosis

Doctoral Thesis

Directed by Siu Kwan SZE, PhD.
tutorized by Joan Ribera, PhD.

Experimental Medicine Department

Universitat de Lleida

Lleida, 2016

Dissertation presented by Xavier Ramon Gallart Palau to obtain the PhD. degree from the University of Lleida. This work was performed under the supervision of Siu Kwan SZE, PhD. from Nanyang Technological University, Joan Ribera, PhD. from University of Lleida and Kah Leong Lim, PhD. from DUKE-National University of Singapore. The present work has been carried out in the Experimental Medicine Department of University of Lleida, in the School of Biological Sciences of Nanyang Tecnological University in Singapore and in the Neuropathology Laboratory of DUKE National University of Singapore. This thesis is included in the health doctorate program of the University of Lleida and was funded by:

a) SAF2011-22908. Funding entity: Ministerio de Ciencia e Innovación of Spain.

b) National Medical Research Council - CBRG of Singapore.

c) Singapore Ministry of Education of Singapore - Tier 1: RGT15/13.

d) NTU-NSH Ageing Research Grant - ARG/1417.

PhD candidate was funded by the University of Lleida Predoctoral Scholarship PREDOCTORAL-101/2012.

For the studies performed in DUKE National University of Singapore the candidate received the scholarship MOBILITAT-204/2012 from the Doctorate School of the University of Lleida.

PhD. Candidate
Xavier Ramon Gallart Palau

Director
Siu Kwan SZE, PhD.
Signature of approval

Tutor
Joan Ribera, PhD.
Signature of approval

“Un pam de terra, un pam de seny i al cor
l’amor etern”

Fra Marc (Monestir de Poblet. Estiu 2012)

AGRAÏMENTS

Arribats a aquest punt, ja acabada d'escriure; sembla que tot està dit en aquesta tesi, però no és així, sóc conscient que falta el més important. Falta el reconeixement i agraïment a la gent que gràcies al seu suport i afecte ha fet possible aquest treball.

No puc oblidar-me en primer lloc dels meus pares, no només em van regalar la vida sinó que em van ensenyar a viure-la, a ells els hi dic que sempre hem estat i estarem un. Tampoc de l'Aida, són ja molts els moments que hem viscut junts i sense la teva empenta alguns moments difícils viscuts durant la consecució d'aquesta tesi m'haurien superat; cap paraula ni gest podrà mai sotregar el meu cor com ho fa la mirada blava i eterna dels teus ulls.

Agraeixo profundament al Dr. Joan Ribera que va acceptar el repte de tirar endavant els moments decissius d'aquesta tesi. Sense el seu consell i suport res d'això hagués estat possible. Recordo el vespre que et vaig contactar des de Singapur com una nit en que el temps i l'espai es comprimien fins al punt de matar el meu desig de seguir fent recerca. Quanta llum quedava mes enllà d'aquell ofuscament! Gràcies de nou a tu Joan per haver-me permès veure-ho i viure-ho.

Els agraïments dedicats als Drs. Siu Kwan SZE i Kah-Leong Lim estàn a la versió anglesa dels agraïments d'aquesta tesi. En català us dic que em sento molt afortunat i impressionat per haver tingut l'oportunitat de conèixer persones amb una ment tant potent i una intel.ligència tant genuina com la vostra.

Agraeixo al Francisco Correa que abans de sortir corriendo em va deixar prou petjada com per incloure'l aquí. Al Javier Sábado, veterano de guerra contra l'ELA, dir-li que 'perdimos la batalla i seguramente perderemos la guerra, pero habremos ganado el honor de aprender a luchar'. A la Marta, Montse i Lídia que sempre van ajudar-me al laboratori quan ho vaig necessitar. També a la Eli per que el poc que vam poder coincidir va ser interessant.

A tota la gent de l'IRB de Lleida incloent l'Alba, el Joaquim, la Carme, el Serafí, la Mª Jose, l'Ester Sala i a altra gent que em puc deixar, ha estat un veritable plaer coincidir amb vosaltres.

I finalment deixeu-me agraïr al silenci. Els *touareg* que estàn atents a les esquerdes i plegs del Sahàra no tenen permès dir: *quin silenci!* només els hi és permès dir: *no hi sento*. Afortunadament jo ara tampoc no hi sento, però reconec que a aquest silenci sempre li deuré part de la bona música.

ACKNOWLEDGMENTS

I first acknowledge this PhD. thesis to the trees as these have been an essential part of my life. I strongly believe that we should behave like an olive tree, it becomes by itself after deep acceptation of the universal laws and lives in harmony with the universe for thousands of years. It keeps the roots in the earth and the head below the heaven sweating wisdom and comprehension from every leaf.

And so while I am thinking about wisdom and comprehension I feel that it is time to thank these two great professors that come to my mind: Kah-Leong Lim and Newman Sze. Kah-Leong from the National University of Singapore taught me the essential principles of neurodegeneration. His expertise on mitochondria impairment and his profound scientific insight keep my mind busy for the intense year that we shared as trainee and master. I am heartfelt thankful to have had the opportunity to meet him and be part of his discussions and teachings during my internship in his laboratory.

Prof. Newman Sze from Nanyang Technological University come later to my life but his imprint will remain forever in my mind and research outcome. He taught me how to write scientific papers and how to improve my scientific thinking, he put the logical order in my chaotic mind allowing me to express all my creativity. He made this thesis possible and guided my research steps. He opened the immensity of proteomics to my narrowed eyes. I am immensely thankful to him and that thankfulness cannot be wholly expressed in words.

I'm also heartfelt thankful to Alice Cronin-Golomb professor at Boston University for her kind teachings and because after my undergraduate internship in her laboratory started my real interest on the brain and Neurosciences. Thanks to Daniel J. Norton for being my first and best mentor, my admiration to you and friendship will always remain. Thanks to Yakeel, Mirella, Abhi from BU Boston,

U.S.A. Thanks to Grace, Adeline, ChengWu, Royston, Eugenia, Chai Chao and Chee Hoe from NUS Singapore, SG. Thanks to Bama, Pilliang, RenYan, Arvind, MenWei, Belinda, HongBin, Juan Wei, Benjamin S. T. Lee, Park and Sunil from NTU Singapore, SG. Finally and forever thanks to my all, my everything Aida.

ABSTRACT

Amyotrophic Lateral Sclerosis (ALS) is an orphan age-associated neurodegenerative disease. All motoneurones in ALS are affected by degenerative flow from the primary motor cortex to the neuromuscular junction. In 1993, mutations of the gene SOD1 opened new research avenues allowing for the generation of familial ALS experimental models in rodents. Since then, the FALS mutation SOD1-G93A has been extensively studied worldwide in ALS to date. Transgenic models for this SOD1 mutation have revealed essential mechanisms of neurodegeneration including excitotoxicity, proteinopathy and axosynaptic degeneration among others. In this dissertation, we explored the molecular changes that occur in C-terminals, a very specialised synapse type from α-motoneurones of SOD1-G93A rodents. Also, we focused on the pathological relationship between the FALS mutant SOD1-G93A and mitochondria in motoneurones. With regard to C-terminals in FALS motoneurones, we found changes that were symptomatically associated with the up-regulated expression of the neurotrophic factor Neuregulin-1 located for the first time in the subsurface system of C-boutons juxtaposed to α-motoneurones. Furthermore, Neuregulin-1 in these endoplasmic reticulum structures was observed inside extracellular vesicles, suggesting that analysis of Neuregulin-1 from extracellular vesicles in ALS holds promise as a potential reliable biomarker for that neurodegenerative disease. We therefore have developed a new method for isolation of extracellular vesicles, as this remains as an essential step for the study of molecules associated with these structures. Our method applied to purify extracellular vesicles from complex biological tissues was able to facilitate the identification of Neuregulin-1 in extracellular vessicles from clinical tissues and biological fluids. Regarding implications of mitochondria in ALS, we have found that the FALS mutant hSOD1-G93A stabilises PINK1 in mitochondria and subsequently activates NFκB in neuronal cells. Sequential interaction between hSOD1 and NFκB impairs the proteosome proteolitic function promoting co-aggregation of SOD1 and PINK1 in these cells. These results add substantial mechanistic insight on the roles of mitochondria in classical ALS-associated neurodegenerative events, including aggregation of dysfuntional proteins in motoneurones. Following our study of mitochondria affectation in ALS, we have created and characterised a novel Drosophila model that expresses human SOD1-G93A in thoracic muscles under the genetic muscular promoter 24B. Flies expressing human SOD1-G93A in thoracic muscles successfully recapitulate FALS mitochondrial phenotype with several advantages in front of the current available rodent models for this FALS mutation. Taken together, the results generated in this thesis provide experimental evidence, further molecular comprehension and promise novel therapeutic approaches to the molecular mechanisms and neurodegenerative events associated with synaptic frailty and mitochondrial disfunction in FALS.

RESUM

L'Esclerosi Lateral Amiotròfica (ELA) és una malaltia neurodegenrativa de la motoneurona. Totes les neurones del sistema motor es veuen afectades pel flux degeneratiu en aquesta malaltia des de l'escorça motora primària fins a la junta neuromuscular. Al 1993, la descoberta de mutacions en el gen SOD1 va obrir nous horitzons experimentals amb la creació dels primers rosegadors transgènics per a aquesta malaltia. Des d'aquell moment i fins a l'actualitat la mutació més estudiada en l'ELA ha estat la SOD1-G93A a tot el món. Els models transgènics per aquesta mutació de la SOD1 han revelat mecanismes essencials de la neurodegeneració en aquesta malaltia incloent l'excitotoxicitat, la disfunció proteica i la degeneració axosinàptica entre altres. En aquest treball hem explorat els canvis moleculars que tenen lloc als terminals C, uns terminals molt especialitzats en les α-moto neurones, dels rosegadors trangènics SOD1-G93A. A més, també hem focalitzat la nostra atenció a la relació patològica que s'estableix en l'ELA familiar (ELAF) entre la mutació SOD1-G93A i les mitocondries de les motoneurones. En relació als terminals C en moto neurones durant la ELAF, hem trobat canvis associats a l'aparició dels símptomes com ara expressió incrementada del factor neurotròfic Neuregulina-1 localitzat també per primer cop a la cisterna subsinàptica dels terminals C aposats a les α-moto neurones. La Neuregulina-1 en aquestes estructures de reticle endoplasmàtic va ser observada a dins de vesicules extrecel·lulars (VEs), suggerint que l'anàlisi de la Neuregulina-1 en VEs durant ELA és especialment prometedor com a biomarcador potencial en aquesta malaltia. Així nosaltres hem desenvolupat també un nou mètode per tal d'aïllar VEs, donat que aquest és un pas essencial previ a l'estudi de les proteïnes associades amb aquestes estructures. El nostre mètode aplicat a la purifcació de VEs en teixits complexos fou capaç de facilitar l'identificació de la Neuregulina-1 en VEs provinents de teixits clínics i fluids biològics. En relació a les implicacions de la mitocondria en la ELA, hem trobat que la mutació SOD1-G93A estabilitza la proteïna PINK1 a la mitocondria seguidament activant el factor nuclear NFκB en neurones. La interacció seqüencial entre la SOD1 mutant i NFκB crea una clara disfunció en la capacitat proteolítica del proteosoma, el qual promou co-agregació de la SOD1 mutant i el PINK1 en aquestes cèl·lules. Aquests resultats afegeixen un substancial coneixement mecanístic sobre els rols de la mitocondria en els events neurodegeneratius clàssics de l'ELA, com ara en l'agregació de proteïnes disfuncionals en moto neurones. Seguint el nostre estudi de l'afectació mitocondrial en la ELA, hem creat i caracteritzat un nou model de *Drosophila* que expressa la mutació humana SOD1-G93A exclusivament en fibres musculars toràciques sota el promotor 24B. Aquest model de Drosophila transgènica recapitula amb èxit el fenotip mitocondrial prèviament observat de l'ELA presentant importants avantatges sobretot en l'elecció de nous compostos terapèutics. En definitiva, els resultats generats en aquesta tesi proporcionen evidència experimental, extensa comprensió molecular i insinuen nous horitzons terapèutics sobre els mecanismes moleculars i els events neurodegeneratius associats a la disfunció sinàptica i mitocondrial en l'ELAF.

RESUMEN

La Esclerosis Lateral Amiotrófica (ELA) es una enfermedad neurodegenerativa de la motoneurona. Todas las motoneuronas se ven afectadas desde la corteza motora primaria hasta la unión neuromuscular. En 1993 la descubierta de mutaciones en el gen SOD1 abrió nuevos límites experimentales con la creación de los primeros roedores transgénicos para esta enfermedad. Desde ese momento y hasta la actualidad, la mutación más estudiada en la ELA ha sido la mutación SOD1-G93A. Los modelos transgénicos de esta mutación han revelado mecanismos esenciales de la neurodegeneración en la ELA, incluyendo la excitotoxicidad, la disfunción proteica y la degeneración axosináptica entre otras. En este trabajo hemos explorado los cambios moleculares que tienen lugar en los terminales C, unos terminales altamente especializados de las α-motoneuronas, en en un modelo murino de ELA con la mutación SOD1-G93A. Ademas, también hemos focalizado nuestra atención sobre la relación patológica que se establece en la ELA familiar (ELAF) entre la mutación SOD1-G93A y las mitocondrias. En relación a los terminales C durante la ELAF, hemos encontrado cambios asociados con la aparición de síntomas, como por ejemplo el incremento de la expresión del factor neurotrófico Neuregulina-1, localizado por primera vez en la cisterna subsináptica de los terminales C. La Neuregulina-1 en esas estructuras de retículo endoplasmático fue observada dentro de vesículas extracelulares (VEs), sugiriendo que el análisis de la Neuregulina-1 dentro de VEs en la ELA resulta especialmente prometedor como biomarcador potencial para esta enfermedad. Así, nosotros hemos desarrollado también un nuevo método para purificar VEs, dado que este es un paso esencial previo al estudio de las proteínas asociadas con estas estructuras. Nuestro método aplicado a la purificación de VEs de tejidos complejos fue capaz de facilitar la identificación de la Neuregulina en VEs provenientes de tejidos clínicos y fluidos biológicos. En relación a las implicaciones de la mitocondria en la ELA, hemos encontrado que la mutación SOD1-G93A estabiliza la proteína PINK1 en las mitocondrias activando el factor nuclear NFκB en neuronas. La interacción sequencial entre la SOD1 mutante y el NFκB crea una clara disfunción sobre la capacidad proteolítica del proteosoma, la cual a su vez promueve co-agregación de la SOD1 mutante y PINK1 en estas células. Estos resultados suman un sustancial conocimiento mecanistico sobre los roles de la mitocondria en eventos degenerativos clásicos de la ELA, como es la agregación de proteínas disfuncionales en motoneuronas. Siguiendo nuestro estudio de la afectación mitocondrial en la ELA, hemos creado y caracterizado un nuevo modelo de Drosophila que expresa la mutación humana SOD1-G93A en fibras musculares torácicas bajo el promotor 24B. Este modelo de Drosophila transgénica recapitula con éxito en fenotipo mitocondrial característico de la ELA presentando importantes ventajas para la elección de nuevos compuestos terapéuticos. En definitiva, los resultados generados en esta tesis proporcionan evidencia experimental, extensa comprensión molecular y insinuan nuevos horizontes terapéuticos acerca de los mecanismos moleculares y eventos neurodegenerativos asociados con la disfunción sináptica y la disfunción mitocondrial en la ELAF.

CONTENT

INTRODUCTION

1. Amyotrophic Lateral Sclerosis: overview and similarities with other motoneuron diseases (MND)

1.1 The great Charcot and the Amyotrophic Lateral Sclerosis (ALS)

Jean-Marie Charcot (1825-1893) was an active professor and doctor in France who introduced the term “Amyotrophic Lateral Sclerosis” for the first time in one of his famed Tuesday seminars held in La Salpetriêre. As documented in his memoir “Leçons du Mardi de la Salpêtrière”, this significant moment in medicine and the study of the central nervous system was a result of Charcot’s interest in the cause of hysteria in ALS patients in addition to symptoms such as muscle stiffness and progressive paralysis of limb muscles. It was then that Charcot discovered an unexpected wreckage of the myelin sheath in the lateral corticospinal tracts of the spinal cord in an autopsied ALS patient. Charcot referred to this pathology as la sclérose latérale or the lateral sclerosis (Vincent Meininger 2011). Since this inceptive description of ALS disease aetiology, its

definition has largely remained unchanged from Charcot's initial reports (Vincent Meininger 2011). Today, ALS is also referred to as Lou Ghering's disease, as Ghering, a former baseball player from the popular New York Yankees suffered from this disease.

1.2 First apparition of ALS diagnosis criteria

Observations made by Charcot and his eminent team of scientists led to the establishment of the first ALS diagnosis criteria (Patrikios 1952) in conjunction with the following specific syndromes (Figure 1):

- Flail arm syndrome, bulbar palsy, lower limb paralysis and exacerbation of muscle contractures or tendonous reflexes.
- Required involvement of the upper motor neurones (UMN) and the lower motor neurones (LMN) in the disease pathogenesis.
- In some cases, there may be possible involvement of the frontal lobes, leading to apparition of frontotemporal dementia (FTD)

1.3 Apparition of contemporary ALS diagnostic features: el Escorial (1994)

The diagnostic criteria for ALS has been used unaltered since it was first discovered by Charcot until the late twentieth century, when newer and clearer diagnostic features were established. The rapid and relentless progression of this devastating disease results in a narrow diagnostic window. As such,

patients generally survive for less than 3 years after the emergence of the initial symptoms (Al-Chalabi and Hardiman 2013).

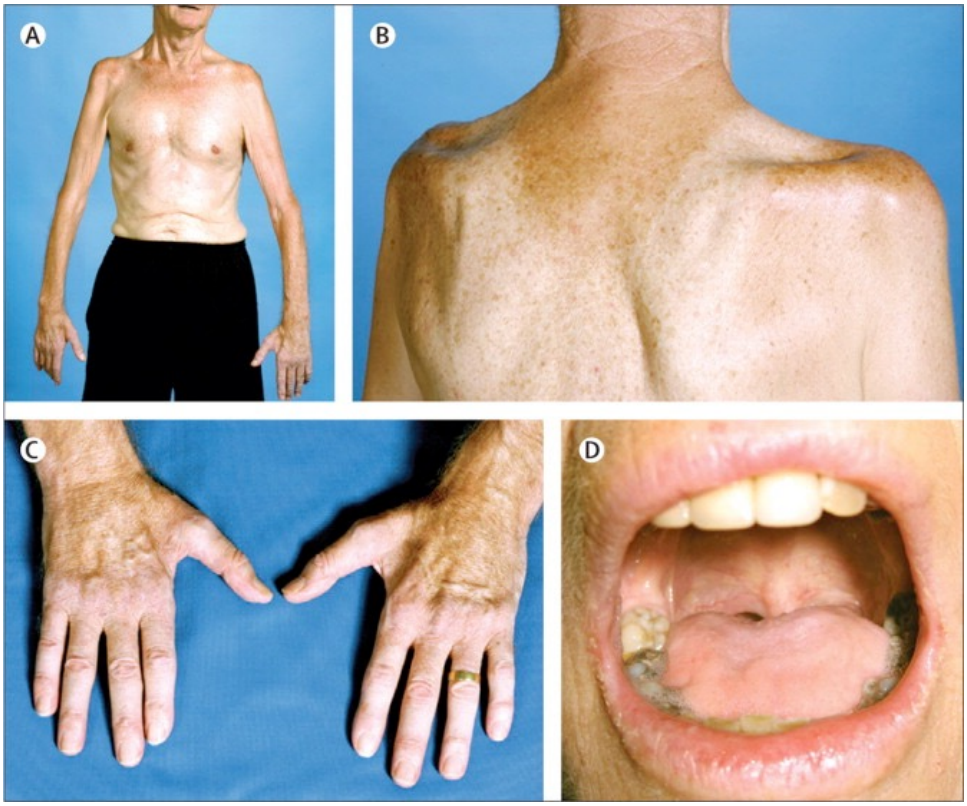

Figure 1. Visual Illustrations of the muscle symptoms observed in ALS. A. Illustration of flail arm syndrome. B. Illustration showing the waste caused by ALS on the spinouts and deltoid muscles. C. Illustration of the split-hand symptom in ALS that indicates a disproportionate waste of the thenar muscles of the hand. D. Illustration of rigidity in the mandibular muscles and difficulties to open the mouth. Clear waste of tongue muscular mass what impedes proper vocalization. (This figure has been adapted for this thesis from the review Kiernan et al. 2011).

While approximately 95% of the ALS cases can be considered as correctly diagnosed (Rowland 1998), the Charcot diagnostic method could not be applied differentially between involvements of the upper motor neurone (UMN)

or the sole involvement of the lower motor neurone (LMN). This was because UMN involvement was considered essential for ALS diagnosis according to the Charcot's criteria. Also, the diagnostic process comprises a time period of nine to 12 months from the emergence of symptoms. It was during the El Escorial (Spain) scientific convention in 1994 when the attributes of ALS were redefined with added diagnostic features, facilitating clinicians to conduct proper and accurate diagnoses.

The following criteria were added (see http://www.wfnals.org/guidelines/1998elescorial/elescorial1998criteria.htm for a review):

- Evidence of LMN and UMN involvement by electrophysiological and neuropathological test examination.
- Progression of symptoms in the whole affected region and the spread to other regions. This is based on the final diagnosis of the disease.
- Possible inclusion of neuroimaging techniques such as diffusion tension image (DTI) of the spinal cord and frontal lobes.

Although this new definition of ALS greatly improved the diagnostic process of ALS, it still remains as a challenge for many physicians when evaluating the involvement of the UMN during their neurological explorations. To date, the motor threshold establishment by transcranial magnetic stimulation (TMS) remains the most reliable analysis in determining delays in the Babinsky sign. This reflex is still considered a crucial diagnostic criterion for ALS as it appears delayed up to a year after the apparition of first symptoms of the disease (V Meininger et al. 1995). Also, body weight loss of more than 10% in the body mass index (BMI) is a a negative predictor of survival in ALS (Piquet 2006). As such, it is important to determine a reliable diagnostic criteria so as to

accurately diagnose ALS differentially among other motor neurone diseases (Kiernan et al. 2011).

1.4 ALS epidemiology and prevalence

The ALS ratio of those affected by the disease amongst a population demonstrates gender-linked differences as men were observed to be more inclined to suffer ALS than women, with a ratio of 1.2 for women and 1.5 for men respectively (Manjaly et al. 2010). The ALS cases in Europeans and European descendants across different countries have been studied extensively in comparison to other ethnicities. Therefore, to enrich current data and to improve epidemiological knowledge of ALS, propositions have been made to study the incidence of ALS in non-European populations. Currently, the incidence of ALS in studied European populations is approximately 2-3 people per 100,000 individuals (Johnston et al. 2006).

The scarcity of individuals with this disease has categorized ALS as an orphan or a rare disease (Ayach et al. 2014) as opposed to more prevalent neurodegenerative diseases Alzheimer's Disease (AD) or Parkinson's Disease (PD). While age progression increases the risk of PD and AD, in ALS the age factor decreases in influence after the threshold point of 75 years. At this age, there is no increase and even a decrease in risk of ALS (Manjaly et al. 2010; Huisman et al. 2011). This may be due to the fact that ALS patients constitute a small group of individuals, as such represent an even smaller group in populations above 75 years of age. (Pugliatti et al. 2013; Wittie et al. 2013).

1.5 ALS risk factors

1.5.1 *Environmental risk factors*

The environmental risk factors of any disease are extremely vast and difficult to characterize. Nonetheless, the environmental risk factors of ALS have been widely studied overtime. Nutrition as a risk factor was proposed as a predominant cause after the discovery of an immoderate ALS prevalence within the Chamorro inhabitants of the Pacific Ocean island of Guam (Cox, Banack, and Murch 2003; Banack and Cox 2003). The consumption of *Cycas micronesica* seeds was common among the Chamorro inhabitants. These fruits are extremely rich in the cyanotoxin β-N-methylamino-L-alanine (BMAA). While the potential neurotoxicity of these cyanotoxins have been proposed to be a risk factor, there has yet to be a clear demonstration of its effects resulting in ALS (Cox et al. 2003).

In research to elucidate ALS environmental risk factors, there has been some evidence that the practice of sports such as soccer and basketball could be risk factors. In countries including the U.S.A and Italy, some professional players and athletes (Scarmeas et al. 2002) were diagnosed with ALS. To evaluate if there was a causal link, a study was conducted in Italy among some professional soccer players reported to suffer from this disease (Chiò et al. 2005). A wide population-based study involving nearly 3000 subjects between ALS patients and healthy controls, was also performed to evaluate this hypothesis. The studies collectively concluded that ALS patients often practice more aerobic exercise as opposed to healthy individuals. However, based on this study, little is still known about the contributions of aerobic exercise in relation to the emergence of ALS (Huisman et al. 2011). In other stratified studies, smoking as a risk factor was more apparent in females than males (Alonso et al. 2010).

In spite of all the aforementioned studies conducted, an explicit and clear relationship between any of these hypothesized environmental risk factors and the apparition and diagnosis of ALS is still lacking (Cox et al. 2003). Some authors have indicated that the study of environmental risk factors independently without the consideration of individual genetic factors yields biased results, due to the continuous interaction between genetic and environmental factors. It would thus be irrelevant to consider one of these elements without evaluating its role in the grander scheme (Dion, Daoud, and Rouleau 2009).

1.5.2 *Inherited ALS and genetic risk factors*

In ALS, genetic factors only account for approximately ten per cent of all ALS cases. The remaining 90 per cent would thus be classified as having occurred by sporadic cause (unexplainable with unknown genetic risk involved) (Al-Chalabi and Hardiman 2013). Cases of ALS involving genetic mutations are known as familial ALS (FALS). In Table 1 we find a description of the genes involved in ALS risk.

The TAR DNA-Binding protein (TARDBP) protein has been linked to ALS and FTD as TDP43 vastly appears in positive-ubiquitin inclusions found in neurones and motor neurones, especially in affected cortical regions (Neumann et al. 2006). Despite the apparition of TDP-43 inclusions in ALS; TARDBP mutations only account for three per cent (Chiò et al. 2012) of FALS cases. The most important gene mutation is A382T, which is frequent in Sardinia, Italy. The disparity between the presence of TDP43 misfolded protein in autopsies and the impact of TARDBP mutations in ALS cases has shifted the research focus to the RNA processes ongoing in motor neurones as TRDBP is a RNA-binding protein.

Table 1. Genes involved on ALS risk (adapted from Al-Chalabi and Hardiman 2013).

Locus	Gene Symb.	Gene Name	Chromosome
ALS 1	SOD1	Superoxide dismutase 1, soluble	21q22.11
ALS 2	ALS2	Amyotrophic lateral sclerosis 2 (juvenile)	2q33.2
ALS 3	Unknown	unknown	18q21
ALS 4	SETX	Senataxin	9q34.13
ALS 5	SPAST	Spastin	2p24
ALS 6	FUS	Fused in Sarcoma	16p11.2
ALS 7	Unknown	Unknown	20p13
ALS 8	VAPB	VAMP (vesicle-associated membrane protein)-associated protein B and C	20q13.33
ALS 9	ANG	Angiogenin, ribonuclease, Rnase A family, 5	14q11.1
ALS 10	TARDBP	TAR DNA-binding protein	1p36.22
ALS 11	FIG4	FIG4 homologue, SAC1 lipid phosphatase domain containing (Saccharomyces cervisiae)	6q21
ALS 12	OPTN	Optineurin	10p13
ALS 13	ATXN2	Ataxin 2	12q23-q24.1
ALS 14	VCP	Valosin-containing protein	9p13
ALS 15	UBQLN2	Ubiquilin 2	3p11.2
ALS 16	SIGMAR1	Sigma non-opioid intracellular receptor 1	17p13.3
ALS 17	Unknown	Unknown	9q21-q22
ALS 18	PFN1	Profilin 1	9p21.1
ALS-FTD 1	Unkwon	Unknown	3p12.1
ALS-FTD 2	C9orf72	Chromosome 9 open readind frame 72	19p13.12
ALS-FTD 3	CHMP2B	Charged multivesicular protein 2B	12q24
ALS	UNC13A	Unc-13 homologue A (Caenorhabditis elegans)	2p13
ALS	DAO	D-amino-acid oxidase	22q12.1-q13.1
ALS	DCTN1	Dynactin 1	12q12
ALS	NEFH	Neurofilament, heavy polypeptide	5q35
ALS	PRPH	Peripherin	17q11.1-q11.2
ALS	SQSTM1	Sequestosome 1	15q14
ALS	TAF15	TAF15 RNA polymerase II, TATA box binding protein (TBP)-associated factor, 68kDA	8p21.1

Another protein that supports this new focus on RNA metabolism in neurones and motor neurones is the FUS (Fused-in-sarcoma) protein encoded by the FUS gene. The FUS mutations account for less than the three per cent of all FALS cases (Vance et al. 2009). The FUS protein acts downstream in the same RNA binding pathway as TDP43 and both proteins have the binding domain in the C-terminus. However, FUS inclusions have been observed in some ALS autopsies while TDP43 inclusions were not (Vance et al. 2009).

Yet another important mutation linked to FALS is Sequestome1 (SQSTM1). This gene encodes the P62 protein, a protein largely involved in neurodegeneration and hence, controls the ubiquitin binding process leading to the misfolding of accumulated proteins and the subsequent activation of the nuclear factor kappa-B signalling (NFκB) (Laurin et al. 2002). Mutations in SQSTM1 only account for nearly one per cent of all FALS cases, thus its apparition is remarkable and introduced NFκB involvement in ALS pathogenesis. As reported in Table1, while several gene mutations have been reported in ALS, these mutations are only observed in less than one per cent of all FALS cases. This however, is not the case with mutations in the Cu and Zn superoxide dismutase-1 (SOD1) gene. Since the introduction and discovery of the first eleven mutations in the gene encoding for SOD1 at chromosome 21q by Rosen et al. in 1993, there has been remarkable improvement in our understanding of ALS. The inceptive discovery made over 20 years ago has made the further understanding of ALS pathological mechanisms possible. With that, the exact mechanisms explaining the disease pathophysiology remain to be elucidated (Ling, Polymenidou, and Cleveland 2013). The discovery of SOD1 mutations has led to the most acclaimed and important development of of FALS SOD1 transgenic animals. These animals are overexpressors of FALS human SOD1 with the ability to reproduce most of the disease features in humans such as shortened life-span, initial paralysis on lower limbs, massive losses on muscle

mass, the initial and exclusive degeneration of motor neurones and the cardio-respiratory failure as the final and fatal symptom (Turner and Talbot 2008).

With regard to the molecular mechanisms governing the ALS pathology, these FALS rodent mutants are also able to replicate crucial features of the disease. These include characteristics such as the glutamate excitotoxicity injury in the spinal cord motor neurones and the generation of reactive oxidative stress species (ROS) during the degeneration of affected neurones (Jeffrey D Rothstein 2009). Despite of the appearance of more than 150 diverse SOD1 mutations in ALS patients worldwide, and the specific penetrance that some of these mutations have in terms of geographical prevalence (see Battistini, et al. 2010 for a review), only a handful of these mutations have been utilized to create familial FALS research models. Amongst the few SOD1 mutations that have been used for FALS research models, we highlight the A4V, the G85R and the widely ALS studied G93A mutation. The G93A mutation is also the focal point of this present thesis. Further details on the contributions with regard to this mutation in ALS establishment and progression are extensively provided in the next chapter of this thesis introductory section.

1.6 Motor neuron diseases: common patterns of neuron degeneration (the case of spinal muscular atrophy (SMA) and ALS)

As described in the earlier paragraphs, ALS is included in a heterogeneous group of diseases known as motor neurone diseases (MNDs). These diseases encompass a common feature of affected regions such as CNS motor neurones and neuromuscular junction unions. There are two main categories of MND pathologies, these are Spinal Muscular Atrophy (SMA) and ALS. Although the scope of this thesis is mainly focused on ALS, some common shared

pathological features between ALS and SMA will also be explored as murine models of both diseases will be discussed.

Spinal muscular atrophies are a family of MNDs with a common genetic background originated by mutations of the survival motor neuron (SMN) gene that encodes the SMN1 protein. The abundance level of the SMN1 protein negatively correlates to the cause and aggressiveness of this disease phenotype (Lefebvre et al. 1995). SMA, unlike ALS, is not associated with the ageing process in all its severe manifestations and usually appears during the childhood, with the exception of a milder variant known as SMA type IV. The SMA type IV variant has an onset from 35 years onward (Orrell 2010).

The degeneration of motor neurones in ALS and SMA share some common mechanisms at the cellular level: the formation of stress granules by the endoplasmic reticulum and the damage of mitochondria by oxidative stress (Blackstone 2012). Even though the common cellular mechanisms between ALS and SMA have been studied, still, little is known about the common shared mechanisms in the degeneration of motor neurones from a broad motor system approach. This is considering that the global insult of the motor system is caused by the effects of the degenerating synapses, axon boutons, afferent terminals and corticospinal tracts commonly causing the degeneration of α-MNs (Talbot 2014).

2. ALS neuropathology revealed by the motor neurone vulnerability to the SOD1-G93A mutation

2.1 SOD enzymes: three enzymes in the animal kingdom with dismutase properties

Superoxide dismutases (SODs) are a family of enzymes widely distributed in various forms in all eukaryotic cells. Their ubiquitous presence are present within the cells of bacterial kingdom, plants, as well as the cells of complex animal cells. The SOD enzymes embody the pivotal role related to the metabolization of $O_2^{\bullet -}$ which counteracts deleterious oxidising chain reactions like reactive oxygen species (ROS) as hydrogen peroxide (H_2O_2), hypochlorite (OCl^-), peroxynitrate (ONO_2^-) and hydroxyl radical ($HO^\bullet$). Without this mechanism in place, the presence of these free radicals could lead to the irreparable damage and consequently, inevitable cell death (Miller AF., 2012). The leading role of SODs in cell survival seems related to an evolutionary shift that came about 2.4 billion of years ago, which elicited a gradual progression

toward an oxygenic photosynthesis environment, which made it difficult for organisms lacking SODs to survive (Miller AF., 2011).

The family of SOD enzymes vary in the aspects of their chemical molecular properties and protein folding. However, these enzymes encompass similar functions and capacities to convert two molecules of superoxide to one dioxygen molecule and one hydrogen peroxide molecule with the consumption of two equivalents of H^+ (Miller AF., 2011). The molecular characteristics of SODs utilize different ions to mediate chemical properties. The variants include one that uses the Ni ion, one that uses Cu combined with Zn, and the last variant which is the most ancient species in biological evolution that uses either a Mn or Fe ion.

In comparison to other less complex cellular organisms, which often utilize only one form of SOD enzymes, mammals often use a combination of two types of SODs. First, a homodimer called SOD1, which chemically uses Cu combined with Zn can be found within the cytoplasm. In the same cell, another enzyme known as the SOD3 with the same chemical properties but comprises a tetramer conformation can be found extracellularly in mammals. Also, a form known as SOD2 which uses Mn as a main chemical property can be found within mitochondria in mammalian cells.

2.2 Abundant and different mutations in SOD1 gene linked to ALS

According to the ALS online genetic database (ALSOD: http://alsod.iop.kcl.ac.uk/), up to date, more than 177 mutations have been discovered in the SOD1 gene related to the ALS phenotype (Abel et al. 2012). More than eighty per cent of those mutations contain amino acid substitutions

whereas the remaining twenty per cent comprises deletions, insertions and polymorphisms.

According to previous epidemiological studies, somewhat of a geographical distribution has been observed to have emerged around the penetrance of diverse SOD1 mutations involved in ALS. In Northern European countries such as Sweden and Finland, the D90A is the most prevalent mutation. In the United States, the A4V mutation is the most prevalent while the Rii5G mutation is most prevalent in Central European countries (see Battistini et al. 2010 for a review). These disparities in geographical prevalence of SOD1 mutant haplotypes are a consequence of the wide ancient migrations across the continents (W J Broom et al. 2008).

With the exception of the D90A isoform, all the SOD1 mutations are inherited in an autosomal dominant manner. The D90A isoform shows moderate onset disparity in terms of ALS symptoms between heterozygote and homozygote subjects, with the mean age of ALS onset being 53.9 years and 46.0 years respectively (Parton et al. 2002). This onset disparity has been hypothesized in relation to a possible correlation between the transcription levels of mutant SOD1 and the severity of ALS symptoms. To date this still remains to be elucidated through further research (Wendy J Broom et al. 2009).

2.3 Disease mechanisms of SOD1-G93A

2.3.1 *Mutant G93A enzymatic properties in ALS*

The discovery of SOD1 mutations in FALS was initially thought to provide an explanation behind the impaired antioxidant properties of the enzyme as the apparition of oxidative stress in motor neurones is a central hallmark of ALS

progression. However, verification studies using SOD1 null mice have observed that mice do not develop any sign of motor neurone disease beyond an increased vulnerability to the experimentally-caused axonal insults (Reaume et al. 1996).

The vast research existing on animal models expressing mutant SOD1-G93A from humans, established the current theory of a possible gain of function behind the toxicity exerted by SOD1 mutants in motor neurones during ALS progression (Bruijn et al. 1997). In 2003, Potter and Valentine presented a classification of two groups for the SOD1 mutants involved in ALS. This classification is based on the structural and functional properties of the mutated enzyme. The G93A mutant was referred by the authors as a wild-type-like mutant since its behaviour remains conformed to the WT enzyme in the assessed condition of copper-mediated catalytic activity through the metal binding site. According to the authors, the G93A showed an increased dismutase activity that reverts in excessive oxidative stress for the expressed cells and may differ from the WT SOD1. This is because it is still unclear if folding stability under manipulated thermal conditions is affected.

Unlike other metal-binding-region mutants, the G93A does not display any abnormal characteristics in its β-barrel plug loop performing a normal binding to Cu and Zn ions through this domain.

Despite all of the aforementioned studies about the enzymatic properties of SOD1 in the context of ALS, specifically the G93A mutant, the relationship between the enzyme capacities and the impact of these in disease onset and progression still remain far from being unraveled.

2.3.2 *Biochemical properties of the mutant SOD1-G93A*

SOD1 is a 32-kDa homodimeric metalloenzyme mostly found in the cytosolic fraction in eukaryotic cells. It can also be present in the mitochondrial membrane, the nucleus and peroxisomes. SOD1 is structurally conformed by two subunits that form eight-stranded Greek key β-barrels which comprise an active site that binds a catalytic Cu ion (binding residues: His46, His48, His63 and His120) and a structural Zn ion (Figure 2) (binding residues: His63, His71, His80 and Asp83) (Banci et al. 2008). The SOD1 developed structure undergoes several post-translational modifications before it reaches mature conformation. The protein suffers a metallation and the formation of a disulphide bond which seems to stabilise the structure. This finally prepares the protein for its normal function (Furukawa, Torres, and O'Halloran 2004).

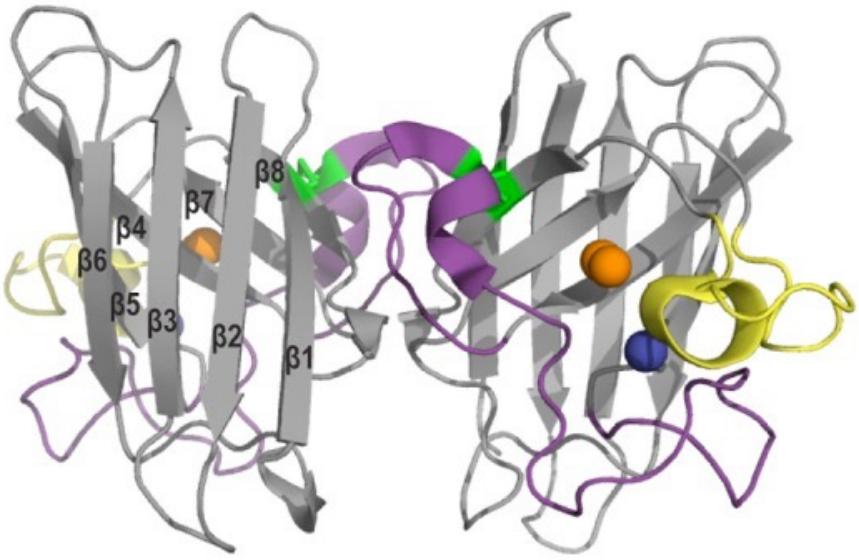

Figure 2. Molecular model illustration in cartoon showing the conformation and the structure of human SOD1 molecule. At the left of the image, the eight-stranded Greek key β-barrel can be identified. (Adapted from Rotunno & Bosco 2013).

It has been proposed that the loss of glycine at residue 93 becomes basic results in the toxicity exerted by the G93A mutant. Also, the toxic properties seem independent of alanine addition (Shipp et al. 2003). Although there is difficulty in finding any discrepancy between the biochemical properties of the WT and the G93A SOD1 isoforms, an emerging hypothesis is that an aberrant binding site may be formed in the mutant structure after the enhanced dynamism of the strand β6 (Shipp et al. 2003). This abnormal dynamism could also be linked to further destabilizations of the protein structure and might promote the motor neuron toxicity through cell signal transduction mechanisms, which are secondary functions of SOD1.

2.3.3 *Mutant SOD1-G93A and the signal transduction mechanism in the disease*

The signal transduction properties of SOD1 have remained an oversight for the research community for a long time (Rotunno and Bosco 2013). The SOD1 enzyme may interact and modify the structure and function of some key-role proteins through oxidation of cysteine and lysine residues involving a modulation of some cellular essential pathways targeting proliferation, gene expression, differentiation and cell death. More precisely, it has been shown how activation of NADPH oxygenases (Nox) is modulated by the oxidation effects of SOD1 in response to pro-inflammatory signals in cell endosomes (Harraz et al. 2008). Contrary to this, the SOD1 in normal conditions has been shown to be liberated by astrocytes in the extracellular spaces. It also acts as a controller of the intracellular calcium homeostasis in cerebellum neurones through the interaction between the SOD1 and the muscarinic M1 receptors (Polazzi et al. 2013). Expression of hSOD1 G93A mutant in astrocytes which were co-cultured with motor neurones demonstrated how G93A is able to enhance the ROS

production interacting with Nox1 which results in an increase in motor neuron cell death. Nox1 silencing is able to rescue this harmful effect (Q. Li et al. 2011).

2.3.4 *Mutant G93A and the prionic propagation hypothesis*

In spite of the fact that SOD1 is ubiquitously expressed, toxic properties of SOD1 G93A are largely exerted in motor neurones in an exclusive manner. However, characteristic SOD1 aggregates have been found present in motor neurones and glial cells apposed to motor neurones in the spinal cord ventral horn (Strong, Kesavapany, and Pant 2005). The mechanisms governing how SOD1 spreads its toxicity from the initial suspected source in motor neurones to other cells still remains unknown. With the assumption that motor neurones are the first and exclusive cells affected by SOD1 cytotoxicity, the propagation of the enzyme toxic properties to surrounding astrocytes and to adjacent extracellular spaces in ventral horn is hypothesized to comprise a prion-like propagation cascade. In mutant mice, it has recently been shown that misfolded SOD1 G93A structures are present in spinal cord dorsal root ganglion (DRG) sensory neurones (Sábado et al. 2014).

Vesicle-contained propagation of SOD1 prionic properties has been largely proposed since it has been shown how culture media from mutant transfected cells can accumulate toxic properties to WT isoforms (Münch, O'Brien, and Bertolotti 2011). According to most recent studies, the prion-like propagation of SOD1 seems independent of exosomes and can also be exerted by aggregates that directly can interact with the motoneuron exocytotic machinery (Grad et al. 2014). The prionic properties of aberrant SOD1 and how it affects the WT protein in the SALS and FALS and how the blockage of abnormal protein clearance mechanisms starts and progresses to promote massive neuronal death is currently a matter of great interest within the ALS research community.

This is because it could provide information about the relationship between sporadic and familial ALS pathophysiological mechanisms and to shed light on some crucial unsolved questions about the disease pathologic mechanisms.

2.3.5 *Mutant G93A motoneuron intracellular inclusions, toxicity and failure of proteostasis mechanisms*

The activity of cellular chaperones is the first step in the quality control mechanism of cells. The chaperone family of molecules is the first to interact with the aberrant proteins to induce their refolding and repair. It has been recently described that the low level of the CRYAB at initial stages of the SOD1G93A ALS exacerbates the disease progression and phenotype of the transgenic mouse (Marino et al. 2014). Imbalances in the chaperone quality control system promote the failure of SOD1G93A re-folding state. It has been reported that in the case of ALS, the aberrant synthesized SOD1G93A in motor neurones is previously confined to detergent insoluble aggregates which are tagged by the ε-ubiquitin ligases at the lysine residue (48) for its subsequent degradation through the proteasome (Basso et al. 2006).

Ubiquitin is a molecule of 76 amino acids ubiquitously expressed in all the eukaryotic cells. When the proteasome degradation machinery switches on, this molecule binds to the lysine residues of the targeted protein and forms a covalent bond (Haizhi Wang and Saunders 2014). It has been demonstrated that the successful degradation of the targeted protein through the proteasome system requires the formation of long ubiquitin bound chains (poly-ubiquitination chains) and the intervention of ε1, ε2 and ε3 ubiquitin ligases (Thrower et al. 2000). Finally, the targeted protein is degraded by the ubiquitin-proteasome system (UPS) composed by the 26S proteasome, which is a complex structure formed by the inner 20S catalytic structure that degrades the targeted proteins

and by the 19S outer complex rings which directly bind to the poly-ubiquitin chains and denature the targeted proteins in mammalian cells (Adams 2003) (Figure 3). In some cases, especially during neurodegeneration under unclear circumstances, the ubiquitin-proteasome system may become overwhelmed. In that case, the SOD1 aggregates present in the motor neurone somata may turn into 'aggresomes', which should be cleared through the lysosome-autophagy pathway (Hongfeng Wang, Ying, and Wang 2012).

SOD1 toxicity is believed to exerts harmful effects on the protein quality control systems within motor neurones. However, this hypothesis has been recently questioned since the toxic effect of SOD1 has been linked to the proteasome protease capacity. When the proteasome is highly active in cells, the mutant SOD1 is extremely prone to form aggregates. The toxicity of this mutant protein is significantly lower than when the proteasome is artificially inhibited by the same mutant SOD1 that creates oligomers with extreme toxic properties that promote cell death (Kitamura et al. 2014).

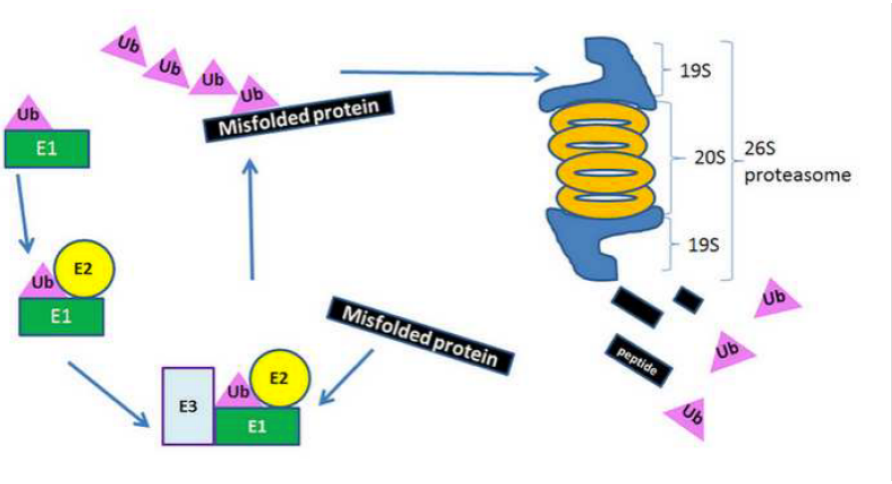

Figure 3: Illustration depicting the cellular degradation machinery of ubiquitinated proteins through the ubiquitin-proteasome system.(UPS). Adapted from Wang and Saunders 2014.

The mechanism of action by which the mutant SOD1 G93A harms the proteasome remains poorly understood even though this harmful effect is apparent in all disease models from in-vitro to mammal models of SOD1 G93A. Experimentally, the detection of SOD1G93A aggregates is usually demonstrated by the use of detergent-insoluble fractionation or by immunoreactive methods (Sábado et al. 2013).

2.3.6 *Mutant G93A toxicity in cellular organelles: mitochondrial dysfunction*

The mitochondrion is crucially involved in more than nine essential pathways for the survival of eukaryotic cells and the extent of that involvement is still far to be completely understood. Perhaps the most recognized amongst them is still the adenosine triphosphate (ATP) production via the matrix effect by oxidative phosphorylation (Nicholls and Budd 2000). Furthermore, the mitochondrion is implicated in cell apoptosis by the BCL2-BH3 complex, synthesis and oxidation of amino acids, metabolism of reactive oxygen species (ROS), urea cycle, etc. (Pickles et al. 2013; Pedrini et al. 2010). The genetic alterations of mitochondria may have fatal consequences for the cells and organisms while in some cases they are centrally implicated in inherited disorders such as juvenile catastrophic epilepsy, myopathies or hepatocerebral disorder (Copeland 2014).

The ancestry of current mammalian mitochondria is derived from the bacterial kingdom and it has been proven that dysfunctions in these organelles display clear tissue-specific manifestations under the same genetic dysfunction (Tan, Pasinelli, and Trotti 2014).

In neurones, it has been established that mitochondria directly affects the activation of neurones by the buffering of Ca^{2+} influx over the neurotransmitter release machinery (Baughman et al. 2011). In addition, the mitochondria is

indirectly implicated in the synthesis of γ-aminobutyric acid (GABA) and glutamate neurotransmitters through the respiratory production of molecular energy (Hertz 2013). Functional alterations in Ca^{2+} buffering capacity have been reported from early and pre-symptomatic disease stages in the SOD1 G93A mouse spinal cord (Damiano et al. 2006; Guatteo et al. 2007). As a consequence, morphologically, the mitochondria may appear swollen and the mitochondrion cristae may appear disorganised and augmented (Sasaki and Iwata 2007). For a long time, the role of mitochondria in ALS appearance and progression was thought to be peripheral, however, as stated in the aforementioned findings, it is now considered crucial and has garnered significant interest. Aggregates of SOD1 G93A are found in the outer membrane of mitochondria in spinal cord of ALS animal models (Pedrini et al. 2010; Pickles et al. 2013). When the healthy mitochondrion is isolated and exposed to the mutant SOD1 G93A, it shows increased susceptibility to structural damage and oxidative stress (Pedrini et al. 2010).

The extent of the mitochondria impairment in ALS goes beyond the common impact this disease has on this cellular organelle in all the cell types. Specifically in neurones, it has been proposed that mitochondrial damage causes the dying back mechanism (Tan, Pasinelli, and Trotti 2014), affecting the complex transport dynamics that takes place in these specialized cells. In spite of this speculation, little is known about the dying back mechanism. It has however, been proposed that the failure of the autophagic flow in the distal areas of axon terminals may cause the accumulation of impaired mitochondria. It may also contribute to axoplasmic transport impairment that finally causes cell death by retrograde degeneration (Fischer-Hayes, Brotherton, and Glass 2013; Tan, Pasinelli, and Trotti 2014).

In relation to the dying back degeneration mechanism, the affectation of mitochondrial dynamics has been described in ALS as well as in PD. In PD, the

impairment of mitochondrial dynamics has been widely explored in relation to neurodegeneration (Tan, Pasinelli, and Trotti 2014). Mitochondria are extremely dynamic organelles that perform the fission and fusion processes according to cell demands and the presence of stress conditions in all the diverse cellular compartments (Szabadkai et al. 2004). In previous studies, it has been stated that the imbalance or impairment mitochondrial dynamics can lead to individual cell death and neurodegeneration (Tan, Pasinelli, and Trotti 2014). The proteins Parkin and PINK1 are involved in the homeostasis of mitochondrial dynamics and the clearance of impaired mitochondria in PD (Lim et al. 2014). The implications of these two proteins in ALS are still unidentified, even though the proteins OPA1 and DRP1 have been implicated in the SOD1 G93A mice impairment of mitochondrial dynamics (Ferri et al. 2010). In the results and discussion sections of this thesis, we will present and discuss novel results with regard to the mitochondrial kinase PINK1 and its implications in ALS pathology.

The described damage in mitochondria during ALS starts early during the pre-symptomatic stages of the G93A mice. At this time, the outer membrane of the mitochondria becomes less permeable (Tan et al. 2013). This damage has been noted to appear solely on the VDAC1 channel, a porin from the outer membrane that controls respiration and the mitochondrial ATP flow. In short, the interaction of mutant SOD1 with this channel results in a high influx of calcium into the mitochondria and promotes the accumulation of ATP in the intermediate membrane. This slows down the capacity of the organelle to translocate ATP or ADP (Mattiazzi et al. 2002). Furthermore, a direct interaction between the mutant SOD1 G93A and the Bcl-2 domain of the mitochondria has been demonstrated to promote the interaction of this complex with the VDAC1 channel. This in turn results in the exposure of the BCH3 toxic domain of the mitochondria and thus the release of the cytochrome C (Tan et al. 2013).

2.3.7 *Mutant SOD1 G93A toxicity in cellular organelles: endoplasmic reticulum stress responses*

The endoplasmic reticulum (ER) is a cellular organelle involved in critical functions of protein synthesis, protein folding and cellular secretory networks. This organelle remains highly interconnected with the mitochondria (Lanner et al. 2010) and is involved in the Ca^{2+} homeostasis in neurones. It has been proposed to be responsible for the calcium intake in mitochondria described above in ALS (Michael J Berridge 2014). Following the increment of misfolded proteins in the cell cytoplasm, the ER activates the unfolded protein response (UPR) mechanism under stress conditions (L. Wang, Popko, and Roos 2011). UPR is a complex mechanism consistent of extensive and intricate molecular events in which a detailed explanation exceeds the purpose and focus of this thesis. However, we consider it important to mention that the ER-UPR activation implies the suppression of nucleus protein synthesis and the reinforcement of the ER synthesis of chaperones via the activation of the enzyme RNA-like ER kinase (PERK) pathway (Cullinan and Diehl 2004). The activation of the aforesaid molecular events under the ER stress condition has been shown that promote the entrance of misfolded proteins into the ER lumen in detriment of newly synthesised proteins. Adding to that, it has been hypothesized that the ER-UPR may promote the activation of the autophagic pathway in the neurodegenerative motoneuron and the activation of the membrane secretory pathway to release toxic misfolded proteins outside of the cell cytoplasm (Appel et al. 2011).

Recent studies have been shown how the ER stress response activation elicits the induction of the NF-κB pathway in a model of SOD1-G93A motor neurone cell line. The increased excitation of this pathway has been suggested to be a pro-survival response to counteract the harmful effects of the ER stress, but the effects of the NF-κB pathway in ALS still remain completely unascertained and

understudied (Prell et al. 2014). In the results section of this thesis, we confirm these findings to provide nau courant results about the NF-κB activation and its implications in the proteasome proteolysis capacity in the presence of mutant SOD1 G93A.

The activation of ER-UPR in mutant SOD1 has been described in vitro (Prell et al. 2012; Kiskinis et al. 2014) and in vivo during the onset of symptomatic stages and the final stage in G93A mutant mice (Kikuchi et al. 2006). UPR activation has also been observed in sporadic ALS cases (Atkin et al. 2008) suggesting an important role of the ER stress scenario in the overall motor neurone pathophysiology prevalent in ALS.

2.3.8 *Motoneurones excitotoxicity in SOD1 G93A ALS*

While these are some molecular mechanisms governing motor neurone degeneration in ALS, other classical pathological mechanisms could aid in discernment of molecular motoneuron injury in ALS. One example of a vital mechanism which is a key in eliciting ALS motor neurone insults is excitotoxicity. Within the spinal cord of ALS patients, glutamate levels have been reported to be highly augmented. In a similar light, the clearance of approximately the 90% of glutamate is executed by the glial glutamate transporter EAAT2 in the motoneuron synaptic clefts located at the ventral horn of the spinal cord (J D Rothstein et al. 1996). Glutamate interacts with three different types of receptors in neurones and produces excitotoxicity by the overactivation of N-methyl-d-aspartate (NMDA), α-amino-3-hydroxy-5-methylisoxazole-4-propionate (AMPA) and kainate receptors (Ayala and Tapia 2003). In this event, the AMPA receptors in motor neurones are likely to exacerbate the effects of motor neurone excitotoxicity, resulting in the detriment of other glutamate receptors (Van Den Bosch et al. 2000). This is especially evident for AMPA receptors that lack the

GluR2 subunit mechanism in which glutamine (Q) is post-transcriptionally substituted by arginine (R) in a Q/R site located in the second membrane domain (M2) since the presence of GluR2 subunit decrease the Ca^{2+} permeability of the receptor. AMPA receptors that lack GluR2 subunit are inclined to quickly increase the Ca^{2+} cytoplasmic concentration when they are agonised by glutamate (Pellegrini-Giampietro et al. 1997; Greig et al. 2000; Van Damme et al. 2002). The excitotoxicity in the cell might be directly linked to the establishment of mitochondrial dysfunction (von Lewinski and Keller 2005; Nicholls and Budd 2000).

Oculomotor neurones, on the other hand, are the last motor neurones to be affected by the neurodegenerative process, exhibiting greater resistance to degeneration in ALS (Robberecht and Philips 2013). This was observed in the SOD1 G93A transgenic mice as well as in patients. As these neurones lack in-depth characterization of their intrinsic traits, the results in this thesis will present some of their newly discovered features in addition to their well-established higher calcium-buffering capacity when compared with spinal motor neurones. This inability of spinal motor neurones to cope with higher calcium levels thus supports this hypothesis of motor neurone excitotoxicity in ALS pathophysiology.

2.3.9 *Contribution of CNS non-neuronal cells to motoneuron degeneration in SOD1 G93A ALS*

Although ALS has been clearly emphasized and described as a motor neurone disease, motor neurones are not solely affected in this fatal disease. The two main populations of cells within the brain: neuronal cells and glial cells vary in function. Neurones are considered unique cells with the ability to contribute to cognition and movement from the time of Cajal. On the contrary, glial cells do not possess these features, and was not considered imperative in the research

field for a significant amount of time. However, with time, as ALS was observed to encompass microglial and astroglial activation as an early feature of the disease. With this, research on the implication of these cells and the study of the pathologic relationship between neurones and glia lead to the discovery of the breakthrough non-cell autonomous theory which amazed the scientific community. In an essence, the exclusive expression of mutant SOD1 in astrocytes does not lead to the apparition of motor symptoms and degeneration of neurones in ALS models. This is also so if the mutant SOD1 is only expressed in neurones where the motor impairment also does not appear. According to this discovery, the ALS pathologic progression caused by SOD1 mutations requires that the mutant enzyme be co-expressed in both neurones and glial cells (Pramatarova et al. 2001; Gong et al. 2000).

On the other hand, more experiments pursuing the further understanding of SOD1 expression mechanisms to cause the ALS pathophysiology were done in chimeric mice. Neurones expressing mutant SOD1 but surrounded by cells that do not express G93A and other mutations were resistant to degeneration (Clement et al. 2003).

Finally, in a recent study, it has been shown how the expression of SOD1 in mice microglia during the late stages of the disease is able to accelerate the progression of the disease (Boillée et al. 2006).

2.4 Generation of monoclonal antibodies against misfolded SOD1 monomers: new opportunities for research and immunotheraphy

Over the past decade, several antibodies have been suggested to recognize misfolded SOD1 species. They have presented a great advantage as they are able to recognize a broad spectra of the sporadic misfolded SOD1 that occur in the 90% of the total ALS cases. A majority of these antibodies are also able to recognize the mutant misfolded SOD1 in patients and ALS experimental models. The first antibody complementary to one covered epitope of SOD1 was the SEDI, which is able to elicit a reaction with urea-denatured SOD1 and oxidized SOD1 monomers (Rakhit et al. 2007). The precipitation of SEDI antibody indicated that the presence of misfolded SOD1 is evident in pre-symptomatic stages of the G93A mice. From there, some other antibodies were discovered, one of them the USOD (Kerman et al. 2010) that shares many characteristics with the SEDI, specially in terms of the reactivity patterns (Pickles and Vande Velde 2012). In 2013, the characterization of the AJ10 antibody was reported (Sábado et al. 2013) subsequent to the demonstration of that the inner hydrophobic region of SOD1 uncovered after misfolding shares structural homology with the peptide sequence of the P2X4 purinergic receptor (Hernández et al. 2010). The AJ10 antibody is able to bind the misfolded SOD1 conformers in different species such as mice, rat and even in *Drosophila melanogaster* tissues as we will show in the results section of this thesis. The availability of these antibodies provides researchers the opportunity to prepare immunotherapy studies together with the opportunity to understand the interactions that mutant and WT SOD1 perform to promote degeneration of the motoneurones.

3. New approaches to ALS: from cell vulnerability to system vulnerability

3.1 From cellular neurobiology to system neurobiology in ALS

The cellular mechanisms that promote the degeneration of motor neurones in ALS as they have been described in the previous chapter of this introduction has attracted the major part of the research interest during decades. Nevertheless, it was only during the span of this decade when a new focus considered the ALS progression as a system failure consequence of broad factors as the progressive neuromuscular junction (NMJ) denervation caused by the degeneration of the alpha motoneuron (α-MN) axons affect the terminals that input the motor neurones in the ventral horn of the spinal cord. Progressive NMJ is also caused by the oscillations in the motoneuron excitability as well as by the degeneration of muscle fibers, among other factors. The consideration that the motor system degenerates in a bidirectional manner from a microscopic to macroscopic approach and vice versa is currently considered as an attractive hypothesis (Talbot 2014). It is not known where and from where the system loses the balance but it is thought to be analogous to an edifice that collapses from

the beams and pillars, the motor system as a whole suffers from its integrators (fibers, tracts and somatic neurones) and finally crumbles.

3.2 The corticospinal Tract (CST)

The CST or pyramidal tract was first identified in the seventeenth century. It was finally mapped two centuries later as a result of the contributions of authors such as Nathan and Smith; Willis; Türck and finally, Charcot. The tract was mapped from the central areas to the distal brain regions and the ventral horn afferents. One limitation of the description of this tract was the fact that the mapping was executed using post-mortem tissues containing lesions, which made it difficult to determine an accurate description (Masri 2011).

The soma of the neurones that originate in the pyramidal tract are located in the V layer of the cerebral cortex. More than 60% of the fibers are from the primary motor area, the premotor area and the supplementary motor area of the frontal cortex (Dum and Strick 1991; Jane et al. 1967). The fibers from the region of origin go through the corona radiata, maintaining a somatotopic representation to the posterior region of the lateral ventricle (Han et al. 2010). It is in the cerebral peduncle in the midbrain where the tract is dissociated, and projects the fibers that represent the upper (anteromedial projections) and lower (posterolateral projections) limbs. It is also in that region where the fibres that innervate the head muscles leave the tract to synapse their respective nuclei in the brainstem. At the caudal medulla, ≈80% of the CST fibers decussate while the remaining ≈20% project ipsilaterally to their origin (Kaneko et al. 1997). In the spinal cord, the fibers bifurcate to form the lateral and the ventral or anterior CST. The decussated fibers are mostly packed in the lateral CST and identified in the lumbosacral spine region while the ipsilateral fibers are mostly packed in

the anterior tract close to the midline of the median fissure and terminate in the middle between the thoracic and the sacral spine (Nathan, Smith, and Deacon 1990; Kaneko et al. 1997).

3.3 Evolution of the corticospinal tract and its genetic susceptibility

The characteristics of the corticospinal tract in humans are exclusive to our species. They are not shared with any of our primate ancestors or any other species in the animal kingdom. It is believed that the evolution of this tract coupled to the neocortex regions of the CNS was done under natural selection by very strong pressure. Therefore, these structures developed very quickly in the evolutionary time process, of less than 200,000 years. It is believed that this evolution was linked to the *Homo sapiens* modified posture so as to interact with the environment, leading tothe development of the human language (Talbot 2014). The intricate complexity of these relatively novel CNS structures derived from these evolutionary patterns that causes individuals that have a genetically susceptible profile to be vulnerable (Eisen 2009). The apparition of the most common neurodegenerative diseases, including ALS, has appeared in the last 200 years. This phenomena has been linked to the increase in life expectancy that has occurred during this time. The exact time of onset for ALS however, still remains unknown. It has been speculated that ALS could start as early as during the crucial periods of CNS development. There are two known crucial periods for the development of the CNS. One is the perinatal period and the other, is the period of adolescence. During adolescence, there is synaptic pruning and the formation of extensive neural circuits and extended myelination. It has been hypothesized that in these periods, individuals with genetic risks can establish the neuronal and system basis of ALS (Eisen 2009).

3.4 Family of spinal and brainstem motoneurones

The human body is composed of more than 100 million of muscle fibers enclosed in 300 bilateral muscle pairs innervated by more than 120,000 motor neurones. As these only originate in the spinal cord, these receive input from the motor neurones that originate in the M1 and pre-motor areas in the frontal lobe of the cortex. The spinal cord motor neurones (MNs) are distributed broadly in columns and pools in the ventral horn and directly innervate the muscle fibers and are distributed according to the fibers that they innervate (Kanning, Kaplan, and Henderson 2010). Gamma motoneurones (γ-MNs) constitute around one third of the total lower motor neurones present in ventral horn pools (Westbury 1982) Morphologically, they exhibit small cell bodies (≈ ½ of smallest α-MNs) while they are functionally distinctive for their exclusive innervation of intrafusal fibers in muscle spindles. Beta motoneurones (β-MNs) innervate muscle spindles together with collaterals to extrafusal fibers, which are the class of motor neurones that are less abundant in ventral horn pools. However, they are functionally determined by their capacity to propioceptive transmission from intrafusal signals to extrafusal fibers. Morphologically, they exhibit soma diameters larger than γ-MNs but are significantly smaller than alpha motor neurons (α-MNs). α-MNs, are the largest motor neurone class present in ventral spinal cord pools. Their distribution in pools is also included in columns along the entire spinal cord according to their projections to extrafusal muscular targets. α-MN axons conform the afferences of the neuromuscular junction. It is thus considered that these motor neurones innervate the skeletal muscles responsible for the execution of voluntary movements. Motor neurone electrophysiological properties have been vastly studied, specifically in α-MNs because of their morphological properties. These cells are the motor neurone class that exhibit extended and copious dendritical tree branches together with large and thick calibre axons which are the best options for nerve conductance

studies. In addition, afferents that synapse the α-MNs soma have been selected as much of the substantial inputs control α-MN excitability. The identification of terminals that synapse motor neurone somas was initially only feasible under ultrastructural electron microscope techniques. At present, the apparition of neurotransmitter vesicular transporter immuno-reactions has made it possible the study of terminals under optical microscopic studies.

The organisation of MNs in columns and pools in the ventral horn of the spinal cord matures from the initial development of the neural tube, thanks to the diffusion of trophic factors in a polarized manner during development. When the the spinal cord reaches its matured conformation, the medial motor column (MMC) innervates the dorsal muscles of the body, the hypaxial motor column (HMC) innervates the ventral muscles of the body and the lateral motor columns (LMC) innervate the limbs muscles. In these described columns, the MN somas are organized in pools and each pool innervates a single skeletal muscle of the body and is composed by all types of the described motor neurones.

3.5 Distribution of terminals that input the spinal motoneurones

Different terminal subtypes have been identified and described as afferents to spinal MNs. These terminals have been classified according to the shape of their containing vesicles, their appositional length and their excitatory or inhibitory nature.

S-terminals and T-terminals are approximately between 1-1.5 μm in appositional length, characteristic spherical vesicle transporters and excitatory nature marked by their glutamate (VGlut) reactivity. F-terminals and M-terminals are between 1-2.6 μm in appositional length, flattened spherical vesicle transporters and positive immuno-reactivity for GABAergic vesicular transporters (VGAT) and

glycine. Ultimately, C-terminals define exclusively α-MNs by their synapses, they are characterised by an appositional length up to 3.5 μm and exhibit both spherical and spherical flattened vesicles though considerably large in comparison to other terminal subtypes.

3.6 The C-terminals: their exclusive features and their enigmatic source in the spinal cord

The presence of C-terminals input to motor neurones in mammals was firstreported by Conradi 1969a; Conradi and Skoglund 1969 as a result of their ultrastructural studies within cat spinal cords. The existence of those terminals was later confirmed in humans by (Pullen 1992). Conradi and Skoglund after the encountering of these terminals emphasized the structure of around 10-nm wide underlying their appositional leng that the bottom of synaptic clefts. This structure was named as the sub-surface cistern (SSC) and inspired the “C” name given to these terminals by the authors of their discovery (Deardorff et al. 2014b). Along these 30 years of history, after discovery of C-Terminals multiple studies aimed to identify the neurotransmitter nature and the proteins and receptors that mediate the synaptic flow of these terminals. From these studies, it was initially hypothesized that the cholinergic nature of C-terminals (W. Li et al. 1995; Nagy, Yamamoto, and Jordan 1993). Thereafter, this was confirmed using immunohistochemistry with vesicular acetylcholine transporter (VAchT) by (Arvidsson et al. 1997). Ultrastructural observation and extensive use of vesicle transporters refuted the hypothesis that as source of C-terminals would be other motor neurones contacting α-MNs (J Hellström et al. 1999). Later, experiments including spinal hemi/transection and dorsal root section and cortical ablation have shown that C-terminals were unaffected in functional absence of the mentioned inputs (Miles et al. 2007; Conradi 1969b; Bodian 1975; Pullen and

Sears 1983).

The enigma involving the origin of C-terminals in the spinal cord was solved by Zagoraiou et al. 2009. The authors found that a Pitx2 positive subpopulation of cholinergic interneurones located in the spinal cord near the central canal project their axons to α-MNs in the ventral horn forming the C-boutons. The authors named these neurones V_0 neurones and found an increased amount of V_0 neurones in cervical and thoracic regions while an apparent decrease in the lumbosacral enlargement. Furthermore, these interneurones were positively stained by the vGlut1 transporter.

3.7 The modulatory function of C-terminals on motoneuron excitability

The function of C-terminals still remains poorly understood beyond the modulation capacity of these boutons upon the activation of α-MNs. C-boutons were later post-synaptically associated with presence of muscarinic m_2 receptors and Kv2.1 potassium channels (Johan Hellström et al. 2003; Wilson, Rempel, and Brownstone 2004) suggesting that muscarinic receptors were agonized in the motor neurone somas by the release of acetylcholine (Ach) from C-boutons. The modulatory effect of m_2 receptors over the rectifier Kv2.1 channels was initially studied in hippocampal cultured neurones (Mohapatra and Trimmer 2006) and later in motoneurones by Miles et al. 2007. Milles at al. found that the modulatory effect of m_2 receptors was linked to a reduction of the after-hyperpolarization (APH) phase in motor neurones. The discovery of the referred cholinergic system input to α-MNs was done in parallel to the discovery of the serotoninergic (5HT) system input. The 5HT neurones projecting to α-MNs were located at the raphe nuclei in the brainstem (Martin, Jordan, and Willis

1978) It was then revealed that both systems are developed in mammals during the post-natal stage (Wilson, Rempel, and Brownstone 2004).

Further studies have shown that the excitability of motor neurones is magisterially controlled by the interaction of both of the systems as the initial activation received in α-MNs. This precedes the contraction of muscles is the input by the 5HT system descending from the supraspinal tracts and the magnification of that initial input is provided by the Ach system through C-boutons (Brownstone 2006). It is assumed that the 5HT system modulates the initial input in α-MNs preceding the voluntary movements while the Ach system modulates the amplitude of the α-MNs output to the muscle fibers.

Despite the mentioned conclusions from the cited functional studies, the puzzle involving the modulation capacities of C-boutons remains understudied and far from being fully understood (Frank 2009). α-MNs outnumber V_0 interneurones in a 10:1 ratio and individual V_0 cells are hypothesized to form around 1000 contacts to a diverse population of α-MNs what gives to that neurones the capacity to modulate the movement affecting a large sources of muscle fibers with their actions. This ratio also increases in the lumbar region where the number of synapses made by V_0 neurones is even larger (Zagoraiou et al. 2009).

3.8 Involvement of C-terminals in motor functions

There are only a few studies that have focused on the function of C-terminals up to date. The most important was done by Zagaraiou and colleagues who generated a new model of transgenic mice able to disrupt the expression of Ach in the Pitx2 V_0 interneurones following previously reported methods of Cre-mediated deletion of coding exons of the mouse ChAT (Buffelli et al. 2003). The newly generated Dbx1::Cre; $ChAT^{fl/fl}$ mice, according to the authors, achieved a

disrupted VAchT function in approximately 55% of the total spinal C-boutons. The elimination of ChAT in C-boutons did not alter the shape and the total number of C-boutons contacting α-MNs. Furthermore, the characteristics described postsynaptic features of the C-terminal synapses were preserved in these animals.

The Dbx1::Cre; $ChAT^{fl/fl}$ mice were normally developed and survived without differences to the WT mice in the adulthood (Zagoraiou et al. 2009). Regarding motor behaviour, these transgenic animals lacking functional C-terminals did not show any alteration when walking and during basic locomotor activities. However, during activities that require further activation, such as swimming, the peak motor neurone burst capacity was significantly diminished when compared to their WT litter mates, altering their motor behaviour exhibited. The output modulation response of the cholinergic C-terminals is thought to appear and evolve after sustained periods of motoneuron excitability that cause the release of Ca^{2+} and the subsequent clustering of $K_{v2.1}$ potassium channels (Deardorff et al. 2014a).

3.9 Implications of C-terminals in MN pathology

Although relationships between C- boutons and ALS or more extensively MND/ injury still remain unclear, recent findings suggest their background role in a basic pathological feature like excitotoxicity during the degeneration of MNs. The existent link between massive releases of Ca^{2+} in neurones and the omnipresent excitoxicity leading to neurodegeneration has been vastly described in ALS and other MNDs. Nevertheless, it is well known that all the SSC underlying post-synaptically the C-terminals act as intracellular sources of stored Ca^{2+} in MNs (M J Berridge 1998). A more recent study suggests that storage and release of Ca^{2+} from SSC may be controlled by C-terminals via the activation of specific receptors (Mavlyutov et al. 2012).

On the other hand, In 1983, Pullen and Sears performed double hemi-section experiments with cat spinal cords. From these studies, the authors confirmed an increase of the overall number of C-terminals input to α-MNs and of their respective presynaptic territory only in these animals showing an efficient process of motor behaviour recovery. This crucial finding supports the increasing interest demonstrated through the study of these terminals as potential actors implicated in the recovery of MNs after damage, with direct implications in the subsequent exhibited motor behaviours. Furthermore, recent studies performed in rodents after motor neurone force injuries have confirmed that recovery of these cells in these animals is done in a close-up relationship with the recovery shown by the C-terminals (Skup et al. 2012). While this has been confirmed as fact, after initial MN contusion (Kitzman 2006) injury, the total number of C-terminals in the spinal cord significantly decreases.

3.10 Neuregulin-1 and Ach terminals synapse to α-MNs: implications in MND

Neuregulin-1 (NRG-1) is a trophic factor from the epidermal growth factor family (EGF). Its level deregulations have been related with schizophrenia and other major disorders (Banerjee et al. 2010). The discovery of NRG-1 in MNs, was found in the NMJ area along with MNs axons. This protein is implicated in the proper establishment of the NMJ and in the maintenance of the myelin sheath along the axons projecting to the muscles from the spinal cord. This is especially so as NRG-1 is synthesized by MNs and acts as a trophic factor for Schwann cells (Shin et al. 2014). A recent study has shown that impaired nerve transmission in Charcot-Marie-Tooth disease can be restored by early expression of NRG-1 as this protein recovers the damage in Schwann cells (Fledrich et al. 2014).

A study published in 2010 indicated that NRG-1 in motor neurones is not only associated to the maintenance of axon myelin and proper neuromuscular transmission (Issa et al. 2010) though it is also located presynaptically in the Ach terminals synapse to phrenic MNs at ventral horn. Accordingly, this was the first study demonstrating the presence of NRG-1 at the level of motor neurone synapses within the mammal´s spinal cord.

Any implication of NRG-1 in MND are still yet to be clarified through further studies. However, a recent study has shown the effect of the ERBB4 mutant receptors in FALS patients. ERBB4 is a member of the EGF family of receptors tyrosine kinases, which forms a homodimer or heterodimer with ERBB2 or ERBB3 when the extracellular ERBB4 ligand domain is stimulated by NRG-1 (Plowman et al. 1993). Stimulation by NRG-1 of the ERBB4 ligand domain produces the phosphorylation of the ERBB4 protein C-terminal (Carpenter 2003). In the FALS subjects presenting mutations for the ERBB4 receptor; the phosphorylation process described in presence of the ligand NRG-1 has been revealed as compromised. This mechanism has been directly implicated by the authors as responsible for the onset of ALS in these patients (Takahashi et al. 2013).

We have considered that all the aforestated evidence from the systems biology approach indicated a crucial role of the C-terminals in MND pathology. Therefore, in a chapter of this thesis, we have further elucidated and characterized some of the changes that have occurred in these terminals during disease progression of two MND murine models.

4. Extracellular vesicles in ALS

4.1 Extracellular vesicles (EVs) and the description of a recently known molecular and cellular communication system

Extracellular vesicles (EVs) are tiny vesicles shed out by cells from different tissues during healthy and diseased conditions that act as containers of proteins, mRNAs and other unknown and unmapped molecules. The field of extracellular vesicles is still incipient, although it is believed that the cargoes carried out by these features change under pathogenic conditions of the organism, such as those caused by cancer and neurodegeneration among others.

EVs have been experimentally identified in several body fluids such as in tears, semen, mucus, blood, lymph, ascites, breast milk, saliva, cerebrospinal fluid, etc. A myriad of shapes and sizes can be identified when one attempts to study EVs. These often range in shape and size: from rounded to elongated and other asymmetric forms and from huge (1000-2000 nm) to minuscule (≈ 50 nm). Diverse nomenclatures have been released from time to time to refer to EVs. They were initially identified in cell culture media and referred as exosomes.

Initial exosomes ranged from 40 to 1000 nm. Currently, that nomenclature is exclusively reserved for EVs released from cell endosome multivesicular bodies (MVE), a subpopulation of EVs that range in diameter from 40 to 100nm. Other identified EVs are generally referred to as microvesicles and these range from 100 to >1000nm. in diameter. Despite the described characteristics of EVs, none of the current available isolation methods can discriminate between exosomes and microvesicles nor demonstrate that the origin of the identified features.

These intercellular communication mechanisms were first identified in the CNS. Through synapses, neurones communicate between them at the molecular level. The molecules released are received by the neighboring cells and influence their function and electrical responses. It has also been demonstrated that the cell affects its own behaviour by the release and subsequent reception of its own vesicles in the autocrine chemical communication. Chemical communication also takes place between cells located at long distances across tissues such as in the paracrine communication of the endocrine system. Also molecules released in various kinds of chemical communication methods are not always in free-form. The release of molecules in vesicles instead being in free-form avoids degradation and facilitates the interaction between cargo released from the messenger cell and the receptors of recipient cell through signalling membrane proteins allocated in the vesicle membranes. This mechanism has been clearly demonstrated in viruses, as these pathogens significantly enhance their diffusion efficiency which are allocated in EVs compared to simple diffusion (Silverman and Reiner 2011).

EVs are generated and released by neurones and glial cells (Guescini et al. 2010; Lachenal et al. 2011; Potolicchio et al. 2005). These can regulate important factors of the CNS such as the formation of new synapses (Lachenal et al. 2011). The study of brain EVs from human subjects is still complex, due to

the lack of proper isolation methods. Thus far, these features have been mainly studied in neuronal cultured cells (Candelario and Steindler 2014). The analysis of EVs isolated from cellular models of neurodegenerative diseases including PD and ALS have revealed the presence of proteins prone to proteinopathy and toxicity in those diseases. Together with other molecules such as mRNAs and miRNAs, these could be involved in the spread of these neurodegenerative conditions (Nonaka et al. 2013; Emmanouilidou et al. 2010).

4.2 Isolation of EVs for experimental and therapeutic purposes

The ratio of EVs to other molecules and contaminants present in body fluids is extremely low. This makes it impractical to conduct a direct study of these significant biological agents. Before this study, the implementation of any isolation method becomes essential (Théry et al. 2006). Isolation methods of EVs often include ultracentrifugation and buoyancy gradients made by sucrose or other dense buffers (Raposo and Stoorvoael 2013). Immuno-adsorption is in some cases, an alternative when the population of EVs is expected to contain the pull-down protein of interest or even newly marketed chemical products used to isolate EVs (Raposo and Stoorvogel 2013). Besides these ultracentrifugation and immunoadsorption methods, the resultant EVs isolated by other methods have not been properly characterized (Raposo and Stoorvogel 2013). Characterization of EV-enriched fractions require the use of mass spectrometry to identify the type of molecules and proteins found in the isolated EVs. This also requires immunoblotting confirmation of the exosome markers and use of imaging techniques. If possible, cryo-electron microscopy should be used to clearly identify shapes and diameters of these vesicles.

The use of ultracentrifuge-based techniques to isolate EVs is the preferred choice, as those methods isolate a heterogeneous population of EVs. These methods can be used to discover the whole EV signature in one specific biological condition. Even so, the implementation of ultracentrifugation methods requires large amounts of sample, and involve complex and long protocols. Moreover, the fractions of EVs isolated by ultracentrifugation often contain large amounts of unwanted plasma molecules, aggregates and other contaminants. The molecular signature that has to be found in an isolated fraction of EVs includes endosome markers as tetraspanins (CD9,63,81 etc.), the protein Alix and annexins among other molecules (van Niel et al. 2006). Some specialized databases including Exocarta (www.exocarta.org) and the more extended Vesiclepedia consortium include all the published molecules associated with EVs.

4.3 Molecules in isolated EVs from ALS models and patients, the hypothesis of toxic SOD1 and NRG-1

It has been demonstrated that toxic SOD1 has an important extracellular role in ALS affected spinal cords and motor cortex that can be successfully targeted by immunotherapy. ALS toxicity *in vivo* may even be abolished (Urushitani, Ezzi, and Julien 2007). As we have clearly explained in the preceding paragraphs, recent ALS studies, as hypothesized in other neurodegenerative diseases, have indicated that SOD1 and other ALS-associated molecules as well as some endogenous therapeutic molecules might be released by neurones and glial cells inside EVs before and during ALS progression.

Beyond that, SOD1 and neuregulin NRG-1 have been associated with MND, as we have already mentioned in the precedent chapter. This last mentioned

molecule It triggers microglia activation when it is hypothetically released from neurones and astrocytes (Song et al. 2012). This thesis attempts to best clarify the varying roles of the NRG-1 molecule. These include ascertaining whether NRG-1 triggers motoneuron degeneration in ALS or if this molecule could have a protective role. The study from where in the MNs NRG-1 is secreted, as well as if it is released in EVs or in free-form delivery.

5. ALS mutant SOD1 animal models: from the wobbler mouse to the invertebrates

5.1 The first MND model: the Wobbler mouse

The Wobbler mouse was created in Edinburgh (Scotland, UK..), being the first animal model that allowed scientists to study the onset and progression of MND, although this mouse was not generated for that purpose (Duchen and Strich 1968). This mouse shows a recessive mutation of the protein VPS54 at the Golgi-associated retrograde protein (GARP). A general deterioration of motor neurones is followed by impaired motor behaviour during the first three months in those mice (Duchen and Strich 1968). The phenotype progression slows down from that age bringing the mean survival age to about one year. These mice did not present any specific MND, despite the mysterious degeneration of motor neurones. Additionally, they showed huge variation across individuals at the phenotype levels. This makes them impractical for an accurate study of MND after the apparition of better mammal models (Rathke-Hartlieb et al. 1999).

5.2 Other unspecific models showing degeneration of MNs

The neuromuscular degeneration mouse model (NMD) was discovered in 1995 after the realization that some mice presented a mutation in chromosome 19. These animals showed a partial loss of motor neurones during the initial stages of development that led to neuromuscular degeneration (Cook et al. 1995). Also, they rarely survive beyond four weeks after birth.

Another non-specific mouse that indicates motor neurone affectation is the progressive motor neuropathy mice (PMN). These animals developed degeneration of the motor axons, while the neuron bodies remained intact and unaffected (Schmalbruch et al. 1991) and did not survive beyond seven weeks of postnatal stage.

The treatment of male mice with 250 mg/kg N-ethyl-N-nitrosourea and posterior crossing with females of the Harwell stock PTP generated in the next generation offsprings with serious affectation of the motor system. The mutant inheritance was passed on to the next generation in a dominant manner and the mice line was named Loa mice. These animals were initially proposed as a good model of ALS, as they presented inclusions in the motor neurones that resembled Lewy bodies, containing the protein SOD1, neurofilament proteins and ubiquitin (Van Den Bosch 2011). The major affectation of motor neurones in Loa mice was at the axon as the amutation affected mostly the protein dynein, which supported the hypothesis of the dying-back degeneration of MNs in ALS. Further research misestimated the use of Loa mice for ALS research, as these animals showed a non-selective loss of MNs without any preference for α-MNs, as originally manifested in the ALS pathology. In addition, these animals showed affectation in the sensory neurones at the spinal cord (Ilieva et al. 2008).

All of these aforementioned unspecific MND mammal models were never considered good experimental models for ALS. However, these studies have contributed to our understandding about the elusive mechanisms of ALS. These demonstrate the inconvenience as well as challenges faced with the lack of an appropriate model in broadening our cognizance and in the development of treatment for this disease.

5.3 Apparition of initial FALS rodent models

In 1993, the discovery of missense mutations in chromosome 21 encoding SOD1 and their implications in ALS provided a new avenue for ALS research (Rosen et al. 1993). The apparition of FALS rodent models, created from over-expressors of mutant SOD1, was revealed as the first ALS experimental model able to resemble "*in vivo*" the progression of the disease in patients. Posterior hind limbs in these animals suffered from initial weakness which progressed to the paralysis of the posterior limbs. These animals eventually die by respiratory failure (Van Den Bosch 2011).

The first SOD1 mutation introduced in a line of transgenic mice was the G93A. This was introduced one year after the discovery of the implications of SOD1 mutation in ALS (Gurney et al. 1994). The apparition of G93A was later followed by the creation of the G85R, D90 and G73R mice models (Van Den Bosch 2011).

Over-expression of SOD1 mutations to create ALS models allowed also the creation of ALS experimental models in Sprague-Dawley rats (Howland et al. 2002) (Figure 4). The apparition of SOD1 G93A rats allowed the study of ALS in animals bigger than mice. Nonetheless, these still present some disadvantages when compared with mice transgenic models as the phenotype in some cases

takes longer time periods to evolve into final stages of disease. These models also show high inter-subject variability (Matsumoto et al. 2006). It is finally remarkable that these animals were extensively used for more than a decade and are still in use in ALS research.

Figure 4: Transgenic rat with the over expression of human SOD1G93A used as a FALS experimental model. The ALS characteristic of the loss of muscular mass in the posterior limbs is recapitulated by these animals at their terminal stage as seen in this picture. [Adapted from Esquerda et al. Mente y cerebro].

5.4 The SOD1 G93A transgenic rodents

The SOD1 G93A are the most used rodent models worldwide for the scientific community in ALS research since their apparition. The first SOD1 G93A mice model generated expressed approximately 20-24 copies of the human coding sequence controlled by a SOD1 promoter (Gurney et al. 1994). Current models also usually use this promoter. However, mice under neuronal-specific and/or

astrocyte-specific promoters have additionally been generated. Rodent animals over-expressing human WT SOD1 are used as controls in the experiments using the G93A mice (McGoldrick et al. 2013).

The multifocal characteristic of neurodegeneration in ALS has been uniquely revealed as a result of the cellular and molecular phenotype shown by the mutant SOD1 G93A mice. Accordingly, these animals show mitochondrial vacuolation, cytoplasmatic aggregates, protein abnormal folding, axonal transport deficits, excitotoxicity and cellular harmful effects by accumulated ROS among other less studied signs of neurodegeneration (Figure 5).

5.5 Use of other vertebrates as mutant SOD1 models: zebrafish

The first zebrafish model over-expressing human G93A was created using mRNA microinjection into the 2-4 blastulae stages. These embryos were studied and created to express ubiquitously the mutant SOD1 to show profound axonopathies in motor neurones. These were considered a promising model to discover the neuron specific affectation in ALS, furthermore, the authors depicted that the up-regulation of vascular endothelial growth factor (VEGF) was able to rescue the axonopathy in those ALS embryos model (Lemmens et al. 2007). Further experiments with adult zebrafish as over-expressors of mutant SOD1 revealed the classical pattern of affectation seen in mammals. This includes neuromuscular junction degeneration, spinal motoneuron loss, partial paralysis, premature death and impaired motor behaviour (difficulty when swimming) (Ramesh et al. 2014). All these mentioned clinical features of the SOD1G93A zebrafish model recapitulate all the disease hallmarks previously seen in mammals. This concludes that the ALS clinical manifestations in the

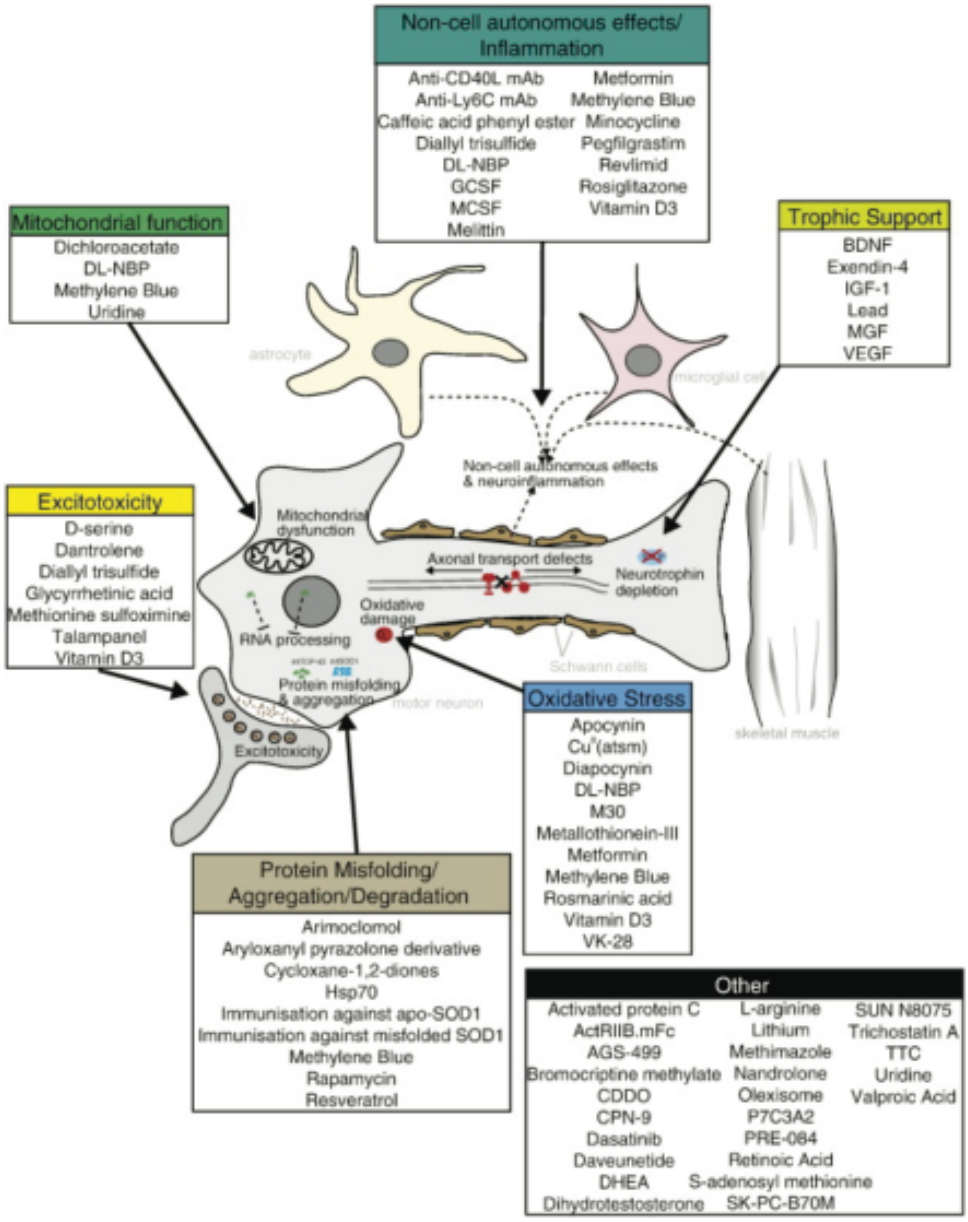

Figure 5. Pathogenic mechanisms of motoneuron degeneration studied in the mutant mice expressing human SOD1 G93A. [Adapted from (McGoldrick et al. 2013)].

motor system are common to all vertebrate organisms.

5.6 Invertebrate ALS transgenic models: the case of SOD1

Caenorhabditis elegans

The use of invertebrate transgenic models (*Drosophila melanogaster* and *C. Elegans*) in ALS research generates high advantages in conjunction with the use of vertebrates. Invertebrate organisms are more cost-effective to maintain. They live for shorter periods and also demonstrate disease signs earlier. They offer a limited genetics background for ease in scientific manipulation and finally, a large amount of transgenic animals that can be easily tested in each experimental condition (Johnson 2014). Despite all the mentioned advantages, the use of invertebrate models present important drawbacks for manipulation as their small size and evolutionary processes. These animals are far from humans making it difficult to find the genetic homologues in humans for some of their genes (Johnson 2014). Still, the use of invertebrate models in ALS research is considered as the use of an *in vivo* model that is halfway between the *in vitro* transgenic models and the mammal transgenic models of the disease.

Diverse ALS models expressing SOD1 under different promoters have been created using *C. Elegans* with the mutations A4V, G73R and G93A under the promoter hsp16-2 which allows the expression of SOD1 in almost all the body tissues of this nematode. The first model was created using the mentioned promoter by Oeda et al. in 2001 and the authors found that the expression of mutant SOD1 in the animal neurones created aggregates that resembled the neuropathologic features in mammals (Oeda et al. 2001). Nonetheless, the expression of mutant G93A SOD1 in the muscle fibers with the specific promoter

unc-54 did not cause substantial affectations at the cellular and motor levels in these animals (Gidalevitz et al. 2009).

5.7 The use of *Drosophila melanogaster* models in ALS: The SOD1 transgenic models

As we have extensively mentioned in the introduction of this thesis, the study of mutant SOD1 permitted the creation of the first experimental FALS model. From then, a huge number of experiments have been performed using the G93A mutation to disclose molecular and motor affectation and eventually, the therapeutic treatments in ALS. The use of murine models impedes a wide and transversal screening of active available compounds that might be useful for the treatment of ALS. This is because a huge number of animals would be required for that purpose and a long period of time would also be needed before to obtain any result. The apparition of *Drosophila* models represented a leap forward in drug screening research, as these could compensate the mentioned deficits found in mice models. *Drosophila* are extremely responsive to drug treatments and have been described as highly 'druggable' based on responses to other neurodegenerative diseases as AD and PD when the compounds are mixed in their vial media (Newman et al. 2011). These animals are able to recapitulate some molecular features of ALS in only few weeks when they reach ageing stages (Watson et al. 2008).

The SOD1 A4V and the G85R mutations have been characterized in a *Drosophila* model of ALS by Watson et al in 2008. The authors found that after the expression of SOD1 in motor neurones using the D42 promoter the animals showed substantial motor climbing defects (Watson et al. 2008). Most recently, a *Drosophila* model expressing the transgenic G41S allele of SOD1 was

generated. The mentioned mutation in the enzyme produces the loss of its zinc-binding residue and the flies expressing this mutation showed mitochondrial affectation, shortened lifespan and motor defects (Bahadorani et al. 2013).

It has been proposed that the expression of A4V and G85R mutations do not produce evident mitochondrial defects in the flies because of their short life-span (Bahadorani et al. 2013). Even though the G93A is the most studied mutation in ALS mammal models currently, nothing is known about its impact in a *Drosophila* model and the mitochondrial integrity. With reference to this, we have generated a new human SOD1 (hSOD1) G93A *Drosophila* line and a human (hWT) SOD1 line to characterize any affectation of the mutation on motor activity and mitochondrial morphology. As such, we also developed a fly model of ALS to further perform drug screening using available natural and synthetic compounds able to ameliorate any observed disease phenotype.

6. References

Abel, Olubunmi, John F Powell, Peter M Andersen, and Ammar Al-Chalabi. 2012. “ALSoD: A User-Friendly Online Bioinformatics Tool for Amyotrophic Lateral Sclerosis Genetics.” Human Mutation 33 (9): 1345–51. doi:10.1002/humu.22157. http://www.ncbi.nlm.nih.gov/pubmed/22753137.

Adams, Julian. 2003. “The Proteasome: Structure, Function, and Role in the Cell.” Cancer Treatment Reviews 29 Suppl 1 (May): 3–9. http://www.ncbi.nlm.nih.gov/pubmed/12738238.

Al-Chalabi, Ammar, and Orla Hardiman. 2013. “The Epidemiology of ALS: A Conspiracy of Genes, Environment and Time.” Nature Reviews. Neurology 9 (11). Nature Publishing Group: 617–28. doi:10.1038/nrneurol.2013.203. http://www.nature.com.ezlibproxy1.ntu.edu.sg/nrneurol/journal/v9/n11/full/nrneurol.2013.203.html.

Alonso, Alvaro, Giancarlo Logroscino, Susan S Jick, and Miguel A Hernán. 2010. “Association of Smoking with Amyotrophic Lateral Sclerosis Risk and Survival in Men and Women: A Prospective Study.” BMC Neurology 10 (January): 6. doi:10.1186/1471-2377-10-6. http://www.pubmedcentral.nih.gov/articlerender.fcgi?artid=2820482&tool=pmcentrez&rendertype=abstract.

Appel, S H, W Zhao, D R Beers, and J S Henkel. 2011. “The Microglial-Motoneuron Dialogue in ALS.” Acta Myologica: Myopathies and Cardiomyopathies: Official Journal of the Mediterranean Society of Myology / Edited by the Gaetano Conte Academy for the Study of Striated

Muscle Diseases 30 (1): 4–8. http://www.pubmedcentral.nih.gov/articlerender.fcgi?artid=3185827&tool=pmcentrez&rendertype=abstract.

Arvidsson, U, M Riedl, R Elde, and B Meister. 1997. “Vesicular Acetylcholine Transporter (VAChT) Protein: A Novel and Unique Marker for Cholinergic Neurones in the Central and Peripheral Nervous Systems.” The Journal of Comparative Neurology 378 (4): 454–67. http://www.ncbi.nlm.nih.gov/pubmed/9034903.

Atkin, Julie D, Manal A Farg, Adam K Walker, Catriona McLean, Doris Tomas, and Malcolm K Horne. 2008. “Endoplasmic Reticulum Stress and Induction of the Unfolded Protein Response in Human Sporadic Amyotrophic Lateral Sclerosis.” Neurobiology of Disease 30 (3): 400–407. doi:10.1016/j.nbd.2008.02.009. http://www.ncbi.nlm.nih.gov/pubmed/18440237.

Ayach, Lucie, Christophe Curti, Marc Montana, Pascale Pisano, and Patrice Vanelle. 2014. “[Amyotrophic Lateral Sclerosis: Update on Etiological Treatment].” Thérapie 68 (2): 93–106. doi:10.2515/therapie/2013012. http://www.ncbi.nlm.nih.gov/pubmed/23773350.

Ayala, Gabriela X, and Ricardo Tapia. 2003. “Expression of Heat Shock Protein 70 Induced by 4-Aminopyridine through Glutamate-Mediated Excitotoxic Stress in Rat Hippocampus in Vivo.” Neuropharmacology 45 (5): 649–60. http://www.ncbi.nlm.nih.gov/pubmed/12941378.

Bahadorani, Sepehr, Spencer T Mukai, Jason Rabie, Joseph S Beckman, John P Phillips, and Arthur J Hilliker. 2013. “Expression of Zinc-Deficient Human Superoxide Dismutase in Drosophila Neurones Produces a Locomotor Defect Linked to Mitochondrial Dysfunction.” Neurobiology of Aging 34 (10). NIH Public Access: 2322–30. doi:10.1016/j.neurobiolaging.2013.03.024. http://europepmc.org/articles/PMC4145400/?report=abstract.

Banack, Sandra Anne, and Paul Alan Cox. 2003. “Biomagnification of Cycad Neurotoxins in Flying Foxes: Implications for ALS-PDC in Guam.” Neurology 61 (3): 387–89. http://www.ncbi.nlm.nih.gov/pubmed/12913204.

Banci, Lucia, Ivano Bertini, Mirela Boca, Stefania Girotto, Manuele Martinelli, Joan Selverstone Valentine, and Miguela Vieru. 2008. “SOD1 and Amyotrophic Lateral Sclerosis: Mutations and Oligomerization.” Edited by Sotirios Koutsopoulos. PloS One 3 (2). Public Library of Science: e1677. doi:10.1371/journal.pone.0001677. http://dx.plos.org/10.1371/journal.pone.0001677.

Banerjee, Anamika, Mathew L Macdonald, Karin E Borgmann-Winter, and Chang-Gyu Hahn. 2010. “Neuregulin 1-erbB4 Pathway in Schizophrenia: From Genes to an Interactome.” Brain Research Bulletin 83 (3-4): 132–39. doi:10.1016/j.brainresbull.2010.04.011. http://www.ncbi.nlm.nih.gov/pubmed/20433909.

Basso, Manuela, Tania Massignan, Giuseppina Samengo, Cristina Cheroni, Silvia De Biasi, Mario Salmona, Caterina Bendotti, and Valentina Bonetto. 2006. “Insoluble Mutant SOD1 Is Partly Oligoubiquitinated in Amyotrophic Lateral Sclerosis Mice.” The Journal of Biological Chemistry 281 (44): 33325–35. doi:10.1074/jbc.M603489200. http://www.ncbi.nlm.nih.gov/pubmed/16943203.

Baughman, Joshua M, Fabiana Perocchi, Hany S Girgis, Molly Plovanich, Casey A Belcher-Timme, Yasemin Sancak, X Robert Bao, et al. 2011. “Integrative Genomics Identifies MCU as an Essential Component of the Mitochondrial Calcium Uniporter.” Nature 476 (7360): 341–45. doi:10.1038/nature10234. http://www.scopus.com/inward/record.url?eid=2-s2.0-80051946060&partnerID=tZOtx3y1.

Berridge, M J. 1998. “Neuronal Calcium Signaling.” Neuron 21 (1): 13–26. http://www.ncbi.nlm.nih.gov/pubmed/9697848.

Berridge, Michael J. 2014. “The Endoplasmic Reticulum: A Multifunctional Signaling Organelle.” Cell Calcium 32 (5-6): 235–49. Accessed September 26. http://www.ncbi.nlm.nih.gov/pubmed/12543086.

Blackstone, Craig. 2012. “Cellular Pathways of Hereditary Spastic Paraplegia.” Annual Review of Neuroscience 35 (January): 25–47. doi:10.1146/annurev-neuro-062111-150400. http://www.ncbi.nlm.nih.gov/pubmed/22540978.

Bodian, D. 1975. “Origin of Specific Synaptic Types in the Motoneuron Neuropil of the Monkey.” The Journal of Comparative Neurology 159 (2): 225–43. doi:10.1002/cne.901590205. http://www.ncbi.nlm.nih.gov/pubmed/1112912.

Boillée, Séverine, Koji Yamanaka, Christian S Lobsiger, Neal G Copeland, Nancy A Jenkins, George Kassiotis, George Kollias, and Don W Cleveland. 2006. “Onset and Progression in Inherited ALS Determined by Motor Neurones and Microglia.” Science (New York, N.Y.) 312 (5778): 1389–92. doi: 10.1126/science.1123511. http://www.ncbi.nlm.nih.gov/pubmed/16741123.

Broom, W J, D V Johnson, K E Auwarter, A J Iafrate, C Russ, A Al-Chalabi, P C Sapp, D McKenna-Yasek, P M Andersen, and R H Brown. 2008. “SOD1A4V-Mediated ALS: Absence of a Closely Linked Modifier Gene and Origination in Asia.” Neuroscience Letters 430 (3): 241–45. doi:10.1016/j.neulet.2007.11.004. http://www.ncbi.nlm.nih.gov/pubmed/18055113.

Broom, Wendy J, Daniel V Johnson, Manuel Garber, Peter M Andersen, Niall Lennon, John Landers, Chad Nusbaum, Carsten Russ, and Robert H Brown. 2009. “DNA Sequence Analysis of the Conserved Region around the SOD1 Gene Locus in Recessively Inherited ALS.” Neuroscience Letters 463 (1): 64–69. doi:10.1016/j.neulet.2009.07.010. http://www.ncbi.nlm.nih.gov/pubmed/19596401.

Brownstone, Robert M. 2006. “Beginning at the End: Repetitive Firing Properties in the Final Common Pathway.” Progress in Neurobiology 78 (3-5): 156–72.

doi:10.1016/j.pneurobio.2006.04.002. http://www.sciencedirect.com/science/article/pii/S0301008206000347.

Bruijn, L I, M W Becher, M K Lee, K L Anderson, N A Jenkins, N G Copeland, S S Sisodia, et al. 1997. "ALS-Linked SOD1 Mutant G85R Mediates Damage to Astrocytes and Promotes Rapidly Progressive Disease with SOD1-Containing Inclusions." Neuron 18 (2): 327–38. http://www.ncbi.nlm.nih.gov/pubmed/9052802.

Buffelli, Mario, Robert W Burgess, Guoping Feng, Corrinne G Lobe, Jeff W Lichtman, and Joshua R Sanes. 2003. "Genetic Evidence That Relative Synaptic Efficacy Biases the Outcome of Synaptic Competition." Nature 424 (6947): 430–34. doi:10.1038/nature01844. http://www.ncbi.nlm.nih.gov/pubmed/12879071.

Candelario, Kate M, and Dennis A Steindler. 2014. "The Role of Extracellular Vesicles in the Progression of Neurodegenerative Disease and Cancer." Trends in Molecular Medicine 20 (7): 368–74. doi:10.1016/j.molmed.2014.04.003. http://www.sciencedirect.com/science/article/pii/S1471491414000641.

Carpenter, Graham. 2003. "ErbB-4: Mechanism of Action and Biology." Experimental Cell Research 284 (1): 66–77. http://www.ncbi.nlm.nih.gov/pubmed/12648466.

Chiò, Adriano, Gianmartino Benzi, Maurizia Dossena, Roberto Mutani, and Gabriele Mora. 2005. "Severely Increased Risk of Amyotrophic Lateral Sclerosis among Italian Professional Football Players." Brain: A Journal of Neurology 128 (Pt 3): 472–76. doi:10.1093/brain/awh373. http://www.ncbi.nlm.nih.gov/pubmed/15634730.

Chiò, Adriano, Andrea Calvo, Letizia Mazzini, Roberto Cantello, Gabriele Mora, Cristina Moglia, Lucia Corrado, et al. 2012. "Extensive Genetics of ALS: A Population-Based Study in Italy." Neurology 79 (19): 1983–89. doi:10.1212/

WNL.0b013e3182735d36. http://www.pubmedcentral.nih.gov/articlerender.fcgi?artid=3484987&tool=pmcentrez&rendertype=abstract.

Clement, A M, M D Nguyen, E A Roberts, M L Garcia, S Boillée, M Rule, A P McMahon, et al. 2003. "Wild-Type Nonneuronal Cells Extend Survival of SOD1 Mutant Motor Neurones in ALS Mice." Science (New York, N.Y.) 302 (5642): 113–17. doi:10.1126/science.1086071. http://www.ncbi.nlm.nih.gov/pubmed/14526083.

Conradi, S. 1969a. "Ultrastructure and Distribution of Neuronal and Glial Elements on the Motoneuron Surface in the Lumbosacral Spinal Cord of the Adult Cat." Acta Physiologica Scandinavica. Supplementum 332 (January): 5–48. http://www.ncbi.nlm.nih.gov/pubmed/4195458.

———. 1969b. "Ultrastructure of Dorsal Root Boutons on Lumbosacral Motoneurones of the Adult Cat, as Revealed by Dorsal Root Section." Acta Physiologica Scandinavica. Supplementum 332 (January): 85–115. http://www.ncbi.nlm.nih.gov/pubmed/5386537.

Conradi, S, and S Skoglund. 1969. "Observations on the Ultrastruture and Distribution of Neuronal and Glial Elements on the Motoneuron Surface in the Lumbosacral Spinal Cord of the Cat during Postnatal Development." Acta Physiologica Scandinavica. Supplementum 333 (January): 5–52. http://www.ncbi.nlm.nih.gov/pubmed/5386538.

Cook, S A, K R Johnson, R T Bronson, and M T Davisson. 1995. "Neuromuscular Degeneration (nmd): A Mutation on Mouse Chromosome 19 That Causes Motor Neuron Degeneration." Mammalian Genome: Official Journal of the International Mammalian Genome Society 6 (3): 187–91. http://www.ncbi.nlm.nih.gov/pubmed/7749225.

Copeland, William C. 2014. "Defects in Mitochondrial DNA Replication and Human Disease." Critical Reviews in Biochemistry and Molecular Biology 47 (1): 64–74. doi:10.3109/10409238.2011.632763. http://

www.pubmedcentral.nih.gov/articlerender.fcgi?artid=3244805&tool=pmcentrez&rendertype=abstract.

Cox, Paul Alan, Sandra Anne Banack, and Susan J Murch. 2003. "Biomagnification of Cyanobacterial Neurotoxins and Neurodegenerative Disease among the Chamorro People of Guam." Proceedings of the National Academy of Sciences of the United States of America 100 (23): 13380–83. doi:10.1073/pnas.2235808100. http://www.pubmedcentral.nih.gov/articlerender.fcgi?artid=263822&tool=pmcentrez&rendertype=abstract.

Cullinan, Sara B, and J Alan Diehl. 2004. "PERK-Dependent Activation of Nrf2 Contributes to Redox Homeostasis and Cell Survival Following Endoplasmic Reticulum Stress." The Journal of Biological Chemistry 279 (19): 20108–17. doi:10.1074/jbc.M314219200. http://www.scopus.com/inward/record.url?eid=2-s2.0-2442542312&partnerID=tZOtx3y1.

Damiano, Maria, Anatoly A Starkov, Susanne Petri, Kathuna Kipiani, Mahmoud Kiaei, Marina Mattiazzi, M Flint Beal, and Giovanni Manfredi. 2006. "Neural Mitochondrial Ca2+ Capacity Impairment Precedes the Onset of Motor Symptoms in G93A Cu/Zn-Superoxide Dismutase Mutant Mice." Journal of Neurochemistry 96 (5): 1349–61. doi:10.1111/j.1471-4159.2006.03619.x. http://www.scopus.com/inward/record.url?eid=2-s2.0-33645102302&partnerID=tZOtx3y1.

Deardorff, Adam S, Shannon H Romer, Patrick M Sonner, and Robert E W Fyffe. 2014a. "Swimming against the Tide: Investigations of the C-Bouton Synapse." Frontiers in Neural Circuits 8 (January): 106. doi:10.3389/fncir.2014.00106. http://www.pubmedcentral.nih.gov/articlerender.fcgi?artid=4167003&tool=pmcentrez&rendertype=abstract.

———. 2014b. "Swimming against the Tide: Investigations of the C-Bouton Synapse." Frontiers in Neural Circuits 8 (January). Frontiers: 106. doi:

10.3389/fncir.2014.00106. http://journal.frontiersin.org/Journal/10.3389/fncir.2014.00106/abstract.

Dion, Patrick A, Hussein Daoud, and Guy A Rouleau. 2009. “Genetics of Motor Neuron Disorders: New Insights into Pathogenic Mechanisms.” Nature Reviews. Genetics 10 (11). Nature Publishing Group: 769–82. doi:10.1038/nrg2680. http://dx.doi.org/10.1038/nrg2680.

Duchen, L. W., and S. J. Strich. 1968. “An Hereditary Motor Neurone Disease with Progressive Denervation of Muscle in the Mouse: The Mutant ‘Wobbler’.” Journal of Neurology Neurosurgery and Psychiatry 31 (6): 535–42. http://www.scopus.com/inward/record.url?eid=2-s2.0-0014368955&partnerID=tZOtx3y1.

Dum, R P, and P L Strick. 1991. “The Origin of Corticospinal Projections from the Premotor Areas in the Frontal Lobe.” The Journal of Neuroscience: The Official Journal of the Society for Neuroscience 11 (3): 667–89. http://www.ncbi.nlm.nih.gov/pubmed/1705965.

Eisen, Andrew. 2009. “Amyotrophic Lateral Sclerosis-Evolutionary and Other Perspectives.” Muscle & Nerve 40 (2): 297–304. doi:10.1002/mus.21404. http://www.ncbi.nlm.nih.gov/pubmed/19609920.

Emmanouilidou, Evangelia, Katerina Melachroinou, Theodoros Roumeliotis, Spiros D Garbis, Maria Ntzouni, Lukas H Margaritis, Leonidas Stefanis, and Kostas Vekrellis. 2010. “Cell-Produced Alpha-Synuclein Is Secreted in a Calcium-Dependent Manner by Exosomes and Impacts Neuronal Survival.” The Journal of Neuroscience: The Official Journal of the Society for Neuroscience 30 (20): 6838–51. doi:10.1523/JNEUROSCI.5699-09.2010. http://www.pubmedcentral.nih.gov/articlerender.fcgi?artid=3842464&tool=pmcentrez&rendertype=abstract.

Ferri, Alberto, Paolo Fiorenzo, Monica Nencini, Mauro Cozzolino, Maria Grazia Pesaresi, Cristiana Valle, Sara Sepe, Sandra Moreno, and Maria Teresa

Carrì. 2010. “Glutaredoxin 2 Prevents Aggregation of Mutant SOD1 in Mitochondria and Abolishes Its Toxicity.” Human Molecular Genetics 19 (22): 4529–42. doi:10.1093/hmg/ddq383. http://www.pubmedcentral.nih.gov/articlerender.fcgi?artid=3298854&tool=pmcentrez&rendertype=abstract.

Fischer-Hayes, Lindsey R, Terrell Brotherton, and Jonathan D Glass. 2013. “Axonal Degeneration in the Peripheral Nervous System: Implications for the Pathogenesis of Amyotrophic Lateral Sclerosis.” Experimental Neurology 246 (August): 6–13. doi:10.1016/j.expneurol.2013.05.001. http://www.scopus.com/inward/record.url?eid=2-s2.0-84879799811&partnerID=tZOtx3y1.

Fledrich, Robert, Ruth M Stassart, Axel Klink, Lennart M Rasch, Thomas Prukop, Lauren Haag, Dirk Czesnik, et al. 2014. “Soluble Neuregulin-1 Modulates Disease Pathogenesis in Rodent Models of Charcot-Marie-Tooth Disease 1A.” Nature Medicine 20 (9): 1055–61. doi:10.1038/nm.3664. http://www.ncbi.nlm.nih.gov/pubmed/25150498.

Frank, Eric. 2009. “A New Class of Spinal Interneurones: The Origin and Function of C Boutons Is Solved.” Neuron 64 (5): 593–95. doi:10.1016/j.neuron.2009.11.030. http://www.ncbi.nlm.nih.gov/pubmed/20005814.

Furukawa, Yoshiaki, Andrew S Torres, and Thomas V O’Halloran. 2004. “Oxygen-Induced Maturation of SOD1: A Key Role for Disulfide Formation by the Copper Chaperone CCS.” The EMBO Journal 23 (14): 2872–81. doi:10.1038/sj.emboj.7600276. http://www.pubmedcentral.nih.gov/articlerender.fcgi?artid=1150991&tool=pmcentrez&rendertype=abstract.

Gidalevitz, Tali, Thomas Krupinski, Susana Garcia, and Richard I Morimoto. 2009. “Destabilizing Protein Polymorphisms in the Genetic Background Direct Phenotypic Expression of Mutant SOD1 Toxicity.” PLoS Genetics 5 (3): e1000399. doi:10.1371/journal.pgen.1000399. http://

www.pubmedcentral.nih.gov/articlerender.fcgi?artid=2642731&tool=pmcentrez&rendertype=abstract.

Gong, Y H, A S Parsadanian, A Andreeva, W D Snider, and J L Elliott. 2000. "Restricted Expression of G86R Cu/Zn Superoxide Dismutase in Astrocytes Results in Astrocytosis but Does Not Cause Motoneuron Degeneration." The Journal of Neuroscience: The Official Journal of the Society for Neuroscience 20 (2): 660–65. http://www.ncbi.nlm.nih.gov/pubmed/10632595.

Grad, Leslie I, Justin J Yerbury, Bradley J Turner, William C Guest, Edward Pokrishevsky, Megan A O'Neill, Anat Yanai, et al. 2014. "Intercellular Propagated Misfolding of Wild-Type Cu/Zn Superoxide Dismutase Occurs via Exosome-Dependent and -Independent Mechanisms." Proceedings of the National Academy of Sciences of the United States of America 111 (9): 3620–25. doi:10.1073/pnas.1312245111. http://www.pnas.org/content/111/9/3620.long.

Greig, A, S D Donevan, T J Mujtaba, T N Parks, and M S Rao. 2000. "Characterization of the AMPA-Activated Receptors Present on Motoneurones." Journal of Neurochemistry 74 (1): 179–91. http://www.ncbi.nlm.nih.gov/pubmed/10617119.

Guatteo, Ezia, Irene Carunchio, Massimo Pieri, Federica Albo, Nadia Canu, Nicola B Mercuri, and Cristina Zona. 2007. "Altered Calcium Homeostasis in Motor Neurones Following AMPA Receptor but Not Voltage-Dependent Calcium Channels' Activation in a Genetic Model of Amyotrophic Lateral Sclerosis." Neurobiology of Disease 28 (1): 90–100. doi:10.1016/j.nbd.2007.07.002. http://www.scopus.com/inward/record.url?eid=2-s2.0-34548790664&partnerID=tZOtx3y1.

Guescini, Michele, Susanna Genedani, Vilberto Stocchi, and Luigi Francesco Agnati. 2010. "Astrocytes and Glioblastoma Cells Release Exosomes

Carrying mtDNA." Journal of Neural Transmission (Vienna, Austria: 1996) 117 (1): 1–4. doi:10.1007/s00702-009-0288-8. http://www.ncbi.nlm.nih.gov/pubmed/19680595.

Gurney, M., H Pu, A. Chiu, M. Dal Canto, C. Polchow, D. Alexander, J Caliendo, et al. 1994. "Motor Neuron Degeneration in Mice That Express a Human Cu,Zn Superoxide Dismutase Mutation." Science 264 (5166): 1772–75. doi: 10.1126/science.8209258. http://www.sciencemag.org/content/264/5166/1772.abstract.

Han, Bong Soo, Ji Heon Hong, Cheolpyo Hong, Sang Seok Yeo, Dong hoon Lee, Hee Kyung Cho, and Sung Ho Jang. 2010. "Location of the Corticospinal Tract at the Corona Radiata in Human Brain." Brain Research 1326 (April): 75–80. doi:10.1016/j.brainres.2010.02.050. http://www.ncbi.nlm.nih.gov/pubmed/20219443.

Harraz, Maged M, Jennifer J Marden, Weihong Zhou, Yulong Zhang, Aislinn Williams, Victor S Sharov, Kathryn Nelson, et al. 2008. "SOD1 Mutations Disrupt Redox-Sensitive Rac Regulation of NADPH Oxidase in a Familial ALS Model." The Journal of Clinical Investigation 118 (2): 659–70. doi: 10.1172/JCI34060. http://www.pubmedcentral.nih.gov/articlerender.fcgi?artid=2213375&tool=pmcentrez&rendertype=abstract.

Hellström, J, U Arvidsson, R Elde, S Cullheim, and B Meister. 1999. "Differential Expression of Nerve Terminal Protein Isoforms in VAChT-Containing Varicosities of the Spinal Cord Ventral Horn." The Journal of Comparative Neurology 411 (4): 578–90. http://www.ncbi.nlm.nih.gov/pubmed/10421869.

Hellström, Johan, Alexandre L R Oliveira, Björn Meister, and Staffan Cullheim. 2003. "Large Cholinergic Nerve Terminals on Subsets of Motoneurones and Their Relation to Muscarinic Receptor Type 2." The Journal of

Comparative Neurology 460 (4): 476–86. doi:10.1002/cne.10648. http://www.ncbi.nlm.nih.gov/pubmed/12717708.

Hernández, Sara, Anna Casanovas, Lidia Piedrafita, Olga Tarabal, and Josep E Esquerda. 2010. "Neurotoxic Species of Misfolded SOD1G93A Recognized by Antibodies against the P2X4 Subunit of the ATP Receptor Accumulate in Damaged Neurones of Transgenic Animal Models of Amyotrophic Lateral Sclerosis." Journal of Neuropathology and Experimental Neurology 69 (2): 176–87. doi:10.1097/NEN.0b013e3181cd3e33. http://www.ncbi.nlm.nih.gov/pubmed/20084016.

Hertz, Leif. 2013. "The Glutamate-Glutamine (GABA) Cycle: Importance of Late Postnatal Development and Potential Reciprocal Interactions between Biosynthesis and Degradation." Frontiers in Endocrinology 4 (January): 59. doi:10.3389/fendo.2013.00059. http://www.pubmedcentral.nih.gov/articlerender.fcgi?artid=3664331&tool=pmcentrez&rendertype=abstract.

Howland, David S, Jian Liu, Yijin She, Beth Goad, Nicholas J Maragakis, Benjamin Kim, Jamie Erickson, et al. 2002. "Focal Loss of the Glutamate Transporter EAAT2 in a Transgenic Rat Model of SOD1 Mutant-Mediated Amyotrophic Lateral Sclerosis (ALS)." Proceedings of the National Academy of Sciences of the United States of America 99 (3): 1604–9. doi:10.1073/pnas.032539299. http://www.pubmedcentral.nih.gov/articlerender.fcgi?artid=122237&tool=pmcentrez&rendertype=abstract.

Huisman, Mark H B, Sonja W de Jong, Perry T C van Doormaal, Stephanie S Weinreich, H Jurgen Schelhaas, Anneke J van der Kooi, Marianne de Visser, Jan H Veldink, and Leonard H van den Berg. 2011. "Population Based Epidemiology of Amyotrophic Lateral Sclerosis Using Capture-Recapture Methodology." Journal of Neurology, Neurosurgery, and Psychiatry 82 (10): 1165–70. doi:10.1136/jnnp.2011.244939. http://www.ncbi.nlm.nih.gov/pubmed/21622937.

Ilieva, Hristelina S, Koji Yamanaka, Shelle Malkmus, Osamu Kakinohana, Tony Yaksh, Martin Marsala, and Don W Cleveland. 2008. “Mutant Dynein (Loa) Triggers Proprioceptive Axon Loss That Extends Survival Only in the SOD1 ALS Model with Highest Motor Neuron Death.” Proceedings of the National Academy of Sciences of the United States of America 105 (34): 12599–604. doi:10.1073/pnas.0805422105. http://www.pubmedcentral.nih.gov/articlerender.fcgi?artid=2527957&tool=pmcentrez&rendertype=abstract.

Issa, Amine N, Wen-Zhi Zhan, Gary C Sieck, and Carlos B Mantilla. 2010. “Neuregulin-1 at Synapses on Phrenic Motoneurones.” The Journal of Comparative Neurology 518 (20): 4213–25. doi:10.1002/cne.22449. http://www.pubmedcentral.nih.gov/articlerender.fcgi?artid=2948240&tool=pmcentrez&rendertype=abstract.

Jane, J A, D Yashon, W DeMyer, and P C Bucy. 1967. “The Contribution of the Precentral Gyrus to the Pyramidal Tract of Man.” Journal of Neurosurgery 26 (2): 244–48. doi:10.3171/jns.1967.26.2.0244. http://www.ncbi.nlm.nih.gov/pubmed/4163618.

Johnson, Thomas E. 2014. “Advantages and Disadvantages of Caenorhabditis Elegans for Aging Research.” Experimental Gerontology 38 (11-12): 1329–32. Accessed December 13. http://www.ncbi.nlm.nih.gov/pubmed/14698813.

Johnston, Clare A, Biba R Stanton, Martin R Turner, Rebecca Gray, Ashley Hay-Ming Blunt, David Butt, Mary-Ann Ampong, Christopher E Shaw, P Nigel Leigh, and Ammar Al-Chalabi. 2006. “Amyotrophic Lateral Sclerosis in an Urban Setting: A Population Based Study of Inner City London.” Journal of Neurology 253 (12): 1642–43. doi:10.1007/s00415-006-0195-y. http://www.ncbi.nlm.nih.gov/pubmed/17219036.

Kaneko, K, S Kawai, T Taguchi, Y Fuchigami, H Morita, A Ofuji, and H Yonemura. 1997. “Spatial Distribution of Corticospinal Potentials Following

Transcranial Electric and Magnetic Stimulation in Human Spinal Cord." Journal of the Neurological Sciences 151 (2): 217–21. http://www.ncbi.nlm.nih.gov/pubmed/9349679.

Kanning, Kevin C, Artem Kaplan, and Christopher E Henderson. 2010. "Motor Neuron Diversity in Development and Disease." Annual Review of Neuroscience 33 (January): 409–40. doi:10.1146/annurev.neuro.051508.135722. http://www.ncbi.nlm.nih.gov/pubmed/20367447.

Kerman, Aaron, Hsueh-Ning Liu, Sidney Croul, Juan Bilbao, Ekaterina Rogaeva, Lorne Zinman, Janice Robertson, and Avijit Chakrabartty. 2010. "Amyotrophic Lateral Sclerosis Is a Non-Amyloid Disease in Which Extensive Misfolding of SOD1 Is Unique to the Familial Form." Acta Neuropathologica 119 (3): 335–44. doi:10.1007/s00401-010-0646-5. http://www.ncbi.nlm.nih.gov/pubmed/20111867.

Kiernan, Matthew C, Steve Vucic, Benjamin C Cheah, Martin R Turner, Andrew Eisen, Orla Hardiman, James R Burrell, and Margaret C Zoing. 2011. "Amyotrophic Lateral Sclerosis." Lancet 377 (9769): 942–55. doi:10.1016/S0140-6736(10)61156-7. http://www.sciencedirect.com/science/article/pii/S0140673610611567.

Kikuchi, Hitoshi, Gabriele Almer, Satoshi Yamashita, Christelle Guégan, Makiko Nagai, Zuoshang Xu, Alexander A Sosunov, Guy M McKhann, and Serge Przedborski. 2006. "Spinal Cord Endoplasmic Reticulum Stress Associated with a Microsomal Accumulation of Mutant Superoxide Dismutase-1 in an ALS Model." Proceedings of the National Academy of Sciences of the United States of America 103 (15): 6025–30. doi:10.1073/pnas.0509227103. http://www.pubmedcentral.nih.gov/articlerender.fcgi?artid=1458691&tool=pmcentrez&rendertype=abstract.

Kiskinis, Evangelos, Jackson Sandoe, Luis A Williams, Gabriella L Boulting, Rob Moccia, Brian J Wainger, Steve Han, et al. 2014. "Pathways Disrupted in

Human ALS Motor Neurones Identified through Genetic Correction of Mutant SOD1." Cell Stem Cell 14 (6): 781–95. doi:10.1016/j.stem.2014.03.004. http://www.ncbi.nlm.nih.gov/pubmed/24704492.

Kitamura, Akira, Noriko Inada, Hiroshi Kubota, Gen Matsumoto, Masataka Kinjo, Richard I Morimoto, and Kazuhiro Nagata. 2014. "Dysregulation of the Proteasome Increases the Toxicity of ALS-Linked Mutant SOD1." Genes to Cells: Devoted to Molecular & Cellular Mechanisms 19 (3): 209–24. doi:10.1111/gtc.12125. http://www.ncbi.nlm.nih.gov/pubmed/24450587.

Kitzman, Patrick. 2006. "Changes in Vesicular Glutamate Transporter 2, Vesicular GABA Transporter and Vesicular Acetylcholine Transporter Labeling of Sacrocaudal Motoneurones in the Spastic Rat." Experimental Neurology 197 (2): 407–19. doi:10.1016/j.expneurol.2005.10.005. http://www.ncbi.nlm.nih.gov/pubmed/16300756.

Lachenal, Gaelle, Karin Pernet-Gallay, Mathilde Chivet, Fiona J Hemming, Agnès Belly, Gilles Bodon, Béatrice Blot, Georg Haase, Yves Goldberg, and Rémy Sadoul. 2011. "Release of Exosomes from Differentiated Neurones and Its Regulation by Synaptic Glutamatergic Activity." Molecular and Cellular Neurosciences 46 (2): 409–18. doi:10.1016/j.mcn.2010.11.004. http://www.ncbi.nlm.nih.gov/pubmed/21111824.

Lanner, Johanna T, Dimitra K Georgiou, Aditya D Joshi, and Susan L Hamilton. 2010. "Ryanodine Receptors: Structure, Expression, Molecular Details, and Function in Calcium Release." Cold Spring Harbor Perspectives in Biology 2 (11): a003996. doi:10.1101/cshperspect.a003996. http://www.pubmedcentral.nih.gov/articlerender.fcgi?artid=2964179&tool=pmcentrez&rendertype=abstract.

Laurin, Nancy, Jacques P Brown, Jean Morissette, and Vincent Raymond. 2002. "Recurrent Mutation of the Gene Encoding Sequestosome 1 (SQSTM1/p62) in Paget Disease of Bone." American Journal of Human Genetics 70

(6): 1582–88. doi:10.1086/340731. http://www.pubmedcentral.nih.gov/articlerender.fcgi?artid=379146&tool=pmcentrez&rendertype=abstract.

Lefebvre, S, L Bürglen, S Reboullet, O Clermont, P Burlet, L Viollet, B Benichou, C Cruaud, P Millasseau, and M Zeviani. 1995. “Identification and Characterization of a Spinal Muscular Atrophy-Determining Gene.” Cell 80 (1): 155–65. http://www.ncbi.nlm.nih.gov/pubmed/7813012.

Lemmens, Robin, Annelies Van Hoecke, Nicole Hersmus, Veerle Geelen, Isabel D’Hollander, Vincent Thijs, Ludo Van Den Bosch, Peter Carmeliet, and Wim Robberecht. 2007. “Overexpression of Mutant Superoxide Dismutase 1 Causes a Motor Axonopathy in the Zebrafish.” Human Molecular Genetics 16 (19): 2359–65. doi:10.1093/hmg/ddm193. http://www.ncbi.nlm.nih.gov/pubmed/17636250.

Li, Qiang, Netanya Y Spencer, Nicholas J Pantazis, and John F Engelhardt. 2011. “Alsin and SOD1(G93A) Proteins Regulate Endosomal Reactive Oxygen Species Production by Glial Cells and Proinflammatory Pathways Responsible for Neurotoxicity.” The Journal of Biological Chemistry 286 (46): 40151–62. doi:10.1074/jbc.M111.279711. http://www.pubmedcentral.nih.gov/articlerender.fcgi?artid=3220533&tool=pmcentrez&rendertype=abstract.

Li, W, P A Ochalski, S Brimijoin, L M Jordan, and J I Nagy. 1995. “C-Terminals on Motoneurones: Electron Microscope Localization of Cholinergic Markers in Adult Rats and Antibody-Induced Depletion in Neonates.” Neuroscience 65 (3): 879–91. http://www.ncbi.nlm.nih.gov/pubmed/7609885.

Lim, Kah-Leong, Doreen S.K. Chua, Xavier Gallart Palau, and Tso-Pang Yao. 2014. Autophagy: Cancer, Other Pathologies, Inflammation, Immunity, Infection, and Aging. Autophagy: Cancer, Other Pathologies, Inflammation, Immunity, Infection, and Aging. Elsevier. doi:10.1016/

B978-0-12-405528-5.00011-0. http://www.sciencedirect.com/science/article/pii/B9780124055285000110.

Ling, Shuo-Chien, Magdalini Polymenidou, and Don W Cleveland. 2013. "Converging Mechanisms in ALS and FTD: Disrupted RNA and Protein Homeostasis." Neuron 79 (3): 416–38. doi:10.1016/j.neuron.2013.07.033. http://www.sciencedirect.com/science/article/pii/S0896627313006570.

Manjaly, Zita R, Kirsten M Scott, Kumar Abhinav, Lokesh Wijesekera, Jeban Ganesalingam, Laura H Goldstein, Anna Janssen, et al. 2010. "The Sex Ratio in Amyotrophic Lateral Sclerosis: A Population Based Study." Amyotrophic Lateral Sclerosis: Official Publication of the World Federation of Neurology Research Group on Motor Neuron Diseases 11 (5): 439–42. doi:10.3109/17482961003610853. http://www.ncbi.nlm.nih.gov/pubmed/20225930.

Marino, Marianna, Simonetta Papa, Valeria Crippa, Giovanni Nardo, Marco Peviani, Cristina Cheroni, Maria Chiara Trolese, et al. 2014. "Differences in Protein Quality Control Correlate with Phenotype Variability in 2 Mouse Models of Familial Amyotrophic Lateral Sclerosis." Neurobiology of Aging, July. Elsevier. doi:10.1016/j.neurobiolaging.2014.06.026. http://www.neurobiologyofaging.org/article/S0197458014004655/fulltext.

Martin, R F, L M Jordan, and W D Willis. 1978. "Differential Projections of Cat Medullary Raphe Neurones Demonstrated by Retrograde Labelling Following Spinal Cord Lesions." The Journal of Comparative Neurology 182 (1): 77–88. doi:10.1002/cne.901820106. http://www.ncbi.nlm.nih.gov/pubmed/701490.

Matsumoto, Arifumi, Yohei Okada, Masanori Nakamichi, Masaya Nakamura, Yoshiaki Toyama, Gen Sobue, Makiko Nagai, Masashi Aoki, Yasuto Itoyama, and Hideyuki Okano. 2006. "Disease Progression of Human SOD1 (G93A) Transgenic ALS Model Rats." Journal of Neuroscience

Research 83 (1): 119–33. doi:10.1002/jnr.20708. http://www.scopus.com/inward/record.url?eid=2-s2.0-30344442440&partnerID=tZOtx3y1.

Mattiazzi, Marina, Marilena D'Aurelio, Carl D Gajewski, Katherine Martushova, Mahmoud Kiaei, M Flint Beal, and Giovanni Manfredi. 2002. "Mutated Human SOD1 Causes Dysfunction of Oxidative Phosphorylation in Mitochondria of Transgenic Mice." The Journal of Biological Chemistry 277 (33): 29626–33. doi:10.1074/jbc.M203065200. http://www.scopus.com/inward/record.url?eid=2-s2.0-0037119407&partnerID=tZOtx3y1.

Mavlyutov, T A, M L Epstein, P Liu, Y I Verbny, L Ziskind-Conhaim, and A E Ruoho. 2012. "Development of the Sigma-1 Receptor in C-Terminals of Motoneurones and Colocalization with the N,N'-Dimethyltryptamine Forming Enzyme, Indole-N-Methyl Transferase." Neuroscience 206 (March): 60–68. doi:10.1016/j.neuroscience.2011.12.040. http://www.pubmedcentral.nih.gov/articlerender.fcgi?artid=3321351&tool=pmcentrez&rendertype=abstract.

McGoldrick, Philip, Peter I Joyce, Elizabeth M C Fisher, and Linda Greensmith. 2013. "Rodent Models of Amyotrophic Lateral Sclerosis." Biochimica et Biophysica Acta 1832 (9): 1421–36. doi:10.1016/j.bbadis.2013.03.012. http://www.sciencedirect.com/science/article/pii/S0925443913000860.

Meininger, V, G Bensimon, L Lacomblez, and F Salachas. 1995. "Natural History of Amyotrophic Lateral Sclerosis. A Discussion." Advances in Neurology 68 (January): 199–207. http://www.ncbi.nlm.nih.gov/pubmed/8787230.

Meininger, Vincent. 2011. "ALS, What New 144 Years after Charcot?" Archives Italiennes de Biologie 149 (1): 29–37. doi:10.4449/aib.v149i1.1265. http://www.architalbiol.org/aib/article/view/14929.

Miles, Gareth B, Robert Hartley, Andrew J Todd, and Robert M Brownstone. 2007. "Spinal Cholinergic Interneurones Regulate the Excitability of Motoneurones during Locomotion." Proceedings of the National Academy

of Sciences of the United States of America 104 (7): 2448–53. doi:10.1073/pnas.0611134104. http://www.pubmedcentral.nih.gov/articlerender.fcgi?artid=1794344&tool=pmcentrez&rendertype=abstract.

Mohapatra, Durga P, and James S Trimmer. 2006. “The Kv2.1 C Terminus Can Autonomously Transfer Kv2.1-like Phosphorylation-Dependent Localization, Voltage-Dependent Gating, and Muscarinic Modulation to Diverse Kv Channels.” The Journal of Neuroscience: The Official Journal of the Society for Neuroscience 26 (2): 685–95. doi:10.1523/JNEUROSCI.4620-05.2006. http://www.ncbi.nlm.nih.gov/pubmed/16407566.

Münch, Christian, John O’Brien, and Anne Bertolotti. 2011. “Prion-like Propagation of Mutant Superoxide Dismutase-1 Misfolding in Neuronal Cells.” Proceedings of the National Academy of Sciences of the United States of America 108 (9): 3548–53. doi:10.1073/pnas.1017275108. http://www.pnas.org/content/108/9/3548.abstract?ijkey=a61f5fdbecf7e24259c37d218126f4fbbfed571e&keytype2=tf_ipsecsha.

Nagy, J I, T Yamamoto, and L M Jordan. 1993. “Evidence for the Cholinergic Nature of C-Terminals Associated with Subsurface Cisterns in Alpha-Motoneurones of Rat.” Synapse (New York, N.Y.) 15 (1): 17–32. doi:10.1002/syn.890150103. http://www.ncbi.nlm.nih.gov/pubmed/8310422.

Nathan, P W, M C Smith, and P Deacon. 1990. “The Corticospinal Tracts in Man. Course and Location of Fibers at Different Segmental Levels.” Brain: A Journal of Neurology 113 (Pt 2 (April): 303–24. http://www.ncbi.nlm.nih.gov/pubmed/2328407.

Neumann, Manuela, Deepak M Sampathu, Linda K Kwong, Adam C Truax, Matthew C Micsenyi, Thomas T Chou, Jennifer Bruce, et al. 2006. “Ubiquitinated TDP-43 in Frontotemporal Lobar Degeneration and Amyotrophic Lateral Sclerosis.” Science (New York, N.Y.) 314 (5796): 130–

33. doi:10.1126/science.1134108. http://www.ncbi.nlm.nih.gov/pubmed/17023659.

Newman, Tracey, Christopher Sinadinos, Alex Johnston, Megan Sealey, and Amrit Mudher. 2011. “Using Drosophila Models of Neurodegenerative Diseases for Drug Discovery.” Expert Opinion on Drug Discovery 6 (2): 129–40. doi:10.1517/17460441.2011.549124. http://www.ncbi.nlm.nih.gov/pubmed/22647132.

Nicholls, D G, and S L Budd. 2000. “Mitochondria and Neuronal Survival.” Physiological Reviews 80 (1): 315–60. http://www.ncbi.nlm.nih.gov/pubmed/10617771.

Nonaka, Takashi, Masami Masuda-Suzukake, Tetsuaki Arai, Yoko Hasegawa, Hiroyasu Akatsu, Tomokazu Obi, Mari Yoshida, et al. 2013. “Prion-like Properties of Pathological TDP-43 Aggregates from Diseased Brains.” Cell Reports 4 (1): 124–34. doi:10.1016/j.celrep.2013.06.007. http://www.ncbi.nlm.nih.gov/pubmed/23831027.

Oeda, T, S Shimohama, N Kitagawa, R Kohno, T Imura, H Shibasaki, and N Ishii. 2001. “Oxidative Stress Causes Abnormal Accumulation of Familial Amyotrophic Lateral Sclerosis-Related Mutant SOD1 in Transgenic Caenorhabditis Elegans.” Human Molecular Genetics 10 (19): 2013–23. http://www.ncbi.nlm.nih.gov/pubmed/11590119.

Orrell, Richard W. 2010. “Motor Neuron Disease: Systematic Reviews of Treatment for ALS and SMA.” British Medical Bulletin 93 (1): 145–59. doi:10.1093/bmb/ldp049. http://bmb.oxfordjournals.org/content/93/1/145.full.

Parton, Matthew J, Wendy Broom, Peter M Andersen, Ammar Al-Chalabi, P Nigel Leigh, John F Powell, and Christopher E Shaw. 2002. “D90A-SOD1 Mediated Amyotrophic Lateral Sclerosis: A Single Founder for All Cases with Evidence for a Cis-Acting Disease Modifier in the Recessive

Haplotype." Human Mutation 20 (6): 473. doi:10.1002/humu.9081. http://www.ncbi.nlm.nih.gov/pubmed/12442272.

PATRIKIOS, J. 1952. "[Pierre Marie and His Work during the First World War]." Revue Neurologique 86 (6 bis): 789–92. http://www.ncbi.nlm.nih.gov/pubmed/13004640.

Pedrini, Steve, Daniela Sau, Stefania Guareschi, Marina Bogush, Robert H Brown, Nicole Naniche, Azadeh Kia, Davide Trotti, and Piera Pasinelli. 2010. "ALS-Linked Mutant SOD1 Damages Mitochondria by Promoting Conformational Changes in Bcl-2." Human Molecular Genetics 19 (15): 2974–86. doi:10.1093/hmg/ddq202. http://www.pubmedcentral.nih.gov/articlerender.fcgi?artid=2901139&tool=pmcentrez&rendertype=abstract.

Pellegrini-Giampietro, D E, J A Gorter, M V Bennett, and R S Zukin. 1997. "The GluR2 (GluR-B) Hypothesis: Ca(2+)-Permeable AMPA Receptors in Neurological Disorders." Trends in Neurosciences 20 (10): 464–70. http://www.ncbi.nlm.nih.gov/pubmed/9347614.

Pickles, Sarah, Laurie Destroismaisons, Sarah L Peyrard, Sarah Cadot, Guy A Rouleau, Robert H Brown, Jean-Pierre Julien, Nathalie Arbour, and Christine Vande Velde. 2013. "Mitochondrial Damage Revealed by Immunoselection for ALS-Linked Misfolded SOD1." Human Molecular Genetics 22 (19): 3947–59. doi:10.1093/hmg/ddt249. http://www.ncbi.nlm.nih.gov/pubmed/23736301.

Pickles, Sarah, and Christine Vande Velde. 2012. "Misfolded SOD1 and ALS: Zeroing in on Mitochondria." Amyotrophic Lateral Sclerosis: Official Publication of the World Federation of Neurology Research Group on Motor Neuron Diseases 13 (4): 333–40. doi:10.3109/17482968.2012.648645. http://www.ncbi.nlm.nih.gov/pubmed/22471903.

Piquet, M-A. 2006. "[Nutritional Approach for Patients with Amyotrophic Lateral Sclerosis]." Revue Neurologique 162 Spec N (June): 4S177–4S187. http://www.ncbi.nlm.nih.gov/pubmed/17128108.

Plowman, G D, J M Green, J M Culouscou, G W Carlton, V M Rothwell, and S Buckley. 1993. "Heregulin Induces Tyrosine Phosphorylation of HER4/p180erbB4." Nature 366 (6454): 473–75. doi:10.1038/366473a0. http://www.ncbi.nlm.nih.gov/pubmed/7902537.

Polazzi, Elisabetta, Ilaria Mengoni, Marco Caprini, Emiliano Peña-Altamira, Ewelina Kurtys, and Barbara Monti. 2013. "Copper-Zinc Superoxide Dismutase (SOD1) Is Released by Microglial Cells and Confers Neuroprotection against 6-OHDA Neurotoxicity." Neuro-Signals 21 (1-2): 112–28. doi:10.1159/000337115. http://www.ncbi.nlm.nih.gov/pubmed/22572742.

Potolicchio, Ilaria, Gregory J Carven, Xiaonan Xu, Christopher Stipp, Richiard J Riese, Lawrence J Stern, and Laura Santambrogio. 2005. "Proteomic Analysis of Microglia-Derived Exosomes: Metabolic Role of the Aminopeptidase CD13 in Neuropeptide Catabolism." Journal of Immunology (Baltimore, Md.: 1950) 175 (4): 2237–43. http://www.ncbi.nlm.nih.gov/pubmed/16081791.

Potter, Soshanna Zittin, and Joan Selverstone Valentine. 2003. "The Perplexing Role of Copper-Zinc Superoxide Dismutase in Amyotrophic Lateral Sclerosis (Lou Gehrig's Disease)." Journal of Biological Inorganic Chemistry: JBIC: A Publication of the Society of Biological Inorganic Chemistry 8 (4): 373–80. doi:10.1007/s00775-003-0447-6. http://www.ncbi.nlm.nih.gov/pubmed/12644909.

Pramatarova, A, J Laganière, J Roussel, K Brisebois, and G A Rouleau. 2001. "Neuron-Specific Expression of Mutant Superoxide Dismutase 1 in Transgenic Mice Does Not Lead to Motor Impairment." The Journal of

Neuroscience: The Official Journal of the Society for Neuroscience 21 (10): 3369–74. http://www.ncbi.nlm.nih.gov/pubmed/11331366.

Prell, T, J Lautenschläger, L Weidemann, J Ruhmer, O W Witte, and J Grosskreutz. 2014. "Endoplasmic Reticulum Stress Is Accompanied by Activation of NF-κB in Amyotrophic Lateral Sclerosis." Journal of Neuroimmunology 270 (1-2): 29–36. doi:10.1016/j.jneuroim.2014.03.005. http://www.ncbi.nlm.nih.gov/pubmed/24666819.

Prell, T, J Lautenschläger, O W Witte, M T Carri, and J Grosskreutz. 2012. "The Unfolded Protein Response in Models of Human Mutant G93A Amyotrophic Lateral Sclerosis." The European Journal of Neuroscience 35 (5): 652–60. doi:10.1111/j.1460-9568.2012.08008.x. http://www.ncbi.nlm.nih.gov/pubmed/22390177.

Pugliatti, Maura, Leslie D Parish, Paola Cossu, Stefania Leoni, Anna Ticca, M Valeria Saddi, Enzo Ortu, et al. 2013. "Amyotrophic Lateral Sclerosis in Sardinia, Insular Italy, 1995-2009." Journal of Neurology 260 (2): 572–79. doi:10.1007/s00415-012-6681-5. http://www.ncbi.nlm.nih.gov/pubmed/23052600.

Pullen, A H. 1992. "Presynaptic Terminal Loss from Alpha-Motoneurones Following the Retrograde Axonal Transport of Diphtheria Toxin." Acta Neuropathologica 83 (5): 488–98. http://www.ncbi.nlm.nih.gov/pubmed/1377857.

Pullen, A H, and T A Sears. 1983. "Trophism between C-Type Axon Terminals and Thoracic Motoneurones in the Cat." The Journal of Physiology 337 (April): 373–88. http://www.pubmedcentral.nih.gov/articlerender.fcgi?artid=1199112&tool=pmcentrez&rendertype=abstract.

Rakhit, Rishi, Janice Robertson, Christine Vande Velde, Patrick Horne, Deborah M Ruth, Jennifer Griffin, Don W Cleveland, Neil R Cashman, and Avijit Chakrabartty. 2007. "An Immunological Epitope Selective for Pathological

Monomer-Misfolded SOD1 in ALS." Nature Medicine 13 (6): 754–59. doi: 10.1038/nm1559. http://www.ncbi.nlm.nih.gov/pubmed/17486090.

Ramesh, Tennore, Alison N Lyon, Ricardo H Pineda, Chunping Wang, Paul M L Janssen, Benjamin D Canan, Arthur H M Burghes, and Christine E Beattie. 2014. "A Genetic Model of Amyotrophic Lateral Sclerosis in Zebrafish Displays Phenotypic Hallmarks of Motoneuron Disease." Disease Models & Mechanisms 3 (9-10): 652–62. doi:10.1242/dmm.005538. http://www.pubmedcentral.nih.gov/articlerender.fcgi?artid=2931540&tool=pmcentrez&rendertype=abstract.

Raposo, Graça, and Willem Stoorvogel. 2013. "Extracellular Vesicles: Exosomes, Microvesicles, and Friends." The Journal of Cell Biology 200 (4): 373–83. doi:10.1083/jcb.201211138. http://www.pubmedcentral.nih.gov/articlerender.fcgi?artid=3575529&tool=pmcentrez&rendertype=abstract.

Rathke-Hartlieb, S, V C Schmidt, H Jockusch, T Schmitt-John, and J W Bartsch. 1999. "Spatiotemporal Progression of Neurodegeneration and Glia Activation in the Wobbler Neuropathy of the Mouse." Neuroreport 10 (16): 3411–16. http://www.ncbi.nlm.nih.gov/pubmed/10599854.

Reaume, A G, J L Elliott, E K Hoffman, N W Kowall, R J Ferrante, D F Siwek, H M Wilcox, et al. 1996. "Motor Neurones in Cu/Zn Superoxide Dismutase-Deficient Mice Develop Normally but Exhibit Enhanced Cell Death after Axonal Injury." Nature Genetics 13 (1): 43–47. doi:10.1038/ng0596-43. http://www.ncbi.nlm.nih.gov/pubmed/8673102.

Robberecht, Wim, and Thomas Philips. 2013. "The Changing Scene of Amyotrophic Lateral Sclerosis." Nature Reviews. Neuroscience 14 (4). Nature Publishing Group: 248–64. doi:10.1038/nrn3430. http://www.nature.com.sire.ub.edu/nrn/journal/v14/n4/full/nrn3430.html.

Rosen, D R, T Siddique, D Patterson, D A Figlewicz, P Sapp, A Hentati, D Donaldson, J Goto, J P O'Regan, and H X Deng. 1993. "Mutations in Cu/Zn

Superoxide Dismutase Gene Are Associated with Familial Amyotrophic Lateral Sclerosis." Nature 362 (6415): 59–62. doi:10.1038/362059a0. http://www.ncbi.nlm.nih.gov/pubmed/8446170.

Rothstein, J D, M Dykes-Hoberg, C A Pardo, L A Bristol, L Jin, R W Kuncl, Y Kanai, et al. 1996. "Knockout of Glutamate Transporters Reveals a Major Role for Astroglial Transport in Excitotoxicity and Clearance of Glutamate." Neuron 16 (3): 675–86. http://www.ncbi.nlm.nih.gov/pubmed/8785064.

Rothstein, Jeffrey D. 2009. "Current Hypotheses for the Underlying Biology of Amyotrophic Lateral Sclerosis." Annals of Neurology 65 Suppl 1 (January): S3–9. doi:10.1002/ana.21543. http://www.ncbi.nlm.nih.gov/pubmed/19191304.

Rotunno, Melissa S, and Bosco, Daryl A. 2013a. "An Emerging Role for Misfolded Wild-Type SOD1 in Sporadic ALS Pathogenesis." Frontiers in Cellular Neuroscience 7 (January): 253. doi:10.3389/fncel.2013.00253. http://www.pubmedcentral.nih.gov/articlerender.fcgi?artid=3863749&tool=pmcentrez&rendertype=abstract.

Rowland, Lewis P. 1998. "Diagnosis of Amyotrophic Lateral Sclerosis." Journal of the Neurological Sciences 160 (October): S6–S24. doi:10.1016/S0022-510X(98)00193-2. http://www.sciencedirect.com/science/article/pii/S0022510X98001932.

Sábado, Javier, Anna Casanovas, Sara Hernández, Lidia Piedrafita, Marta Hereu, and Josep E Esquerda. 2013. "Immunodetection of Disease-Associated Conformers of Mutant Cu/zn Superoxide Dismutase 1 Selectively Expressed in Degenerating Neurones in Amyotrophic Lateral Sclerosis." Journal of Neuropathology and Experimental Neurology 72 (7): 646–61. doi:10.1097/NEN.0b013e318297fd10. http://www.ncbi.nlm.nih.gov/pubmed/23771221.

Sábado, Javier, Anna Casanovas, Olga Tarabal, Marta Hereu, Lídia Piedrafita, Jordi Calderó, and Josep E Esquerda. 2014. “Accumulation of Misfolded SOD1 in Dorsal Root Ganglion Degenerating Proprioceptive Sensory Neurones of Transgenic Mice with Amyotrophic Lateral Sclerosis.” BioMed Research International 2014 (January): 852163. doi:10.1155/2014/852163. http://www.ncbi.nlm.nih.gov/pubmed/24877142.

Sasaki, Shoichi, and Makoto Iwata. 2007. “Mitochondrial Alterations in the Spinal Cord of Patients with Sporadic Amyotrophic Lateral Sclerosis.” Journal of Neuropathology and Experimental Neurology 66 (1): 10–16. doi:10.1097/nen.0b013e31802c396b. http://www.scopus.com/inward/record.url?eid=2-s2.0-33846087291&partnerID=tZOtx3y1.

Scarmeas, N, T Shih, Y Stern, R Ottman, and L P Rowland. 2002. “Premorbid Weight, Body Mass, and Varsity Athletics in ALS.” Neurology 59 (5): 773–75. http://www.ncbi.nlm.nih.gov/pubmed/12221178.

Schmalbruch, H, H J Jensen, M Bjaerg, Z Kamieniecka, and L Kurland. 1991. “A New Mouse Mutant with Progressive Motor Neuronopathy.” Journal of Neuropathology and Experimental Neurology 50 (3): 192–204. http://www.ncbi.nlm.nih.gov/pubmed/2022963.

Shin, Yoon Kyung, So Young Jang, So Young Park, Joo Youn Park, Jong Kuk Kim, Jong Phil Kim, Duk Joon Suh, Hye Jeong Lee, and Hwan Tae Park. 2014. “Grb2-Associated Binder-1 Is Required for Neuregulin-1-Induced Peripheral Nerve Myelination.” The Journal of Neuroscience: The Official Journal of the Society for Neuroscience 34 (22): 7657–62. doi:10.1523/JNEUROSCI.4947-13.2014. http://www.ncbi.nlm.nih.gov/pubmed/24872569.

Shipp, Eric L, Francesca Cantini, Ivano Bertini, Joan Selverstone Valentine, and Lucia Banci. 2003. “Dynamic Properties of the G93A Mutant of Copper-Zinc Superoxide Dismutase as Detected by NMR Spectroscopy:

Implications for the Pathology of Familial Amyotrophic Lateral Sclerosis." Biochemistry 42 (7). American Chemical Society: 1890–99. doi:10.1021/bi026704y. http://dx.doi.org/10.1021/bi026704y.

Silverman, Judith Maxwell, and Neil E Reiner. 2011. "Exosomes and Other Microvesicles in Infection Biology: Organelles with Unanticipated Phenotypes." Cellular Microbiology 13 (1): 1–9. doi:10.1111/j.1462-5822.2010.01537.x. http://www.ncbi.nlm.nih.gov/pubmed/21040357.

Skup, Malgorzata, Olga Gajewska-Wozniak, Paulina Grygielewicz, Tatsyana Mankovskaya, and Julita Czarkowska-Bauch. 2012. "Different Effects of Spinalization and Locomotor Training of Spinal Animals on Cholinergic Innervation of the Soleus and Tibialis Anterior Motoneurones." The European Journal of Neuroscience 36 (5): 2679–88. doi:10.1111/j.1460-9568.2012.08182.x. http://www.ncbi.nlm.nih.gov/pubmed/22708650.

Song, Fei, Pohung Chiang, Jiajing Wang, John Ravits, and Jeffrey A Loeb. 2012. "Aberrant Neuregulin 1 Signaling in Amyotrophic Lateral Sclerosis." Journal of Neuropathology and Experimental Neurology 71 (2): 104–15. doi:10.1097/NEN.0b013e3182423c43. http://www.pubmedcentral.nih.gov/articlerender.fcgi?artid=3270561&tool=pmcentrez&rendertype=abstract.

Stefania Battistini, Michele Benigni, Claudia Ricci and Alessandro Rossi. 2010. "SOD1 Mutations in Amyotrophic Lateral Sclerosis." EUROPEAN NEUROLOGICAL JOURNAL, no. 000: 1–11.

Stefania Battistini, Michele Benigni, Claudia Ricci and Alessandro Rossirnal. 2010. "SOD1 Mutations in Amyotrophic Lateral Sclerosis." European Neurological Journal, no. 000.

Strong, Michael J, Sashi Kesavapany, and Harish C Pant. 2005. "The Pathobiology of Amyotrophic Lateral Sclerosis: A Proteinopathy?" Journal of Neuropathology and Experimental Neurology 64 (8): 649–64. http://www.ncbi.nlm.nih.gov/pubmed/16106213.

Szabadkai, György, Anna Maria Simoni, Mounia Chami, Mariusz R Wieckowski, Richard J Youle, and Rosario Rizzuto. 2004. “Drp-1-Dependent Division of the Mitochondrial Network Blocks Intraorganellar Ca2+ Waves and Protects against Ca2+-Mediated Apoptosis.” Molecular Cell 16 (1): 59–68. doi:10.1016/j.molcel.2004.09.026. http://www.scopus.com/inward/record.url?eid=2-s2.0-4944222095&partnerID=tZOtx3y1.

Takahashi, Yuji, Yoko Fukuda, Jun Yoshimura, Atsushi Toyoda, Kari Kurppa, Hiroyoko Moritoyo, Veronique V Belzil, et al. 2013. “ERBB4 Mutations That Disrupt the Neuregulin-ErbB4 Pathway Cause Amyotrophic Lateral Sclerosis Type 19.” American Journal of Human Genetics 93 (5): 900–905. doi:10.1016/j.ajhg.2013.09.008. http://www.pubmedcentral.nih.gov/articlerender.fcgi?artid=3824132&tool=pmcentrez&rendertype=abstract.

Talbot, Kevin. 2014. “Amyotrophic Lateral Sclerosis: Cell Vulnerability or System Vulnerability?” Journal of Anatomy 224 (1): 45–51. doi:10.1111/joa.12107. http://www.ncbi.nlm.nih.gov/pubmed/24010870.

Tan, Wenzhi, Nicole Naniche, Alexey Bogush, Steve Pedrini, Davide Trotti, and Piera Pasinelli. 2013. “Small Peptides against the Mutant SOD1/Bcl-2 Toxic Mitochondrial Complex Restore Mitochondrial Function and Cell Viability in Mutant SOD1-Mediated ALS.” The Journal of Neuroscience: The Official Journal of the Society for Neuroscience 33 (28): 11588–98. doi:10.1523/JNEUROSCI.5385-12.2013. http://www.scopus.com/inward/record.url?eid=2-s2.0-84880430220&partnerID=tZOtx3y1.

Tan, Wenzhi, Piera Pasinelli, and Davide Trotti. 2014. “Role of Mitochondria in Mutant SOD1 Linked Amyotrophic Lateral Sclerosis.” Biochimica et Biophysica Acta 1842 (8): 1295–1301. doi:10.1016/j.bbadis.2014.02.009. http://www.ncbi.nlm.nih.gov/pubmed/24568860.

Théry, Clotilde, Sebastian Amigorena, Graça Raposo, and Aled Clayton. 2006. “Isolation and Characterization of Exosomes from Cell Culture

Supernatants and Biological Fluids." Current Protocols in Cell Biology / Editorial Board, Juan S. Bonifacino ... [et Al.] Chapter 3 (April): Unit 3.22. doi:10.1002/0471143030.cb0322s30. http://www.ncbi.nlm.nih.gov/pubmed/18228490.

Thrower, J S, L Hoffman, M Rechsteiner, and C M Pickart. 2000. "Recognition of the Polyubiquitin Proteolytic Signal." The EMBO Journal 19 (1): 94–102. doi:10.1093/emboj/19.1.94. http://www.pubmedcentral.nih.gov/articlerender.fcgi?artid=1171781&tool=pmcentrez&rendertype=abstract.

Turner, Bradley J, and Kevin Talbot. 2008. "Transgenics, Toxicity and Therapeutics in Rodent Models of Mutant SOD1-Mediated Familial ALS." Progress in Neurobiology 85 (1): 94–134. doi:10.1016/j.pneurobio.2008.01.001. http://www.sciencedirect.com/science/article/pii/S0301008208000026.

Urushitani, Makoto, Samer Abou Ezzi, and Jean-Pierre Julien. 2007. "Therapeutic Effects of Immunization with Mutant Superoxide Dismutase in Mice Models of Amyotrophic Lateral Sclerosis." Proceedings of the National Academy of Sciences of the United States of America 104 (7): 2495–2500. doi:10.1073/pnas.0606201104. http://www.pubmedcentral.nih.gov/articlerender.fcgi?artid=1790867&tool=pmcentrez&rendertype=abstract.

Van Damme, P, L Van Den Bosch, E Van Houtte, G Callewaert, and W Robberecht. 2002. "GluR2-Dependent Properties of AMPA Receptors Determine the Selective Vulnerability of Motor Neurones to Excitotoxicity." Journal of Neurophysiology 88 (3): 1279–87. http://www.ncbi.nlm.nih.gov/pubmed/12205149.

Van Den Bosch, L. 2011. "Genetic Rodent Models of Amyotrophic Lateral Sclerosis." Journal of Biomedicine & Biotechnology 2011 (January):

348765. doi:10.1155/2011/348765. http://www.pubmedcentral.nih.gov/articlerender.fcgi?artid=3022221&tool=pmcentrez&rendertype=abstract.

Van Den Bosch, L, W Vandenberghe, H Klaassen, E Van Houtte, and W Robberecht. 2000. "Ca(2+)-Permeable AMPA Receptors and Selective Vulnerability of Motor Neurones." Journal of the Neurological Sciences 180 (1-2): 29–34. http://www.ncbi.nlm.nih.gov/pubmed/11090861.

Van Niel, Guillaume, Isabel Porto-Carreiro, Sabrina Simoes, and Graça Raposo. 2006. "Exosomes: A Common Pathway for a Specialized Function." Journal of Biochemistry 140 (1): 13–21. doi:10.1093/jb/mvj128. http://www.ncbi.nlm.nih.gov/pubmed/16877764.

Vance, Caroline, Boris Rogelj, Tibor Hortobágyi, Kurt J De Vos, Agnes Lumi Nishimura, Jemeen Sreedharan, Xun Hu, et al. 2009. "Mutations in FUS, an RNA Processing Protein, Cause Familial Amyotrophic Lateral Sclerosis Type 6." Science (New York, N.Y.) 323 (5918): 1208–11. doi:10.1126/science.1165942. http://www.ncbi.nlm.nih.gov/pubmed/19251628.

Von Lewinski, Friederike, and Bernhard U Keller. 2005. "Ca2+, Mitochondria and Selective Motoneuron Vulnerability: Implications for ALS." Trends in Neurosciences 28 (9): 494–500. doi:10.1016/j.tins.2005.07.001. http://www.ncbi.nlm.nih.gov/pubmed/16026864.

Wang, Haizhi, and Aleister J Saunders. 2014. "The Role of Ubiquitin-Proteasome in the Metabolism of Amyloid Precursor Protein (APP): Implications for Novel Therapeutic Strategies for Alzheimer's Disease." Discovery Medicine 18 (97): 41–50. Accessed August 11. http://www.discoverymedicine.com/Haizhi-Wang/2014/07/the-role-of-ubiquitin-proteasome-in-the-metabolism-of-amyloid-precursor-protein-app-implications-for-novel-therapeutic-strategies-for-alzheimers-disease/.

Wang, Hongfeng, Zheng Ying, and Guanghui Wang. 2012. "Ataxin-3 Regulates Aggresome Formation of Copper-Zinc Superoxide Dismutase (SOD1) by

Editing K63-Linked Polyubiquitin Chains." The Journal of Biological Chemistry 287 (34): 28576–85. doi:10.1074/jbc.M111.299990. http://www.jbc.org/content/287/34/28576.long.

Wang, Lijun, Brian Popko, and Raymond P Roos. 2011. "The Unfolded Protein Response in Familial Amyotrophic Lateral Sclerosis." Human Molecular Genetics 20 (5): 1008–15. doi:10.1093/hmg/ddq546. http://www.pubmedcentral.nih.gov/articlerender.fcgi?artid=3033190&tool=pmcentrez&rendertype=abstract.

Watson, Melanie R, Robert D Lagow, Kexiang Xu, Bing Zhang, and Nancy M Bonini. 2008. "A Drosophila Model for Amyotrophic Lateral Sclerosis Reveals Motor Neuron Damage by Human SOD1." The Journal of Biological Chemistry 283 (36): 24972–81. doi:10.1074/jbc.M804817200. http://www.jbc.org/content/283/36/24972.short.

Westbury, D R. 1982. "A Comparison of the Structures of Alpha and Gamma-Spinal Motoneurones of the Cat." The Journal of Physiology 325 (April): 79–91. http://www.pubmedcentral.nih.gov/articlerender.fcgi?artid=1251381&tool=pmcentrez&rendertype=abstract.

Wilson, Jennifer M, Jeremy Rempel, and Robert M Brownstone. 2004. "Postnatal Development of Cholinergic Synapses on Mouse Spinal Motoneurones." The Journal of Comparative Neurology 474 (1): 13–23. doi:10.1002/cne.20089. http://www.ncbi.nlm.nih.gov/pubmed/15156576.

Wittie, Michael, Lorene M Nelson, Sharon Usher, Kevin Ward, and Michael Benatar. 2013. "Utility of Capture-Recapture Methodology to Assess Completeness of Amyotrophic Lateral Sclerosis Case Ascertainment." Neuroepidemiology 40 (2): 133–41. doi:10.1159/000342156. http://www.ncbi.nlm.nih.gov/pubmed/23095852.

Zagoraiou, Laskaro, Turgay Akay, James F Martin, Robert M Brownstone, Thomas M Jessell, and Gareth B Miles. 2009. "A Cluster of Cholinergic

Premotor Interneurones Modulates Mouse Locomotor Activity." Neuron 64 (5): 645–62. doi:10.1016/j.neuron.2009.10.017. http://www.pubmedcentral.nih.gov/articlerender.fcgi?artid=2891428&tool=pmcentrez&rendertype=abstract.

HYPOTHESIS AND OBJECTIVES

Amyotrophic Lateral Sclerosis (ALS) is a complex neurodegenerative disease that eventually results in paralysis and death of affected patients. The affectation of the motor neurons that controls voluntary movements occurs in this disease at different levels. This includes affectation of the motor neurone cellular organelles and affectation of the motor neurone terminals/axons according to the previous research conducted in SOD1-G93A ALS-associated transgenic models.

Affectation of the motoneuron terminals is generally studied from the systems neurobiology approach. This approach comprises the analysis of the molecular changes in the terminal proteins that can be associated with any pathological or compensatory aspect of motor neurones from ALS-associated models. On the other hand, affectation of cellular organelles in ALS primordially includes the affectation of the proteasome and dysfunction of mitochondria that is associated with presence of mutant SOD1 in familial forms of ALS. The study of these pathological hallmarks is conducted by the scrutinization of neuronal intrinsic molecular pathways that could be altered in these cells in presence of mutant SOD1-G93A. By the same token, the development of invertebrate models that resemble mitochondrial affectation for the study of those mitochondrial dysfunctions associated with SOD1-G93A is currently lacking and might be a promising strategy to accelerate the understanding of this harmful association and the development of novel therapeutic agents.

In this thesis, we have hypothesized that substantial molecular changes associated with recently discovered proteins such as Neuregulin-1 (NRG-1) in the soma of alpha motor neurones could be associated with molecular alterations in the C-terminals apposed to spinal cord motor neurones. These in turn could occur in line with the progression of familial ALS symptoms in SOD1-G93A transgenic mice. The presence of these altered proteins could remain associated with extracellular vesicles in these terminals and the development of

a reliable and easy-to-perform method for the isolation of these vesicles should be achieved to perform a proper study of these altered synaptic proteins in familial ALS.

By the same token, with regard to the mechanisms that promote degeneration of motor neurones in ALS, we hypothesized that affectation of mitochondria could be linked to the affectation of the ubiquitin proteasome system and formation of aggregates in this disease. We also hypothesized that the expression of human ALS mutant SOD1-G93A in *Drosophila* muscles could create a novel *Drosophila* model to be used for the study of mitochondria affectation and the development of massive therapeutic compound screenings in familial ALS.

With reference to the aforementioned hypotheses, the objectives proposed are:

I. To study the potential presence of NRG-1 in C-terminals of SOD1-G93A mice and WT litter mates spinal cord motor neurones and quantify any substantial disease-associated change.

II. Ultrastructural characterization of the NRG-1 in C-terminals of spinal cord motor neurones

III. Development of a reliable and easy-to-perform protocol for isolation of EVs from biological fluids and neuronal tissues for the study and characterization of NRG-1 in EVs.

IV. Study of the existent links between housekeeping mitochondrial proteins such PINK1 and Parkin and SOD1-G93A.

V. Find currently unknown pathways that might control the proteasome function in presence of the ALS mutant SOD1-G93A.

VI. Express mutant SOD1-G93A in *Drosophila* muscles under the 24B promoter to create a new invertebrate ALS model that efficiently develops ALS-associated mitochondrial dysfunction phenotype.

RESULTS AND DISCUSSION

Chapter 1.

Characterization of neuregulin-1 from C-terminal extracellular vesicles in spinal cord motoneurons: a systems approach in ALS

Gallart-Palau et al. The FASEB Journal (2014) 28 (8), 3618-3632.

Gallart-Palau et al. Scientific Reports (2015) 5, 14664.

Chapter 1 Annex. (Unpublished).

Neuregulin-1 is concentrated in the postsynaptic subsurface cistern of C-bouton inputs to α-motoneurons and altered during motoneuron diseases.

Gallart-Palau et al. The FASEB Journal (2014) 28 (8), 3618-3632

The FASEB Journal (2014) 28 (8), 3618-3632

The FASEB Journal • Research Communication

NEUREGULIN-1 IS CONCENTRATED IN THE POSTSYNAPTIC SUBSURFACE CISTERN OF C-BOUTON INPUTS TO α-MOTONEURONS AND ALTERED DURING MOTONEURON DISEASES

Xavier Gallart-Palau,[1] Olga Tarabal,[1] Anna Casanovas, Javier Sábado, Francisco J. Correa, Marta Hereu, Lídia Piedrafita, Jordi Calderó,[2] and Josep E. Esquerda[2]

Unitat de Neurobiologia Cellular, Departament de Medicina Experimental, Facultat de Medicina, Institut de Recerca Biomèdica de Lleida (IRBLLEIDA), Universitat de Lleida, Lleida, Catalonia, Spain

Abstract

C-boutons are large, cholinergic, synaptic terminals that arise from local interneurones and specifically contact spinal α-motoneurones (MNs). C boutons characteristically display a postsynaptic specialization consisting of an endoplasmic reticulum-related subsurface cistern (SSC) of unknown function. In the present work, by using confocal microscopy and ultrastructural immunolabeling, we demonstrate that neuregulin-1 (NRG1) accumulates in the SSC of mouse spinal MNs. We also show that the NRG1 receptors erbB2 and erbB4 are presynaptically localized within C boutons, suggesting that NRG1-based retrograde signaling may occur in this type of synapse. In most of the cranial nuclei, MNs display the same pattern of NRG1 distribution as that observed in spinal cord MNs. Conversely, MNs in oculomotor nuclei, which are spared in amyotrophic lateral sclerosis (ALS), lack both C boutons and SSC-associated NRG1. NRG1 in spinal MNs is developmentally regulated and depends on the maintenance of nerve-muscle interactions, as we show after nerve transection experiments. Changes in NRG1 in C boutons were also investigated in mouse models of MN diseases: i.e., spinal muscular atrophy (SMNΔ7) and ALS ($SOD1^{G93A}$). In both models, a transient increase in NRG1 in C boutons occurs during disease progression. These data increase our understanding of the role of C boutons in MN physiology and pathology.—Gallart-Palau, X., Tarabal, O., Casanovas, A., Sábado, J., Correa, F. J., Hereu, M., Piedrafita, L., Calderó, J., Esquerda, J. E. Neuregulin-1 is concentrated in the postsynaptic subsurface cistern of C-bouton inputs to α-motoneurones and altered during motoneuron diseases.

Abbreviations: Abbreviations: ALS, amyotrophic lateral sclerosis; ANOVA, analysis of variance; CGRP, calcitonin gene-related peptide; DAPI, 4=,6-diamidino-2-phenylindole dihydrochloride; E, embryonic day; ER, endoplasmic reticulum; GABA, -aminobutyric acid; LMC, lateral motor column; MN, motoneuron; NGS, normal goat serum; NRG1, neuregulin-1; P, posthatching day; PB, phosphate buffer; PBS, phosphate-buffered saline; PFA, paraformaldehyde; SMA, spinal muscular atrophy; TBST, Tris-buffered-saline containing Triton X-100; VAChT, vesicular acetylcholine transporter; VGAT, vesicular GABA transporter; VGLUT1/2, vesicular glutamate transporter 1/2; WT, wild type

1 These authors contributed equally to this work.
2 Correspondence: Unitat de Neurobiologia Cellular, Departament de Medicina Experimental, Facultat de Medicina, IRBLLEIDA, Universitat de Lleida, Av. Rovira Roure 80, 25198 Lleida, Catalonia, Spain. E-mail: J.E.E., josep.esquerda@ mex.udl.cat; J.C., jordi.caldero@mex.udl.cat

The FASEB Journal (2014) 28 (8), 3618-3632

Keywords: Spinal cord ventral horn; interneurones; erB receptors; spinal cord muscular atrophy; amyotrophic lateral sclerosis

1 INTRODUCTION

Motoneurones (MNs) located in the spinal cord and brainstem motor nuclei project axons to skeletal muscles and represent the ultimate efferent pathways of the complex neuronal circuitry that controls voluntary motor activity. MNs innervating distinct muscle groups cluster into pools that receive specific synaptic inputs, which modulate MN excitability. By using a variety of neurotransmitter molecules acting on specific postsynaptic receptors, nerve afferents to MNs shape the appropriate patterns of activity determining motor behavior. There are several reports in which the major transmitter systems that constitute the synaptic input on MNs have been described; these include glutamate, glycine, γ-aminobutyric acid (GABA), acetylcholine, serotonine, norepinephrine, and neuropeptides (reviewed in ref. 1). All of them operate through specific postsynaptic ionotropic and metabotropic receptors.

Pioneering studies using electron microscopy have described the structural diversity of the synaptic inputs on MNs. On the basis of vesicle shape, pre- and postsynaptic membrane specializations, and other ultrastructural characteristics, a number of distinct types of synapses were defined, which include F-, S-, and C-type boutons (2,–,4). The F and S types are the major classes of boutons contacting MN cell bodies. Whereas S-type boutons mainly correspond to glycine- or GABA-containing inhibitory synapses, F-type boutons match with glutamate-containing excitatory terminals (5,–,8). C boutons are unusually large nerve terminals (3–5 μm length) characteristic of somatic α-MNs that contain a high number of densely packed, round or slightly flattened, and clear synaptic vesicles. At the postsynaptic region, the C termini display a unique structure consisting of a 10-nm-wide subsurface cistern adjacent to the MN membrane and associated with a stack of underlying lamellae of rough endoplasmic reticulum (9). Although the cholinergic nature of C termini has been well established (10, 11), the neuronal origin of these inputs was long not known. More recently, the origin and function of C termini have been revealed (12, see also ref. 13 for review) as a small cluster of cholinergic interneurones (VOc interneurones) located near the central canal that modulate MN activity during locomotor behavior (14).

In a recent study examining neuregulin-1 (NRG1) expression on phrenic spinal cord MNs, it was reported that this factor was expressed in nearly all cholinergic nerve terminals (15). Here, we have reexamined this and confirmed that NRG1 is closely associated with the cholinergic C boutons that innervate both the somatic and proximal dendritic regions of lower MNs. However, a more detailed analysis by confocal and immunoelectron microscopy revealed that NRG1 was absent from C-type presynaptic terminals, but it is concentrated in the associated postsynaptic component, within the subsurface cistern. The C termini are poorly investigated structures that are reported to suffer plastic changes in sick MNs after spinal cord injury (16, 17) or in amyotrophic lateral sclerosis (ALS; refs. 18,–,20). Accordingly, we extended our analysis of C-terminal-associated NRG1 expression in developing and injured chick embryo MNs and, also, in

transgenic mouse models of MN diseases, including spinal muscular atrophy (SMA) and ALS. Preliminary results have been previously presented in abstract form (21).

2 EXPERIMENTAL

Animals

Fertilized chicken eggs were purchased from SADA (Lleida, Catalonia, Spain) and incubated in the laboratory at 37°C and 60% relative humidity. At the time of sampling, embryos were staged according to the Hamburger and Hamilton stage series (22). For developmental studies, chickens were euthanizeded at different days from embryonic day 6 (E6) to posthatching day 8 (P8).

For experiments in normal mice, CD1 nontransgenic animals purchased from Harlan Laboratories (Castellar del Vallès, Barcelona, Catalonia, Spain) were used. Two mouse transgenic lines were also used in our experiments, $SOD1^{G93A}$ and SMNΔ7, which were purchased from The Jackson Laboratory (Sacramento, CA, USA). $SOD1^{G93A}$ mice were maintained as hemizygotes by breeding transgenic males with C57BL/6 females. SMNΔ7 ($Smn^{-/-}$;$SMN2^{+/+}$;$SMN\Delta7^{+/+}$) mice were obtained by breeding pairs of SMA carrier mice ($Smn^{+/-}$;$SMN2^{+/+}$;$SMN\Delta7^{+/+}$) on a FVB/N background. Transgenic progeny of both lines were identified by PCR genotyping of DNA extracted from the tail by using specific primers as described previously (23, 24). Age-matched wild-type (WT) littermates of transgenic animals were used as controls. All animal experimentation procedures were performed according to the committee for Animal Care and Use of the University of Lleida, in line with the Generalitat de Catalunya Norms (DOGC 2073, 1995).

Nerve transection experiments

For *in ovo* pharmacological experiments and embryonic surgery, the eggs were windowed on E6. Unilateral limb amputation (axotomy) was performed in some E16 embryos after local application of xylocaine anesthesia (25). For this, the right hindlimb was tightly sutured above the knee with sterile silk, and the limb was cut distally to the suture; embryos were killed 2 d after the operation. The side contralateral to the surgery was used as a control.

For axotomy experiments in adult mice, the sciatic nerve was transected and ligated at midthigh level while animals were under inhalant anesthesia with 4% isoflurane and maintained with a 10% ketamine-2% xylazine combination. Animals were subjected to postoperative analgesia with buprenorphine (0.05 mg/kg, intraperitoneal).

Tissue preparation for light and confocal microscopy

Chick embryos and chicks were killed by decapitation, and the spinal cords were rapidly dissected into saline and fixed by immersion in 4% paraformaldehyde (PFA) in 0.1 M phosphate buffer (PB) at pH 7.4. Mice were deeply anesthetized with pentobarbital and transcardially perfused with physiological saline solution followed by 4% PFA in 0.1 M PB (pH 7.4); lumbar spinal cord samples were dissected and maintained in the same fixative for 24 h. After fixation, samples were transferred to 30% sucrose in 0.1 M PB and 0.02% sodium azide for cryoprotection and subsequently frozen. Transverse cryostat sections (16 μm thick) were obtained and

collected on gelatin-coated glass slides. In experiments referring to "normal adult mice," samples were taken from CD1 mice at P60 to P90.

Immunocytochemistry and image analysis

Sections were permeabilized with phosphate-buffered saline (PBS) containing 0.1% Triton X-100 for 1 h, blocked with 10% normal horse serum (NHS; Sigma-Aldrich, St. Louis, MO, USA) in PBS for 1 h, and incubated overnight at 4°C with 1 or 2 of the following primary antibodies: rabbit polyclonal anti-NRG1 1α/β1/2 (1:300; sc-348; Santa Cruz Biotechnology, Santa Cruz, CA, USA); rabbit polyclonal anti-Neu E-18 (1:300; sc-284; Santa Cruz Biotechnology); rabbit polyclonal anti-p-Neu tyr1248 (p-erbB2; 1:300; sc-12352-R; Santa Cruz Biotechnology); rabbit polyclonal anti-erbB4 (1:400; sc-283; Santa Cruz Biotechnology); mouse monoclonal anti-σ-1 receptor (1:50; sc-137075; Santa Cruz Biotechnology); guinea pig polyclonal anti-vesicular acetylcholine transporter (VAChT; 1:250; 139 105; Synaptic Systems, Goettingen, Germany); guinea pig polyclonal anti-vesicular glutamate transporter 1 (VGLUT1; 1:250; 135 304; Synaptic Systems); guinea pig polyclonal anti-VGLUT2 (1:250; 135 404; Synaptic Systems); guinea pig polyclonal anti-vesicular GABA transporter (VGAT; 1:200; 131 004; Synaptic Systems); goat polyclonal anti-parvalbumin (1:1000; pv-235; Swant, Marly, Switzerland); rabbit polyclonal anti-m2 muscarinic receptor (1:100; AMR-002; Alomone Labs, Jerusalem, Israel); rabbit polyclonal anti-calcitonin gene-related peptide (CGRP, 1:1000; C-8198; Sigma-Aldrich); mouse monoclonal anti-KDEL receptor (1:50; VAA-PT048; Stressgen Biotechnologies, Victoria, BC, Canada); mouse monoclonal anti-PDI (1:100; SPA-891; Stressgen Biotechnologies); mouse monoclonal anti-early endosome marker (EEA1[1G11], 1:100; ab70521; Abcam, Cambridge, UK); mouse monoclonal anti-Rab5 (1:100; 108 011; Synaptic Systems); and mouse monoclonal anti-Rab11 (1:100; R56320; Transduction Laboratories, Lexington, KY, USA).

After being washed, sections were incubated at room temperature for 1 h with the appropriate secondary antibody labeled with one of the following fluorochromes at 1:500 dilution: Alexa Fluor 488 and Alexa Fluor 546 (both from Molecular Probes, Eugene, OR, USA) or Cy3, Cy5, or DyLight 488 (Jackson ImmunoResearch Laboratories, West Grove, PA, USA). Nuclear counterstaining was performed by using 4′,6-diamidino-2-phenylindole dihydrochloride (DAPI; 50 ng/ml; Molecular Probes). Finally, spinal cord sections were labeled with fluorescent NeuroTrace Nissl staining (1:150; Molecular Probes). Preparations were mounted with Vectashield (Vector Laboratories, Burlingame, CA, USA) or with a laboratory-made antifading mounting medium containing 0.1 M Tris-HCl buffer (pH 8.5), 20% glycerol, 10% Moviol, and 0.1% 1,4-diazabicyclo[2,2,2]octane. Slides from the different animals to be compared were processed in parallel for immunocytochemistry and subsequent imaging.

Digital images were obtained from every 30th section of the entire lumbar spinal cord using Fluoview FV-500 or Fluoview FV-1000 Olympus confocal laser-scanning microscopes (Olympus, Hamburg, Germany). The same scanning parameters were used for the acquisition of images corresponding to different experimental groups. Image analysis was

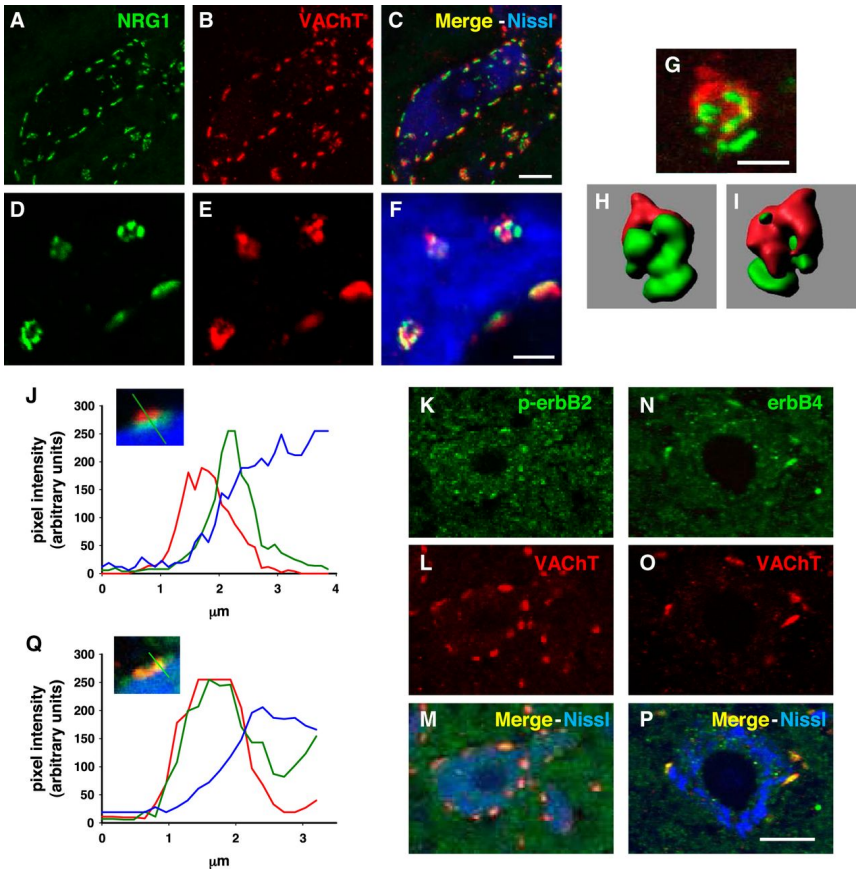

Figure 1. NRG1 and its receptors ErbB2 and ErbB4 are associated with cholinergic C-bouton afferents on ventral horn MNs. *A–C*) MN soma after double immunolabeling for NRG1 (green; *A*) and VAChT (red; *B*), in combination with fluorescent Nissl staining (blue; *C*); note the close association of NRG1-positive spots with cholinergic C-type terminals. *D–F*) En face view of NRG1-positive spots at the surface of MN soma demonstrates that they are organized as clustered subunits (green; *D*) closely related, but not colocalized, with VAChT-labeled presynaptic terminals (red; *E*); a Nissl counterstained (blue) merged image is shown (*F*). *G–I*) Projected high-magnification confocal image of a single C-type terminal double immunolabeled with anti-NRG1 (green) and anti-VAChT (red) antibodies (*G*) was processed to make a volume rendering (*H*, *I*) demonstrating a complementary fitting of axon terminal (red) in the synaptic arrangement containing NRG1 (green). *J*) Pixel profile along a line crossing a multifluorescent labeled C-type synapse demonstrated the dissociation of the presynaptic marker VAChT (red) from the NRG1 (green), suggesting that the NRG1-containing spot is postsynaptically located at the MN soma surface (Nissl staining in blue). *K–P*) phosphorylated ErbB2 (green; *K*) and ErbB4 (green; *N*) are present in VAChT-labeled C boutons (red; *L*, *O*); merged images combined with Nissl staining are shown (*M*, *P*). *Q*) Pixel profile along a line crossing a multifluorescent labeled C-type synapse demonstrated the coincidence of the presynaptic marker VAChT (red) with p-ErbB2 (green), indicating the presynaptic localization of this NRG1 receptor; a blue Nissl labeling was used to delimitate the MN cell body. Scale bars = 10 µm (*A–C*, *K–P*); 4 µm (*D–F*); 2 µm (*G–I*).

performed using Visilog 6.3 software (Noesis, Orsay, France) or ImageJ software (U.S. National Institutes of Health, Bethesda, MD, USA), and only those MNs showing a large nucleus, a visible nucleolus, and a healthy appearance were considered. Immunolabeled profiles of NRG1 and of distinct vesicle transporter proteins studied were manually counted on the screen for each MN soma. The area and perimeter of MN somata were also measured. Three-dimensional reconstructions were performed by using Bitplane (Imaris, Bitplane, CT, USA) on 0.5-μm-thick Z step obtained with the confocal microscope.

Ultrastructural immunolabeling

Animals used for ultrastructural immunolabeling analysis were perfused with 4% paraformaldehyde and 0.1% glutaraldehyde in 0.1 M PB (pH 7.4). Dissected spinal cords were submerged in the same fixative for 6 h.

For preembedding procedures, vibratome sections (50 μm thick) of lumbar spinal cord were treated with 50 mM glycine in PB for 30 min, cryoprotected in 30% sucrose in 0.1M PB, permeabilized performing 4 freeze/thaw cycles in liquid N_2, blocked with 10% normal goat serum (NGS) in PBS for

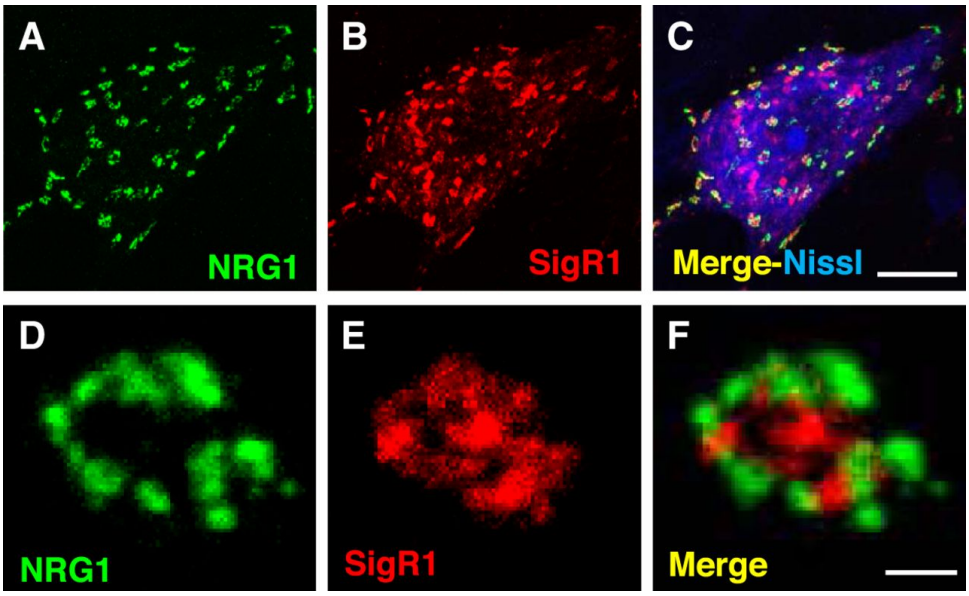

Figure 2. In C-type synapses, NRG1 is accumulated in the MN compartment closely associated with the ER-related subsurface cistern domain enriched in σ-1 receptor (SigR1). A–C) Spinal cord MNs were immuno-labeled for simultaneous detection of NRG1 (green; A) and SigR1 (red; B); both markers co-localize in C-type synapses (yellow; C); MN somata were visualized by fluorescent Nissl staining (blue; C). D–F) High-magnification imaging under the confocal microscope demonstrates that although subcellular compartments containing NRG1 (green; D) and SigR1 (red; E) are closely linked, both proteins are differentially sorted in spatially distinct and poorly overlapping domains within a subsurface cistern (F). Scale bars = 20 μm (A–C); 1 μm (D–F).

1 h, and incubated overnight at 4°C with the primary rabbit polyclonal antibody anti-NRG1α/β1/2 (1:200; Santa Cruz Biotechnology). After several washes, sections were incubated for 1 h with a secondary anti-rabbit biotinylated antibody (1:100; Vector Laboratories) and visualized using Vectastain Elite ABC (Vector Laboratories) followed by incubation in a 0.05% 3,3-diaminobenzidine (DAB)/0.01% H_2O_2 mixture. Labeled sections were flat embedded in Embed 812, sectioned, and counterstained with uranyl acetate and lead citrate.

For postembedding immunolabeling, lumbar spinal cord samples were sectioned at 200 μm using a McIlwain Tissue Chopper (Mickle Laboratory Engineering, Gomshall, UK). Samples were also processed for either freeze substitution or ultrathin cryosectioning. For the freeze-substitution procedure, a Leica EM system (Leica Microsystems, Wetzlar, Germany) was used; samples were low temperature embedded in Lowicryl HM20 resin (Electron Microscopy Sciences, Hatfield, PA, USA), following a protocol similar to that described elsewhere (26). Ultrathin sections were collected on nickel grids and treated for 10 min at room temperature with 0.1% sodium borohydride in Tris-buffered-saline (pH 7.4) containing 0.1% Triton X-100 (TBST) and 50 mM glycine. After being washed with TBST, sections were first incubated for 10 min in 10% NGS in TBST, and then for 2 h in anti-NRG1α/β1/2 (1:200; Santa Cruz Biotechnology) at room temperature. After being rinsed in TBST, they were incubated in 10 nm gold-conjugated goat anti-rabbit IgG (Sigma-Aldrich) diluted at 1:20 in TBST containing 10% NGS and 5 mg/ml polyethylene glycol 20,000 for 1 h at room temperature. After being washed in TBST and distilled water, sections were counterstained with uranyl acetate and lead citrate before observation.

For immunolabeling of ultrathin cryosections, samples were cryoprotected in 2.3 M sucrose in PB, mounted on specimen holders, and frozen by immersion in liquid N_2. Sections were obtained with a Leica EM FC cryoultramicrotome, according to a previously described procedure (27), and labeled using the anti-NRG1 antibody (1:200; Santa Cruz Biotechnology) and 10 nm gold-conjugated goat anti-rabbit IgG (Sigma-Aldrich) according to established procedures (28).

Observations were performed with a Zeiss EM 910 electron microscope (Zeiss, Oberkochen, Germany).

Statistical analysis

Data are expressed as means ± se. The statistical analysis was assessed by either Student's t test or 1-way analysis of variance (ANOVA) followed by post hoc Bonferroni's test. The level of significance was chosen as $P < 0.05$.

3 RESULTS

NRG1 immunoreactivity in normal adult mouse spinal cord

Immunostaining with the antibody against NRG1 revealed a large number of intensely labeled small punctate structures, mainly distributed in the spinal cord ventral horn. NRG1-immunopositive spots decorated the soma and proximal dendrites of large MNs at a density of 16.20 ± 2.18/100 μm of somatic perimeter (n=67 somata from P90 mice). Their size (area 0.93±0.06 μm^2; n=112) and distribution suggest that they could be

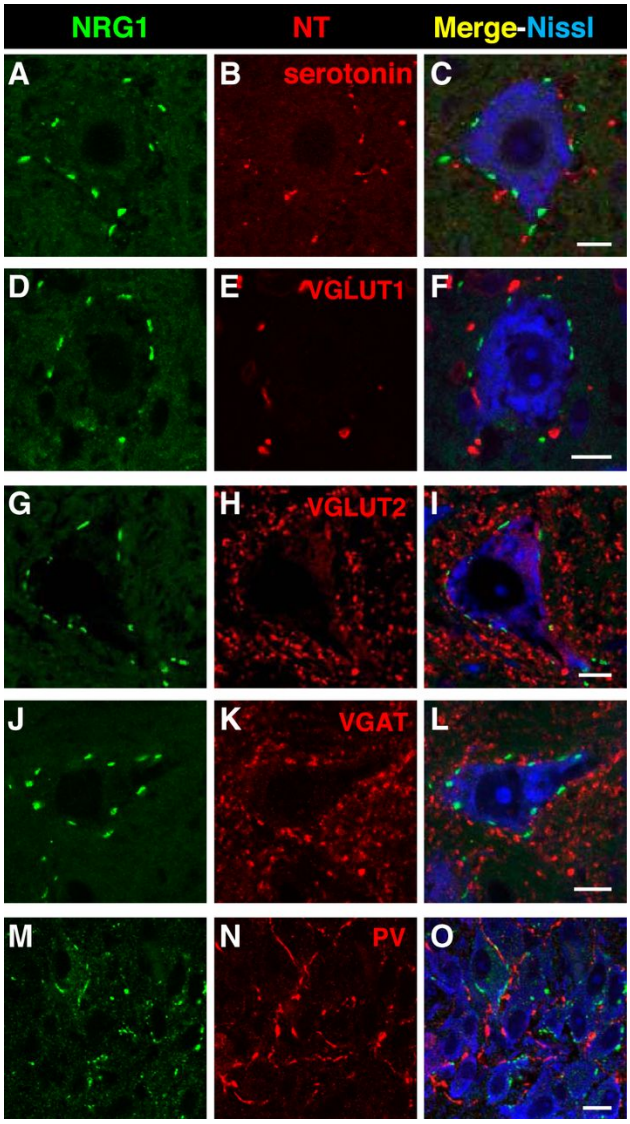

Figure 3. NRG1 is specifically associated with cholinergic MN afferent boutons in ventral horn MNs of adult mice. A–L) Single optical sections at the ventral horn MN somata were immuno-labeled for simultaneous detection of NRG1 (green; A, D, G, J) and markers for the distinct neurotransmitters (NT; red) serotonin (B), VGLUT1 (E), VGLUT2 (H), and VGAT (K); combined images in which MN somata were also labeled with fluorescent Nissl stain (blue; C, F, I, L) demonstrate the absence of association with any of these markers. M–O) NRG1 (green; M) is not associated with nerve terminals coming from proprioceptive muscle spindles, identified after PV (red; N, and merge image, O) immuno-staining in embryonic (E18) mouse spinal cord. Scale bars = 10 μm.

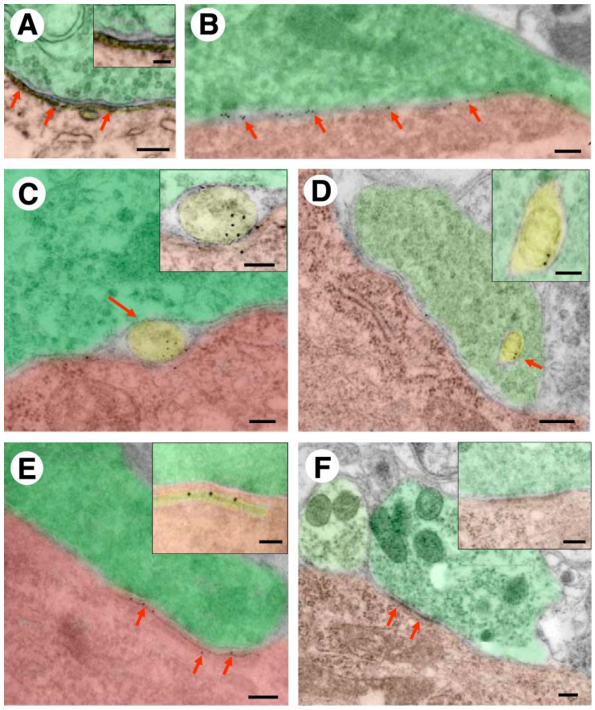

Figure 4. Ultrastructural immunolocalization of NRG1 at C-type synapses on spinal cord MNs. In all panels, presynaptic terminals were shaded in green, and the adjacent postsynaptic region was shaded in red. In some panels, an enlarged detail of the respective micrographs is shown as an inset. A) NRG1 immunolabeling after the preembedding protocol is seen in form of amorphous electrondense deposit within the postsynaptic subsurface cistern (arrows). B) NRG1 was detected by an immunogold (12 nm) postembedding procedure after freeze-substitution tissue preparation, showing the gold particles aligned close to postsynaptic membrane of a large C-type terminal. C) C bouton displaying a NRG1-labeled multivesicular body (arrowed and shaded in yellow) interposed between the pre- and postsynaptic sides of the synapse. D) NRG1-labeled vacuolar structures are occasionally intermixed with synaptic vesicles (dashed in yellow) within presynaptic terminals of C-type synapses. E) NRG1 immunogold labeling in an ultrathin cryosection of C-type synapse; note the localization of NRG1 in the postsynaptic subsurface cistern (arrowed and shaded in yellow). F) Absence of NRG1 immunolabeling in afferent MN synapses other than C type as exemplified here by an asymmetric bouton displaying a prominent postsynaptic density (arrows). Scale bars = 200 nm (panels); 100 nm (insets).

related with afferent synaptic structures. For this reason, their association with synaptic markers was further studied. It was found that NRG1-containing spots were closely associated, but not superimposed, with cholinergic synaptic boutons identified by their positive VAChT immunoreactivity (Fig. 1A–C). The size of individual VAChT-containing spots (1.57±0.1 μm^2; n=61) was slightly, although significantly, larger than those containing NRG1 ($P<0.001$). The vast

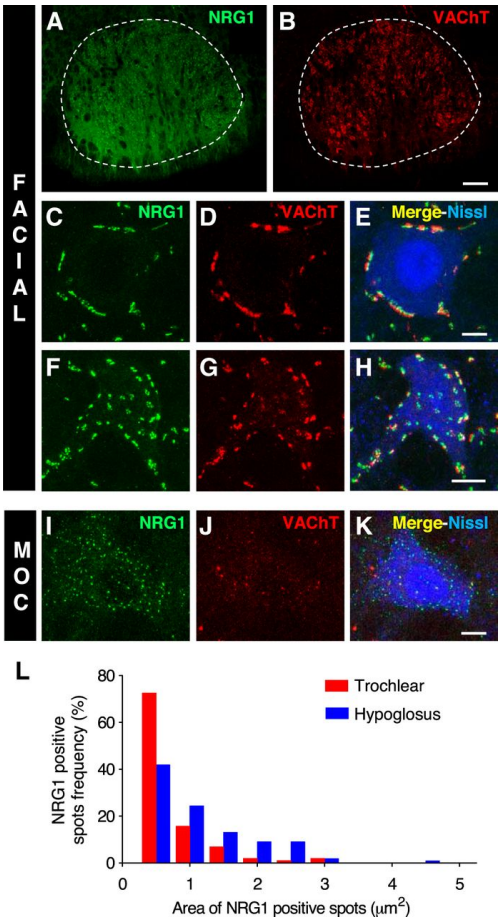

Figure 5. NRG1 immunolabeling in brain stem motor nuclei showing dissimilarities between oculomotor MNs vs. other cranial and spinal MNs. Samples were imaged after immunolabeling for NRG1 (green; A, C, F, I) combined with VAChT (red; B, D, G, J) and Nissl fluorescent staining (blue; E, H, K). A–H) Micrographs taken from the facial nucleus. A, B) Low-magnification images in which positive NRG1 immunolabeling can be seen within the whole facial nucleus (delimitated by dashed line). C–E) At higher magnification, NRG1 immunolabeling can be detected in facial MN somata in association with VAChT-immunoreactive C boutons. F–H) In a tangential section of MN surface, the clustered subunits of NRG1-positive spots at C-synapses can be seen. I–K) Representative images of a MN soma taken from oculomotor nucleus (MOC), showing the low numbers of VAChT-positive cholinergic inputs that are devoid of associated NRG1 deposits; instead, NRG1 immunoreactivity is present as widely distributed small particles on MN somata. L) Relative frequency histogram of areas of NRG1-positive spots taken from MN somata in the trochlear and hypoglosus nuclei. Note the reduced size of NRG1-positive spots in oculomotor (trochlear) MNs. Scale bars = 100 μm (A, B); 10 μm (C–K).

majority of MN synaptic boutons containing VAChT displayed closely associated NRG1-immunoreactive spots (84.6±3.6%; n=185 boutons from 27 MN somata). However, the analysis of fluorescent signals coming from NRG1 and VAChT double-labeled samples after high-resolution (0.5-μm-thick) optical sectioning in the confocal microscope revealed a clear spatial dissociation between 2 markers. This can be demonstrated after the examination of pixel profile values along a line traced on double-labeled (NRG1 plus VAChT) axosomatic synapses (Fig. 1J). Tangential optical sections allowed en face NRG1-positive patches at the MN membrane to be viewed and revealed that they were shaped by subunits of smaller spots clustered into large (~1 μm) disc-like aggregates (Fig. 1D–F). After 3D reconstruction, it was found that the organization of NRG1-containing structures closely matched complementary VAChT-containing presynaptic axonal endings (Fig. 1G–I), as expected for postsynaptic localization of NRG1.

The biological effects of NRG are mediated by the tyrosine kinase receptors erbB2-4, which are members of the epidermal growth factor receptor family (29, 30). ErbB2 cannot bind NRG1 directly but is essential for signal transduction after NRG1 binding to its receptors erbB3 or erbB4, which results in transactivation of erbB2 tyrosine kinase activity. To test whether postsynaptic NRG1 in MNs is spatially related to activated erbB2, the distribution of p-erbB2 was examined in relation to VAChT/NRG1-containing boutons. Because the only antibody available against p-erbB2 was produced in rabbits, the simultaneous double labeling with NRG1 was not feasible. However, clusters of p-erbB2 immunoreactive spots were seen colocalized presynaptically with VAChT-immunopositive synaptic boutons (Fig. 1K–M, Q). Experiments using a nonphosphorylated erbB2 antibody gave similar results but with a higher background (not shown). We also found that erbB4 was concentrated in the presynaptic nerve terminals with a similar distribution to that of erbB2 (Fig. 1N–P). These results are consistent with retrograde transcellular NRG1 signaling. Moreover, we confirmed previously reported data (31, 32) showing that postsynaptic muscarinic m2 receptors were clustered adjacent to VAChT-containing C termini. Unfortunately, the direct colocalization of muscarinic m2 receptors with NRG1 was not feasible because our antibodies were both raised in rabbits. We also corroborated the presence of NRG1 within presynaptic terminals at the neuromuscular junction (not shown) as described elsewhere (33).

The σ-1 receptor is an endoplasmic reticulum (ER) protein that has been reported to be associated with C-type synapses on MNs, with a suggested location at the postsynaptic subsurface cistern (34). Therefore, we examined whether the σ-1 receptor and NRG1 share the same subcellular compartment. We confirmed that the σ-1 receptors were present at postsynaptic sites of C boutons but, when this protein was simultaneously imaged with NRG1 at the highest magnification, both proteins were closely related but they accumulated in clearly separate domains (Fig. 2).

The possible relationship of NRG1 with other classical neurotransmitter systems on MNs was also explored. NRG1 spots were clearly dissociated from GABAergic or serotoninergic boutons identified by immunostaining of VGAT or serotonin,

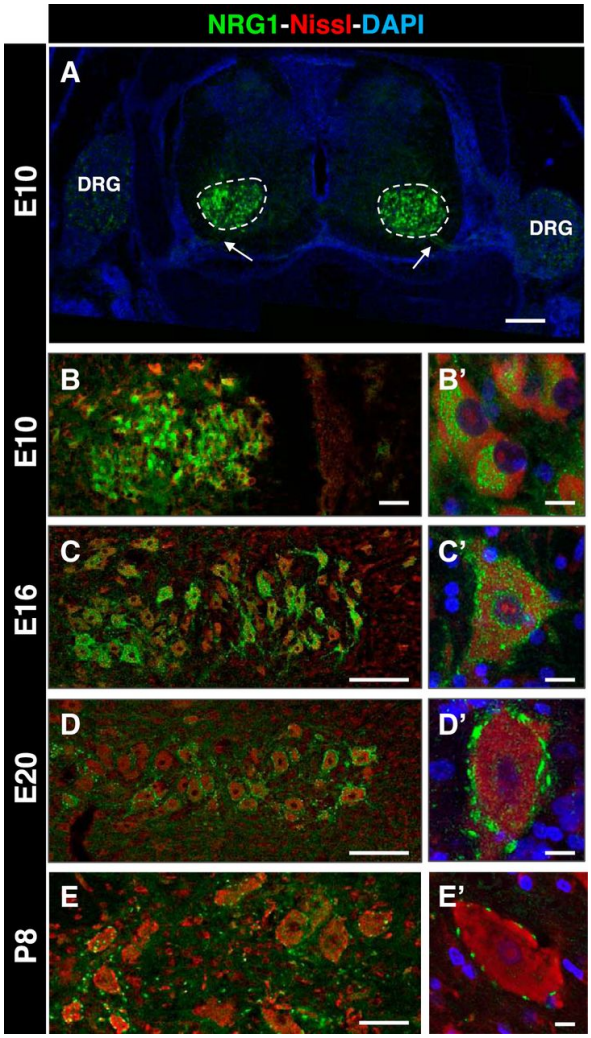

Figure 6. Developmental analysis of NRG1 expression in chick embryo spinal cord MNs. Samples at the indicated embryonic ages were processed for simultaneous visualization of NRG1 immunoreactivity (green), neuronal profiles (fluorescent Nissl staining, red) and nuclei (DAPI, blue). A) Low-magnification view of E10 whole spinal cord showing highly labeled MNs in the LMC (delimitated with a dashed line) with their emerging axons in the ventral root (arrows); DRG indicates the location of dorsal root ganglia. B–E) Developmental changes of NRG1 expression in the whole LMC are displayed at distinct ages between E10 and P8: E10 (B), E16 (C), E20 (D), and P8 (E). B′–E′) Developmental changes in NRG1 distribution within MN cell bodies are depicted from E10 to P8; note the progressive sorting of intracellular NRG1-containing structures from disseminated organization at E10–E16 (B′, C′) to a submembrane compartment at E20 (D′) and finally their concentration in the C-bouton-like region at P8 (E′). Scale bars = 200 μm (A); 50 μm (B–E); 10 μm (B′–E′).

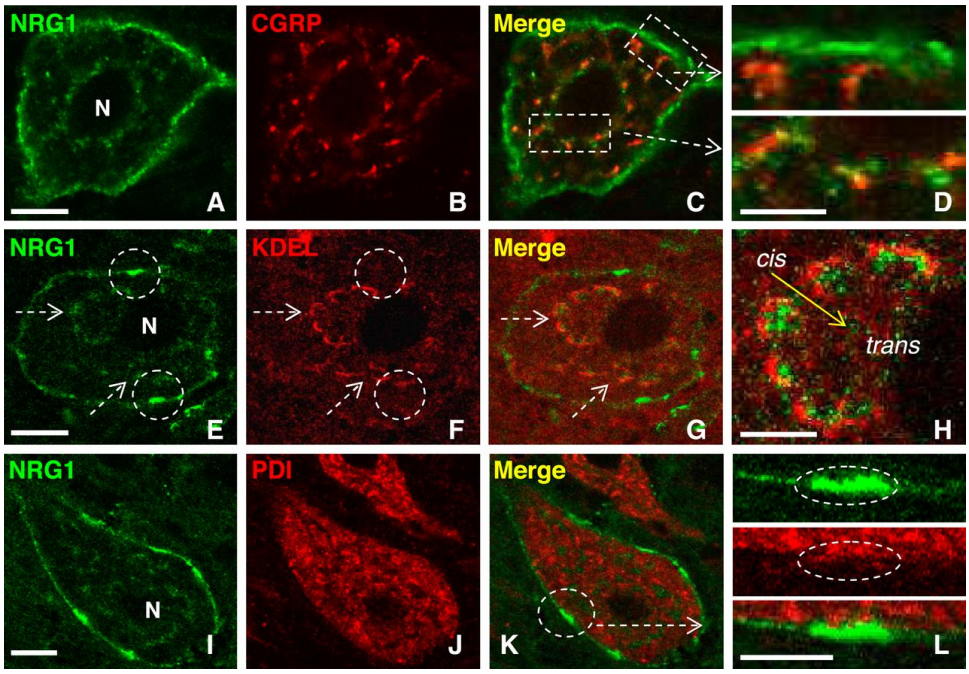

Figure 7. Accumulation of NRG1 in the submembrane compartment during subsurface cistern formation suggests differential membrane trafficking along the secretory pathway. A–C) NRG1-containing cellular compartments (green; A) were visualized in mature (E20) chick embryo MNs in combination with CGRP immunolabeling (red; B) as a marker for Golgi-secretory pathways. Note that NRG1 and CGRP colocalize extensively within membrane compartments in MN cell bodies (C), except in a region forming a marginal collar adjacent to the plasma membrane. D) Enlarged details of boxed regions in C. E–H) NRG1 immunostaining (green; E) of P8 chick spinal cord MNs was combined with KDEL receptor immunolabeling (red; F). NRG1 in the subsurface compartment is not associated with KDEL receptor (encircled); however, the NRG1 and KDEL receptors are very close to each other, without overlapping, within the Golgi region (arrows; G). H) Enlargement of the Golgi region depicted in G, in which the segregation of KDEL receptor and NRG1 into cis-trans region of Golgi is shown. I–L) NRG1 immunostaining (green; I) was combined with the ER marker PDI (red; J) in P8 chick spinal cord MNs; note the absence of colocalization between both markers (encircled in K; enlarged in L). Scale bars = 10 μm (A, E, I); 5 μm (D, H, L).

respectively (Fig. 3A–L). However, a proportion of glutamatergic boutons, containing vesicular glutamate transporter were associated with NRG1 spots (for VGLUT1: 22.1±9.5%; n=58 boutons, and for VGLUT2: 26.3±5.4%, n=68 boutons; from 5 MN somata). NRG1-positive synaptic sites did not colocalize with proprioceptive nerve terminals on MNs examined in embryonic spinal cord by their expression of parvalbumin (35; Fig. 3M–O).

Ultrastructural localization of NRG1 immunoreactivity at the C boutons

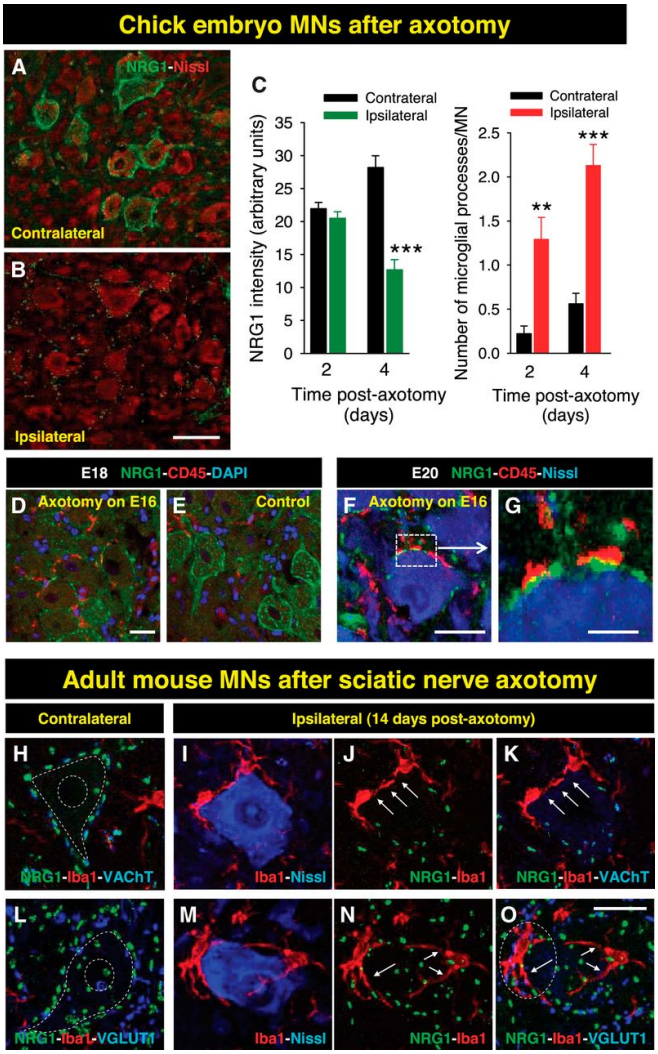

Figure 8. Changes in NRG1 expression in injured chick embryo MNs. A, B) NRG1 (green) was visualized in E20 spinal cord MNs within the lumbar lateral motor column 4 d hours after performing a peripheral nerve transection (limb amputation); contralateral (no transection surgery) side served as a control. Note that NRG1 immunolabeling was notably decreased in cell bodies of axotomized (ipsilateral) MNs (B) when compared with nonaxotomized (contralateral) control (A). Red Nissl counterstaining was applied to delimitate MN cell bodies. C) Intensity of NRG1 immunostaining (left) in MN somata and the number of CD45-positive microglial profiles (right) contacting the MN surface were quantified 2 and 4 d after axotomy performed on E16. **P < 0.01, ***P < 0.001 vs. contralateral (Student's t test). D, E) Peripheral nerve axotomy induces a microglial activation around MN cell bodies, as can be seen using anti-CD45 antibody (red), as a microglial marker, in combination with NRG1 immunostaining (green); note the increase in red profiles near MNs that are depleted of NRG1 on the surgery side (D) in relation to the control side (E). DAPI

(blue) was used as a counterstain. F, G) Detail of CD45-positive microglial profiles (red) contacting a presumably denervated C-bouton site, which can be recognized by NRG1 remnants (green); Nissl staining (blue) was applied for identification of MN soma profiles. H–O) Spinal cord MNs 14 d after sciatic nerve axotomy performed on adult mice, visualized after multiple fluorescent labeling for detection of microglia (Iba1, red), NRG1 (green), VAChT (blue; H, K), VGLUT1 (blue; L, O), and Nissl (blue; I, M). Images from nonaxotomized (contralateral; H, L) and axotomized (ipsilateral; I–K, M–O) sides are shown. Note that activated microglial cells are recruited around the soma of axotomized MNs (I, M); in regions in which microglial cells contact MN surface, a depletion of NRG1/VAChT-positive C boutons can be seen (arrows; J, K). MN afferent glutamatergic terminals, which do not colocalize with NRG1-positive spots (M–O), were also depleted in regions adjacent to microglial cell processes (arrows; N, O). Presumably synaptic stripping of glutamatergic boutons by microglial processes can be seen in the encircled region in O. MN soma profiles in H and L are delimited by dashed lines. Scale bars = 100 μm (A, B, D, E); 20 μm (F, H–O); 5 μm (G).

To determine the subcellular localization of NRG1 in MN central synapses, high-resolution immunoelectron microcopy was performed in samples of adult mouse spinal cord by using preembedding procedures (immunoperoxidase) and postembedding procedures (immunogold after either freeze-substitution or ultrathin cryosectioning). All procedures gave the same result, showing an exquisite localization of NRG1 within the postsynaptic subsurface cistern in association with MN C termini (Fig. 4A–E). C termini are large nerve boutons that contact α-MNs, displaying a characteristic cisternal formation (C, cistern) located subsynaptically and connected with MN ER (2, 3). Occasionally, intensely NRG1-immunolabeled structures resembling multivesicular bodies were seen at the intersynaptic space (Fig. 4C). NRG1-containing vacuolar structures intermixed with presynaptic vesicles at the nerve terminals were also occasionally seen (Fig. 4D). These observations may reflect a post- to presynaptic trafficking of NRG1 mediated by exosome-like vesicles, similar to what has been described for Wnt signaling at *Drosophila* neuromuscular junctions (36, 37). No labeling was found in asymmetric terminals that likely correspond to glutamatergic excitatory synapses (Fig. 4F).

NRG1 immunoreactivity in cranial motor nuclei

Serial sections of brainstem from adult mice were processed for triple labeling for Nissl to identify MN cell bodies, VAChT to visualize cholinergic synaptic terminals and NRG1 (Fig. 5A–K). In some cases, sections were also processed for either VGLUT1 or VGLUT2 immunostaining. A pattern of punctate NRG1-immunolabeling, comparable to that found in spinal cord ventral horn MNs, was associated with MN soma and proximal dendrites in most of the cranial motor nuclei, including the trigeminal (nV), facial (nVII), ambiguus (nIX/nX), and hypoglossal (nXII) motor nuclei (Fig. 5A–H). As expected, NRG1-immunopositive spots were closely associated with cholinergic VAChT-positive terminals, similar to our observations in the spinal cord described above. However, NRG1-immunoreactive spots were abundant, but noticeably small, in MNs from oculomotor nuclei [oculomotor (nIII), trochlear (nIV), and abducens (nVI); Fig. 5I–L], and these were poorly associated

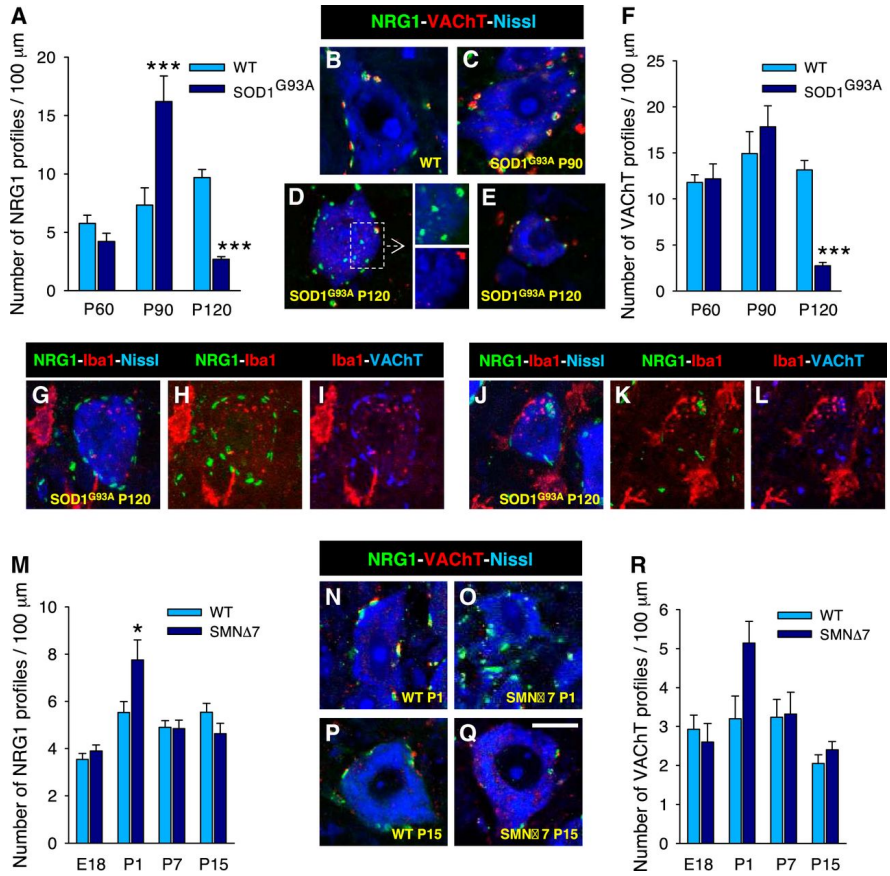

Figure 9. Changes in NRG1 and VAChT immunoreactivity in spinal cord MNs of transgenic mouse models of MN disease. Results obtained from SOD1^{G93A} ALS mice (A–L) and SMNΔ7 SMA mice (M–R). WT, age-matched wild-type animals of the corresponding disease model. A, M) Number of NRG1-positive spots at the surface of MN somata are shown infor SOD1^{G93A} (A) and SMNΔ7 (M) mice. B–E, N–Q) Representative images of counts for SOD1^{G93A} (B–E) and SMNΔ7 (N–Q) mice in which NRG1 (green), VAChT (red) immunolabeled spots, and MNs somata (blue, fluorescent Nissl labeling) are visualized. D) Insets show details of labeled area in which some NRG1-immunopositive spots (green) are devoid of VAChT staining (red) in a degenerating MN from an end-stage SOD1 ALS mouse. G–L) MNs from end-stage ALS mice in which NRG1 (green) and VAChT (blue) immunostaining were combined with Iba1 labeling (red) for microglia. G, J) VAChT staining was omitted, and MN somata were visualized by means of Nissl blue staining. G–I) In an MN in which C boutons are preserved, few microglial processes are seen adjacent to neuronal soma. J–L) Other MNs that are depleted of C boutons show extensive microglial covering. F, R) Number of VAChT-immunoreactive cholinergic boutons contacting MN somata counted in SOD1^{G93A} (F) and SMNΔ7 (R) animals and their respective WT littermates. Data in all graphs are expressed as means ± se; immunoreactive spots were counted in 70–140 MNs from 3 mice/age and experimental condition. Scale bar = 10 µm. *P < 0.05, ***P < 0.001 vs. age-matched WT animals (ANOVA with Bonferroni's test).

with synaptic structures when observed after coimmunostaining with either VAChT or VGLUT1 antibodies.

Developmental profile of NRG1 expression during MN development in the chick embryo and changes after MN injury

Many aspects of MN development have been investigated in the chick embryo model. MNs in the lateral motor column (LMC) of lumbar spinal cord start to innervate peripheral muscle after E6. During the main period of neuromuscular synaptogenesis (E6-10), chick MNs that fail to contact muscle cells are normally eliminated by apoptosis (38). Few axosomatic synapses at the LMC MNs are present before E10 but their number markedly increases between E10 and E14 and later (39). Accordingly, we analyzed the developmental profile of NRG1 immunoreactivity in chick embryo LMC MNs from E6 to posthatching (P8) ages (Fig. 6A–E′). Between E6 (not shown) and E10, NRG1 was highly expressed in the MN somata and motor axons emerging in the ventral root (Fig. 6A, B′). Within the MN soma, NRG1 immunoreactivity showed a small punctate pattern clustered in an area adjacent to the nucleus (Fig. 6B′) indicating a localization of NRG1 in the ER-Golgi secretory compartment (40). Between E14 and E20, the intracellular pool of NRG1 was progressively translocated from the paranuclear region to the most peripheral area of the MN soma close to cell surface (Fig. 6C, D′). In the most advanced developmental stages analyzed (E20–P8), the peripherally located and homogeneous-distributed NRG1 became clustered in sharply defined spots that adopted the same morphology as that described above in association with C termini in mice (Fig. 6D, E′). Thus, it appears that intracellular NRG1 is sorted into at least 2 intracellular membrane compartments: one located adjacent to MN surface, and the other shared with the secretory pathway. Because the anterograde delivered NRG1 exerts a well-defined function at the neuromuscular junction stabilizing postsynaptic nicotinic acetylcholine receptors (41, 42), we examined whether a subset of the intracellular NRG1 compartmentation is shared with CGRP, a MN neuropeptide that is known to be accumulated in trans-Golgi stacks and transported to the neuromuscular junction (43,–,46). We found that most of the intracellular NRG1-containing particles, but not those located near the MN surface, were distributed together with CGRP and dissociated from the ER-Golgi intermediate compartment involved in the retrograde transport of vesicles from Golgi to ER, as evidenced after KDEL-receptor immunolabeling (Fig. 7A–H). The subsurface compartment containing NRG1 did not colocalize with the ER marker PDI, indicating that the former is a particular domain of this organelle (Fig. 7I–L). In addition, we did not find any colocalization of the subsurface NRG1 with the endosomal markers EEA1, Rab5, and Rab11 (not shown). Since the VAChT antibodies used here do not work in chicken, we were not able to visualize the association of NRG1 spots with cholinergic nerve terminals.

To explore whether the maintenance of expression of NRG1 in chick embryo MNs is dependent on the integrity of peripheral neuromuscular connections, unilateral limb amputation (axotomy) was performed *in ovo* (47, 48). It was clearly shown that NRG1 was strongly downregulated in MNs 4 d after axotomy (Fig. 8A–C). Peripheral nerve axotomy in

the chick embryo resulted in a progressive increase, starting 2 d after lesion, in the number of CD45-immunoreactive microglial cells present in the lumbar LMC of the surgery side (ref. 25 and Fig. 8D–G). Therefore, microglial reaction precedes NRG1 down-regulation. This microglial reaction corresponds to the well-described phenomenon in axotomized rodent MNs by which microglial processes, interposed between synaptic boutons and the MN surface, mediate the removal of axosomatic synapses (49). This process of synaptic disconnection is often referred as synaptic stripping (50). In the chick embryo model, we saw that residual NRG1 immunoreactive profiles, still remaining in axotomized MNs, are intimately juxtaposed to CD45-positive microglial profiles (Fig. 8F, G). This demonstrates that, at least transiently, NRG1 persists at postsynaptic sites after removal of presynaptic boutons by synaptic stripping. To further evaluate the relationship between microglial recruitment around MNs and C-bouton removal, microglial cells identified with the anti-Iba1 antibody were examined in axotomized mouse MNs in conjunction with NRG1 and VAChT immunolabeling. It was evidenced that regions on the MN surface in which C boutons have been disappeared correspond to those that were contacted by microglial processes (Fig. 8H–K). The removal of afferent boutons contacting axotomized MNs was not specific for cholinergic terminals, since it was also observed after immunolabeling of glutamatergic boutons by means of VGLUT1 (Fig. 8L–O).

Changes in NRG1 immunolabeling in C boutons during MN disease

It has been reported that alterations in excitability play an important role in MN disease. For example, in ALS, excitability regulates the selective vulnerability of distinct MN subtypes (51,–,53), and it has been proposed that deregulation of glutamate-mediated neurotransmission causes MN excitotoxic damage (54, 55). C termini are involved in the regulation of MN activity by the activation of m2-type muscarinic receptors (12, 56) and changes in this type of synapse have been observed in ALS (20, 57, 58). On the other hand, C-bouton-mediated excitability is reported to decrease MN subtype vulnerability in ALS (53). By contrast, MN subtypes do not appear to exhibit differential susceptibility to degeneration in SMA (59). However, altered excitability and loss of afferent synaptic inputs have been observed at early stages of SMA, preceding MN cell death (60,–,62). Based on the above studies, we investigated whether correlative changes in the distribution of C-bouton-related NRG1 occur in models of MN disease. Spinal cord MNs from $SOD1^{G93A}$ mice were analyzed after double immunostaining for NRG1 and VAChT. The association between these two proteins at the synaptic boutons on the MN soma surface showed an organization similar to that described above in WT animals. Nevertheless, quantitative analysis demonstrated that changes in NRG1-positive profiles occurred during disease progression.

In $SOD1^{G93A}$ mice, the first overt clinical symptoms appear at about P90, leading to death at about P120 (63). Before symptom onset, no changes in the density of NRG1-positive profiles on MN somata were found. A significant increase in NRG1-positive spots was detected beginning at symptomatic stages (P90), whereas a decrease in NRG1 in MNs was seen at end stages of the disease (P120, Fig. 9A–E). A similar time course profile

was seen when VAChT-immunoreactive afferent boutons were quantified, although data collected at P90, due to individual variability, did not reach statistical significance (Fig. 9F). At P120, both cholinergic synapses and NRG1 immunoreactive spots showed a remarkable variability when observed in individual MNs: whereas the majority of MNs are highly depleted of C boutons containing both NRG1 and VAChT (Fig. 9E), some MNs depleted of VAChT-positive boutons displayed high numbers of NRG1-positive spots (Fig. 9D), suggesting that degeneration of cholinergic afferents precedes NRG1 loss in the SSC. To analyze the relationship between C-bouton loss and microglia activation, P120 tissue samples were additionally immunolabeled with anti-Iba1 antibody. We observed that the extent of microglial covering on degenerating MNs correlates with the degree of C-bouton loss (Fig. 9G–L), in a similar way that occurs in axotomized MNs. Interestingly, a transient increase in NRG1-positive spots was also observed early (P1) in SMNΔ7 mice (Fig. 9M–Q). This is in concordance with ultrastuctural studies showing an increase in C boutons and a decrease in other MN afferent terminals in SMNΔ7 mice (63). In this model, the mean life span is of ~14–15 d, and symptoms begin at P7–P8 (64); therefore, NRG1 up-regulation takes place before the onset of symptoms. The results on VAChT immunoreactivity were similar to those for NRG1 (Fig. 9R).

4 DISCUSSION

C termini are intriguing synaptic structures that are specific for α-MNs and were morphologically identified >40 yr ago (2, 9). More recently, there has been an increased interest in C termini. After the cholinergic phenotype of C boutons and their association with m2 muscarinic receptors is recognized (11, 31, 65), other molecular aspects of these synapses such as expression of voltage-gated Kv2.1 (66), Ca^{2+}-activated K^+ (SK) channels (67), connexin32 (68), VAMP-2 (11), and σ-1 receptors (69) have also been described. NRG1, a ligand for erbBs, has been previously suggested to be present in cholinergic terminals apposed to MNs (15), but its exact localization was unknown. Here, we show unambiguously that NRG1 is associated with C boutons and is concentrated in postsynaptic sites within the subsurface cistern. We also observed that erbB2 and erbB4 receptors are present in the presynaptic compartment indicating that NRG1 acts as a retrograde signaling molecule in C-type synapses. Since NRG1-immunolabeled exosome-like vesicles were occasionally seen within the synaptic cleft, the possibility that exosomes participate in NRG1 retrograde synaptic signaling should be further investigated (see ref. 70).

NRG1 has pleiotropic regulatory actions in different vertebrate cell types. It is involved in the development and maintenance of cardiovascular and nervous systems and appears to play a role in pathological conditions such as schizophrenia and cancer (71). In the neuromuscular system, NRG1 is expressed by MNs and regulates the differentiation and survival of Schwann cells, and its delivery at the neuromuscular junction determines the expression of postsynaptic AChRs (33, 72,–,75). We show here that, in contrast to NRG1 associated with C boutons, this protein is also localized with CGRP in the MN endomembrane system. This suggests that NRG1 is differentially sorted into 2 distinct pathways: one addressed to subsurface cisterns at C-

type synapses, and the other, shared with CGRP but not with KDEL receptor, destined to be anterogradely transported either for axon-Schwann cell signaling or for delivery to the neuromuscular junction.

Note that substantial differences in NRG1 immunolabeling exist in MNs of oculomotor nuclei when compared with other MN population: NRG1 immunoreactivity in oculomotor MN somata is exclusively located in small, punctate, and scattered particles, whereas larger structures, with the typical morphology of C-bouton-associated NRG1, are absent. This is consistent with the absence of C-type synaptic afferents on these MN subtypes. Type m2 cholinergic receptors are also not found in oculomotor MNs (31).

The role of subsurface cistern in C-type synapses is not known. The only molecule previously reported to accumulate in this compartment is the σ-1 receptor (34). However, we show here that NRG1 is also present in the subsurface cistern, but predominantly located in a different subcompartment.

It is known that peripheral nerve injury induces the loss of synapses on axotomized MNs (49) as well as the redistribution of molecules present in C boutons (76). Our results on NRG1 in axotomized MNs are in concordance with the down-regulation of this protein in mouse MNs after nerve injury (77). The prominent morphological changes in ER-Golgi-derived membrane compartments described in chromatolytic MNs may account for the NRG1 alterations we observed postaxotomy (78). In addition, the possible role of NRG1 in the recruitment of microglial cells and synaptic stripping in MNs after axotomy should be further investigated. It should be taken into account that microglia express ErBbs, and NRG1 signaling, via these receptors, is involved in postinjury microglial activation and chemotaxis in spinal dorsal horn after sensory nerve transection (79).

A variety of alterations in C-type synapses have been reported in ALS, some of which involve the subsurface cistern components. For instance, it has been reported the following: mutations in σ-1 receptor causes juvenile ALS (80); in a mouse model of ALS, life span is decreased in the absence of σ-1 receptor (69); and treatment with a σ-1 receptor agonist is neuroprotective (81, 82). In addition, the σ-1 receptor in human spinal cord MNs is abnormally distributed in ALS (83). Other morphological alterations of the subsurface cisterns also appear to be present in ALS-linked mutations of vesicle-associated membrane protein-associated protein B, which is abnormally targeted to C boutons altering their function (VAPB, ALS8; ref. 84). On the other hand, NRG1-erbB signaling is involved in ALS pathogenesis and erbB4 mutations, which lead to a reduced autophosphorylation of erbB4 protein after NRG1 stimulation and are associated with a hereditary late onset ALS (85). Reduced amounts of NRG1 in spinal cord MNs have been observed in human sporadic ALS and in $SOD1^{G93A}$ mice (86).

ErbB4 receptor protein is particularly enriched in glutamatergic synapses on cerebral inhibitory interneurones (87). On the other hand, NRG1 stimulates the formation of synapses and increases their size in adults suggesting that NRG1 strengthens existing synapses (88). C boutons originate from spinal cord cholinergic interneurones that, among others, drive MN activity (12) The

blockade of m2 muscarinic receptors at C boutons leads to in a decrease in MN firing (56). It is plausible that NRG1-ErbB4 signaling contributes to regulation of MN activity by modulating the function of cholinergic interneurones. In pathological conditions, this may have important consequences determining MN vulnerability. For example, blocking cholinergic neurotransmission through C boutons results in an increase in neurotoxic mifolded SOD1 in MNs of SOD1 ALS mouse model (53). Another aspect that may be relevant in ALS and SMA is whether NRG1-ErbB4 takes also a role in the regulation of neuroinflammatory events mediated by microglial in these diseases.

Our findings locating NRG1 within subsurface cistern and the changes we observed in MN diseases open new avenues for revealing the role of this protein in the alterations of C termini in ALS and its relevance in the pathogenesis of the disease (19, 20, 53, 58, 89, 90). Future pharmacological assays targeting NRG1/ErbBs signaling pathway associated to C boutons should be performed to further evaluate its potential therapeutic relevance.

5 ACKNOWLEDGEMENTS

The authors thank Dr. Ronald W. Oppenheim and Sherry Vinsant for critical reading of the manuscript and for helpful comments and suggestions. The authors also thank Dr. Elisabet Dachs, Clàudia Cerveró, and Alexandra Eritja for help in some parts of this study.

This work was supported by grants from the Ministerio de Ciencia y Tecnología and Ministerio de Economía y Competitividad, financed jointly with Federación Española de Enfermedades Raras (SAF2011-22908; SAF2012-31831) and the Fundación Genoma España/ Fundación Atrofia Muscular Espinal.

6 REFERENCES

1. Rekling, J.C., Funk, G.D., Bayliss, D.A., Dong, X.W., Feldman, J.L. (2000) Synaptic control of motoneuronal excitability. Physiol. Rev. 80, 767-852.

2. Conradi, S. (1969) Ultrastructure and distribution of neuronal and glial elements

on the surface of the proximal part of a motoneuron dendrite, as analyzed by serial sections. Acta Physiol. Scand. 332(Suppl), 49–64.

3. Bodian, D. (1970) An electron microscopic characterization of classes of synaptic vesicles by means of controlled aldehyde fixation. J. Cell Biol. 44, 115-124.

4. Bernstein, J.J., Bernstein, M.E. (1976) Ventral horn synaptology in the rat. J. Neurocytol. 5, 109-123.

5. Destombes, J., Horcholle-Bossavit, G., Thiesson D. (1992) Distribution of glycinergic terminals on lumbar motoneurones of the adult cat: an ultrastructural study. Brain Res. 599, 353–360.

6. Destombes, J., Horcholle-Bossavit, G., Simon, M., Thiesson D. (1996) GABAlike immunoreactive terminals on lumbar motoneurones of the adult cat. A quantitative ultrastructural study. Neurosci. Res. 24, 123-130.

7. Murphy, S.M., Pilowsky, P.M., Llewellyn-Smith, I.J. (1996) Vesicle shape and amino acids in synaptic inputs to phrenic motoneurones: do all inputs contain either

glutamate or GABA? J. Comp. Neurol. 373, 200-219.

8. Örnung, G., Shupliakov, O., Linda, H., Ottersen, O.P., Storm-Mathisen, J., Ulfhake, B., Cullheim, S. (1996) Qualitative and quantitative analysis of glycine- and GABA-immunoreactive nerve terminals on motoneuron cell bodies in the cat spinal cord: a postembedding electron microscopic study. J. Comp. Neurol. 365, 413-426.

9. Conradi, S. (1969) Ultrastructure and distribution of neuronal and glial elements on the motoneuron surface in the lumbosacral spinal cord of the adult cat. Acta Physiol. Scand. 332 (Suppl), 5-48.

10. Nagy, J.I., Yamamoto, T., Jordan. L.M. (1993) Evidence for the cholinergic nature of C-terminals associated with subsurface cisterns in alpha-motoneurones of rat. Synapse 15, 17-32.

11. Hellström, J., Arvidsson, U., Elde, R., Cullheim, S., Meister, B. (1999) Differential expression of nerve terminal protein isoforms in VAChT-containing varicosities of the spinal cord ventral horn. J. Comp. Neurol. 411, 578-590.

12. Zagoraiou, L., Akay, T., Martin, J.F., Brownstone, R.M., Jessell, T.M., Miles, G.B. (2009) A cluster of cholinergic premotor interneurones modulates mouse locomotor activity. Neuron 64, 645-662.

13. Witts, E.C., Zagoraiou, L., Miles, G.B. (2013) Anatomy and function of cholinergic C bouton inputs to motor neurones. J. Anat. 224, 52-60.

14. Frank, E. (2009) A new class of spinal interneurones: the origin and function of C-bouton solved. Neuron 64, 593-595.

15. Issa, A.N., Zhan, W.Z., Sieck, G.C., Mantilla, C.B. (2010) Neuregulin-1 at synapses on phrenic motoneurones. J. Comp. Neurol. 518, 4213-4225.

16. Pullen, A.H., Sears, T.A. (1983) Trophism between C-type axon terminals and thoracic motoneurones in the cat. J. Physiol. 337, 373-388.

17. Novikov, L.N., Novikova, L.N., Holmberg, P., Kellerth. J. (2000) Exogenous brain-derived neurotrophic factor regulates the synaptic composition of axonally lesioned and normal adult rat motoneurones. Neuroscience 100, 171-181.

18. Pullen, A.H. (1992) Presynaptic terminal loss from alpha-motoneurones following the retrograde axonal transport of diphtheria toxin. Acta Neuropathol. 83, 488-498.

19. Nagao, M., Misawa, H., Kato, S., Hirai, S. (1998) Loss of cholinergic synapses on the spinal motor neurones of amyotrophic lateral sclerosis. J. Neuropathol. Exp. Neurol. 57, 329-333.

20. Pullen, A.H., Athanasiou, D. (2009) Increase in presynaptic territory of Cterminals on lumbar motoneurones of G93A SOD1 mice during disease progression. Eur. J. Neurosci. 29, 551-561

21. Gallart-Palau, X., Tarabal, O., Casanovas, A., Sábado, J., Correa, F., Cerveró, C., Hereu, M., Piedrafita, L., Calderó, J., Esquerda, J.E. (2013) Neuregulin-1 is associated with postsynaptic sites contacting afferent C-type cholinergic terminals on lower motoneurones: changes in murine models of motoneuron diseases. Amyotroph. Lateral. Scler. Frontotemporal Degener.

14 (Suppl. 2), 186. Doi: 10.3109/21678421.2013.838424/228

22. Hamburger, V., Hamilton, H.L. (1951) A series of normal stages in the development of the chick embryo. J. Morphol. 88, 49-92.

23. Ripps, M.E., Huntley, G.W., Hof, P.R., Morrison, J.H., Gordon, J.W. (1995) Transgenic mice expressing an altered murine superoxide dismutase gene provide an animal model of amyotrophic lateral sclerosis. Proc. Natl. Acad. Sci. U.S.A. 92, 689-693.

24. Le, T.T., Pham, L.T., Butchbach, M.E.R., Zhang, H.L., Monani, U.R., Coovert, D.D., Gavrilina, T.O., Xing, L., Bassell, G.J., Burghes, A.H.M. (2005) SMNDelta7, the major product of the centromeric survival motor neuron (SMN2) gene, extends survival in mice with spinal muscular atrophy and associates with full-length SMN. Hum. Mol. Genet. 14, 845-857.

25. Calderó, J., Brunet, N., Ciutat, D., Hereu, M., Esquerda, J.E. (2009) Development of microglia in the chick embryo spinal cord: implications in the regulation of motoneuronal survival and death. J. Neurosci. Res. 87, l2447-2466.

26. Rubio, M.E., Wenthold, R.J. (1999) Differential distribution of intracellular glutamate receptors in dendrites. J. Neurosci. 19, 5549-5562.

27. Tokuyasu, K.T. (1997). Immunocytochemistry on ultrathin cryosections. In Cells: A laboratory manual (Spector, D.L., Goldman, R.D., Leonwand, L.A., eds), 131, 1-27, Cold Spring Harbor Laboratory Press, NY.

28. Slot, J.W., Geuze, H.J. (2007) Cryosectioning and immunolabeling. Nat. Protoc. 2, 2480-2491.

29. Sliwkowski, M.X., Schaefer, G., Akita, R.W., Lofgren, J.A., Fitzpatrick, V.D., Nuijens, A., Fendly, B.M., Cerione, R.A., Vandlen, R.L., Carraway III, K.L. (1994) Coexpression of erbB2 and erbB3 proteins reconstitutes a high affinity receptor for heregulin. J. Biol. Chem. 269, 14661-14665.

30. Mei, L., Xiong, W.C. (2008) Neuregulin 1 in neural development, synaptic plasticity and schizophrenia. Nat. Rev. Neurosci. 9, 437-452.

31. Hellström, J., Oliveira, A.L., Meister, B., Cullheim, S. (2003) Large cholinergic nerve terminals on subsets of motoneurones and their relation to muscarinic receptor type 2. J. Comp. Neurol. 460, 476-486.

32. Wilson, J.M., Rempel, J., Brownstone, R.M. (2004) Postnatal development of cholinergic synapses on mouse spinal motoneurones. J. Comp. Neurol. 474, 13-23.

33. Rimer, M., Cohen, I., Lømo, T., Burden, S.J., McMahan, U.J. (1998) Neuregulins and erbB receptors at neuromuscular junctions and at agrin-induced postsynaptic-like apparatus in skeletal muscle. Mol. Cell Neurosci. 12, 1-15.

34. Mavlyutov, T.A., Epstein, M.L., Andersen, K.A., Ziskind-Conhaim. L., Ruoho. A.E. (2010) The sigma-1 receptor is enriched in postsynaptic sites of Cterminals in mouse motoneurones. An anatomical and behavioral study. Neuroscience 167, 247-255.

35. Ichikawa, H., Mo, Z., Xiang, M., Sugimoto, T. (2004) Effect of Brn-3a deficiency on parvalbumin-immunoreactive primary sensory neurones in the dorsal root ganglion. Brain Res. Dev. Brain Res. 150, 41-45.

36. Korkut, C., Ataman, B., Ramachandran, P., Ashley, J., Barria, R., Gherbesi, N., Budnik, V. (2009) Trans-synaptic transmission of vesicular Wnt signals through Evi/Wntless. Cell 139, 393-404.

37. Korkut, C., Li, Y., Koles, K., Brewer, C., Ashley, J., Yoshihara, M., Budnik, V. (2013) Regulation of postsynaptic retrograde signaling by presynaptic exosome release. Neuron 77, 1039-1046.

38. Oppenheim, R.W. (1981) Neuronal death and some related regressive phenomena during neurogenesis: A selective historical review and progress report. In Studies in Developmental Neurobiology: Essays in Honor of Viktor Hamburger (Cowan, W.M., ed.) pp. 74-133, Oxford University Press, New York.

39. Oppenheim, R.W., Chu-Wang, I.W., Foelix, R.F. (1975) Some aspects of synaptogenesis in the spinal cord of the chick embryo: a quantitative electron microscopic study. J. Comp. Neurol. 161, 383-418.

40. Tarabal, O., Calderó, J., Casas, C., Oppenheim, R.W., Esquerda, J.E. (2005) Protein retention in the endoplasmic reticulum, blockade of programmed cell death and autophagy selectively occur in spinal cord motoneurones after glutamate receptor-mediated injury. Mol. Cell Neurosci. 29, 283-298.

41. Schaeffer, L.., de Kerchove d'Exaerde, A., Changeux, J.P. (2001). Targeting transcription to the neuromuscular synapse. Neuron 31, 15-22.

42. Schmidt, N., Akaaboune, M., Gajendran, N., Martinez-Pena y Valenzuela, I., Wakefield, S., Thurnheer, R., Brenner, H.R. (2011) Neuregulin/ErbB regulate neuromuscular junction development by phosphorylation of α-dystrobrevin. J. Cell Biol. 195, 1171-1184.

43. Calderó J, Casanovas A, Sorribas A, Esquerda JE (1992) Calcitonin gene-related peptide in rat spinal cord motoneurones: subcellular distribution and changes induced by axotomy. Calcitonin gene-related peptide in rat spinal cord motoneurones: subcellular distribution and changes induced by axotomy. Neuroscience 48, 449-461.

44. Tarabal O, Calderó J, Lladó J, Oppenheim RW, Esquerda JE (2001) Longlasting aberrant tubulovesicular membrane inclusions accumulate in developing motoneurones after a sublethal excitotoxic insult: a possible model for neuronal pathology in neurodegenerative disease. J. Neurosci. 21, 8072-8081.

45. Sala, C., Andreose, J.S., Fumagalli, G., Lømo, T. (1995) Calcitonin gene-related peptide: possible role in formation and maintenance of neuromuscular junctions. J. Neurosci. 15, 520-528.

46. Tarabal, O., Calderó, J., Ribera, J., Sorribas, A., López, R., Molgó, J., Esquerda, J.E. (1996) Regulation of motoneuronal calcitonin gene-related peptide (CGRP) during axonal growth and neuromuscular synaptic plasticity

induced by botulinum toxin in rats. Eur. J. Neurosci. 8, 829-836.

47. Houenou, L.J., Li, L., Lo, A.C., Yan, Q., Oppenheim, R.W. (1994) Naturally occurring and axotomy-induced motoneuron death and its prevention by neurotrophic agents: a comparison between chick and mouse. Prog. Brain Res. 102, 217-226.

48. Brunet, N., Tarabal, O., Portero-Otín, M., Oppenheim, R.W., Esquerda, J.E., Calderó, J. (2007) Survival and death of mature avian motoneurones in organotypic slice culture: trophic requirements for survival and different types of degeneration. J. Comp. Neurol. 501, 669-690.

49. Blinzinger, K., Kreutzberg, G. (1968) Displacement of synaptic terminals from regenerating motoneurones by microglial cells. Z. Zellforsch Mikrosk. Anat. 85, 145-157.

50. Moran, L.B., Graeber, M.B. (2004) The facial nerve axotomy model. Brain Res. Rev. 44, 154–178.

51. Pun, S., Santos, A.F., Saxena, S., Xu, L., and Caroni, P. (2006). Selective vulnerability and pruning of phasic motoneuron axons in motoneuron disease alleviated by CNTF. Nat. Neurosci. 9, 408–419.

52. Kanning, K.C., Kaplan, A., Henderson, C.E. (2010). Motor neuron diversity in development and disease. Annu. Rev. Neurosci. 33, 409–440.

53. Saxena, S., Roselli, F., Singh, K., Leptien, K., Julien, J.P., Gros-Louis, F., Caroni, P. (2013) Neuroprotection through excitability and mTOR required in ALS motoneurones to delay disease and extend survival. Neuron 80, 80-96.

54. Rothstein, J.D., Martin, L.J., Kuncl, R.W. (1992) Decreased glutamate transport by the brain and spinal cord in amyotrophic lateral sclerosis. N. Engl. J. Med. 326, 1464–1468.

55. Van Den Bosch, L., Van Damme, P., Bogaert, E., Robberecht, W. (2006). The role of excitotoxicity in the pathogenesis of amyotrophic lateral sclerosis. Biochim. Biophys. Acta 1762, 1068-1082.

56. Miles, G.B., Hartley, R., Todd, A.J., Brownstone, R.M. (2007) Spinal cholinergic interneurones regulate the excitability of motoneurones during locomotion. Proc. Natl. Acad. Sci. U.S.A. 104, 2448-2453.

57. Vinsant, S., Mansfield, C., Jimenez-Moreno, R., Moore, V.D.G., Yoshikawa, M., Hampton, T.G., Prevette, D., Caress, J., Oppenheim, R.W., Milligan, C. (2013) Characterization of early pathogenesis in the SOD1 G93Amouse model of ALS: part I, background and methods. Brain Behav. 3, 335-50.

58. Vinsant, S., Mansfield, C., Jimenez-Moreno, R., Del Gaizo Moore, V., Yoshikawa, M., Hampton, T.G., Prevette, D., Caress, J., Oppenheim, R.W., Milligan, C. (2013). Characterization of early pathogenesis in the SOD1G93A mouse model of ALS: part II, results and discussion. Brain Behavior. 3, 431- 457.

59. Thomson, S.R., Nahon, J.E., Mutsaers, C.A., Thomson, D., Hamilton, G., Parson, S.H., Gillingwater, T.H. (2012) Morphological characteristics of motor neurones do not determine their relative susceptibility to degeneration in a mouse

model of severe spinal muscular atrophy. PLoS One 7, e52605.

60. Ling, K.K., Lin, M.Y., Zingg, B., Feng, Z., Ko, C.P. (2010) Synaptic defects in the spinal and neuromuscular circuitry in a mouse model of spinal muscular atrophy. PLoS One 5, e15457.

61. Mentis, G.Z., Blivis, D., Liu, W., Drobac, E., Crowder, M.E., Kong, L., Alvarez, F.J., Sumner, C.J., O'Donovan, M.J. (2011) Early functional impairment of sensory-motor connectivity in a mouse model of spinal muscular atrophy. Neuron 69, 453-467.

62. Turner, B.J., Talbot, K. (2008) Transgenics, toxicity and therapeutics in rodent models of mutant SOD1-mediated familial ALS. Prog. Neurobiol. 85, 94–134.

63. Tarabal O, Caraballo-Miralles V, Cardona-Rossinyol A, Correa FJ, Olmos G, Lladó J, Esquerda JE, Calderó J (2014) Mechanisms involved in spinal cord central synapse loss in a mouse model of spinal muscular atrophy. J. Neuropathol Exp. Neurol. (in press).

64. Sleigh, J.N., Gillingwater, T.H., Talbot, K. (2011) The contribution of mouse models to understanding the pathogenesis of spinal muscular atrophy. Dis. Model Mech. 4, 457-467.

65. Li, W., Ochalski, P.A., Brimijoin, S., Jordan, L.M., Nagy, J.I. (1995) Cterminals on motoneurones: electron microscope localization of cholinergic markers in adult rats and antibody-induced depletion in neonates. Neuroscience 65, 879-891.

66.Muennich, E.A., Fyffe, R.E. (2004) Focal aggregation of voltage-gated, Kv2.1 subunit-containing, potassium channels at synaptic sites in rat spinal motoneurones. J. Physiol. 554, 673-685.

67. Deardorff, A.S., Romer, S.H., Deng, Z., Bullinger, K.L., Nardelli, P., Cope, T.C., Fyffe, R.E. (2013) Expression of postsynaptic Ca2+-activated K+ (SK) channels at C-bouton synapses in mammalian lumbar α-motoneurones. J. Physiol. 591, 875-897.

68. Yamamoto, T., Hertzberg, E.L., Nagy, J.I. (1991) Subsurface cisterns in alphamotoneurones of the rat and cat: immunohistochemical detection with antibodies against connexin32. Synapse 8, 119-136.

69. Mavlyutov, T.A., Epstein, M.L., Verbny, Y.I., Huerta, M.S., Zaitoun, I., Ziskind-Conhaim, L., Ruoho, A.E. (2013) Lack of sigma-1 receptor exacerbates ALS progression in mice. Neuroscience 240, 129-134.

70. Ronnevi, L.O. (1979) Spontaneous phagocytosis of C-type synaptic terminals by spinal alpha-motoneurones in newborn kittens. An electron microscopic study. Brain Res. 162, 189-199.

71. Banerjee, A., Macdonald, M.L., Borgmann-Winter, K.E., Hahn, C.G. (2010) Neuregulin 1-erbB4 pathway in schizophrenia: From genes to an interactome. Brain Res. Bull. 83, 132-139.

72. Corfas, G., Rosen, K.M., Aratake, H., Krauss, R., Fischbach, G.D. (1995) Differential expression of ARIA isoforms in the rat brain. Neuron 14, 103-115.

73. Syroid, D.E., Maycox, P.R., Burrola, P.G., Liu, N., Wen, D., Lee, K.F., Lemke, G., Kilpatrick, T.J. (1996) Cell death in the Schwann cell lineage and its regulation

by neuregulin. Proc. Natl. Acad. Sci. U.S.A. 93, 9229–9234.

74. Jessen, K.R., Mirsky, R. (2005) The origin and development of glial cells in peripheral nerves. Nat. Rev. Neurosci. 6, 671-682.

75. Rimer, M. (2007) Neuregulins at the neuromuscular synapse: past, present, and future. J. Neurosci. Res. 85, 1827-1833.77.

76. Romer, S.H., Dominguez, K.M., Gelpi, M.W., Deardorff, A.S., Tracy, R.C., Fyffe, R.E. (2013) Redistribution of Kv2.1 ion channels on spinal motoneurones following peripheral nerve injury. Brain Res. doi: 10.1016/j.brainres.2013.12.012.

77. Stassart, R.M., Fledrich, R., Velanac, V., Brinkmann, B.G., Schwab, M.H., Meijer, D., Sereda, M.W., Nave, K.A. (2013) A role for Schwann cell-derived neuregulin-1 in remyelination. Nat. Neurosci. 16, 48-54.

78. Fujita, Y., Watabe, K., Ikeda, K., Mizuno, Y., Okamoto, K. (2011) Morphological changes of Golgi apparatus in adult rats after facial nerve injuries. Neuropathology 31, 42-47.

79. Calvo M1, Zhu N, Tsantoulas C, Ma Z, Grist J, Loeb JA, Bennett DL (2010) Neuregulin-ErbB signaling promotes microglial proliferation and chemotaxis contributing to microgliosis and pain after peripheral nerve injury. J. Neurosci. 30:5437-5450.

80. Al-Saif, A., Al-Mohanna, F., Bohlega, S. (2011) A mutation in sigma-1 receptor causes juvenile amyotrophic lateral sclerosis. Ann. Neurol. 70, 913-919.

81. Mancuso, R., Oliván, S., Rando, A., Casas, C., Osta, R., Navarro, X. (2012) Sigma-1R agonist improves motor function and motoneuron survival in ALS mice. Neurotherapeutics 9, 814-826.

82. Peviani, M., Salvaneschi, E., Bontempi, L., Petese, A., Manzo, A., Rossi, D., Salmona, M., Collina, S., Bigini, P., Curti, D. (2013) Neuroprotective effects of the Sigma-1 receptor (S1R) agonist PRE-084, in a mouse model of motor neuron disease not linked to SOD1 mutation. Neurobiol. Dis. 62, 218-232.

83. Prause, J., Goswami, A., Katona, I., Roos, A., Schnizler, M., Bushuven, E., Dreier, A., Buchkremer, S., Johann, S., Beyer, C., Deschauer, M., Troost, D., Weis, J. (2013) Altered localization, abnormal modification and loss of function of Sigma receptor-1 in amyotrophic lateral sclerosis. Hum. Mol. Genet. 22, 1581-1600.

84. Aliaga, L., Lai, C., Yu, J., Chub, N., Shim, H., Sun, L., Xie, C., Yang, W.J., Lin, X., O'Donovan, M.J., Cai, H. (2013) Amyotrophic lateral sclerosis-relatedVAPB P56S mutation differentially affects the function and survival of corticospinal and spinal motor neurones. Hum. Mol. Genet. 22, 4293-4305.

85. Takahashi, Y., Fukuda, Y., Yoshimura, J., Toyoda, A., Kurppa, K., Moritoyo, H., Belzil, V.V., Dion, P.A., Higasa, K., Doi, K., Ishiura, H., Mitsui, J., Date, H., Ahsan, B., Matsukawa, T., Ichikawa, Y., Moritoyo, T., Ikoma, M., Hashimoto, T., Kimura, F., Murayama, S., Onodera, O., Nishizawa, M., Yoshida, M., Atsuta, N., Sobue, G.; JaCALS, Fifita, J.A., Williams, K.L., Blair, I.P., Nicholson, G.A., Gonzalez-Perez, P., Brown, R.H. Jr., Nomoto, M., Elenius, K., Rouleau, G.A., Fujiyama, A., Morishita, S., Goto, J., Tsuji, S. (2013) ERBB4 Mutations

that Disrupt the Neuregulin-ErbB4 Pathway Cause Amyotrophic Lateral Sclerosis Type 19. Am. J. Hum. Genet. 93, 900-905.

86. Song, F., Chiang, P., Wang, J., Ravits, J., Loeb, J.A. (2012) Aberrant neuregulin 1 signaling in amyotrophic lateral sclerosis. J. Neuropathol. Exp. Neurol. 71, 104-115.

87. Vullhorst D1, Neddens J, Karavanova I, Tricoire L, Petralia RS, McBain CJ, Buonanno J Neurosci. (2009) Selective expression of ErbB4 in interneurones, but not pyramidal cells, of the rodent hippocampus. J. Neurosci. 29,12255–12264

88. Ting AK1, Chen Y, Wen L, Yin DM, Shen C, Tao Y, Liu X, Xiong WC, Mei L. (2011) Neuregulin 1 promotes excitatory synapse development and function in GABAergic interneurones. J. Neurosci. 3,15-25

89. Chang, Q., Martin, L.J. (2009) Glycinergic innervation of motoneurones is deficient in amyotrophic lateral sclerosis mice: a quantitative confocal analysis. Am. J. Pathol. 174, 574-585.

90. Herron, L.R., Miles, G.B. (2012) Gender-specific perturbations in modulatory inputs to motoneurones in a mouse model of amyotrophic lateral sclerosis. Neuroscience 226, 313-323.

Received for publication January 22, 2014.
Accepted for publication April 21, 2014.

Extracellular vesicles are rapidly purified from human plasma by PRotein Organic Solvent PRecipitation (PROSPR).

Gallart-Palau et al. Scientific Reports 5, (2015) Article number: 14664.

Scientific Reports 5 (2015), Article number 14664

EXTRACELLULAR VESICLES ARE RAPIDLY PURIFIED FROM HUMAN PLASMA BY PROTEIN ORGANIC SOLVENT PRECIPITATION (PROSPR)

Xavier Gallart-Palau[1], Aida Serra[1], Andrew See Weng Wong[1], Sara Sandin[1], Mitchell K. P. Lai[2,3], Christopher P. Chen[2,3], Oi Lain Kon[4], Siu Kwan Sze[1*]

[1]School of Biological Sciences, Nanyang Technological University, Singapore, 637551.
[2]Department of Pharmacology, Yong Loo Lin School of Medicine, National University of Singapore, Singapore.
[3]Memory, Aging and Cognition Centre, National University Health System, Singapore.
[4]Division of Medical Sciences, Humphrey Oei Institute of Cancer Research, National Cancer Centre Singapore, 11 Hospital Drive, Singapore 169610.

Abstract

Extracellular vesicles (EVs) such as exosomes and microvesicles mediate intercellular communication and regulate a diverse range of crucial biological processes. Host cells that are damaged, infected or transformed release biomarker-containing EVs into the peripheral circulation, where they can be readily accessed for use in diagnostic or prognostic testing. However, current methods of EV isolation from blood plasma are complex and often require relatively large sample volumes, hence are inefficient for widespread use in clinical settings. Here, we report a novel and inexpensive method of rapidly isolating EVs from small volumes of human blood plasma by PRotein Organic Solvent PRecipitation (PROSPR). PROSPR encompasses a rapid three-step protocol to remove soluble proteins from plasma via precipitation in cold acetone, leaving the lipid-encapsulated EVs behind in suspension. This generates higher purity EVs that can then be obtained from filtration or classical ultracentrifugation methods. We foresee that PROSPR-based purification of EVs will significantly accelerate the discovery of new disease biomarkers and the characterization of EVs with potential for clinical applications.

Keywords: Extracellular vesicles, Exosome, Blood plasma, PROSPR, Biomarker, Biochemical Purification

* Corresponding author
Siu Kwan SZE, PhD
School of Biological Sciences
Division of Chemical Biology & BioTechnology
Nanyang Technological University,
60 Nanyang Drive, Singapore 637551
Tel: +65: 6514-1006
Fax: +65: 6791-3856
Email: skszе@ntu.edu.sg

INTRODUCTION

Extracellular vesicles (EVs) are critical mediators of intercellular communication that regulate a diverse range of biological and pathological processes including leukocyte responses, cancer development and neurodegeneration. Host cells that are damaged, infected or transformed release biomarker-containing EVs into the peripheral circulation, where they can readily be accessed for study and potential use in diagnostic or prognostic testing. The characterization of plasma EVs are likely to be paramount to our current understanding of fundamental biological processes and disease pathophysiology. However, current methods of EV isolation have proven ineffective and time-consuming for extensive use in clinical settings[1]. In spite of some progress made in recent years, basic classification of EVs categorized by morphological criteria or protein composition remains highly inaccurate[2,3]. Current nomenclature categorizes major EV subtypes as exosomes (30–100 nm vesicles secreted from the cytoplasmic multivesicular body machinery) or as microvesicles (100–1000 nm vesicles secreted from the endosome-like domains of the plasma membrane), which exhibit a heterogeneous composition[4].

Efficient methods of EV purification from complex biological fluids and tissues such as blood plasma will be vital to enable their characterization and future use in medical practice. Patient samples frequently contain large quantities of soluble proteins, aggregates and contaminants that restrict EV analysis using current 'omics' platforms. The most common method of EVs isolation is ultracentrifugation coupled with sucrose gradient or cushion separation[5,6]. However, this laborious and time-consuming approach requires large volumes of blood plasma (>2 ml), and often the process results in EV co-separation with unwanted contaminants[1,7,8,9]. More efficient methods of EVs purification are therefore required to accelerate the study of EVs biology and assist the translation of these data into clinical applications.

Here, we hypothesize a more effective approach comprising the removal of soluble proteins from biological samples by precipitation, leaving a supernatant enriched in a heterogeneous population of EVs for further analysis. In our study, we report that the isolation of EVs from small volumes of human blood plasma can be achieved by PRotein Organic Solvent PRecipitation (PROSPR); a fast and simple procedure that could significantly propel technological advances in the study of EVs biological implications and biomarker discovery.

RESULTS

Optimization of the PROSPR method for isolation of extracellular vesicles (EVs)

Extracellular vesicles (EVs) are rich in cargoes that may be identified as potential biomarkers of disease processes. However, current methods of isolating EVs from complex biological fluids are inefficient and slow. We thus sought to optimize an alternative approach based on PRotein Organic Solvent Precipitation (PROSPR). We first used healthy control blood plasma to test the ability of three different organic solvents (acetone, chloroform and trichloroacetic acid) to precipitate plasma

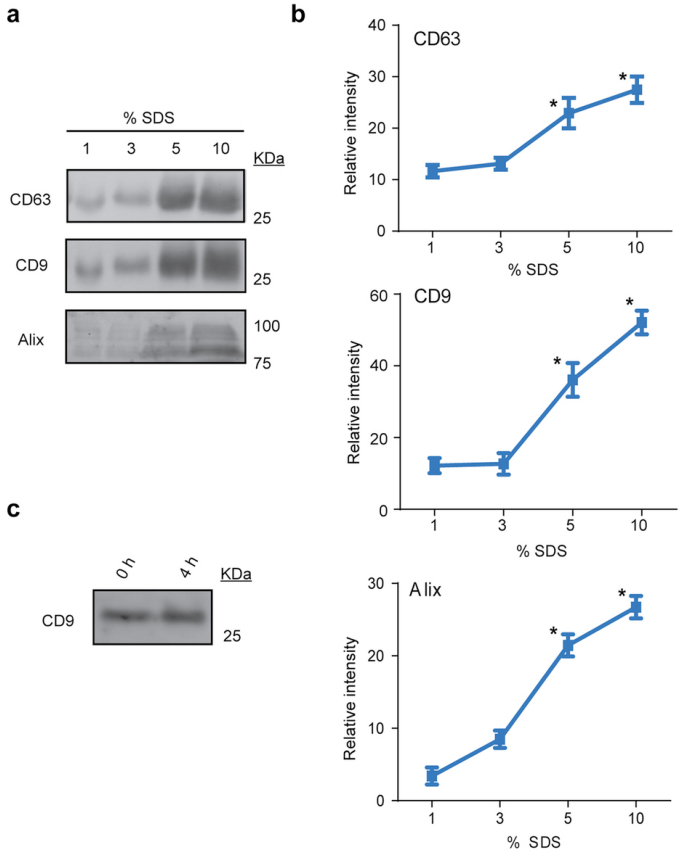

Figure 1. Western blot detection **(a)** and relative quantification **(b)** of characteristic EV markers in PROSPR-separated EV samples after treatment with a range of varying doses of SDS detergent. Significantly higher amounts of CD63, CD9 and Alix proteins were detected at SDS concentrations ≥5% in the lysis buffer (*$p < 0.05$). The SDS dose-dependent western blots of plasma EVs were performed in triplicate. The stability of EVs was also assessed by western blot **(c)** and no clear differences between the time intervals studied were revealed. These data suggest that the isolated EVs remain stable for at least four hours in the PROSPR buffer and require higher concentrations of solubilizing agent to be properly lysed.

proteins under similar optimal conditions (1:4 v/v solvent to plasma ratio[10,11,12]). The purified EVs were further processed for proteomic analysis. The LC-MS/MS analysis of the tryptic-digested proteins contained in the PROSPR-purified EVs revealed that acetone was the most efficient of the three solvents tested (Supplementary Data Set 1). The proteomic profile obtained by chloroform-based PROSPR exhibited a short list of identified proteins and none of the exosomal markers was identified by this method (Supplementary Data Set 2). It is thus likely that EVs may have been deteriorated in chloroform. We also concluded that trichloroacetic acid-based PROSPR was highly complex and

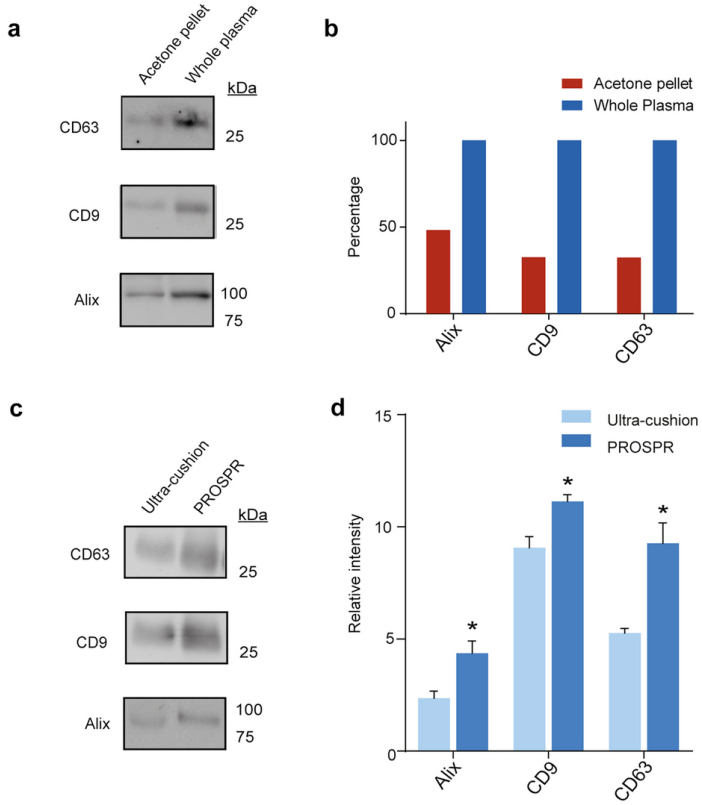

Figure 2. Western blot detection **(a)** and percentage of relative quantification **(b)** of whole plasma and acetone pellet fractions before and after perform PROSPR isolation of EVs.The obtained results show that PROSPR is able to successfully isolate between the 50 and 70 percent of the characteristic EV markers (CD63, CD9 and Alix) present in whole plasma samples. Presence of EV markers was also analyzed in ultra-cushion and PROSPR fractions and the ESCRT adaptor protein Alix and the tetraspanins CD9 and CD63 were used as indicators of purified EVs (c). Higher isolation capacity of the PROSPR method (d) was achieved for each of the three tested EV markers (*$p < 0.05$).

inefficient during the evaporation step, and would not contribute to our pursuit for a rapid and efficient isolation method.

Since detailed biochemical analysis of EV contents requires membrane disaggregation and release of vesicular cargoes, we next assessed the efficiency of EV disruption by Western Blot with a range of different SDS concentrations (1–10% SDS in PBS). EV lysis was determined by detection of common EV markers (Fig. 1a,b). We observed that maximal detection of the EV-associated proteins CD9, CD63, and Alix was achieved using SDS concentrations ≥5%. Our data further indicated that higher SDS concentrations were associated with improved release of total EV proteins, consistent with earlier reports that ultracentrifugation-separated EVs include distinct subsets with detergent-resistant

properties[13]. We next assessed the stability of the plasma EVs over time when plasma was incubated in PROSPR precipitation buffer at −20 °C up to four hours. Western blot determination of CD9 levels clearly demonstrated that EVs prevailed during the time interval assessed in acetone precipitation buffer, with no significant differences in antigen detection (Fig. 1c). Finally, we assessed the relative yielding profile of PROSPR by western blot (Fig. 2a,b). The results showed that PROSPR isolated between the 50%–70% of the whole amount of EV characteristic antigens from blood plasma. These data collectively suggest that blood plasma EVs can be successfully isolated by acetone-based PROSPR separation and remain stable in PROSPR buffer during at least 4 hours, furthermore these EVs can only be efficiently lysed using high concentrations of denaturing agents.

Ultrastructural characterization of PROSPR-separated EVs

Having established that PROSPR is an efficient method for the separation of EVs from human blood plasma, we next proceeded to assess the structural integrity and diversity of the vesicles obtained using this method. Cryo-electron microscopy was used to determine the ultra-structural morphology of PROSPR-separated EVs for comparison with vesicles isolated by a standard ultra-cushion protocol. Using this approach, we observed that both PROSPR and ultra-cushion techniques generated a heterogeneous mix of circular, membrane-encapsulated structures with diameters ranging from 20–300 nm (Fig. 3). The morphologies and sizes of the structures we detected were consistent with those widely reported for exosomes (50–100 nm) and microvesicles (100–1000 nm)[14]. In addition, both the PROSPR and ultra-cushion methods yielded multi-layered and elongated vesicles of various sizes[15], and separated non-membranous particles of ~30 nm diameter that resembled lipoproteins in size and morphology[15,16,17,18]. Although there was no difference in EV size distribution between the two methodologies tested here (data not shown), PROSPR separation appeared to generate a higher density of EVs. In order to obtain definitive evidence that PROSPR is an efficient method of EVs purification, we next conducted a confirmatory experiment using cryo-immunogold labeling to confirm the presence of characteristic EV markers (Alix and CD9) in PROSPR-separated EVs. Visualization of the immunogold-labeled EVs obtained by PROSPR confirmed and validated the presence of membrane-associated Alix and CD9 proteins on both multi-layered and single-layer EVs (Fig. 4). These data indicate that the plasma EVs obtained by PROSPR separation exhibit size distribution and biochemical features previously shown by those of EVs isolated using conventional techniques.

Comparison of EV-derived proteins obtained by PROSPR versus sucrose ultra-cushion

High concentrations of unwanted plasma proteins in ultra-centrifuged samples are likely to impede the identification of EV-associated proteins and mRNAs with potential for use as disease biomarkers[19]. We therefore proceeded to use LC-MS/MS label-free proteomics to evaluate the relative levels of contaminating proteins present in the EV fractions obtained by ultra-cushion and PROSPR. When compared with the EV fraction obtained

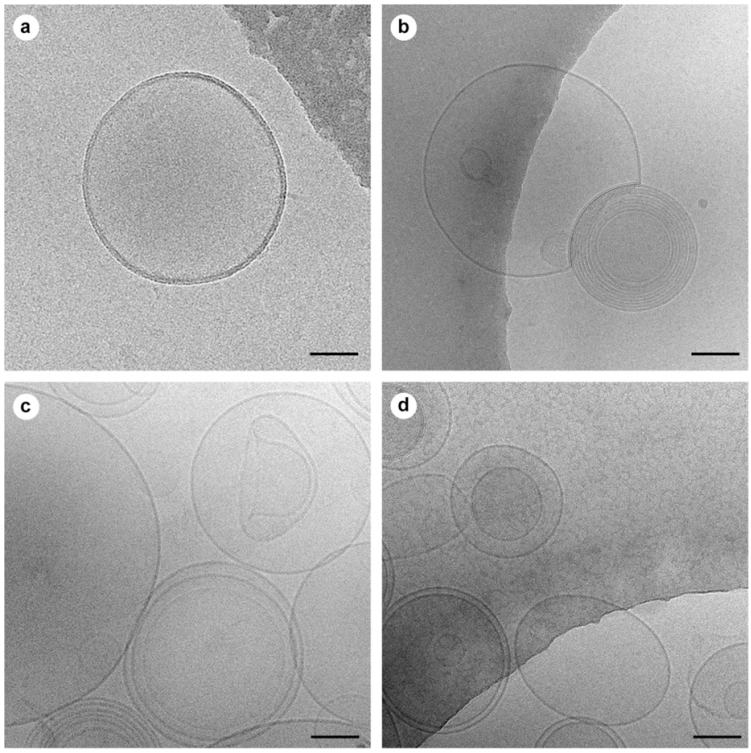

Figure 3. Cryo-EM ultrastructural characterization of EVs isolated from blood plasma by ultra-cushion and PROSPR methods. A heterogeneous population of EVs was observed in both methods including single layered vesicles, multilayered vesicles, exosomes (~100 nm) and microvesicles (>100 nm.) isolated by ultra-cushion **(a,b)** and PROSPR **(c,d)**. Higher density of EVs was observed in PROSPR preparations including an odd-shaped vesicle as shown in micrograph **(c)**. Scale bars in all images represent 55 nm.

by ultra-cushion, we observed that the PROSPR-separated EV fraction exhibited dramatically reduced levels of serum albumin (ALB) and lower quantities of other plasma high abundant proteins (Fig. 5a). Indeed, albumin is the most abundant protein in human plasma, and the PROSPR-separated EV fractions contained less than 1% of the albumin levels present in the ultra-cushion purified fractions. When subsequently analyzed using the high-throughput Orbitrap mass spectrometers Elite and QExactive (Thermo Scientific Inc., Bremen, Germany), we detected a total of 1539 proteins in the PROSPR-isolated fraction, and a total of 610 proteins in the ultra-cushion EVs fraction (Supplemental Data Set 1). We then compared the percentage of match of these respective obtained datasets with Vesiclepedia, an extensive database containg proteins previously identified in isolated EVs[20]. The PROSPR-isolated fractions exhibited 90.7% of match with vesiclepedia and the ultra-cushion isolated fractions exhibited 78.0% of match (Fig. 5b). A total of 1396 EV proteins were identified in common

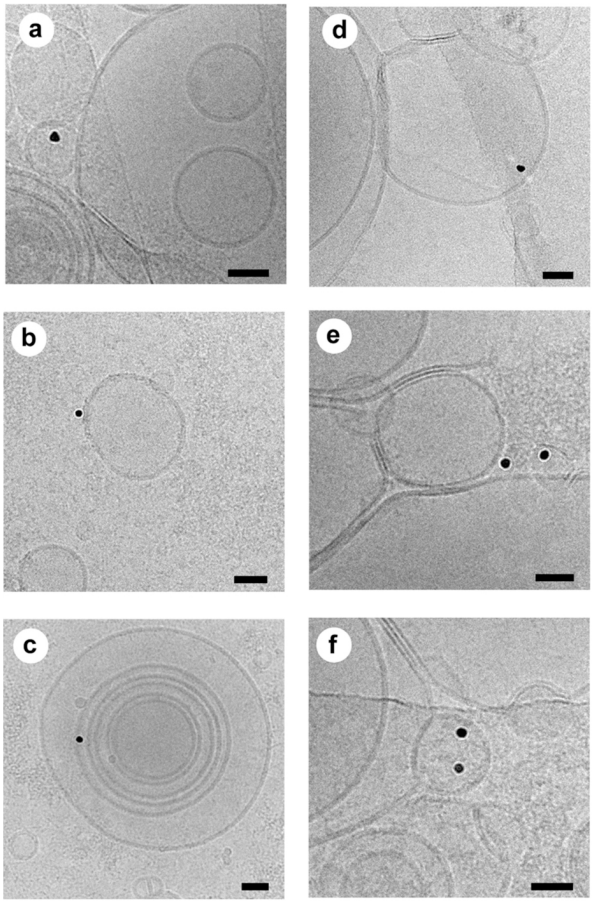

Figure 4. Cryo-immunogold EM micrographs of PROSPR isolated EVs. Presence of tetraspanin CD9 (10 nm colloidal gold particles) was observed as attached to the internal/external face of the membrane in single layered exosome-like vesicles **(a,b)** and in multilayered exosome-like vesicles **(c)**. Presence of the ESCRT protein Alix was also confirmed (10 nm colloidal gold particles) in exosome-like vesicles isolated by PROSPR from blood plasma **(d–f)**. Scale bars in all images represent 40 nm.

between PROSPR and vesiclepedia and a total of 476 EV proteins were identified in common between ultra-cushion and vesiclepedia.

Isolation of EVs by ultra-cushion often results in co-isolation of high-density lipoproteins; accordingly we have analyzed the presence of these proteins in the PROSPR and ultra-cushion EV isolated fractions. Of the most abundant lipoproteins the A-II and C-III were highly present in PROSPR whereas ultra-cushion exhibited higher levels of apolipoproteins A-I, E, A-IV, M and D (Fig. 5c). Globally, these data indicated that PROSPR separation yields higher purity plasma EVs as opposed to conventional approaches. This was consistent with our earlier Western Blot results determining that PROSPR-separated fractions contained substantial levels of characteristic EV markers including CD9, CD63, Alix (Fig. 2c,d) and CD81 (Supplementary Figure 1).

We next sought out to elucidate if there were any significant differences in the EV-associated proteins/genes identified by LC-MS/MS when using PROSPR and

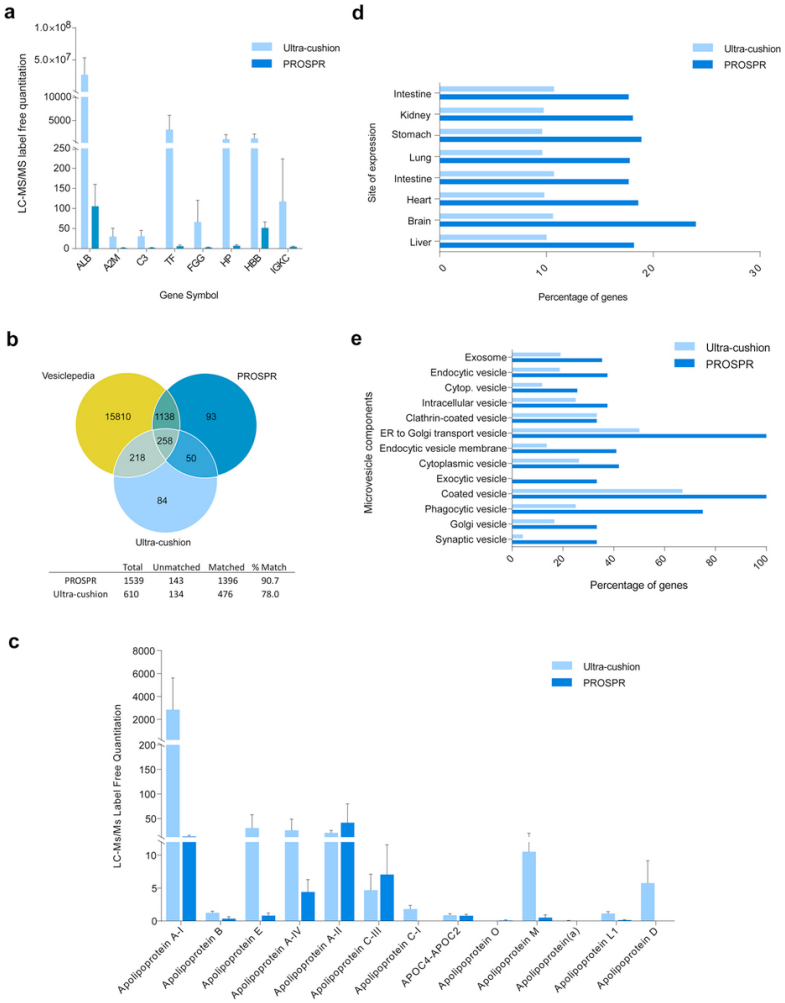

Figure 5. PROSPR generates higher purity plasma EVs as opposed to conventional ultra-cushion methods. LC-MS/MS label-free quantitation revealed that PROSPR separation yields high purity microvesicle fractions containing lower levels of contaminating plasma proteins when compared with samples obtained by ultra-cushion **(a)**. The list of EV proteins identified by LC-MS/MS in ultra-cushion and PROSPR isolated fractions were compared with the list of human EV proteome contained in vesiclepedia[20] as shown by the venn diagrams **(b)**. Percentage of match between ultra-cushion and PROSPR was analyzed; PROSPR revealed higher percentage of match 90.7% compared to ultra-cushion 78.0% with vesiclepedia EV proteins. Cross-contamination in ultra-cushion and PROSPR isolated EV between proteins and high density lipoproteins was analyzed **(c)** the lipoproteins A-II and C-III were found at higher levels in PROSPR EV fractions whereas the lipoproteins A-I, E, A-IV, M and D were found at higher levels in ultra-cushion EV fractions. EV protein datasets were subjected to functional enrichment analyses using the FunRich tool21. Higher percentage of genes was identified in PROSPR fractions compared to ultra-cushion regarding site of expression **(d)** and analyzed microvesicle components **(e)**.

ultra-cushion separated EVs. We performed a functional enrichment analysis of both datasets using FunRich[21], an open source software which considers data from EV specialized databases including Vesiclepedia and Exocarta[20,22]. The percentage of gene identifications in PROSPR clearly outperformed those in ultra-cushion in all the analyzed categories (Fig. 5d,e). Of note, the higher percentage of exosome and brain proteins identified in PROSPR isolated EVs including several specific synaptic proteins. Furthermore, the percentage of proteins attributable to coated vesicles and ER to golgi categories which matched from PROSPR the 100% of the gene background lists in Funrich. Altogether it can be established that the EVs obtained by PROSPR separation are highly consistent with those currently being used in 'omics'-based biomarker discovery studies.

DISCUSSION

In our current study, we report a novel method of isolating extracellular vesicles (EVs) from human plasma by PRotein Organic Solvent PRecipitation (PROSPR), which is simpler and quicker to use as opposed to conventional purification methods, yielding high-purity EVs suitable for detailed proteomic analyses. While EV preparations obtained using centrifugation-based techniques often include high concentrations of contaminating plasma proteins, our approach comprising the use of organic solvents to remove unwanted soluble proteins by precipitation represents an au courant and effective method of isolating EVs in human plasma samples for clinical use.

We observed that EV isolation by PROSPR removes the vast majority of contaminating plasma proteins and unwanted aggregates that would otherwise complicate analysis of EV cargo. After the removal of contaminating proteins by solvent-based precipitation, the lipid-encapsulated EVs are left behind in suspension and can easily be separated by vacuum centrifugation or MWCO filtration by centrifugation. Unlike ultracentrifugation, the PROSPR protocol involves only a few steps and takes a total time of less than two hours to complete. Furthermore, it only requires an acetone solvent which is extremely safe, inexpensive and widely available. The PROSPR method is a suitable method for biomarker measurements of individual patients in diverse clinical settings. Observed to generate an abundant heterogeneous population of EVs from small volumes of blood plasma, PROSPR is a viable and favourable alternative to conventional methods.

Our optimized PROSPR protocol utilizes a vacuum concentrator to concentrate the EVs prior to analysis by LC-MS/MS. Alternatively, a 300 kDa molecular weight cut-off (MWCO) filter could be used instead to separate the EVs out of suspension and remove additional small molecules, salts and metabolites prior to imaging studies. The extensive removal of soluble proteins is crucial to the success of the PROSPR method of EV purification. Protein molecules in aqueous solution are stabilized by exposing their hydrophilic regions in aqueous medium under constant dielectric strength[23], which allows acetone to promote the attraction of opposing charged ions and induce protein aggregation[24]. In addition, Crowell

et al. demonstrated that acetone-based protein precipitation could be enhanced by the presence of salts, which are abundant in human biological fluids[25]. The ion-pairing effects of these salts are thus likely to contribute to the efficacy of EV isolation by PROSPR. Contrary to our initial conjectures, our ultrastructural analyses revealed that EV diversity, structural integrity and intravesicular cargo remain stable for extended periods in cold 80% acetone. As such, this suggests that the PROSPR method is likely to be suitable for a wide range of biomarker discovery studies and clinical applications.

The reliable and economical method approach discussed in this study is highly advantageous in the aspects of cost, time and labour as opposed to conventional isolation methods. The use of PROSPR would therefore significantly accelerate the study of plasma-derived EVs and the translation of these data into novel clinical tests.

MATERIALS AND METHODS

Biological samples

Blood plasma samples from a total of 20 healthy subjects were obtained at the Singapore General Hospital and National University Hospital of Singapore by standard protocol. Heparin was added to fresh whole blood samples and these were immediately centrifuged at 4200 × g for 10 min at 22 °C. Plasma was then frozen at −150 °C until analysis. Informed consent was obtained from all participants prior to the donation of blood samples used in our study. All experimental procedures were approved by the Institutional Review Board at Nanyang Technological University and were performed according to institutional guidelines.

Antibodies and Reagents

All reagents were purchased from Sigma-Aldrich (MO., USA) unless otherwise indicated. Secondary antibodies HRP-conjugated rabbit anti-mouse (sc-358914), HRP-conjugated goat anti-rabbit (sc-2030) and primary antibodies rabbit polyclonal against CD81 (sc-9158), mouse monoclonal against CD9 (sc-13118) and mouse monoclonal against CD63 (sc-365604) were purchased from Santa Cruz Biotechnology (CA, USA). The mouse polyclonal antibody against Alix (ab88746) was purchased from Abcam (Cambridge, UK.). Protease inhibitor cocktail tables were obtained from Roche (Basel, Switzerland) and sequencing-grade modified trypsin was obtained from Promega (WI, USA).

PRotein Organic Solvent PRecipitation (PROSPR)

Isolation of Evs by solvent-based precipitation was performed by directly mixing 500–1000 µl of neat plasma with four times the volume of cold acetone (−20 °C). The mixture was vortexed for a few seconds and then centrifuged at 3000 × g for one minute.

After centrifugation is completed, the pellet was either discarded or kept for further experiments. The EV-containing supernatant was removed and dehydrated in a vacuum concentrator (Concentrator Plus, Eppendorf AG,

Hamburg, Germany) during approximately 1 hour. For imaging experiments the EV-containing supernatant was concentrated using a 300 kDa MWCO (see cryo-EM in the materials and methods section) for approximately 40 minutes (Fig. 6 and Supplementary Figure 1). The dried microvesicle fraction was resuspended and homogenized in bi-distilled water prior to be used in further analyses and the MWCO microvesicle fraction was directly used in further analyses.

Microvesicle isolation by ultracentrifugation on a sucrose cushion (ultra-cushion)

Microvesicle isolation by ultracentrifugation onto a sucrose cushion was performed as previously described[26,27,28,29,30,31,32] with some modifications for use with human plasma. Plasma was centrifuged at 300 × g, 4 °C for 30 minutes to remove cell debris. The resultant pellet was discarded, while the supernatant (S1) was centrifuged again at 16500 × g, 4 °C for 30 more minutes. The pellet from the second centrifugation step was removed and the supernatant (S2) was collected and mixed with chilled HPLC water (4 °C) to decrease sample density. The diluted supernatant was then transferred carefully into an ultracentrifuge tube containing 1 ml cold sucrose (5.5% solution chilled to 4 °C; approximate density 1.02 g/ml[33]) and centrifuged at 200,000 × g, 4 °C for 120 minutes to obtain the microvesicle pellet (P3) and supernatant (S3), which was then ultracentrifuged overnight (200,000 × g at 4 °C) to obtain the final pellet (P4).

Western blot analysis

Microvesicles were transferred into lysis buffer (5% SDS in PBS) together with Complete Protease Inhibitor Cocktail (COMPLETE; Roche, Mannheim, Germany) and then boiled for 5 min at 95 °C under reducing conditions with 2-mercaptoethanol (5%) in BioRad 2× Laemmli sample buffer (CA, USA). Protein concentration was quantified by the Bradford assay and equal amounts of protein were used for Western blot analysis. To ensure that equal quantities of EVs were used in each experimental condition, EVs were first isolated from a pool of mixed plasma. The acetone fraction was later split equally for testing in each experimental condition. Proteins were subsequently resolved using either 10% or 15% SDS-PAGE and blotted onto nitrocellulose membranes. Protein detection was conducted using the appropriate primary antibodies at 1:1000 dilution (CD9, CD63, CD81 and Alix). Finally, appropiate HRP-conjugated secondary antibodies at 1:2000 dilution were used together with the Invitrogen ECL detection system (CA, USA).

Ultrastructural studies of EVs

Cryo-electron microscopy

Microvesicles were PROSPR-separated from 1 ml total blood plasma. A 5 ml volume of the resultant EV-containing supernatant was later diluted in three-fold in 1× PBS, then concentrated 150-fold using a 300 kDa Pall Life Science Nanosep Centrifugal Device (MI, USA). EVs isolated by ultra-cushion were re-dissolved in 1× PBS and then concentrated similarly. The EV

preparations were then directly deposited onto glow-discharged Quantifoil R2/2 grids coated with 2 nm carbon (Jena, Germany). Grids were blotted (1 second) at 95% humidity and plunge-frozen in liquid ethane using a Vitrobot plunger (FEI). Grids were imaged on an Arctica transmission electron microscope (FEI) operated at 200 kV on a Falcon II (FEI) direct electron detector. Images were recorded at −3 µm underfocus, with an electron dose of 15 e/Å2 and a nominal magnification of X 53,000. The object pixel size was 0.2 nm.

Cryo-immunogold EM abeling

Isolated microvesicles were deposited onto carbon-coated Quantifoil grids and washed with bi-distilled water in blocking solution (0.5% BSA/ddH2O) for 5 minutes. Samples were then incubated in a drop of primary antibody (CD9/Alix, 1:100 dilution) for 20 minutes. The grids were washed twice for 3 minutes in blocking solution, followed by adding 10 nm colloidal gold coated with a secondary antibody (goat anti-mouse 1:100 dilution, purchased from Aurion, Netherlands). Samples were washed twice again in bi-distilled water for 3 minutes and plunge-frozen as described above.

Digestion of plasma EVs

Extracellular vesicles were lysed in 16 M urea, 50 mM ABB buffer together with Complete Protease Inhibitor Cocktail. Urea buffer was diluted to 8 M urea, 25 mM ABB with bi-distilled water prior to put the samples in reducing conditions. Proteins were then reduced in a final concentration of 10 mM dithiothreitol (DTT) for 3 h at 30 °C and alkylated using a final concentration of 20 mM IAA during 45 min at room temperature in the dark. After alkylation, urea concentration was diluted to <1 M using 25 mM ABB and digested overnight at 30 °C with trypsin at 1:50 dilution. Tryptic digestion was stopped by acidification diluting the digested samples to a 0.5% final concentration of FA. Peptides were reconstituted and desalted using Waters Sep-pack 50 mg C18 cartridges (MA., USA) performing several washes of 0.1% trifluoroacetic acid (TFA). Elution was carried out using 75% acetonitrile, 0.1% formic acid (FA), and the eluted samples were concentrated using vacuum concentrator.

Fractionation of EV peptides

Desalted EV peptides were fractionated in order to decrease sample complexity. Briefly, samples were dissolved in 200 µL mobile phase A (85% ACN 0.1% acetic acid) and fractionated using a Fortis Amino column (4.6×200 mm, 3 µm, Fortis Technologies Ltd., Cheshire, UK) on a Shimadzu Prominence UFLC system monitored at 280 nm. Seventy-two fractions were collected with a 72 min gradient of mobile phase B (10% ACN, 0.1% FA), at 0% for 5 min, 0–20% B for 25 min, 20–33% B for 10 min, 33–60% B for 10 min, and 60–100% B for 5 min, followed by 17 min at 100% B at a flow rate of 1 ml/min. Fractions were dried to decrease the volume under vacuum and subsequently pooled according to peak intensities. Finally, peptides were completely dried and reconstituted with 3% ACN, 0.1% FA prior to be analyzed by mass spectrometry.

LC-MS/MS spectrometry

LC-MS/MS analysis of digested peptides was performed on a Thermo Scientific Inc. Orbitrap Elite and QExactive mass spectrometers (Bremen, Germany) coupled with a Dionex UltiMate 3000 UHPLC system from Thermo Scientific Inc. Samples were sprayed using a Bruker-Michrom Inc. Michrom's Thermo CaptiveSpray nanoelectrospray ion source (AL., USA). Approximately 2 µg of peptides were injected into a reverse phase Acclaim PepMap RSL column (Thermo Scientific; 75 µm ID × 15 cm, 2 µm particles) at a temperature of 35 °C and flow rate of 300 nl/min. Eluent A (0.1% FA in water) and eluent B (90% ACN/0.1% FA) were used to establish a 60 min gradient with elution starting at 3% eluent B for 1 min, which was then linearly increased to 35% eluent B over 47 minutes, before being increased to 50% eluent B over four minutes, and then increased to 80% eluent B in six seconds and kept isocratic for 78 seconds. Finally, the conditions were reverted to their initial state over six seconds and maintained for 6.5 minutes.

Thermo Scientific Orbitrap mass spectrometers were set to positive ion mode using LTQ Tune Plus software for data acquisition mode, alternating between a Full FT-MS (350–1600 m/z, resolution 60,000, with one µscan per spectrum) and a FT-MS/MS where the 10 most intense ions above a 500 count threshold were selected for fragmentation in high-energy collisional dissociation (HCD) mode (32% normalized collision energy, 150–2000 m/z, resolution 15,000, one µscan per spectrum, capillary temperature 250 °C, source voltage 1.5 kV). The automatic gain control target for FT-MS and MS/MS was set at 1e+06 and precursor ion charge state screening was activated.

Bioinformatics and data analysis

Raw MS/MS data were de-isotoped and converted into Mascot Generic Format (mgf) files using Thermo Proteome Discoverer (version 1.4.1.14, Thermo Fisher Scientific Inc). Database searches were performed using an in-house Mascot server (version 2.3.02, Matrix Science, MA, USA) with a precursor MS tolerance of 10 ppm and MS/MS fragment tolerance of 0.02 Da. A false discovery rate (FDR) correction of 1% was applied to the identified peptides to enhance the confidence level of identified proteins (Supplementary Figure 2). The Mascot reported exponentially modified protein abundance index (emPAI) was used for protein quantitation as previously described[34]. Western blot signal was quantified by ImageJ software[35]. Student's t test analyses were performed between PROSPR and ultra-cushion data using GraphPad Prism 6 (CA., USA) and p-values < 0.05 were considered significant unless specified otherwise. Error bars indicate SEM.

Data deposition

Proteomics data have been deposited to the ProteomeXchange Consortium[36] via the PRIDE partner repository with the following identifier PXD002668.

ACKNOWLEDGEMENTS

This research is supported by the Singapore National Research Foundation

under its CBRG (NMRC/CBRG/0004/2012) and administered by the Singapore Ministry of Health's National Medical Research Council, the Singapore Ministry of Education (Tier 1: RGT15/13), NTU-NHG Ageing Research Grant (ARG/14017) and NTU iFood (Grant #: S006). Sara Sandin contributions were supported by a NTU start-up grant and the Singapore Ministry of Education (Tier 1: RG39/14). Andrew See Weng Wong contributions were supported by Nanyang Structural Biology Institute, Singapore. The authors sincerely thank See-Toh Rachel for her helpful and critical readings of the manuscript and Mei Ling for generously providing us with the gold conjugated antibody used in the cryo-immunogold EM experiments.

AUTHOR CONTRIBUTIONS

S.K.S. conceived the idea and X.G.P. arranged the experiments. X.G.P. and A.S. performed proteomics experiments and analyzed data. X.G.P., A.S.W.W. and S.S. conducted ultrastructural studies. M.K.P.L, C.P.C. and O.L.K. collected and provided clinical samples. X.G.P., A.S. and S.K.S. wrote the paper. All authors have read and approved the manuscript.

COMPETING FINANCIAL INTERESTS

X.G.P, C.P.C and S.K.S are named as co-inventors on a patent application that covers the analysis of biomarkers in plasma EVs isolated by PROSPR.

REFERENCES

1 Taylor, D. D., Zacharias, W. & Gercel-Taylor, C. Exosome isolation for proteomic analyses and RNA profiling. Methods in molecular biology (ed Clifton, N. J.) Ch. 728, 235–246, 10.1007/978-1-61779-068-3_15 (Humana Press, 2011).

2 Bobrie, A., Colombo, M., Raposo, G. & Thery, C. Exosome secretion: molecular mechanisms and roles in immune responses. Traffic 12, 1659–1668, 10.1111/j.1600-0854.2011.01225.x (2011).

3 Couzin, J. Cell biology: The ins and outs of exosomes. Science 308, 1862–1863, 10.1126/science.308.5730.1862 (2005).

4 Robbins, P. D. & Morelli, A. E. Regulation of immune responses by extracellular vesicles. Nat Rev Immunol 14, 195–208, 10.1038/nri3622 (2014).

5 Van Deun, J. et al. The impact of disparate isolation methods for extracellular vesicles on downstream RNA profiling. J Extracell Vesicles 3, 10.3402/jev.v3.24858 (2014).

6 Witwer, K. W. et al. Standardization of sample collection, isolation and analysis methods in extracellular vesicle research. J Extracell Vesicles 2, 10.3402/jev.v2i0.20360 (2013).

7 He, M., Crow, J., Roth, M., Zeng, Y. & Godwin, A. K. Integrated immunoisolation and protein analysis of circulating exosomes using microfluidic technology. Lab Chip 14, 3773–3780, 10.1039/c4lc00662c (2014).

8 Kalra, H. et al. Comparative proteomics evaluation of plasma exosome isolation techniques and assessment of the stability of exosomes in normal human blood plasma. Proteomics 13, 3354–3364, 10.1002/pmic.201300282 (2013).

SUPPLEMENTAL INFORMATION

9 Caby, M. P., Lankar, D., Vincendeau-Scherrer, C., Raposo, G. & Bonnerot, C. Exosomal-like vesicles are present in human blood plasma. Int Immunol 17, 879–887, 10.1093/intimm/dxh267 (2005).

10 Botelho, D. et al. Top-down and bottom-up proteomics of SDS-containing solutions following mass-based separation. J Proteome Res 9, 2863–2870, 10.1021/pr900949p (2010).

11 Davidsson, P., Westman, A., Puchades, M., Nilsson, C. L. & Blennow, K. Characterization of Proteins from Human Cerebrospinal Fluid by a Combination of Preparative Two-Dimensional Liquid-Phase Electrophoresis and Matrix-Assisted Laser Desorption/Ionization Time-of-Flight Mass Spectrometry. Anal Chem 71, 642–647, 10.1021/ac980672w (1998).

12 Jiang, L., He, L. & Fountoulakis, M. Comparison of protein precipitation methods for sample preparation prior to proteomic analysis. J Chromatogr A 1023, 317–320, http://dx.doi.org/10.1016/j.chroma.2003.10.029 (2004).

13 Buschow, S. I. et al. MHC II in dendritic cells is targeted to lysosomes or T cell-induced exosomes via distinct multivesicular body pathways. Traffic 10, 1528–1542, 10.1111/j.1600-0854.2009.00963.x (2009).

14 Masyuk, A. I. et al. Biliary exosomes influence cholangiocyte regulatory mechanisms and proliferation through interaction with primary cilia. Am J Physiol Gastrointest Liver Physiol 299, G990–999, 10.1152/ajpgi.00093.2010 (2010).

15 Yuana, Y. et al. Cryo-electron microscopy of extracellular vesicles in fresh plasma. J Extracell Vesicles 2, 10.3402/jev.v2i0.21494 (2013).

16 Han, M. et al. Disruption of human plasma high-density lipoproteins by streptococcal serum opacity factor requires labile apolipoprotein A-I. Biochemistry 48, 1481–1487, 10.1021/bi802287q (2009).

17 Liu, Y. & Atkinson, D. Immuno-electron cryo-microscopy imaging reveals a looped topology of apoB at the surface of human LDL. J Lipid Res 52, 1111–1116, 10.1194/jlr.M013946 (2011).

18 Zhang, L. et al. Structural basis of transfer between lipoproteins by cholesteryl ester transfer protein. Nat Chem Biol 8, 342–349, 10.1038/nchembio.796 (2012).

19 Thery, C., Amigorena, S., Raposo, G. & Clayton, A. Isolation and characterization of exosomes from cell culture supernatants and biological fluids. (eds. Bonifacino J. S. et al.) Ch 3, Unit 3.22, 10.1002/0471143030.cb0322s30 (Wiley & Sons, 2006).

20 Kalra, H. et al. Vesiclepedia: a compendium for extracellular vesicles with continuous community annotation. PLoS Biol 10, e1001450, 10.1371/journal.pbio.1001450 (2012).

21 Pathan, M. et al. Technical brief funrich: An open access standalone functional enrichment and interaction network analysis tool. Proteomics 15, 2597–2601, 10.1002/pmic.201400515 (2015).

22 Mathivanan, S., Fahner, C. J., Reid, G. E. & Simpson, R. J. ExoCarta 2012: database of exosomal proteins, RNA and

lipids. Nucleic acids Res 40, D1241–1244, 10.1093/nar/gkr828 (2012).

23 Arakawa, T. & Timasheff, S. N. Theory of protein solubility. Methods Enzymol 114, 49–77 (1985).

24 Green, A. A. & Hughes, W. L. Protein fractionation on the basis of solubility in aqueous solutions of salts and organic solvents. Methods Enzymol 1, 67–90, 10.1016/0076-6879(55)01014-8 (1955).

25 Crowell, A. M. J., Wall, M. J. & Doucette, A. A. Maximizing recovery of water-soluble proteins through acetone precipitation. Anal ChimActa 796, 48–54, http://dx.doi.org/10.1016/j.aca.2013.08.005 (2013).

26 Kadiu, I., Narayanasamy, P., Dash, P. K., Zhang, W. & Gendelman, H. E. Biochemical and biologic characterization of exosomes and microvesicles as facilitators of HIV-1 infection in macrophages. J Immunol 189, 744–754, 10.4049/jimmunol.1102244 (2012).

27 Datta, A., Chen, C. P. & Sze, S. K. Discovery of prognostic biomarker candidates of lacunar infarction by quantitative proteomics of microvesicles enriched plasma. PLoS One 9, e94663, 10.1371/journal.pone.0094663 (2014).

28 Park, J. E. et al. Hypoxic tumor cell modulates its microenvironment to enhance angiogenic and metastatic potential by secretion of proteins and exosomes. Mol Cell Proteomics 9, 1085–1099, 10.1074/mcp.M900381-MCP200 (2010).

29 Lai, R. C. et al. Proteolytic Potential of the MSC Exosome Proteome: Implications for an Exosome-Mediated Delivery of Therapeutic Proteasome. Int J Proteomics 2012, 971907, 10.1155/2012/971907 (2012).

30 de Hoog, V. C. et al. Serum extracellular vesicle protein levels are associated with acute coronary syndrome. Eur Heart J Acute Cardiovasc Care 2, 53–60, 10.1177/2048872612471212 (2013).

31 Tan, K. H. et al. Plasma biomarker discovery in preeclampsia using a novel differential isolation technology for circulating extracellular vesicles. Am J Obstet Gynecol 211, 380.e381–313, 10.1016/j.ajog.2014.03.038 (2014).

32 Wang, J. W. et al. Plasma extracellular vesicle protein content for diagnosis and prognosis of global cardiovascular disease. Neth Heart J 21, 467–471, 10.1007/s12471-013-0462-3 (2013).

33 Asadi, M. Beet-Sugar Handbook. (John Wiley & Sons 2005).

34 Ishihama, Y. et al. Exponentially modified protein abundance index (emPAI) for estimation of absolute protein amount in proteomics by the number of sequenced peptides per protein. Mol Cell Proteomics 4, 1265–1272, 10.1074/mcp.M500061-MCP200 (2005).

35 Schneider, C. A., Rasband, W. S. & Eliceiri, K. W. NIH Image to ImageJ: 25 years of image analysis. Nat Methods 9, 671–675 (2012).

36 Vizcaino, J. A. et al. ProteomeXchange provides globally coordinated proteomics data submission and dissemination. Nat Biotech 32, 223–226, 10.1038/nbt.2839 (2014).

Received for publication March 18, 2015.
Accepted for publication September 03, 2015.

SUPPLEMENTARY FIGURES

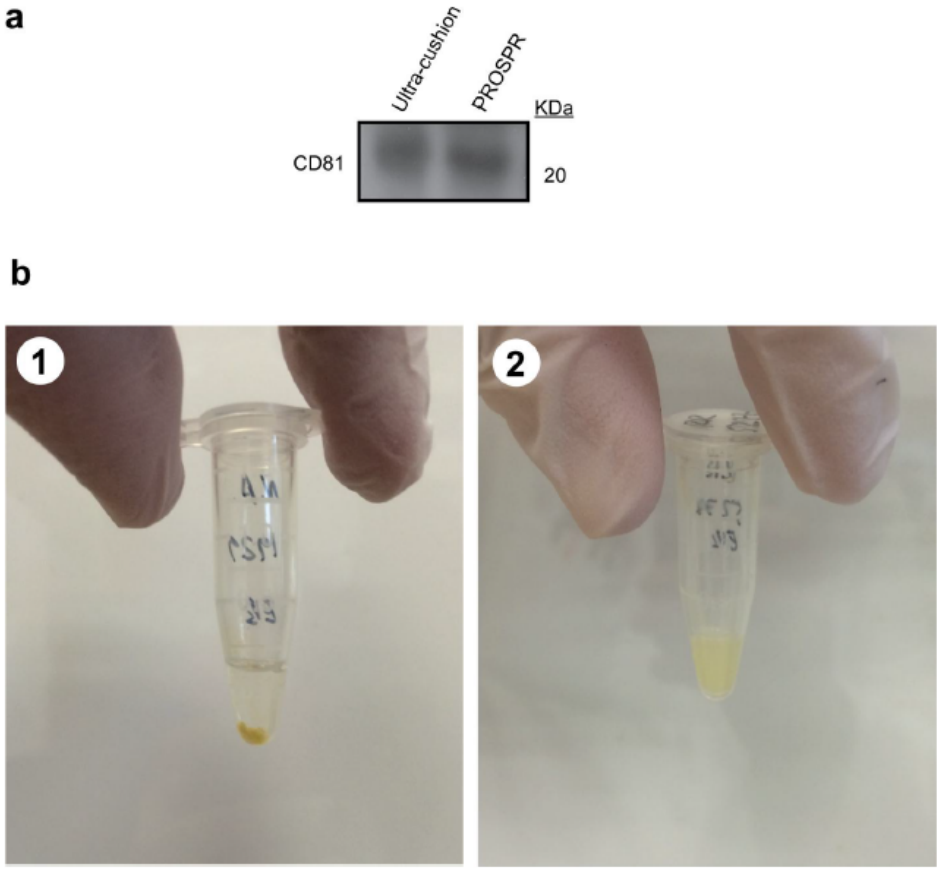

Supplementary Figure 1. (a) Western blot showing the presence of CD81 in plasma EVs isolated by ultra-cushion and PROSPR methods. **(b1)** The pellet containing separated EVs after vacuum evaporation of PROSPR supernatant is shown after addition of bi-distilled water. (b2) PROSPR EVs pellet resuspended in bi-distilled water.

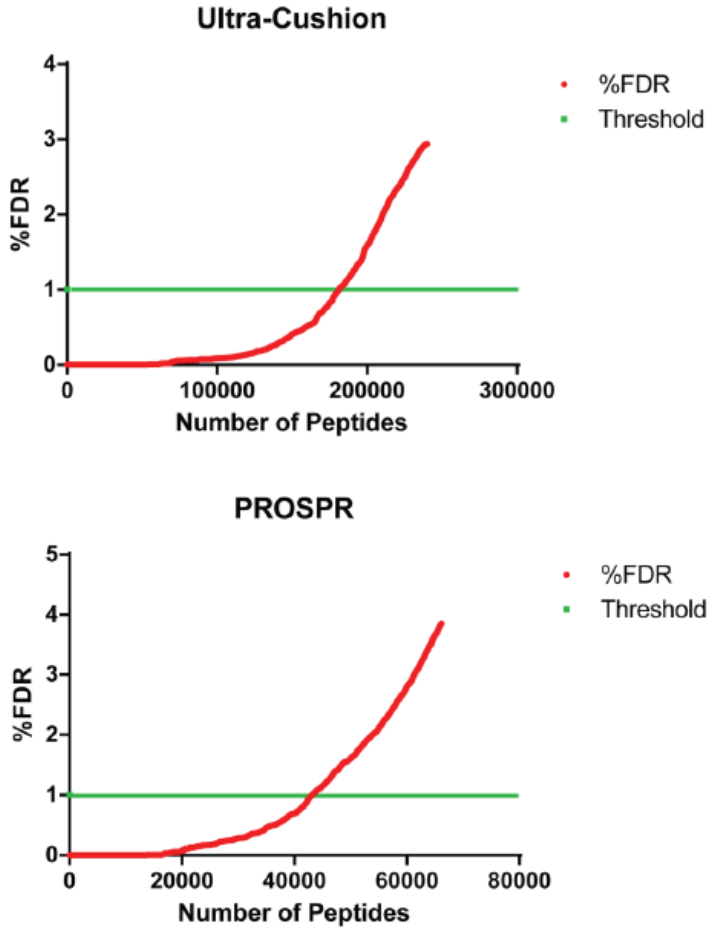

Supplemental Figure 2: FDR distribution of peptides identified by Ultra-Cushion and PROSPR.

Chapter 1 Annex. Neuregulin-1 in PROSPR-isolated extracellular vesicles from biological fluids (Unpublished)**.**

NEUREGULIN-1 IN PROSPR-ISOLATED EXTRACELLULAR VESICLES FROM BIOLOGICAL FLUIDS

Abstract

Neuregulin-1 (NRG-1) is a growth factor implicated in both healthy and pathological conditions of the central nervous system. These include neuropsychiatric disorders and neurodegenerative diseases. In Amyotrophic Lateral Sclerosis (ALS), we have found the presence of Neuregulin-1 in close association with C-boutons apposed to α-motor neurones. These newly discovered NRG-1 molecules were found inside extracellular vesicles (EVs) likely to be released through the exocytotic exosomal pathway. We have therefore developed PROSPR, a novel protocol that provides a more efficient, easy-to-use and inexpensive than current available methods to isolate EVs. Here, we describe the successful application of the PROSPR method to study and characterize NRG-1 present in EVs in the context of healthy and motor neurone diseases conditions.

INTRODUCTION

Neuregulins are growth factor molecules that were discovered more than three decades ago as key mediators of the axon-muscle and Schwann-axon interactions in the peripheral nervous system (PNS) (Falls et al. 1993). Neuregulins found in the PNS are encoded by the NRG-1 gene, thereby these proteins were dubbed as neuregulin-1 proteins (NRG-1). Isoforms of NRG-1 are in essence signalling factors that act as binding ligands of the ErbB family of receptors (Falls 2003). Bioactive forms of NRG-1 are mandatory containers of the epidermal growth factor-like domain (EGF-like) thus that domain in this molecule is essential to activate the ErbB tyrosine-kinase receptors (Buonanno & Fischbach 2001).

The study of NRG-1 functions in the central nervous system (CNS) is highly complex, since most of the knock-out (KO) mice for NRG-1 are non-viable. In spite of this complexity, the presence and functions of NRG-1 have been successfully studied and discovered during the embryogenesis stages of these KO mice. Mice lacking the isoform III of NRG-1 are embryonic viable. However, they die at the birth point as they are unable to breathe due to lack of formation of neuromuscular junctions (Falls 2003). Additionally, significant reduction in motor neurones was accounted for the CNS motor areas of these KO mice (Falls 2003).

Molecules of NRG-1 were found in the endoplasmic reticulum subsurface cistern of cholinergic C-terminals apposed to α-motor neurones in lumbar spinal cord of $SOD1^{G93A}$ Amyotrophic Lateral Sclerosis (ALS) transgenic mice (Gallart-Palau et al. 2014). We found levels of this C-bouton associated protein as up-regulated at ALS symptomatic stage (post-natal 90 days) of these transgenic animals. Furthermore, NRG-1 was found inside vesicles that resembled extracellular vesicles (EVs) and more specifically exosomes (Gallart-Palau et al. 2014; Mavlyutov et al. 2015). The study of EVs in neurodegenerative diseases are currently in its incipient stage, this fact is even more evident in sporadic and familial forms of ALS (Basso et al. 2013). The presence of NRG-1 in EVs is a controversial matter, mainly due

to the lack of a reliable and 'easy-to-perform' method to isolate circulating EVs from biological fluids and tissues.

In the present application, we have used our newly developed PROSPR protocol for the isolation of EVs from plasma tissue and urine fluid. Our results indicate that PROSPR is an improved and referential method to be used in the characterization and further study of NRG-1 from circulating EVs from biological fluids and tissues of ALS subjects.

MATERIALS AND METHODS

Material and methods used in all the applications described here of the PROSPR protocol have been previously detailed in the material and methods section of the PROSPR manuscript , which is included in the current thesis chapter. LC-MS/MS data was searched in this annex against a restricted human Uniprot database. Additionally, to the samples used in the PROSPR manuscript, early morning fresh urine from a healthy subject was collected and analyzed here following the exact referred manuscript methods and indications.

RESULTS

Presence of NRG-1 was found in the PROSPR isolated EVs from plasma and urine samples as described in Tables 1. Spectrum of the most confident peptide identified by our high-throughput mass spectrometer Orbitrap Elite (Thermo Inc., Germany) for the NRG-1 is being shown in (Figure 1). Label-free proteomics relative quantification in plasma tissues showed an equal amount of NRG-1 and CD9, a marker of EVs, in the analyzed samples. Furthermore, our quantitative results suggest substantial presence of NRG-1 in PROSPR isolated EVs from biological tissues and fluids.

DISCUSSION

We found the presence of NRG-1 in post-synaptical association with C-terminals and the protein was enclosed in EVs likely to be released by the exosomal exocytotic pathway (Gallart-Palau et al. 2014; Mavlyutov et al. 2015). We also found increase of these molecules during ALS symptomatic stages of transgenic $SOD1^{G93A}$ mice (Gallart-Palau et al. 2014), which suggests a potential use of this protein as a promising and reliable

Table 1. Identification of NRG1 and an EV-specific tetraspanin CD9 in PROSPR EVs isolated from human plasma and urine samples.

	Plasma			Urine		
	Sequence coverage (%)	Matched spectrums	emPAI[a]	Sequence coverage (%)	Matched spectrums	emPAI
NRG1	76	69	0,06	69	110	0,12
CD9	67	18	0,18	n.d.	n.d.	n.d.

n.d. Not detected.
[a] Exponential Modified Protein Index (emPAI) defined as 10^{PAI} where Protein Abundance Index (PAI) represents the ratio of observed to observable proteins.

a.

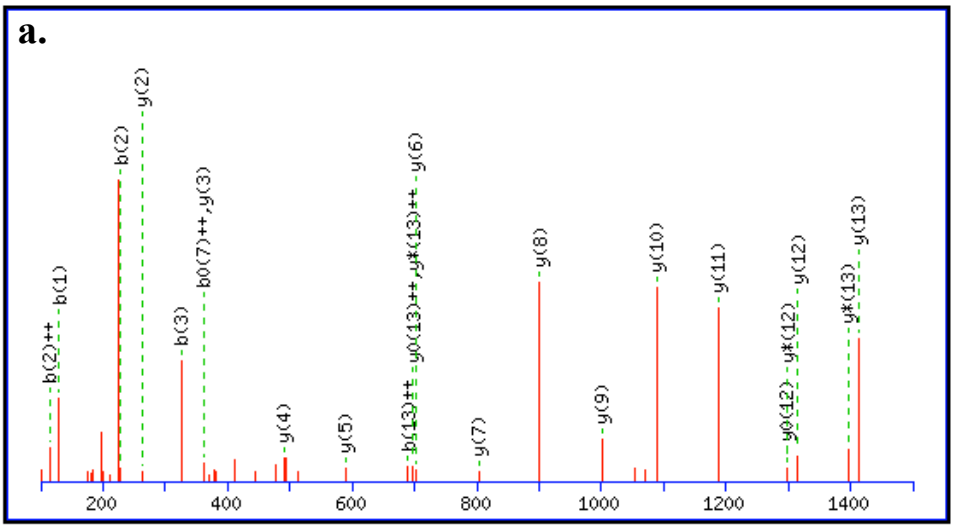

b.

#	b	b^{++}	b*	b^{*++}	b^0	b^{0++}	Seq.	y	y^{++}	y*	y^{*++}	y^0	y^{0++}	#
1	129.1022	65.0548	112.0757	56.5415			K							15
2	228.1707	114.5890	211.1441	106.0757			V	1511.8428	756.4250	1494.8162	747.9118	1493.8322	747.4197	14
3	325.2234	163.1153	308.1969	154.6021			P	*1412.7744*	706.8908	1395.7478	698.3775	1394.7638	697.8855	13
4	453.2820	227.1446	436.2554	218.6314			Q	*1315.7216*	658.3644	1298.6951	649.8512	1297.7110	649.3592	12
5	552.3504	276.6788	535.3239	268.1656			V	*1187.6630*	594.3352	1170.6365	585.8219	1169.6525	585.3299	11
6	639.3824	320.1949	622.3559	311.6816	621.3719	311.1896	S	*1088.5946*	544.8009	1071.5681	536.2877	1070.5841	535.7957	10
7	740.4301	370.7187	723.4036	362.2054	722.4196	361.7134	T	*1001.5626*	501.2849	984.5360	492.7717	983.5520	492.2796	9
8	837.4829	419.2451	820.4563	410.7318	819.4723	410.2398	P	*900.5149*	450.7611	883.4884	442.2478	882.5043	441.7558	8
9	938.5306	469.7689	921.5040	461.2556	920.5200	460.7636	T	*803.4621*	402.2347	786.4356	393.7214	785.4516	393.2294	7
10	1051.6146	526.3109	1034.5881	517.7977	1033.6041	517.3057	L	*702.4145*	351.7109	685.3879	343.1976	684.4039	342.7056	6
11	1150.6830	575.8452	1133.6565	567.3319	1132.6725	566.8399	V	*589.3304*	295.1688	572.3039	286.6556	571.3198	286.1636	5
12	1279.7256	640.3665	1262.6991	631.8532	1261.7151	631.3612	E	*490.2620*	245.6346	473.2354	237.1214	472.2514	236.6293	4
13	1378.7940	689.9007	1361.7675	681.3874	1360.7835	680.8954	V	*361.2194*	181.1133	344.1928	172.6001	343.2088	172.1081	3
14	1465.8261	733.4167	1448.7995	724.9034	1447.8155	724.4114	S	*262.1510*	131.5791	245.1244	123.0659	244.1404	122.5738	2
15							R	175.1190	88.0631	158.0924	79.5498			1

Figure 1. The most confident NRG-1 peptide, with peptide score 103 and MS tolerance error of 0.47 ppm, identified by LC-MS/MS in PROSPR EVs isolated from human plasma. **(a)** Annotated MS/MS spectrum. **(b)** Ion assigment table.

biomarker of the ALS progression in isolated EVs from ALS patients. Here in this application, we demonstrate that NRG-1 can be found in isolated EVs of tissues and biological fluids. Subsequently, we are currently optimizing our described PROSPR method to isolate EVs from CNS tissues. We hypothesize that human CNS tissue homogenization prior to the PROSPR application can be achieved in 100mM ammonium acetate buffer (pH. 6) with a mechanical tissue homogenizer controlling the homogenization time in the bullet blender (Next Advance, Inc., NY, USA) to short intervals (≈2 min.) and using a small amount of metallic beads (¼ of tissue

amount, w/w) following the bullet blender manufacturer´s protocol.

Isolation of EVs from ALS tissues following the previously described method and the PROSPR protocol can facilitate the characterization of C-terminals NRG-1 by top-down proteomics. Application of top-down proteomics to the characterization of NRG-1 isolated from C-terminals EVs can map the whole structure of the protein, allowing the specific identification of the NRG-1 subtype found in motoneuron C-terminals. Furthermore, top-down proteomics characterization of NRG-1 could allow the description of the post-translational modifications that the NRG-1 molecule might undergo in patients and experimental models through the progression of ALS. Additionally, the characterization of extracellular vesicle receptors that might be involved in the NRG-1 signalling could provide new and crucial insight in FALS motoneuron pathophysiology.

REFERENCES

Basso, M. et al., 2013. Mutant copper-zinc superoxide dismutase (SOD1) induces protein secretion pathway alterations and exosome release in astrocytes: implications for disease spreading and motor neuron pathology in amyotrophic lateral sclerosis. The Journal of biological chemistry, 288(22), pp.15699–711.

Buonanno, A. & Fischbach, G.D., 2001. Neuregulin and ErbB receptor signaling pathways in the nervous system. Current opinion in neurobiology, 11(3), pp.287–96.

Falls, D., 2003. Neuregulins: functions, forms, and signaling strategies. Experimental Cell Research, 284(1), pp. 14–30.

Falls, D.L. et al., 1993. ARIA, a protein that stimulates acetylcholine receptor synthesis, is a member of the neu ligand family. Cell, 72(5), pp.801–15.

Gallart-Palau, X. et al., 2014. Neuregulin-1 is concentrated in the postsynaptic subsurface cistern of C-bouton inputs to α-motoneurones and altered during motoneuron diseases. FASEB journal: official publication of the Federation of American Societies for Experimental Biology, 28(8), pp.3618–32.

Mavlyutov, T.A. et al., 2015. Role of the Sigma-1 receptor in Amyotrophic Lateral Sclerosis (ALS). Journal of pharmacological sciences, 127(1), pp.10–16.

Chapter 2.

SOD1^{G93A} and mitochondria: a pathogenic relationship beyond cell death and energetic depletion

Gallart-Palau *et al.* Neuroscience Letters (2016). 624, 47-52.
Gallart-Palau et al. Manuscript in preparation

Drosophila expressing human SOD1 succesfully recapitulates mitochondrial phenotypic features of familial amyotrophic lateral sclerosis.

Gallart-Palau *et al*. Neuroscience Letters (2016).624, 47-52

Contents lists available at ScienceDirect

Neuroscience Letters

journal homepage: www.elsevier.com/locate/neulet

DROSOPHILA EXPRESSING HUMAN SOD1 SUCCESSFULLY RECAPITULATES MITOCHONDRIAL PHENOTYPIC FEATURES OF FAMILIAR AMYOTROPHIC LATERAL SCLEROSIS

Xavier Gallart-Palau[1,2,3*], Chee-Hoe Ng[5,6], Joan Ribera[1,2], Siu Kwan Sze[3], and Kah-Leong Lim[4,5,6]

[1]Departament de Medicina Experimental, Facultat de Medicina, Universitat de Lleida 25198 Lleida, Catalonia, Spain.

[2]Institut de Recerca Biomèdica de Lleida (IRBLLEIDA), 25198 Lleida, Catalonia, Spain.

[3]School of Biological Sciences, Nanyang Technological University, Singapore, 637551.

[4]Department of Physiology, National University of Singapore, Singapore 117543, Singapore.

[5]Department of Research, National Neuroscience Institute, Singapore 308433, Singapore.

[6]Duke-NUS Graduate Medical School, Singapore 169857, Singapore.

Abstract

Mitochondrial pathology is a seminal pathogenic hallmark of familial amyotrophic lateral sclerosis (FALS) which is extensively manifested by human patients and mutant SOD1G93A mammalian models. Rodents expressing human FALS-associated mutations successfully mimic several human disease features; although they are not as amenable to genetic and therapeutic compound screenings as non-mammalian models. In this study, we report a newly generated and characterized Drosophila model that expresses human SOD1G93A in muscle fibers. Presence of SOD1G93A in thoracic muscles causes mitochondrial pathology and impairs normal motor behavior in these flies. Use of this new FALS-24B-SOD1G93A fly model holds promise for better understanding of the mitochondrial affectation process in FALS and for the discovery of novel therapeutic compounds able to reverse mitochondrial dysfunction in this fatal disease.

Keywords: FALS, SOD1^{G93A}, mitochondria, Drosophila.

* Correspondence:
Xavier Gallart-Palau
Facultat de Medicina, IRBLLEIDA, Universitat de Lleida.
Dept. Medicina Experimental, Unitat de Neurobiologia cel·lular.
Av. Rovira Roure 80, 25198 Lleida, Catalonia, Spain.
Phone: +34-973-702427, Fax: +34-973-702426. E-mail: xavgallart@gmail.com

INTRODUCTION

Amyotrophic lateral sclerosis (ALS) is a devastating motor neuron disease that involves the progressive loss of motor neurons leading to paralysis and death. Although the etiology of ALS remains unclear, mitochondrial pathology has been found even at pre-symptomatic stages of ALS and is currently considered a converging point of multiple pathological pathways in that disease [19]. From the apparition of familial amyotrophic lateral sclerosis (FALS) human SOD1 mutants in 1993 [16], research in ALS has been almost exclusively conducted in FALS rodent models. The advantages regarding the use of these animals have been properly and extensively justified although its use dramatically limits the possibilities to perform extensive primary therapeutic compound screenings in ALS. Prohibitive economic and ethical costs together with discouraging time periods prior to the manifestation of disease features are the classical disadvantages of rodents for that purpose [9].

On the contrary, the fly Drosophila melanogaster fulfils the empty space between in vitro models and mammal models for primary drug screenings in neurodegenerative diseases [21] and [8]. Use of Drosophila implies extremely low cost of maintenance and handling, fast development of disease hallmarks and the possibility to test different forms of administration and toxic effects of promising therapeutic compounds [10] and [12].

In this study we report a new fly model of ALS expressing the human FALS mutant SOD1G93A under the 24B-GAL4 muscle-specific promoter. Expression of SOD1G93A in thoracic muscles, the region of flies that contains higher presence of mitochondria and higher energetic expenses, shortens lifespan, impairs motor behavior and causes mitochondria dysfunction in these animals. Characterization of SOD1G93A-24B-GAL4 flies opens new venues for genetic and extensive primary drug screenings aimed to treat FALS mitochondrial pathology.

MATERIALS AND METHODS

Fly stocks

GAL4/Uas system was used for expression of our transgenes in Drosophila flies as previously described [4]. The fly line 24B-GAL4 used in our experiments was obtained from the Bloomington Stock Center (IN., U.S.A.). Flag-tagged wild-type human SOD1 and human FALS-associated mutant SOD1G93A cDNAs were cloned into pUAST expression vectors. Sequencing of cloned products was performed and pUAST generated plasmids were sent to BestGene (CA., U.S.A.) for microinjection. Eight lines of each transgene were generated and at least two transgenic lines of each mentioned fly transgene (male) were used in our experiments.

Immunohistochemistry and western blotting

All antibodies and reagents were purchased from Sigma Aldrich (MO, USA) unless specified otherwise. AJ10 antibody was kindly provided by Esquerda and colleagues. Flies were submerged in a fixative solution (4% PFA in 1x PBS) overnight at 4 °C. Tissues were then cryoprotected and frozen at −80 °C in cryogenic solution buffer as

previously described by Gallart-Palau et al. [6]. Cryostat sectioning at 14 μm were performed (LEICA, Germany) and tissue sections were mounted in gelatinized slides. Immunohistochemistry protocol was followed as previously described by Gallart-Palau et al. [6]. Mouse anti-flag (1:300), rabbit AJ10 (1:250) and anti-mouse Alexa-488 and anti-rabbit Alexa-594 (1:500) were used as primary and secondary antibodies respectively. Slides were mounted with a drop of Vectashield mounting media (Vectorlabs CA, USA) prior to image acquisition using a confocal microscope Fluoview FV-1000 (Olympus, Germany).

Western blotting to validate transgenes expression was done in denaturant conditions as previously reported [5] and 24B-GAL4/+ lines were used as negative controls. Briefly, SOD1WT and SOD1G93A independent pools were formed by including a total of 10 flies from each respective line. Whole flies were homogenized in 1% SDS and proteins were resolved in a SDS-PAGE gel. Mouse anti-flag-HRP (1:1000) and mouse-γ-tubulin (1:1000) were incubated on blotted nitrocellulose membranes as primary antibodies. Anti-mouse-HRP (1:500) was used as secondary antibody.

Transmission electron microscopy of thoracic muscles

Preparation of thoracic muscles was performed as previously described [23]. Briefly, 15d-old flies were deeply anesthetized with CO2 and thoraces were dissected and removed under the binocular loupe. Muscle tissues were extracted, submerged overnight into a fixative solution (2.5% glutaraldehyde in 0.1 M phosphate buffer, pH 7.2) and postfixed in 1% OsO4 for 1 h. Tissues were next dehydrated in ethanol series and embedded in Spurr's resin. Ultrathin sections were stained with uranyl acetate and lead citrate prior to be observed under a JEM-1230 electron microscope (Jeol, Peabody, MA).

Survival and climbing assays

Male flies were transferred to clean food vials every 2–3 days and scored for death. Food vials containing non-yeasted standard food housed a maximum of 20 individuals. A total of 25 individuals per line expressing human wild-type and G93A-SOD1 transgenes and 24B-GAL4/+ were CO2 anesthetized and placed into vertical plastic columns of 15 cm length and 1.5 cm diameter for climbing assays. One hour was given to each group for recovery purposes and then flies were gently tapped to the bottom of the column and the number of individuals that reached the top at 1 min was scored. Climbing assays were performed in triplicate for each line in intervals of 15 min.

Image analysis and statistical analyses

Confocal microscope images were obtained using a Fluoview FV-500 (Olympus, Hamburg, Germany). Scanning parameters were kept constant during the acquisition of all images. Images were analyzed using fluoview software (Olympus, Hamburg, Germany) and imageJ (NIH, MD., USA) [18] and antibody spots were manually counted. Only clearly visible and round shaped spots were quantified. Quantitative data between 24B-GAL4/+, hSOD1WT and hSOD1G93A fly lines was compared by one-way analysis of variance. Kaplan–Meier analysis was performed and survival log rank trends were analyzed by Chi-square. Level of significance in all

analyses was established at $p < 0.05$ unless specified otherwise.

RESULTS AND DISCUSSION

hSOD1^{G93A} expression in *Drosophila* thoracic muscles

Mass distribution of muscle fibers in Drosophila is highly prominent in thoracic regions to sustain the dynamism of legs and wings [1]. A clear advantage of the UAS-GAL4 system is the selective spatial expression of transgenes in specific cells, tissues and body regions [10]. We analyzed the expression of human SOD1WT and hSOD1G93A under the 24B promoter and found that more than 80 percent of hSOD1 expression was successfully confined to thoracic muscle fibers in all transgenic flies (Fig. 1A and B).

Exclusive expression of hSOD1G93A in skeletal muscles of transgenic mice was initially performed by Dobrowolny et al. [3]. The authors found that this FALS mutant restrictively expressed in skeletal muscles causes reduction of the metabolic activity, atrophy, sarcolemma and higher accumulation of ROS. Later, restricted expression of FALS mutant SOD1G93A in skeletal muscles promoted motor neuron degeneration via retrograde degeneration of motoneuron axons [24]. These studies suggest that affectation of SOD1G93A in muscle fibers is a crucial event on the triggering of neuropathology in FALS; that justifies the investigation of the effects of this transgene following muscle-restricted expression in a novel Drosophila FALS model. Flies expressing neurodegenerative disease-associated mutants under the 24B-GAL4 promoter, a muscle tissue specific driver, have been also previously used to study mitochondrial dysfunction in Parkinson's Disease (PD) by our group [11].

We believed thus that expression of human SOD1G93A in muscles would

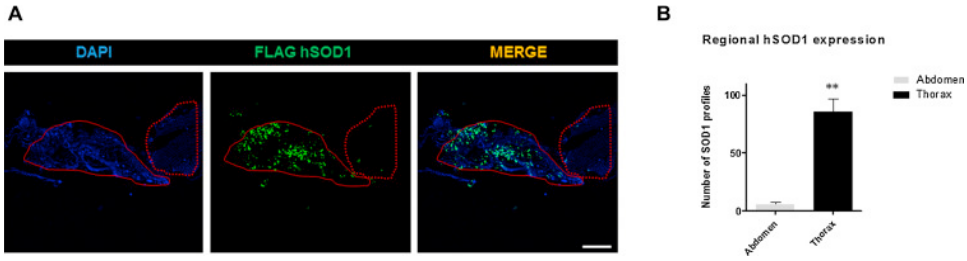

Figure 1: Spatial expression of hSOD1 in Drosophila flies. Immunohistochemistry experiments were performed to confirm the spatial expression of FALS transgenes (hSOD1G93A and hSOD1WT) in our newly generated transgenic Drosophila lines. (A) Image panel showing Dapi staining, hSOD1 anti-flag staining and the merged image in thoracic and abdominal regions of Drosophila body. Continous line shapes Drosophila body thoracic region whereas dashed line shapes Drosophila body abdominal region. Scale bar represents 850 µm. (B) Quantification of hSOD1 expression in thoracic and abdominal regions of Drosophila body in our transgenic lines. As shown in the graph, thoracic expression of hSOD1 was significantly higher than abdominal expression of these transgenes under the 24B promoter ($p < 0.001$).

cause ALS-associated mitochondrial pathology in Drosophila flies. To further confirm expression of SOD1 in our transgenic Drosophila lines; we analyzed hSOD1WT and hSOD1G93A expression levels by anti-flag antibody image quantification and no significant differences were found on the expression of these transgenes between these two groups (Fig. 2H). Additionally, hSOD1 expression in transgenic lines was validated by WB (Fig. 2I).

Toxic isoforms of misfonded SOD1 in thoracic fibers of hSOD1^{G93A} flies

Toxicity of hSOD1G93A is associated with apparition of misfolded isoforms of the protein that can be identified by specific antibodies [14]. One of these antibodies is AJ10 which was characterized by Sabado et al. as able to specifically bind to misfolded and toxic isoforms of hSOD1 [17]. We used the AJ10 antibody to identify misfolded and toxic isoforms of hSOD1 in our generated transgenic flies. Positive colocalization (57.6%) (Fig. 2G) was evidenced in thoracic tissues of hSOD1G93A flies whereas no positive staining was found in same tissues from hSOD1WT control flies (Fig. 2A–F).

Expression of hSOD1^{G93A} in thoracic muscles causes mitochondrial pathology

An unforeseen upheld wing phenotype was uniquely observed in between the 30–40% of our 24B-hSOD1G93A flies (Fig. 3A). A very close phenotype to our findings was previously reported by Deak [1] during analysis of upheld mutant flies. According to the author, those mutants held-up their wings vertically and stacked, were flightless and unable to jump as we observed only in hSOD1G93A flies. Deak also observed abnormalities on the legs and cuticle density of upheld mutant flies and these defects were not apparently resembled by our model. The author observed that upheld mutants displayed dramatic disorganization of indirect flight muscles including extreme loss of fibers and abnormal mitochondria distribution whereas no specific mitochondria pathology was reported in those mutants by histological analyses [1]. Although muscle disorganization can cause abnormal wings posture in flies (upheld or flapwing) as referred by Deak, recently, singular alterations in normal mitochondrial dynamics caused by neurodegenerative mutants have been associated to the apparition of abnormal wing phenotype without affectation of muscle fibers which may help to explain our hSOD1G93A encountered phenotype [2], [11] and [15].

It has been shown that toxic and misfolded isoforms of hSOD1 as those identified in our hSOD1G93A flies by the AJ10 antibody affect preferentially the mitochondria organelles in FALS models [14]. In order to characterize the tissues expressing ALS-SOD1G93A in upheld phenotypic flies and hSOD1WT in control flies, thoracic ultrastructural analyses by transmission electronic microscopy (TEM) were performed. ALS-SOD1G93A TEM images showed, in general terms, normal organization of muscle fibers as it was also observed in controls (Fig. 3B–D). However, a clear pattern of mitochondrial affectation was observed in ALS fly mutants in concordance to what was previously reported in ALS-SOD1G93A rodent models [22], [13] and [20]. Mitochondria in 24B-SOD1G93A flies exhibit the inner structures including

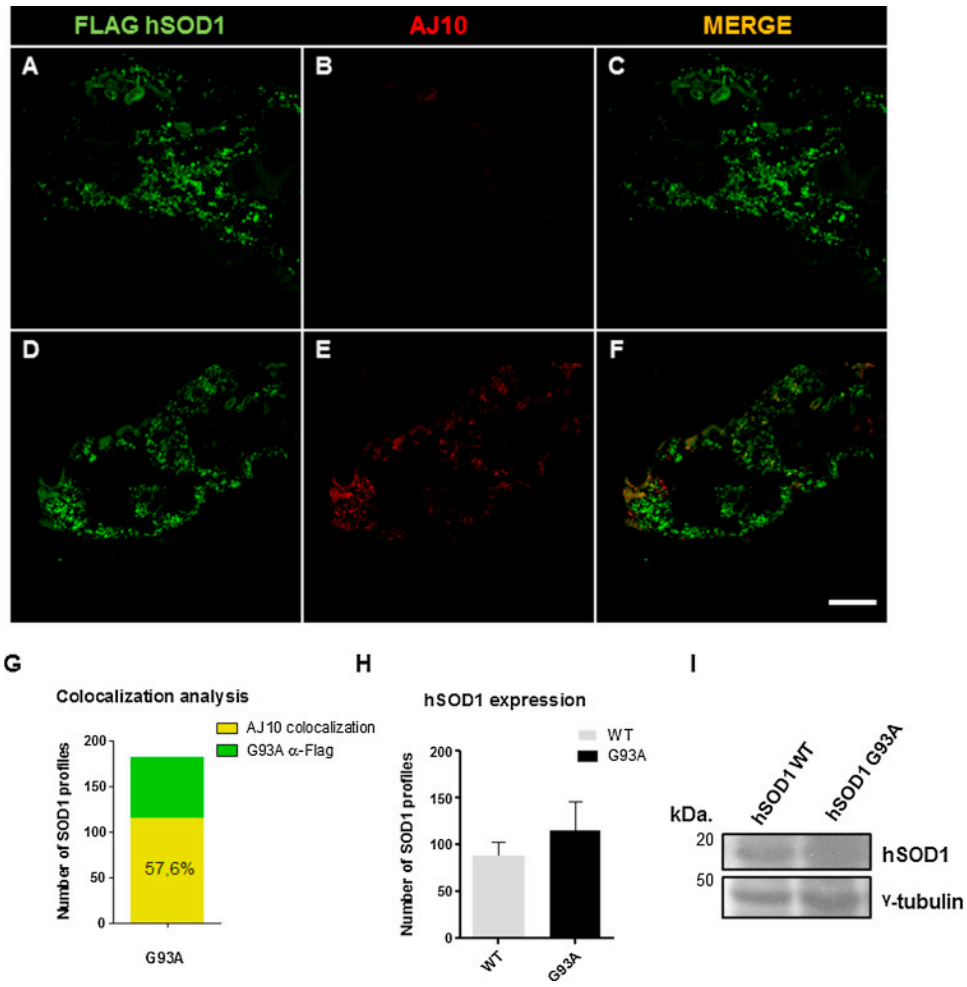

Figure 2: Analysis of hSOD1 expression in Drosophila transgenic lines. (A) Confocal image showing anti-flag hSOD1 antibody signal in thoracic tissues of hSOD1WT transgenic flies. (B) Confocal image showing anti-AJ10 antibody signal in thoracic tissues of hSOD1WT transgenic flies. (C) Confocal image showing the merged image of anti-flag and AJ10 signal in thoracic tissues of hSOD1WT transgenic flies. Merged image shows absence of colocalization between both antibodies in WT transgenic flies. (D) Confocal image showing anti-flag antibody signal in thoracic tissues of hSOD1G93A transgenic flies. (E) Confocal image showing anti-AJ10 antibody signal in thoracic tissues of hSOD1G93A transgenic flies. (F) Confocal image showing the merged image of anti-flag and AJ10 signal in thoracic tissues of hSOD1G93A transgenic flies. Merged image shows colocalization (yellow spots) between both antibodies in G93A transgenic flies. Scale bar represents 500 μm. (G) Percentage quantification of colocalized hSOD1G93A to misfolded and toxic isoforms of hSOD1 stained by AJ10 antibody. (H) SOD1 expression in WT and G93A flies was quantified and no significant differences were found on the expression pattern of these transgenes between groups. (I) hSOD1 expression was validated by WB. (For interpretation of the references to colour in this figure legend, the reader is referred to the web version of this article.)

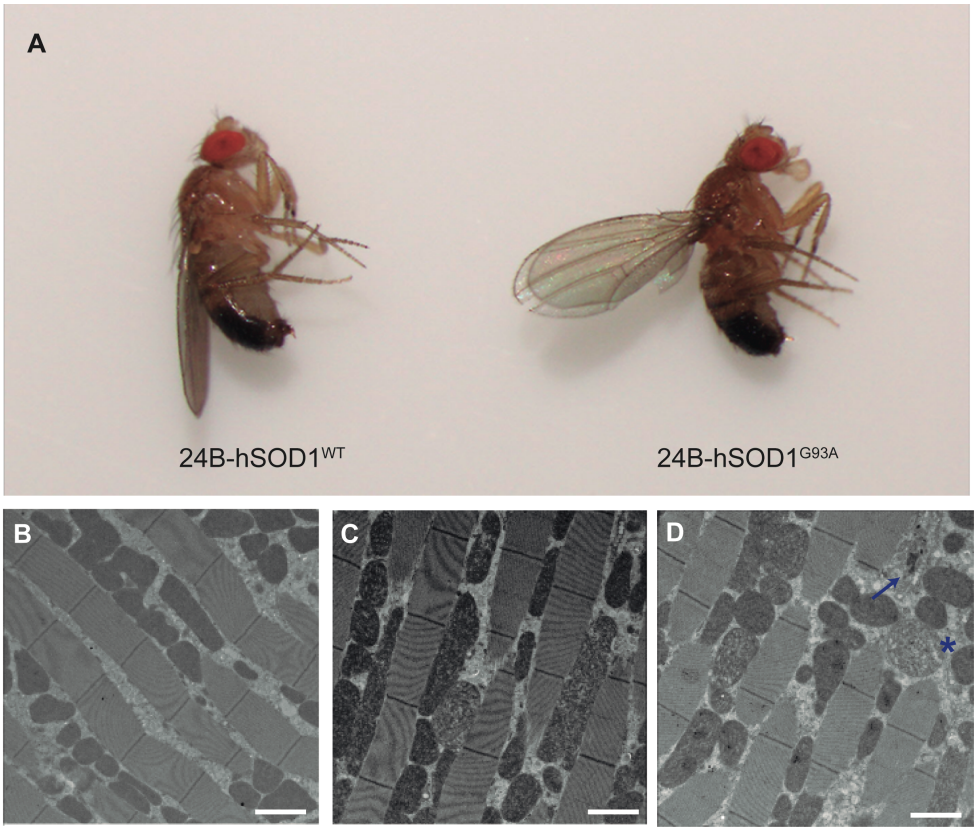

Figure 3: Characterization of the newly generated FALS-24B-hSOD1G93ADrosophila lines. (A) Image showing the upheld phenotype caused by expression of hSOD1G93A in thoracic muscles of Drosophila flies. Expression of hSOD1WT in Drosophila thoracic muscles does not cause any apparent phenotype. (B) Ultrastructural image showing the thoracic muscular fibers and mitochondria of Drosophila flies following expression of hSOD1WT. (C) Ultrastructural image of Drosophila thoracic muscles following expression of the FALS mutant of hSOD1G93A, mitochondria show clear dynamic dysfunction (pro-fusion pattern) and the inner structures are visible showing damage on the mitochondria outer and intermediate membranes. (D) Ultrastructural image of Drosophila thoracic muscles were swollen mitochondria (pointed by *) and autophagosome-like structures (pointed by blue arrow) are apparent following expression of hSOD1G93A in Drosophila flies. Scale bar in B, C and D ultrastructural images represents 2 μm. (For interpretation of the references to colour in this figure legend, the reader is referred to the web version of this article.)

cristae, what clearly suggests impairment of the cellular organelle membranes. In addition, elongated mitochondria were often observed together with rounded and swollen organelle profiles (Figs. 2 D and 3 C; swollen mitochondria indicated by an asterisk). None of these ALS pathological hallmarks were seen in hSOD1WT flies (Fig. 3B). In the same light, presence of autophagosome-like features were also observed in 24B-GAL4-SOD1G93A flies mitochondria (Fig.

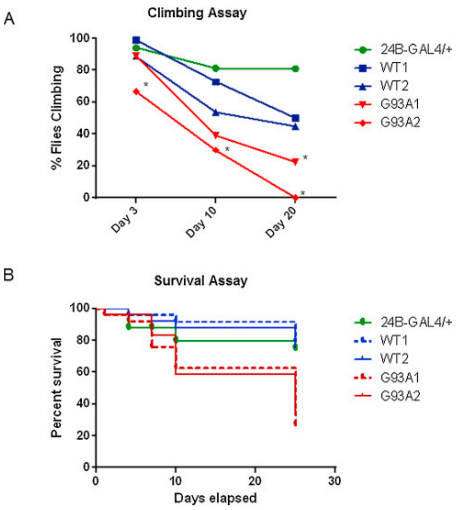

Figure 4 Behavioral characterization of FALS-24B-hSOD1G93ADrosophila lines. (A) Trend line graph showing the climbing assay performance of Drosophila lines. 24B-GAL4/+, hSOD1WT and hSOD1G93A fly lines were analyzed and climbing defects were apparent hSOD1G93A transgenic flies from day 10 post-eclosion onwards. Significance level * $p < 0.05$. (B) Kaplan–Meier analysis of survival was performed in 24B-GAL4/+, hSOD1WT and hSOD1G93A fly lines. Significant survival declination peak was found at day 25 post-eclosion. Chi-square log rank trend analysis 13.85, p-value < 0.001.

3D; dark blue arrow). Ultrastructural characterization confirmed that disorganized and impaired mitochondria, as these identified in our ALS mutant flies, is associated to depletion of energy in thoracic muscle fibers what promotes apparition of the identified upheld phenotype [11].

SOD1^{G93a} impairs *Drosophila* motor behavior and shortens lifespan

Upheld wings phenotype arose around 7–10 postnatal days in 24B-hSOD1G93A and rendered only the affected flies as flightless. Impaired climbing ability was clearly manifested in one of the analyzed 24B-hSOD1G93A lines at 15 day post-eclosion whereas in the other 24B-hSOD1G93A line the impaired climbing ability was evidenced around five days later, in all cases the climbing ability was compared to 24B-hSOD1WT control flies (Fig. 4A). Climbing ability of upheld wing 24B-hSOD1G93A flies was highly similar to non-upheld wing flies in the same lines. Additionally, survival studies showed decline in survival for the ALS-mutant flies after ~25 days post-eclosion compared to controls although the survival decline was especially apparent in the upheld wing flies (Fig. 4B). Despite the fact that significant differences on the expression level of transgenes between transgenic lines were not identified in our study, higher in-line variation as it has been recently described [7] may explain some encountered behavioral discrepancies between same transgene lines observed in our study.

Behavioral assays as climbing and survival assays reflect disease phenotypes in several neurodegenerative transgenic fly models. Similarly, and as shown by our 24B-SOD1G93A flies characterized here, mitochondrial affectation has also been mainly manifested by abnormal wings posture and impaired climbing abilities in PD transgenic models [11]. Furthermore, impaired motor ability was observed near the terminal stage of FALS flies, what would be in close accordance to what is observed on hSOD1G93A mammal models [6].

CONCLUSIONS

We demonstrate here that overexpression of hSOD1G93A in Drosophila muscle fibers causes a characteristic pathogenic phenotype that includes flightless upheld wings, climbing defects and mitochondrial dysfunction; features that resemble human FALS. Due to the easy handling, simple genetic modification and highly "druggable" capacity, we believe that the new hSOD1G93ADrosophila FALS model reported here will provide significant opportunities to study and rescue the pathogenic interactions between SOD1 mutants and mitochondria in ALS.

ACKNOWLEDGEMENTS

This study was funded in Singapore by grants from the National Medical Research Council-CBRG to K.L.L. and in Spain by doctoral scholarships from the University of Lleida to X.G.P. The authors sincerely thank Royston Tan for his invaluable technical help. We wish also to thank members of the Neurodegeneration Research Labotarory at the National Neuroscience Institute of Singapore, especially Dr. Zhang Chengwu and Dr. Grace Lim.

REFERENCES

[1] Deak, II (1977) Mutations of Drosophila melanogaster that affect muscles. Journal of embryology and experimental morphology 40:35-63.

[2] Deng H, Dodson MW, Huang H, Guo M (2008) The Parkinson's disease genes pink1 and parkin promote mitochondrial fission and/or inhibit fusion in Drosophila. Proceedings of the National Academy of Sciences of the United States of America 105:14503-14508.

[3] G. Dobrowolny, M. Aucello, E. Rizzuto, S. Beccafico, C. Mammucari, S. Boncompagni, S. Belia, F. Wannenes, C. Nicoletti, Z. Del Prete, N. Rosenthal, M. Molinaro, F. Protasi, G. Fano, M. Sandri, A. Musaro. Skeletal muscle is a primary target of SOD1G93A-mediated toxicity. Cell Metab., 8 (2008), pp. 425–436

[4] J.B. Duffy. GAL4 system in Drosophila: a fly geneticist's Swiss army knife. Genesis, 34 (2002), pp. 1–15

[5] X. Gallart-Palau, A. Serra, A.S. Wong, S. Sandin, M.K. Lai, C.P. Chen, O.L. Kon, S.K. Sze. Extracellular vesicles are rapidly purified from human plasma by PRotein Organic Solvent PRecipitation (PROSPR). Sci. Rep., 5 (2015), p. 14664

[6] Gallart-Palau X, Tarabal O, Casanovas A, Sabado J, Correa FJ, Hereu M, Piedrafita L, Caldero J, Esquerda JE (2014) Neuregulin-1 is concentrated in the postsynaptic subsurface cistern of C-bouton inputs to alpha-motoneurones and altered during motoneuron diseases. FASEB journal : official publication of the Federation of American Societies for Experimental Biology 28:3618-3632.

[7] W. Huang, M.A. Carbone, M.M. Magwire, J.A. Peiffer, R.F. Lyman, E.A. Stone, R.R. Anholt, T.F. Mackay. Genetic basis of transcriptome diversity in Drosophila melanogaster. Proc. Natl. Acad. Sci. U. S. A., 112 (2015), pp. E6010–6019

[8] Imai Y, Venderova K, Lim KL (2012) Animal models of Parkinson's disease 2012. Parkinson's disease 2012:729428.

[9] Lee S, Bang SM, Lee JW, Cho KS (2014) Evaluation of traditional medicines for neurodegenerative diseases using Drosophila models. Evidence-based complementary and alternative medicine : eCAM 2014:967462.

[10] K.A. Matthews, T.C. Kaufman, W.M. Gelbart. Research resources for Drosophila: the expanding universe. Nat. Rev. Genet., 6 (2005), pp. 179–193

[11] C.H. Ng, M.S. Guan, C. Koh, X. Ouyang, F. Yu, E.K. Tan, S.P. O'Neill, X. Zhang, J. Chung, K.L. Lim. AMP kinase activation mitigates dopaminergic dysfunction and mitochondrial abnormalities in Drosophila models of Parkinson's disease. J. Neurosci., 32 (2012), pp. 14311–14317

[12] U.B. Pandey, C.D. Nichols. Human disease models in Drosophila melanogaster and the role of the fly in therapeutic drug discovery. Pharmacol. Rev., 63 (2011), pp. 411–436

[13] S. Pickles, L. Destroismaisons, S.L. Peyrard, S. Cadot, G.A. Rouleau, R.H. Brown Jr., J.P. Julien, N. Arbour, C. Vande Velde. Mitochondrial damage revealed by immunoselection for ALS-linked misfolded SOD1. Hum. Mol. Genet., 22 (2013), pp. 3947–3959

[14] S. Pickles, C. Vande Velde. Misfolded SOD1 and ALS: zeroing in on mitochondria. Amyot. Lat. Scler., 13 (2012), pp. 333–340

[15] M. Rai, P. Katti, U. Nongthomba. Drosophila erect wing (Ewg) controls mitochondrial fusion during muscle growth and maintenance by regulation of the Opa1-like gene. J. Cell Sci., 127 (2014), pp. 191–203

[16] D.R. Rosen, T. Siddique, D. Patterson, D.A. Figlewicz, P. Sapp, A. Hentati, D. Donaldson, J. Goto, J.P. O'Regan, H.X. Deng. Mutations in Cu/Zn superoxide dismutase gene are associated with familial amyotrophic lateral sclerosis. Nature, 362 (1993), pp. 59–62

[17] Sabado J, Casanovas A, Hernandez S, Piedrafita L, Hereu M, Esquerda JE (2013) Immunodetection of disease-associated conformers of mutant cu/zn superoxide dismutase 1 selectively expressed in degenerating neurones in amyotrophic lateral sclerosis. Journal of neuropathology and experimental neurology 72:646-661.

[18] C.A. Schneider, W.S. Rasband, K.W. Eliceiri. NIH image to ImageJ: 25 years of image analysis. Nat. Methods, 9 (2012), pp. 671–675

[19] Shi P, Wei Y, Zhang J, Gal J, Zhu H (2010) Mitochondrial dysfunction is a converging point of multiple pathological pathways in amyotrophic lateral sclerosis. Journal of Alzheimer's disease : JAD 20 Suppl 2:S311-324.

[20] Song W, Song Y, Kincaid B, Bossy B, Bossy-Wetzel E (2013) Mutant SOD1G93A triggers mitochondrial fragmentation in spinal cord motor neurones: neuroprotection by SIRT3 and PGC-1alpha. Neurobiology of disease 51:72-81.

[21] Tickoo S, Russell S (2002) Drosophila melanogaster as a model system for drug discovery and pathway screening. Current opinion in pharmacology 2:555-560.

[22] Vande Velde C, McDonald KK, Boukhedimi Y, McAlonis-Downes M,

Lobsiger CS, Bel Hadj S, Zandona A, Julien JP, Shah SB, Cleveland DW (2011) Misfolded SOD1 associated with motor neuron mitochondria alters mitochondrial shape and distribution prior to clinical onset. PloS one 6:e22031.

[23] Wang C, Lu R, Ouyang X, Ho MW, Chia W, Yu F, Lim KL (2007) Drosophila overexpressing parkin R275W mutant exhibits dopaminergic neuron degeneration and mitochondrial abnormalities. The Journal of neuroscience : the official journal of the Society for Neuroscience 27:8563-8570.

[24] M. Wong, L.J. Martin. Skeletal muscle-restricted expression of human SOD1 causes motor neuron degeneration in transgenic mice. Hum. Mol. Genet., 19 (2010), pp. 2284–2302

NFκB influences proteasome function and co-aggregation of SOD1

Amyotrophic Lateral Sclerosis.

In preparation

NFκB INFLUENCES PROTEASOME FUNCTION AND CO-AGGREGATION OF SOD1^{G93A} AND PINK1 IN FAMILIAL AMYOTROPHIC LATERAL SCLEROSIS

Xavier Gallart-Palau[1,2,3], Grace G. Y. Lim[4,5], Zhang Cheng Wu[5], Siu Kwan Sze[3], Joan Ribera[1,2] and Kah-Leong Lim[4,5,6]

[1]Departament de Medicina Experimental, Facultat de Medicina, Universitat de Lleida 25198 Lleida, Catalonia, Spain.

[2]Institut de Recerca Biomèdica de Lleida (IRBLLEIDA), 25198 Lleida, Catalonia, Spain.

[3]School of Biological Sciences, Nanyang Technological University, Singapore, 637551.

[4]Department of Physiology, National University of Singapore, Singapore 117543, Singapore.

[5]Department of Research, National Neuroscience Institute, Singapore 308433, Singapore.

[6]Duke-NUS Graduate Medical School, Singapore 169857, Singapore.

Abstract

Mutant SOD1^{G93A} is known to impair the proteasome and promote dysfunction of mitochondria in Familial Amyotrophic Lateral Sclerosis (FALS). Proteasome impairment precedes degeneration of motoneurones in FALS however the mechanisms that cause failure of the proteasome remain unclear. Additionally, apparition of mitochondria toxicity involves the activation of PINK1; a protein that triggers degradation of these organelles by autophagy. Although mitochondria toxicity and proteasome dysfunction are clearly known as pathological hallmarks of FALS the interactions between SOD1^{G93A}, UPS and mitochondria in this motoneuron disease are largely unknown. Here we confirmed a significant translocation of expressed SOD1^{G93A} into mitochondria that promotes activation of PINK1. Furthermore, we found co-aggregation of SOD1 ^{G93A} and PINK1 in cells and in SOD1 ^{G93A} transgenic rodent motoneurones. Finally, we encountered in the nuclear factor NFκB a convergence element that activates nuclear expression of PINK1 and promotes dysfunction of the proteasome under presence of the FALS-associated mutant SOD1^{G93A}. Taken together our results provide novel insight on the existent link between mitochondria toxicity and the molecular mechanisms that promote impairment of the proteasome in FALS.

Keywords: ALS, SOD1^{G93A}, Mitochondria, NFκB, PINK1, Proteasome.

BACKGROUND

Motoneurones (MNs) are very specialized cells with highly energetic expenses to sustain their fast excitable nature. This idiosyncratic feature is likely to make these cells especially vulnerable to imbalances in bioenergetics homeostasis (Le Masson et al. 2014). Mitochondria regulate MNs energetic supply through generation of adenosine triphosphate

(ATP) and release of cytosolic calcium during excitability (Bergmann & Keller 2004). Additionally, these cellular organelles influence cell death and survival by controlling the liberation of pro-apoptotic signals (Cozzolino et al. 2015). In familial forms of Amyotrophic Lateral Sclerosis (FALS) caused by toxic mutants of the protein superoxide dismutase 1 (SOD1); alterations of mitochondria in axon and dendrites of MNs have been evidenced even at pre-symptomatic stages of the disease (Pickles & Vande Velde 2012). Furthermore, it is proposed that $SOD1^{G93A}$ indirectly may affect mitochondria via the impairment of the proteasome ubiquitin system (UPS) (Tradewell et al. 2011; Sullivan et al. 2004) although the interactions between the triad $SOD1^{G93A}$, UPS and mitochondria still remain poorly understood in FALS.

Damaged mitochondria in MNs activate the expression of some key proteins proposed to trigger mitochondrial degradation by autophagy. The expression of PTEN-induced putative kinase 1 (PINK1), a mitochondrial transmembrane protein, promotes clearance of dysfunctional mitochondria abolishing UPS degradation of pro-mitophagic proteins (Muqit et al. 2006). Alteration on the expression of PINK1 in FALS caused by $SOD1^{G93A}$ has been recently described (Knippenberg et al. 2013) anyhow the role of PINK1 in FALS still remains elusive. Activation of PINK1 in neurones has been proposed as regulated by the nuclear factor kappa-light-chain-enhancer of activated B cells (NFκB) (Duan et al. 2014). In normal conditions, NFκB remains attached to the protein IκB forming a complex in the cellular cytoplasm, although under presence of stressful stimulus IκB is degraded and NFκB released for nuclear translocation. Activation of NFκB in FALS has been previously reported however insight about the interactions between NFκB and PINK1 under presence of ALS-associated SOD1 mutants is currently lacking.

Here we have examined the capacity of the ALS mutant $SOD1^{G93A}$ to translocate to mitochondria, damage the proteasome protease capacity and activate PINK1 expression via translocation of NFκB into the nuclei of neurones. We show how PINK1 co-aggregates with $SOD1^{G93A}$ in neuronal cells and in the spinal cord of $SOD1^{G93A}$ transgenic mice. Strikingly, we found that inactivation of the NFκB pathway under presence of $SOD1^{G93A}$ and PINK1 reverses proteasome affectation and reduces the co-aggregation of $SOD1^{G93A}$ and PINK1 in neuronal cells. Our results provide new insight on the currently unknown degenerative interactions that take place amongst the triad $SOD1^{G93A}$, UPS and mitochondria in FALS.

METHODS

Plasmids, antibodies and reagents

cDNA plasmids expressing FLAG-tagged $SOD1^{WT}$, FLAG-tagged $SOD1^{G93A,}$ NFκB mutants K44 and IκB were kind gifts from Takahashi R. (Kyoto University, Japan). cDNA plasmid expressing PINK1 was obtained from G. Sobue (Nagoya University, Japan). Ubiquitinated GFP (GFPu) plasmid was a generous gift from N. Matsuda (Tokyo Metropolitan Institute of Medical Science, Japan). Anti-FLAG

mouse monoclonal antibody was purchased from Sigma (MO, USA), rabbit polyclonal primary antibody anti-PINK1 was acquired from Novus Biologicals (CO, USA), Rabbit anti-GFP was purchased from Abcam (Cambridge, UK) and custom raised rabbit monoclonal AJ10 antibody against misfolded SOD1 was characterized and previously published by our research group (Sábado et al. 2013). Horseradish peroxidase conjugated (Hrp) secondary antibodies anti-rabbit and anti-mouse were purchased from Sigma (MO, USA) and secondary antibodies anti-mouse Alexa Fluor 488, anti-rabbit Rhodamine-Red and anti-rabbit Alexa Fluor Cy3 were acquired from Jackson ImmunoResearch (Suffolk, UK). All reagents were purchased from Sigma (MO, USA) with the exception of MG-132 acquired from A.G. Scientific (CA, USA).

Cell culture, mitochondrial enrichment, particulate fractionation and Western blot

Human SH-SY5Y neuroblastoma cells were cultured as described (Lim et al. 2005). Briefly, cells were grown in 10% FBS DMEM enriched media into a CO_2 controlled incubator. Around 70% of confluence, cells were transiently transfected with cDNA plasmids using lipofectAMINE PLUS from Invitrogen, (CA., USA) following the manufacturer´s protocol. For our mitochondria enrichment studies, 48h after transfection cell media was aspirated and cells were washed two times with 1X cold phosphate-buffer saline (PBS). Subsequently, cells were lysed in a Tris buffer containing (200mM sucrose, 1M Tris pH 7.4, PMSF and Aprotonin) and briefly sonicated at low amplitude (≈20%). Then lysates were centrifuged at 100g for five minutes at 4ºC and supernatant (S/N) was collected and centrifuged again at 8000g for 20 minutes. Pellet containing the mitochondrial enriched fraction (Mito) was washed once in cold PBS. Protein from both fractions was resuspended in custom made 2X Laemmli buffer added fresh with 5% β-mercaptoethanol. Samples were boiled at 95º for 5 minutes under reducing conditions and finally 40µg of protein were resolved in a SDS-PAGE gel and analyzed by Western blot. In our particulate fractionation experiments we followed the protocol described by (Wang et al. 2005) to obtain two fractions, by one side the soluble fraction (S/N) containing of the cells soluble proteins and the particulate fraction (P) containing of the cells oligomeric proteins. Briefly, cells were lysed on ice in 1X Triton-X100 added with protease inhibitors and ultracentrifuged at 50.000 rpm for 30 minutes. The S fraction was collected and the P fraction was processed as previously described for the Mito fraction. Both fractions were finally analyzed by Western Blot.

NFκB activation and proteasome assays

The Ready-To-Glow secreted luciferase assay (SEAP) Clontech (CA., USA) was performed to monitor NFκB activation in SH-SY5Y cells. Cells were plated in 10cm plates and respectively transfected with the NFκB reporter + PSEAP; NFκB reporter + PSEAP + $SOD1^{WT}$; NFκB reporter + PSEAP + $SOD1^{G93A}$ and NFκB reporter + PSEAP + TRAF6 used as positive control. Twenty-four hours after transfection cell media was collected

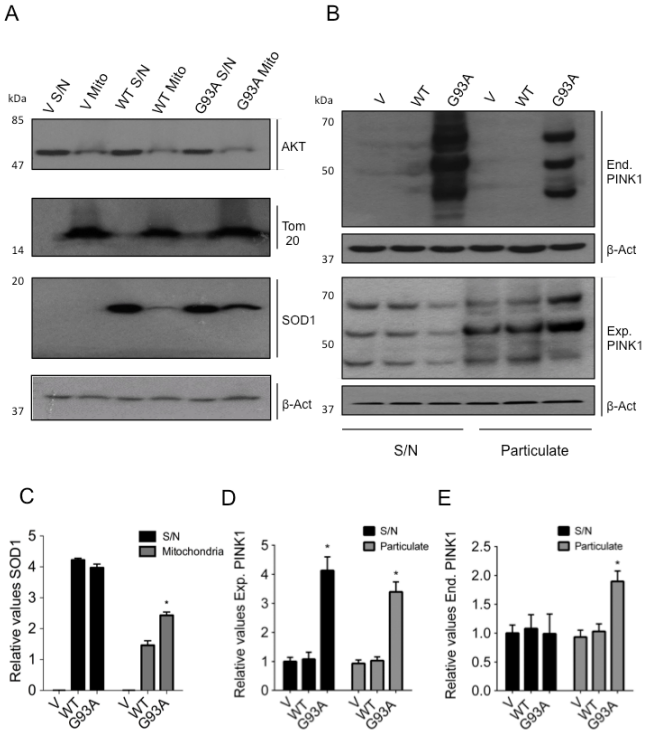

Figure 1. Western blot characterization of mitochondria and particulate fractions of the hSOD1 and PINK1 transfected SHSY5Y cells. A. Mitochondrial fractionation unraveled the high capacity of the mutant hSOD1G93A to translocate to the mitochondrial compared to hSOD1WT. The proteins Tom 20 and AKT were used as internal controls during the mitochondria isolation protocol. Tom 20 is an exclusive mitochondrial marker while the AKT presence has only been linked to the cytosol and nuclear fractions (Rosner et al., 2007) . Accordingly, the Tom 20 protein was only detected in the mitochondrial fraction while the AKT presence was primordially detected in the cytosolic fraction. B. The soluble/particulate fractionation demonstrates the capacity of mutant SOD1 to activate PINK1 levels. The upright caption shows the activation of PINK1 in both the cytosolic and the particulate fraction while PINK1 was co-expressed with hSOD1G93A. The downright caption shows the activation of endogenous PINK1 in the particulate fraction under the presence of overexpressed hSOD1G93A. C. Western blot values including statistical analysis of the relative hSOD1 presence in the mitochondrial fraction. (* $P<0.05$) shows the difference between hSOD1WT and hSOD1G93A. D. Western blot values including statistical analysis of the relative endogenous PINK1 levels in the hSOD1 transfected cells. The values for the WT and the mutant transfected cells were independently compared for the insoluble and the particulate fractions. (t test * $P<0.05$) between hSOD1WT and hSOD1 G93A. E. Western blot values including statistical analysis of the relative co-expressed PINK1 level in hSOD1 transfected cells. The values for the co-expressed PINK1 in WT and mutant co-transfected cells were independently compared for the insoluble and the particulate fractions. (t test * $P<0.05$) between hSOD1WT and hSOD1G93A. The average values are expressed with SEM.

(100 µL.) and assayed according to the manufacturer´s instructions. To study the activity of the 20S proteasome cells were washed in cold PBS and assayed by the Chemicon´s proteasome activity kit Chemicon (MA., USA) following the manufacturer´s protocol. Samples and blanks were analyzed in triplicate and MG-132 was used as control of the proteasome baseline activity at a concentration of 10µM.

Immunocytochemistry

SH-SY5Y cells were cultured on Poly-D-Lysine coated coverlips and transfected as described above. At the harvesting point cells were washed two times with cold 1X PBS and submerged overnight in fixative solution (2.5% paraformaldehyde in 1X PBS) at 4ºC. Then, cells were washed three times with 1X PBS and permeabilized with 0.1% Triton-X100 for 1 minute. After permeabilization cells were labeled with the respective primary antibodies overnight at 4ºC, washed with 1X PBS for three times and incubated with Alexa 488 and Rhodamine-Red secondary antibodies at room temperature for 1h. Finally, cells were mounted on slides using Vectashield mounting media Vectorlabs (CA, USA) prior to be analyzed under confocal microscope.

Animals

SOD1^{G93A} rats (Sprague Dawley background) and SOD1^{G93A} mice used in our experiments were purchased from the Jackson Laboratory (Sacramento, CA). Transgenic rats were directly housed in our specialized animal facilities and SOD1^{G93A} mice were maintained as hemizygotes by breeding transgenic males with C57BL/6 females. Mice transgenic progeny was identified by PCR genotyping of DNA extracted from the tail by using specific primers as previously described (Sábado et al. 2013; Gallart-Palau et al. 2014). Age-matched WT littermates of transgenic animals were used as controls. All experimentation procedures were performed according to the committee for Animal Care and Use of the University of Lleida in line with the Generalitat de Catalunya guidelines (DOGC 2073, 1995).

Tissue preparation, tissue homogenization and immunohistochemistry

Mice were deeply anesthetized and transcardially perfused with saline buffer followed by fixative buffer (4% PFA in 0.1M PB pH 7.4). Lumbar spinal cord tissues were extracted and conserved in fixative buffer for 24 hours prior to be kept in cryoprotective buffer (30% sucrose in 0.1M PB and 0.02% sodium azide). Subsequently, samples were frozen in optimal cutting temperature media Tissue-Teck (Flemingweg, The Netherlands) and cryostate blocks were formed and sectioned (16 µm.) in a cryostat Leica (Wetzlar, Germany). Spinal cord tissues from rats were extracted and kept at -80ºC freezer after the animals were deeply anesthetized and transcardially perfused with saline buffer. For our spinal cord particulate study, one-hundred micrograms of tissue were homogenized in 1X Triton X-100, processed and analyzed by Western Blot as previously detailed in the particulate fractionation paragraph of this methods section.

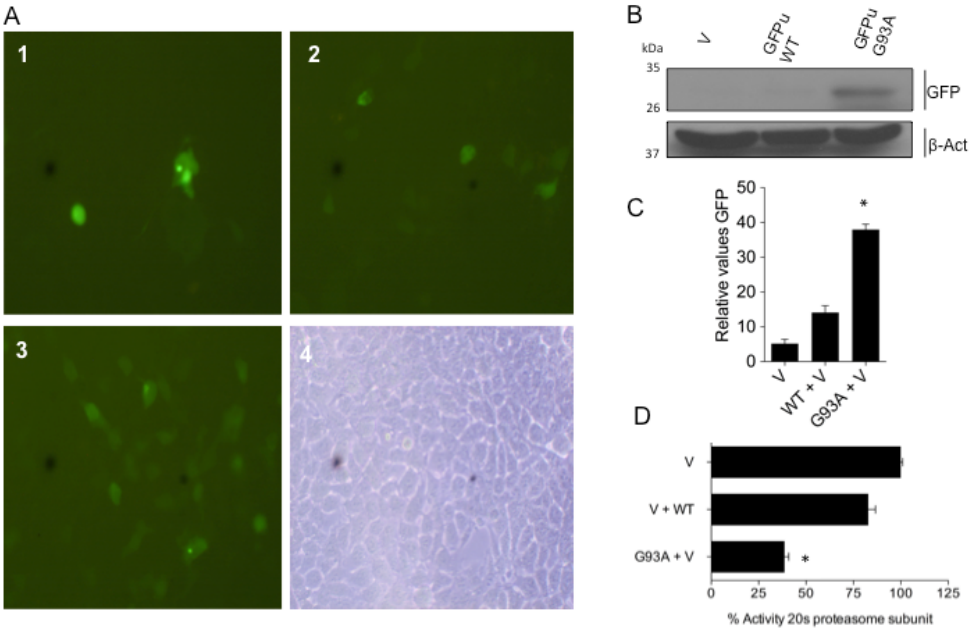

Figure 2. Proteasome assay captions measuring the proteolytic capacity of the 26s and the 20s proteasome subunits in the presence of transfected hSOD1WT and hSOD1G93A in SH-SY5Y cells. A. 1. Fluorescence microscope representative image showing GFPu signal after the PCDNA vector and 0.3µg of the GFPu vector were co-transfected. The GFPu protein is constitutively ubiquitinated and degraded by the 26S proteasome subunit with a half-life <30 minutes in the cells (Djakovic et al., 2009; Gilon et al., 1998). 2. Fluorescence microscope representative image showing GFPu signal after the hSOD1WT and 0.3µg of the GFPu vector were co-transfected. 3. Fluorescence microscope representative image showing GFPu signal after the mutant hSOD1G93A and 0.3µg of the GFPu vector were co-transfected. 4. Cell density control image. B. The GFPu levels in the respective co-transfected cell lysates were evaluated by western blot. C. Western blot representative values including statistical analysis of the relative GFPu levels in WT and mutat hSOD1G93A co-transfected cells. (* $P<0.05$) shows the detrimental effect of hSOD1G93A on the 26S proteasome subunit compared between the respectively described conditions. D. The 20s proteasome peptidase activity (fluorimetric assay) in the cell lysates transfected with PCDNA, hSOD1WT and hSOD1G93A was measured by fluorimeter as has been described in the material and methods. (* $P<0.05$) shows the detrimental effect of hSOD1G93A on the 20S proteasome subunit compared to the respectively described conditions. The average values are in all cases expressed with the SEM.

Spinal cord sections were collected onto gelatinized slides and permeabilized with 0.1% Triton X-100 in PBS for 1h, blocked in 10% normal horse serum for 1h and incubated overnight at 4ºC with the respective primary antibodies. Then sections were washed thrice in 1X PBS for 10 minutes and incubated with the

appropriate secondary antibodies for 1 h at room temperature. After washes, spinal cord sections were labeled with NeuroTrace Nissl staining Molecular Probes (MA, USA) and mounted with a laboratory made antifading mounting media (0.1 M Tris-HCl buffer, pH 8.5, 20% glycerol, 10% Moviol and 0.1% 1,4-diazabicyclo [2.2.2] octane).

Confocal microscopy

Confocal images were obtained using Fluoview FV-1000 Olympus confocal laser-scanning microscope (Olympus, Hamburg, Germany). For the spinal cord sections, digital images were obtained from every 30th section of the entire lumbar spinal cord and same scanning parameters were used to acquire images corresponding to different experimental groups.

Statistical Analysis

Data are expressed as mean ± SEM. Student's t-test and ANOVA analyses were performed to compare between

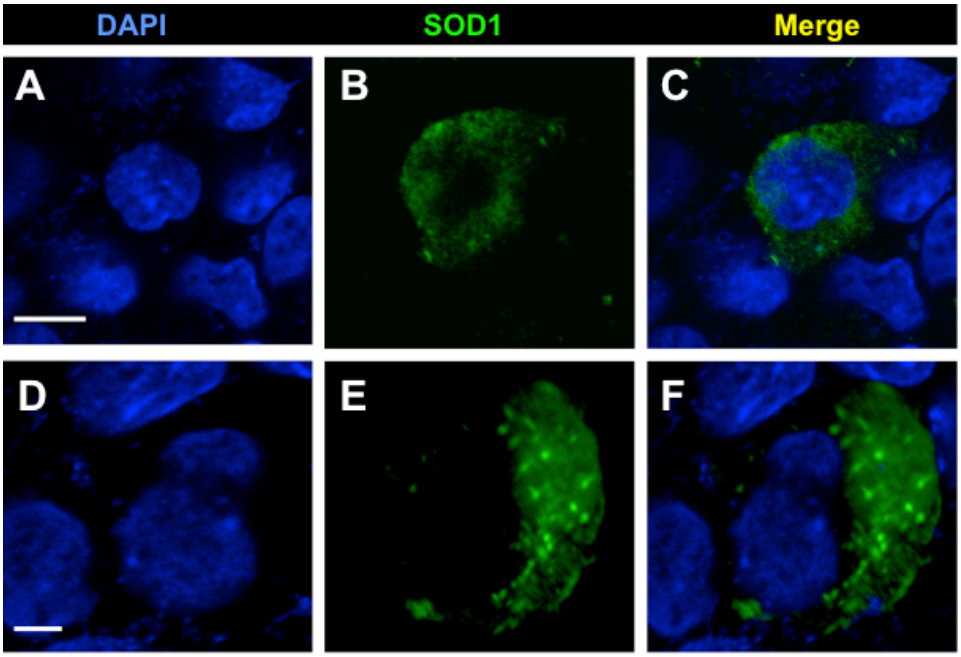

Figure 3. Confocal micrographs showing the aggregation capacity of hSOD1G93A when is overexpressed in SH-SY5Y cells. The cells transfected by the PCDNA vector did not show any signal for the Alexa 488 channel, accordingly the confocal images from this condition were not shown. A. Cell nuclei of hSOD1WT transfected cells stained by DAPI. B. Anti-flag reactivity stained by Alexa 488 in the flagged-hSOD1WT transfected cells. C. Merge of DAPI and flag stained by ALEXA 488 channels. D. Cell nuclei of hSOD1G93A transfected cells stained by DAPI. E. Anti-flag reactivity stained by Alexa 488 in the flagged-hSOD1G93A transfected cells. F. Merged image. (Bar for the A,B,C and the D,E,F images corresponds to 7 µm.)

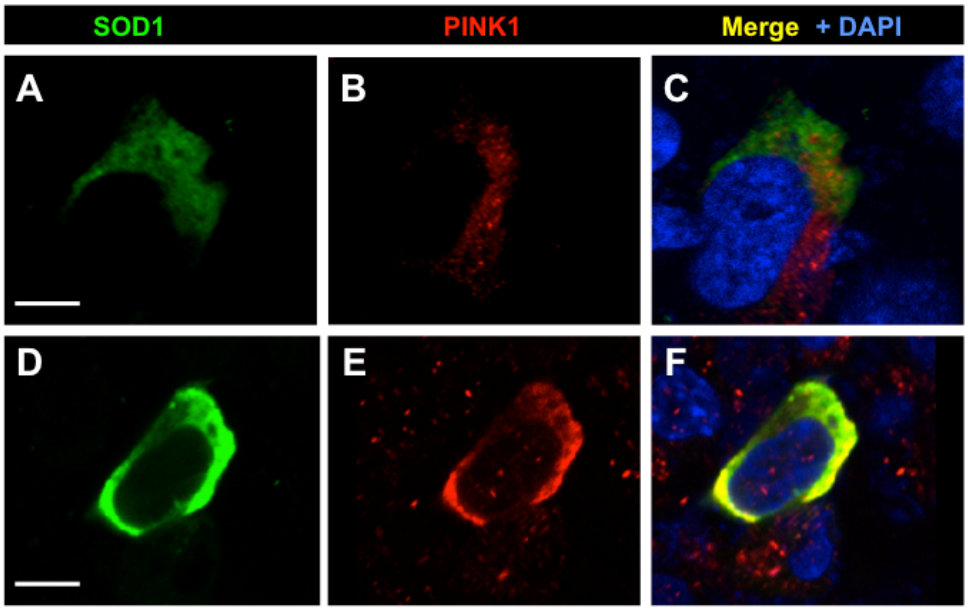

Figure 4. Confocal micrographs showing the aggregation capacity of hSOD1G93A when is co-expressed with PINK1 in SH-SY5Y cells. The cells transfected by the PCDNA vector did not show further signal than background for the Alexa 488 and the Cy3 confocal channels, accordingly were not shown. A. hSOD1WT reactivity pattern (anti-flag) after its co-expression with PINK1. B. PINK1 reactivity pattern stained by Cy3 after its co-expression with hSOD1WT. C. Merge image including DAPI staining, hSOD1WT and PINK1 patterns. D. hSOD1G93A reactivity pattern (anti-flag) after its co-expression with PINK1. E. PINK1 reactivity pattern stained by Cy3 when is co-expressed with hSOD1G93A. F. Merge image that shows in yellow the collocalization of hSOD1G93A and PINK1 in the neuron aggregates. (Bar for the A,B,C images corresponds to 6 µm.; Bar for the D,E,F images corresponds to 10 µm.).

experimental conditions. Level of significance was set at $p < 0.05$ unless specified otherwise.

RESULTS AND DISCUSSION

SOD1^{G93A} in mitochondria causes up-regulation and aggregation of PINK1

A protective dismutative role that justifies the translocation of SOD1 from cytosolic domains to mitochondria was firstly reported by O'Brien and colleagues in yeast (O'Brien et al. 2004). Later, several authors have described novel import mechanisms of this enzyme to mitochondria and its interaction with cytochrome-C in the intermembrane space (IMS) of these organelles under presence of reactive oxygen species (ROS) (see Vehviläinen et al. 2014 for review). Although the mechanism by which the ALS mutant SOD1^{G93A} incorporates into mitochondria is still

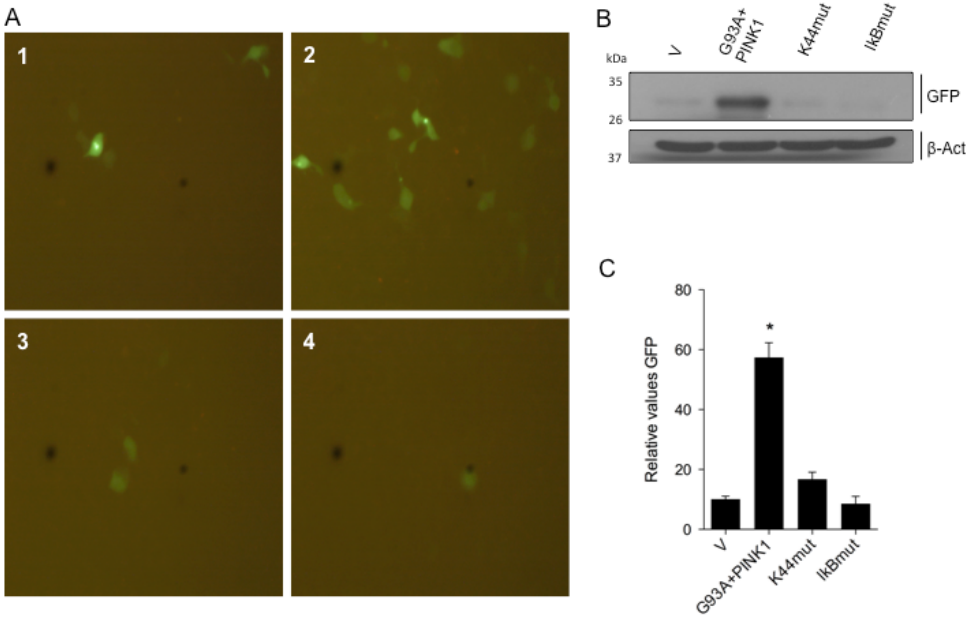

Figure 5. Effect of the NFκB pathway on the activity of the 26S proteasome under the co-expression of hSOD1G93A and PINK1 . A 1. Fluorescence microscope representative image showing the GFPu signal after the PCDNA vector expression together with 0.3µg of the GFPu vector. 2. Fluorescence microscope representative image showing GFPu signal after the co-expression of hSOD1G93A and PINK1 with 0.3µg of the GFPu vector. 3. Fluorescence microscope representative image showing the rescue effect on the proteasome activity through the GFPu signal after the co-expression with hSOD1G93A, PINK1 and the K44 mutant (NFκB pathway inactivation). 4. Fluorescence microscope representative image showing the rescue effect on the proteasome activity through the GFPu signal after the co-expression with hSOD1G93A, PINK1 and the IKBα mutant (NFκB pathway inactivation). B. The GFPu levels in the respective co-transfected cell lysates were evaluated by western blot. C. Western blot representative values including statistical analysis of the relative GFPu in the following conditions: (PCDNA expression, hSOD1G93A + PINK1, hSOD1G93A + PINK1 + K44 mutant, hSOD1G93A + PINK1 + IKBα mutant). * P<0.01 level of significance between the detrimental effect of hSOD1G93A+PINK1 co-expression in the 26S proteasome, and the rescue of the proteasome activity after the inhibiton of the NFκB pathway.

unclear; the prominent ability of this mutant to bind mitochondrial IMS was firstly reported by Ahtoniemi et al. 2008 in transgenic rats.

Here we show how over-expressed $SOD1^{G93A}$ in SH-SY5Y cells is stabilized into the mitochondrial fraction at significantly higher rates than $SOD1^{WT}$ (Figure 1A and C). The toxic effects of $SOD1^{G93A}$ in mitochondria have been vastly hypothesized and partially studied (Palomo & Manfredi 2014; Vehviläinen et al. 2014) however the interactions

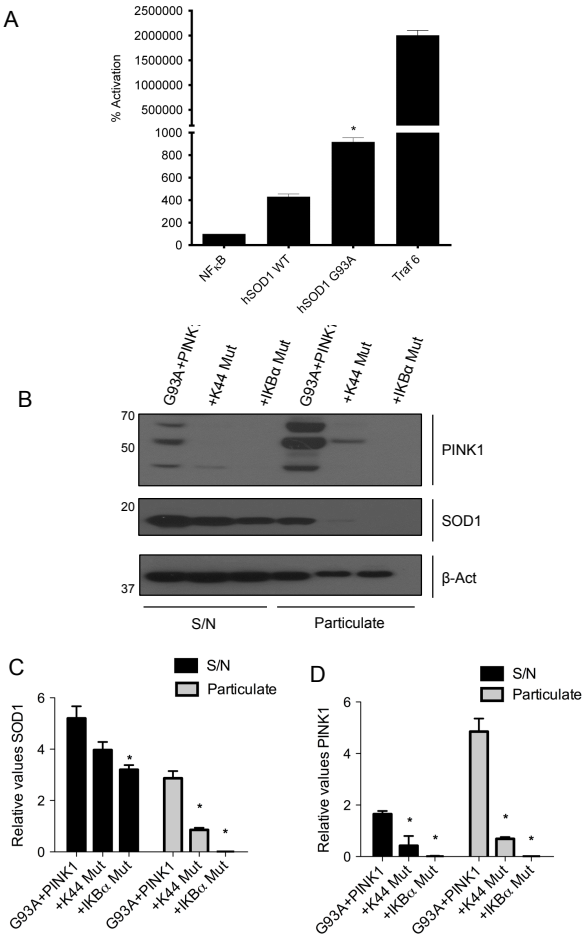

Figure 6. Activation of NFκB pathway by sod1-G93A. A. Luciferase assay PSEAP indicated significantly higher up-regulation of NFκB in SH-SY5Y neuroblastoma cells under the presence of sod1-G93A. In this experiment the NFκB activation pathway protein was used as control of the assay. B. Co-aggregation of PINK1 and sod1-G93A in the particulate fraction was clearly ihnibited under suppression of the NFκB pathway by the κB mutants K44 and IKBα. C. Relative quantifaction of SOD1 western blot signal in the supernatant and th particulate fractions under presence of NFκB inhibitors. D. Relative quantification of PINK1 western blot signal in the supernatant and th particulate fractions under presence of NFκB inhibitors. significance (* P< 0.05).

between SOD1^{G93A} and essential proteins that regulate housekeeping of damaged mitochondria in neurones remain unexplored. We analyzed the levels of PINK1 under the presence of SOD1^{WT} and SOD1^{G93A}, and we found that either the endogenous and over-expressed PINK1 levels were increased under presence of SOD1^{G93A} in SH-SY5Y cells (Figure 1B, D and E). Additionally, levels of endogenous and over-expressed PINK1 in the particulate fraction of these cells were substantially up-regulated under presence of SOD1^{G93A} (Figure 1B, D and E). Willing to further characterize the up-regulation of PINK1, we performed a timepoint analysis of the PINK1 endogenous levels after expression of SOD1^{G93A} and found a positive correlation between ALS mutant expression levels and endogenous PINK1 levels; thus the higher level of endogenous PINK1 was found at 24h post-transfection of SOD1^{G93A} (Supplemental Figure 1B). Up-regulation of PINK1 caused by SOD1^{G93A} could be determined by an increased

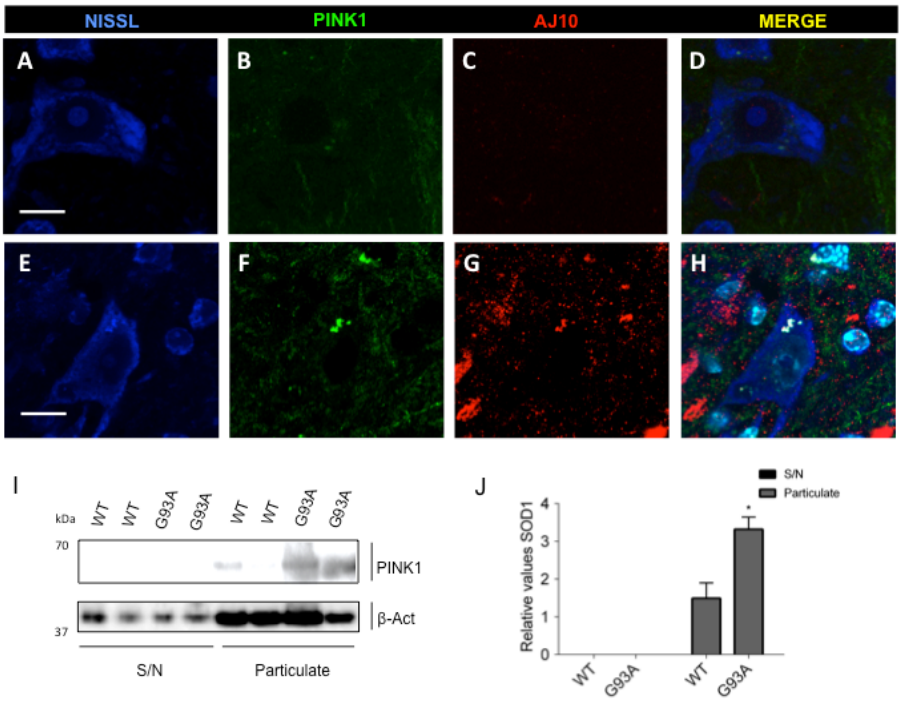

Figure 7 Study of the PINK1 and hSOD1 abundance and localization in the spinal cord ventral horn of hSOD1G93A transgenic animals. A. Confocal micrograph image showing the somata of a representative α-motoneuron from hSOD1G93A terminal (120 d.) transgenic mouse stained by Nissl. B. Confocal micrograph image showing the PINK1 aggregates in the α-motoneuron somata from hSOD1G93A terminal (120 d.) transgenic mouse. C. Confocal micrograph image showing the AJ10 specific antibody signal against misfolded hSOD1. The image shows the presence of intracellular and extracellular sopts of misfolded protein. D. Merge confocal micrograph image showing the collocalization between the AJ10 intracellular signal and the PINK1 aggregates in the α-motoneuron from hSOD1G93A terminal (120 d.) transgenic mouse. E. Confocal micrograph image showing the somata of a representative α-motoneuron from hSOD1WT (120 d.) transgenic mouse stained by Nissl. F. Confocal micrograph showing the PINK1 signal in the α-motoneuron somata from hSOD1GWT (120 d.) transgenic mouse. G. Confocal micrograph image showing the AJ10 specific antibody signal against misfolded hSOD1. H. Merge confocal micrograph image from hSOD1WT (120 d.) transgenic mouse. (Bar for the A,B,C,D and the E,F,G,H images is corresponding to 10 μm.). I. Analysis by western blot of the PINK1 presence in hSOD1G93A and hSOD1WT spinal cord from transgenic animals. The image shows the PINK1 antibody signal after the spinal cord tissue fractionation between supernatant and particulate fractions. The presence of PINK1 was only detected in the particulate fraction where an increase in abundance was detected for the hSOD1G93A animals compared to the hSOD1WT . J. Western blot representative values including statistical analysis of the relative PINK1 levels in the supernatant and particulate fractions of hSOD1 WT and hSOD1G93A transgenic animals, the presence of PINK1 was independently compared between supernatant and particulate conditions (* $P<0.05$).

expression of that protein or by an impaired degradation of PINK1. We therefore performed a nuclear synthesis inhibition experiment with puromycin, a potent protein synthesis inhibitor in SH-SY5Y cells (Croons et al. 2008). We found in this experiment that up-regulation of endogenous PINK1 under presence of SOD1^{G93A} was abolished when transfected cells were treated with puromycin at 12h post-transfection (Supplemental Figure 1A). The results found in our initial experiments seem to indicate that translocation of SOD1^{G93A} into mitochondria up-regulated the expression of PINK1 levels and additionally promoted aggregation of this mitochondrial kinase in neuroblastoma cells.

The tendency of PINK1 to be found in the particulate fraction of neuroblastoma cells was previously described by Um and colleagues in 2010 after treatment of these cells with toxins that induce Parkinson´s Disease-like degenerative signs. These authors found a marked interaction between PINK1 and the E3 ubiquitin-ligase Parkin in those cells in where both proteins were co-aggregated to achieve the formation of protective aggresomes. We have further analyzed in this study the roles of Parkin in presence of SOD1^{G93A} however we could not find any clear interaction between PINK1 and Parkin nor any change in the Parkin levels in our co-transfected cells (data not shown). Interaction between PINK1 and UPS was reported by Muqit and colleagues in 2006. The authors found that PINK1 influenced the formation of aggresomes in PD brains when the UPS was inhibited under stress conditions. Additionally, when PINK1 is localized in the cytoplasm this protein is mainly degraded by the UPS (Pilsl & Winklhofer 2012). Despite that interaction between PINK1 and the proteasome system has been only partially studied in PD, the existence of any interaction between these two cellular agents during FALS pathophysiology currently remains unknown.

Up-regulation of PINK1 promote its co-aggregation with SOD1 ^{G93A} and dysfunction of UPS

Formation of insoluble aggregates is one of the most characteristic pathological hallmarks of familial ALS. Aggregates found in the spinal cord motoneurones of terminal SOD1 ^{G93A} transgenic mice occasionally can be large and contain misfolded proteins, chaperones, cytoskeleton structures and proteasome subunits (Johnston et al. 2000). Whether the formation of these singular aggregates can be protective or toxic for the host cells still remains a controversial matter in all neurodegenerative diseases (Ying et al. 2013) although the dysfunction of the UPS seems the common and essential step that precedes apparition of these insoluble features in SOD1^{G93A} mutants (Cheroni et al. 2005; Valentine & Hart 2003). Johnston and colleagues found for the first time that expression of SOD1^{G93A} in cells caused the formation of aggresomes after impairment of the UPS by the treatment with proteasome inhibitors (Johnston et al. 2000). In this study, we found that expression of SOD1^{G93A} in neuroblastoma cells caused a clear dysfunction in the 26S and 20S proteasome subunits (Figure 2A-D). Our immunocytochemistry experiments

revealed a pattern of misfolded SOD1^{G93A} with formation of tiny oligomerized features that were not resembled by the cells expressing SOD1^{WT}. Anyhow we would not be able to find a clear pattern of aggregation and aggresome formation in our SOD1^{G93A} cells after transfection of this FALS-associated mutant (Figure 3A-F). On the contrary, co-expression of SOD1^{G93A} with PINK1 in neuroblastoma cells clearly promoted apparition of large aggregates and aggresome-like formations that included collocalization of both proteins inside (Figure 4D-F). These insoluble structures were unseen after co-expression of PINK1 and SOD1^{WT} (Figure 4A-C). Our immunocytochemistry results were further confirmed in our particulate fractionation experiments. In these blots, PINK1 was found at significant higher levels in the particulate fraction of neuroblastoma cells in presence of SOD1^{G93A} (Figure 1B, D and E). Furthermore, we analyzed whether activation of PINK1 after be co-expressed with SOD1^{G93A} could be involved on the dysfunction of the UPS. This study revealed how co-expression of both proteins markedly worsened any previous found UPS dysfunction as we show in our 26S GFPu fluorescence signal and subsequent western blot experiments (Figure 5A2, B and C).

Activation of NFκB pathway by SOD1^{G93A} influences PINK1 up-regulation, proteasome function and apparition of protein aggregates

Regulation of PINK1 expression in neurones remained elusive for long time however it has been very recently clarified when Duan and colleagues found that expression of PINK1 in neuroblastoma cells was regulated by previous activation of the NFκB pathway (Duan et al. 2014). Additionally, the activation of the NFκB pathway in presence of SOD1^{G93A} has also been recently reported in ALS using 'in vitro' neuronal models (Prell et al. 2014). Here we analyzed the activation of the NFκB pathway in neuroblastoma cells transfected with SOD1^{G93A} and SOD1^{WT}. We found a significant increased nuclei translocation of the NFκB factor in presence of SOD1 ^{G93A} (Figure 6A). This result was found in accordance with the previous result described by Prell and colleagues.

To study any functional convergence between the NFκB pathway and our previously described PINK1 up-regulation in ALS, we inhibited the NFκB pathway with the IκBα and K44 mutants in presence of SOD1^{G93A}. Our particulate fractionation experiments strikingly revealed that inhibition of NFκB dramatically prevented any up-regulation of the co-expressed PINK1 and any further aggregation of this protein in the particulate fraction of neuroblastoma cells (Figure 6B and D). Additionally, inhibition of the NFκB pathway significantly prevented translocation of SOD1^{G93A} into the particulate fraction showing up-regulation of SOD1^{G93A} uniquely in the isolated soluble fraction (Figure 5B and C). Clearance of SOD1^{G93A} from the particulate following inactivation of the NFκB pathway prompted us to study the function of the proteasome in that happenstance. Proteasome experiments revealed a dramatic rescue effect exerted by inhibition of the NFκB pathway in presence of co-expressed proteins SOD1^{G93A} and PINK1 (Figure 5A-

C). To our knowledge the findings described here link for the first time the function of the proteasome with activation of the NFκB pathway. At the same time, these findings shed novel and substantial light to the molecular mechanisms that sustain formation of SOD1 protein aggregates in neurones affected by the progression of FALS.

SOD1^{G93A} and PINK1 co-aggregate in the spinal cord of transgenic rodents

To complement our previous 'in vitro' finding regarding up-regulation of PINK1 in familial ALS we have analyzed the levels of PINK1 in the spinal cord of terminal transgenic SOD1^{G93A} rats. Levels of PINK1 were significantly higher especially in the particulate fraction of our SOD1^{G93A} animals analyzed compared with their SOD1^{WT} littermates (Figure 7 I and J). Additionally, we have studied the collocalization of misfolded SOD1^{G93A} and PINK1 in lumbar spinal cord motoneurones of SOD1^{G93A} mice by immunohistochemistry. We analyzed tissues from pre-symptomatic mice at postnatal 60 days, symptomatic animals at postnatal 90 days and terminal animals at postnatal ≈120 days. Co-aggregation of SOD1^{G93A} and PINK1 was only spotted in motoneurones from mice at the terminal stage (Figure 7 A-D) whereas other timepoints studied did not show any significant difference on the PINK1 levels nor in the PINK1 and SOD1^{G93A} co-aggregation ability compared to SOD1^{WT} littermates (data not shown).

Immunohistochemistry levels of PINK1 in lumbar spinal cord motoneurones were recently reported as increased in terminal SOD1^{G93A} mice (Knippenberg et al. 2013). These authors also found increased mRNA levels for this protein in lumbar spinal cord tissues of these transgenic ALS animals at terminal stage. These findings from Knippenberg and colleagues suggest that increase in PINK1 levels in transgenic FALS mice is linked to the transcriptional expression of PINK1 and would be consistent with our current reported findings found in neuroblastoma cells. Furthermore, co-aggregation of PINK1 and misfolded SOD1 in SOD1^{G93A} transgenic mice spinal motoneurones was spotted using our in-home raised antibody AJ10 against misfoded SOD1 (Sábado et al. 2013) what justifies that increase in PINK1 is followed by the toxic effects of mutant SOD1.

ACKNOWLEDGEMENTS

This study was funded by grants from the National Medical Research Council-CBRG to K.L.L and scholarships from the University of Lleida to X.G.P. The authors thank See Toh Rachel for the critical readings on that draft manuscript.

The authors declare no conflict of interest regarding to this report.

REFERENCES

Ahtoniemi, T. et al., 2008. Mutant SOD1 from spinal cord of G93A rats is destabilized and binds to inner mitochondrial membrane. Neurobiology of disease, 32(3), pp.479–85.

Bergmann, F. & Keller, B.U., 2004. Impact of mitochondrial inhibition on excitability and cytosolic Ca2+ levels in brainstem motoneurones from mouse. The Journal of physiology, 555(Pt 1), pp.45–59.

Cheroni, C. et al., 2005. Accumulation of human SOD1 and ubiquitinated deposits in the spinal cord of SOD1G93A mice during motor neuron disease progression correlates with a decrease of proteasome. Neurobiology of Disease, 18(3), pp.509–522.

Cozzolino, M. et al., 2015. Mitochondrial dynamism and the pathogenesis of Amyotrophic Lateral Sclerosis. Frontiers in cellular neuroscience, 9, p.31.

Croons, V. et al., 2008. Differential effect of the protein synthesis inhibitors puromycin and cycloheximide on vascular smooth muscle cell viability. The Journal of pharmacology and experimental therapeutics, 325(3), pp. 824–32.

Duan, X. et al., 2014. Upregulation of human PINK1 gene expression by NFκB signalling. Molecular Brain, 7(1), p.57.

Gallart-Palau, X. et al., 2014. Neuregulin-1 is concentrated in the postsynaptic subsurface cistern of C-bouton inputs to α-motoneurones and altered during motoneuron diseases. FASEB journal: official publication of the Federation of American Societies for Experimental Biology, 28(8), pp. 3618–32.

Johnston, J.A. et al., 2000. Formation of high molecular weight complexes of mutant Cu, Zn-superoxide dismutase in a mouse model for familial amyotrophic lateral sclerosis. Proceedings of the National Academy of Sciences of the United States of America, 97(23), pp. 12571–6.

Knippenberg, S. et al., 2013. Altered expression of DJ-1 and PINK1 in sporadic ALS and in the SOD1(G93A) ALS mouse model. Journal of neuropathology and experimental neurology, 72(11), pp.1052–61.

Lim, K.L. et al., 2005. Parkin mediates nonclassical, proteasomal-independent ubiquitination of synphilin-1: implications for Lewy body formation. The Journal of neuroscience: the official journal of the Society for Neuroscience, 25(8), pp.2002–9.

Le Masson, G., Przedborski, S. & Abbott, L.F., 2014. A computational model of motor neuron degeneration. Neuron, 83(4), pp.975–88.

Muqit, M.M.K. et al., 2006. Altered cleavage and localization of PINK1 to aggresomes in the presence of proteasomal stress. Journal of neurochemistry, 98(1), pp.156–69.

O'Brien, K.M. et al., 2004. Mitochondrial protein oxidation in yeast mutants lacking manganese-(MnSOD) or copper- and zinc-containing superoxide dismutase (CuZnSOD): evidence that MnSOD and CuZnSOD have both unique and overlapping functions in protecting mitochondrial proteins from . The Journal of biological chemistry, 279(50), pp.51817–27.

Palomo, G.M. & Manfredi, G., 2014. Exploring new pathways of neurodegeneration in ALS: The role of mitochondria quality control. Brain research, 1607, pp.36–46.

Pickles, S. & Vande Velde, C., 2012. Misfolded SOD1 and ALS: zeroing in on mitochondria. Amyotrophic lateral sclerosis: official publication of the World Federation of Neurology

Research Group on Motor Neuron Diseases, 13(4), pp.333–40.

Pilsl, A. & Winklhofer, K.F., 2012. Parkin, PINK1 and mitochondrial integrity: emerging concepts of mitochondrial dysfunction in Parkinson's disease. Acta neuropathologica, 123(2), pp. 173–88.

Prell, T. et al., 2014. Endoplasmic reticulum stress is accompanied by activation of NF-κB in amyotrophic lateral sclerosis. Journal of neuroimmunology, 270(1-2), pp.29–36.

Sábado, J. et al., 2013. Immunodetection of disease-associated conformers of mutant cu/zn superoxide dismutase 1 selectively expressed in degenerating neurones in amyotrophic lateral sclerosis. Journal of neuropathology and experimental neurology, 72(7), pp. 646–61.

Sullivan, P.G. et al., 2004. Proteasome inhibition alters neural mitochondrial homeostasis and mitochondria turnover. The Journal of biological chemistry, 279(20), pp.20699–707.

Tradewell, M.L. et al., 2011. Calcium dysregulation, mitochondrial pathology and protein aggregation in a culture model of amyotrophic lateral sclerosis: mechanistic relationship and differential sensitivity to intervention. Neurobiology of disease, 42(3), pp. 265–75.

Um, J.W. et al., 2010. Formation of parkin aggregates and enhanced PINK1 accumulation during the pathogenesis of Parkinson's disease. Biochemical and biophysical research communications, 393(4), pp.824–8.

Valentine, J.S. & Hart, P.J., 2003. Misfolded CuZnSOD and amyotrophic lateral sclerosis. Proceedings of the National Academy of Sciences, 100(7), pp.3617–3622.

Vehviläinen, P., Koistinaho, J. & Gundars, G., 2014. Mechanisms of mutant SOD1 induced mitochondrial toxicity in amyotrophic lateral sclerosis. Frontiers in cellular neuroscience, 8, p.126.

Wang, C. et al., 2005. Alterations in the solubility and intracellular localization of parkin by several familial Parkinson's disease-linked point mutations. Journal of neurochemistry, 93(2), pp.422–31.

Ying, Z., Wang, H. & Wang, G., 2013. The ubiquitin proteasome system as a potential target for the treatment of neurodegenerative diseases. Current pharmaceutical design, 19(18), pp. 3305–14.

SUPPLEMENTARY INFORMATION

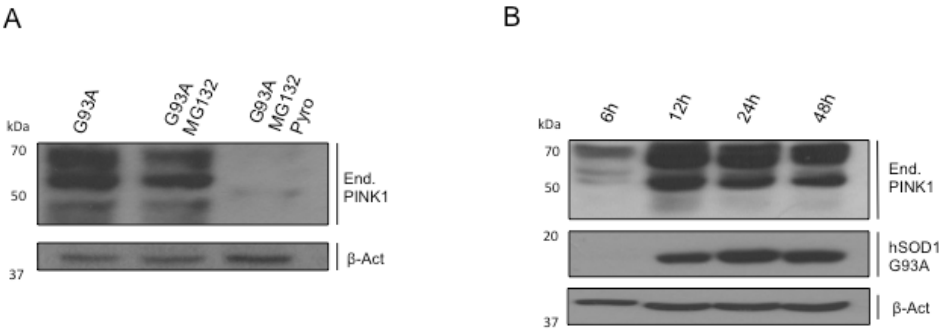

Supplemental Figure. A. Western blot analysis of the transcriptional increase of endogenous PINK1 in hSOD1G93A transfected SH-SY5Y cells when the cells were treated with the RNA translation process inhibitor pyromicin. The proteasome inhibitor was used to avoid the degradation of pyromicin in the cells, and its effect on the PINK1 increase was controlled. B. Time-course analysis by western blot of the increase of endogenous PINK1 in hSOD1G93A transfected SH-SY5Y cells, the levels of SOD1 were also analyzed. The PINK1 level shows the most stable increase at 24h after the hSOD1G93A transfection.

GLOBAL DISCUSSION

1. SOD1G93A and Familial Amyotrophic Lateral Sclerosis (FALS) a degenerative relationship

Over 100 mutations of the SOD1 gene have been associated with familial forms of ALS (Andersen 2000). The mutation most widely studied and also primarily used in the experiments of this thesis is the amino acid substitution guanine to alanine in the residue 93 of the human SOD1 sequence (G93A) (Henriques, Kastner et al. 2015). Transgenic mice expressing human SOD1G93A show a clear motor degenerative phenotype that resembles in several facets the symptoms found in patients affected by ALS. A detailed description of the clinical symptoms observed in these mice are shown in (Figure 1) further detail and historical association of this SOD1 mutation with ALS can be found in (Vinsant, Mansfield et al. 2013).

2. Onset of motor neurones degeneration in SOD1G93A FALS and the essential role of synaptic decay

The emergence and progression of FALS in patients and animal models is marked by massive loss of motor neurones in the ventral horn of the spinal cord. Onset of FALS pathophysiology remains uncertain, although some authors agree that the loss of synaptic terminals might be the initial factor that triggers neurodegeneration in that disease (Dadon-Nachum, Melamed, and Offen 2011) . This theory is known as the “dying-back effect” and its main hypothesis extends to other neurodegenerative diseases including Alzheimer´s disease (AD) and Vascular dementia. The characterization of the $SOD1^{G93A}$ mice performed by Vinsant and colleagues demonstrated how the loss of synapses is the first event of the neurodegenerative chain in these mice (Vinsant et al. 2013). Also, the authors detected an increase in the number of C-boutons when

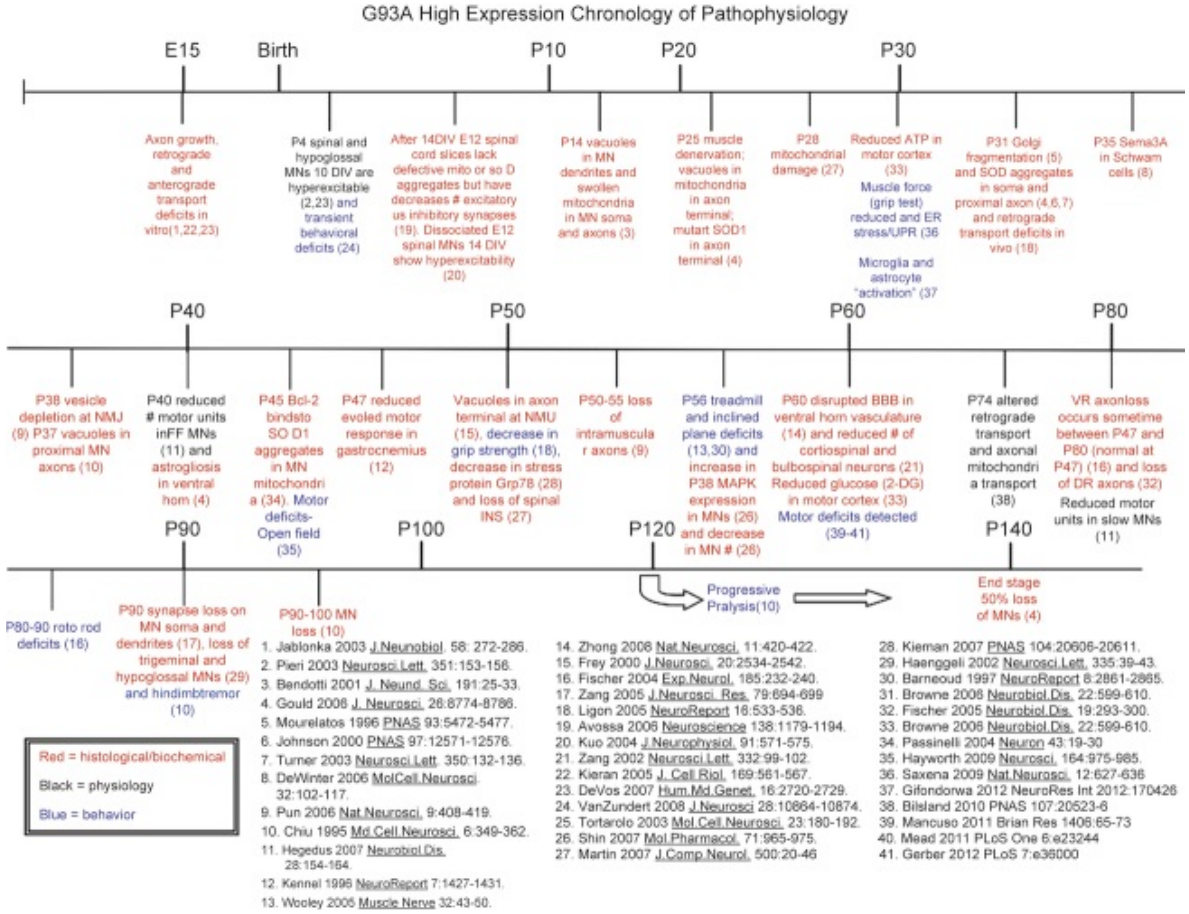

Figure 1. Pathophysiology of the ALS-associated SOD1G93A transgenic mice. Adapted from (Vinsant, Mansfield et al. 2013).

the synapse loss becomes evident in these animals (Vinsant et al. 2013). In this thesis, we studied the molecular changes of C-boutons during ALS progression in SOD1^{G93A} mice as we reported in the chapter 1 of the results section. For a long time, the origin of C-boutons was unknown and only that these synapses were absent of association with corticospinal tracts affectation was known. Most recently, the origin of these synapses was identified as a Pitx-2 expressing cholinergic interneurones in the spinal cord (Frank 2009). We found that C-boutons are clearly the latest synapses to degenerate on affected motor neurones. Additionally, these terminals do not seem to be affected by synaptic stripping (Moran and Graeber 2004). In spite of that, excitatory synapses including cholinergic and glutamatergic terminals apposed to injured motor neurones were cleaved through this effect by reactive microglia. Imbalances on the motor neuron homeostasis from a systems biology approach have ledme to hypothesize that C-terminals despite of be protective for MNs could contribute to the degeneration of motor neurones via activation of microglia and stripping of other synapses. We can conclude following our obtained results and previous publications that excitatory synapses are partially affected at the disease onset and completely removed from motor neurones during ALS progression, whereas C-terminals are the unique source of excitatory nature that remains in sick α-MNs till the absolute degeneration of these cells. A potential pathogenic role regarding NRG-1 and C-boutons is based on our results, since we found that NRG-1 and C-terminals are practically absent in ocular nuclei motor neurones, a subclass of motor neurones that remain unaffected in FALS and idiopathic ALS even amongst other degenerating motor neurones. This fact justifies a future thorough and careful study to discern the role of C-boutons in the MNDs context since previous studies have been exclusively centered on determining the morphological changes that C-terminals go through in MNDs. We found, therefore, that the molecular characterization of these terminals was not previously performed in a proper manner in the context of ALS. Morphologically,

it was reported that C-terminals increase their apposing territory as the motoneuron injury progresses (Pullen 1992). However, what causes this elongation and the functional repercussions that this phenomena would have at the cellular and system levels remain unknown. Initially, it was hypothesized that the epidermal growth factor neuregulin-1 would be present at cholinergic terminals apposed to α-MNs (Issa et al. 2010), we predicted that these terminals found by Issa and colleagues would most likely be C-terminals which led us to perform our own studies following this hypothesis. We found that NRG-1 is not present in any synaptic terminal itself but it can be found in normal and neurodegenerative motor neurones enclosed in the endoplasmic reticulum organelle dubbed as subsurface cistern (SSC) (Li et al. 1995). The SSC is known to be enriched with the presence of sigma-1 receptors in α-MNs. In addition, alterations of this receptor have been linked with the apparition of certain forms of FALS (Al-Saif, Al-Mohanna, and Bohlega 2011) and its progression (Mavlyutov et al. 2013). The protein NRG-1 found in the SSC of α-MNs relies on the sigma-1 receptor. Notwithstanding, this protein shows clear interaction with these receptors and seems located in another compartment of these cellular structures. While we are currently unable to clarify the role of NRG-1 in the FALS-associated degeneration of α-MNs, we have found that this molecule was enclosed in vesicles likely to be secreted from the motoneuron membrane. The function of NRG-1 is associated with the erbB family of receptors (Xiang et al. 2015; Wen et al. 1992), this molecule binds to the erbb receptors and activates the function of the erbb-tyrosine kinase (Calvo et al. 2010; Falls 2003).

Analysis of our results with regard to the C-terminals and NRG-1 from a biological competition approach leads to suggest a pathogenic role for the C-terminals as mentioned above in the degeneration of motor neurones during FALS. Albeit, if we consider that the spinal cord α-MNs and oculomotor nuclei MNs are highly different, we can easily conclude that the role of C-boutons

might be protective as support for affected cells providing excitatory flux during the degenerative process to clearly slow the FALS-associated neurodegeneration. Our results, contextually interpreted with the previous findings at the current stage can support both interpretative approaches as we will review in the following paragraphs.

3. NRG-1 and erbB receptors as key activators of reactive microglia in spinal cord

Microglia is distributed in the brain and spinal cord remain in close association with astrocytes and neurones. The pattern of expression of microglia cells in the CNS is shown in (Figure 2).

Expression of erbB receptors in brain microglia and neurones has been previously reported by (Gerecke et al. 2001). The authors highlighted in their study a significant increase in erbB3 receptors in the neuronal axons surrounded by reactive microglia that was did not resemble the neuronal soma of the same cells. Later, Dimayuga et al. found that the protein neuregulin glial growth factor (GGF2) attenuated the ROS generated by reactive microglia (Dimayuga et al. 2003). Calvo and colleagues in 2010 found experimental evidence that NRG-1 had a potent effect in cultured cells activating the erbB receptors in microglia to generate microgliosis. Additionally, the authors tested this fact *in vivo* and the results determined that the NRG-1 activation of erbB receptors in microglia are key role mediators of the inflammation response especially in motor neurones after axonal injury (Calvo et al. 2010). Song and colleagues found an increase in secreted isoforms of NRG-1 in spinal cord of $SOD1^{G93A}$ mice and this increase was strongly associated with progression of microgliosis and MNs degeneration in these animals (Song et al. 2012). These

authors were also able to replicate these results in post-mortem human spinal cord tissues from sporadic ALS patients. Currently, there is no clear evidence that shows the association between secreted NRG-1 isoforms and synaptic stripping in the spinal cord. This is an experimental hypothesis that requires further exploration in our humble opinion. By the same token, our newly discovered isoforms of NRG-1 in the SSC of α-MNs need to be further characterized to study the associations between these molecules and activation of erbB receptors in C-boutons and synapse stripping through microgliosis in FALS.

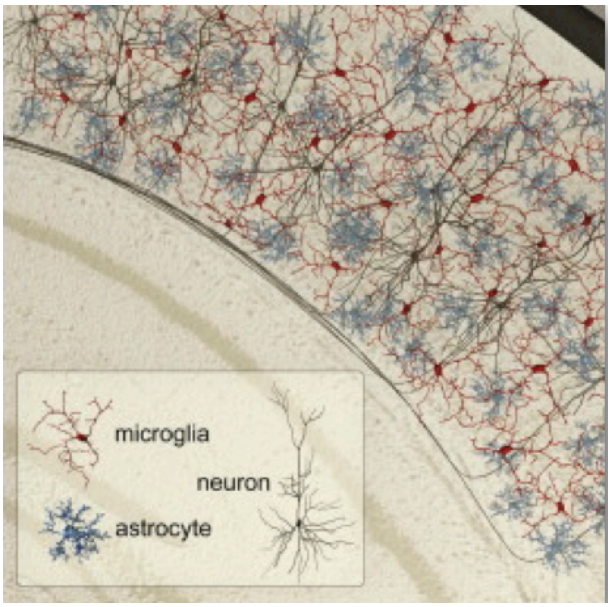

Figure 2. Distribution of microglia, astrocytes and pyramidal neurones in the CNS. Adapted from (Kettenmann, Kirchhoff, and Verkhratsky 2013).

4. Characterization of NRG-1 isoforms from SSC by their association with extracellular vesicles (EVs)

Our discovery of NRG-1 inside EVs closely associated with C-terminals in α-MNs and their associated-increase in motor neurone diseases including ALS has provided a new avenue to characterize these NRG-1 molecules from isolated EVs. In this thesis, we focused on expounding on this possibility, since characterization of these NRG-1 molecules can help us to understand the role of EVs in this disease. EVs have been associated with neurodegeneration and increase of these secreted vesicles during pathogenesis of the CNS including ALS, seems to illustrate a strong association (Lachenal et al. 2011; Grad et al. 2014; Basso et al. 2013). Although the promising advantages following characterization of our spotted EVs/NRG-1 molecules in ALS tissues and biological fluids, the study of EVs faces currently a substantial bottleneck regarding the use of available isolation methods (Van Deun et al. 2014). Isolation methods co-isolate aggregated proteins and several soluble proteins that hinder the proper study of EVs, as well as the levels and functions of their associated proteins (Lin et al. 2015). Our initial consideration following our NRG-1 studies took into account the fact of the increase of the EVs/NRG-1 molecules in motor neurone diseases, and especially in ALS. This validated fact proposes this protein as a precious biomarker for that disease. We therefore developed a novel and easy-to-perform method of EVs isolation that we dubbed as PROSPR that is able to quantify EVs-associated proteins in human biological fluids as we show in the chapter 1 of the results section. The identification and quantification of NRG-1 in these isolated EVs from biological fluids was successful, following the application of this method as we show in the above mentioned chapter. Our proteomics studies indicate that following isolation of EVs by PROSPR even from CNS tissues can help to specifically characterize the NRG-1 molecules isolated from EVs. Presence of NRG-1 in EVs from essential biological fluids as urine and

human tissues as blood was not reported clearly before; we consider that this was probably due to the lack of proper EVs isolation methods. Further applications of the PROSPR isolation method for the study and characterization of EVs/NRG-1 will shed light on the roles of this molecule in ALS and the potential consideration of this protein as a reliable biomarker for the diagnosis, progression and treatment of ALS.

5. C-boutons as excitatory terminals that might slow degenerative pathogenesis in motor neurones

Motor neurones have been largely revealed as vulnerable cells to excitability imbalances (Kanning, Kaplan, and Henderson 2010). Additionally, the symptoms associated with hyperexcitability of motoneurones was clearly revealed in patients and FALS mammalian models during the progression of that disease (Saxena and Caroni 2011). However, the role of excitability in the α-MNs degeneration process remained unclear for long time. Caroni an d colleagues in 2013 demonstrated how the excitability of α-MNs modulates degeneration of these cells in the spinal cord of $SOD1^{G93A}$ mice. The authors in the same study describe how pharmacological inhibition of acetylcholine metabotropic receptors predominant in the C-boutons also as we found in our studies rescues endoplasmic reticulum stress associated with the disease progression in FALS transgenic mice. The main hypothesis of the authors is that initially the changes in C-terminals could account for beneficial outcome in the affected MNs. This would be in accordance with our above described hypothesis that changes in NRG-1 in FALS, which could be linked to a protective role providing balanced excitatory input to α-MNs once cholinergic and other excitatory inputs linked to the corticospinal tract in the ventral horn of the spinal cord has been lost. This

hypothesis requires to further elucidation in SOD1^{G93A} mice however experimental evidence to confirm this theory in FALS is currently lacking.

6. Mitochondria dysfunction and synaptic decay: essential pathogenic factors of motor neurone degeneration in FALS

Loss in synaptic terminals largely observed in FALS transgenic models including the SOD1^{G93A} mice strengthens the dying-back hypothesis of MNs degeneration in ALS. Several authors have described how the dying back effect cannot be dissociated of the mitochondria degeneration in the affected axons and the mitochondria induced cell death seems to be the central mechanism of degeneration following this hypothesis (Tan, Pasinelli, and Trotti 2014; Cozzolino and Carrì 2012; Rothstein 2009). As we have noticed in the previous paragraphs of this global discussion, the implications of the C-terminals in the degeneration of motor neurones are only incipiently studied thus any association between mitochondrial dysfunction and the C-terminal molecular changes occurred during ALS progression might be a good approach for the study neurodegenerative progression in FALS. Anyhow, it is already known that mitochondria affectation in the α-MNs axon may be the crucial mechanism that triggers cell death in FALS.

Mitochondria in FALS by the effect of human mutant SOD1^{G93A} becomes affected in its inner and outer structures, thus the whole organelle becomes swollen when examined under ultrastructural electron microscope (Higgins, Jung, and Xu 2003; P. C. Wong et al. 1995). Mitochondria dysfunction in ALS is currently considered the convergence point where all the known neurodegenerative mechanisms meet to promote cell death. Among these pathogenic mechanisms, we find excitotoxicity, cellular transport imbalances

protein mis-folding, etc. The association between protein mis-folding and mitochondria affectation seems unclear. In this thesis, we show how there is a specific association between these two essential phenomena of neurodegeneration in SOD1^{G93A} FALS. This striking association that we have discovered will be discussed later in the subsequent paragraphs.

The central role of mitochondria dysfunction thus, seems out of discussion in SOD1^{G93A} FALS. However, currently, there is no specific model to test therapeutic approaches which include genetic and pharmacological approaches in ALS. The use of transgenic mice for that purpose is clearly unethical and totally unviable considering time to apparition of symptoms, economic and human costs. Considering the drawbacks of the mammalian models, invertebrate models including *Drosophila* fill the gaps between *in vitro* models and mammalians for pharmacological and genetic screenings. *Drosophila* flies are highly 'druggable' animals, with the advantages that this fact implies at the time to perform therapeutic compound screenings. These animals offer unbeatable genetic manipulation flexibility to further investigate the pathways of action of the tested compounds and to confirm the molecular mechanisms that sustain the identified pathological phenotype and the pharmacological rescue effects (Pandey and Nichols 2011).

The discovery of novel therapeutic compounds is extremely imperative in ALS, since this neurodegenerative disease is currently lacking of any specific and available treatment. We have therefore created a new transgenic *Drosophila* model expressing hSOD1^{G93A} in thoracic muscles under the 24B GAL4 specific muscle promoter. Restricted expression of transgenes in *Drosophila* is performed under the transcriptional control of the yeast upstream activating sequence GAL4 that is recognized by the combined GAL4/UAS system (McGuire, Roman, and Davis 2004). Our generated FALS-24B-hSOD1^{G93A} flies show a clear mitochondrial and motor phenotype that resembles FALS

symptoms being positioned as a relevant model for the future study of mitochondrial pathology in FALS. Mitochondria in FALS-24B-hSOD1^{G93A} *Drosophila* were found clearly swollen and showing the inner structures including cristae, as it had been previously found in FALS hSOD1^{G93A} mammalian models (Pickles and Vande Velde 2012; Pasinelli et al. 2004; Tan, Pasinelli, and Trotti 2014). Additionally, a clear pro-fusion phenotype that had not clearly reported before was spotted in our FALS transgenic flies that might be consequence of interactions between hSOD1^{G93A} and VDAC1 mitochondrial channel proteins in *Drosophila.* This hypothesis with important implications thus needs to be further studied. With regard to our FALS-24B-hSOD1^{G93A,} we would like to notify that after the acceptance of our submitted manuscript included in the Chapter 2 of results section of this thesis, we manifested our intention to make this model publicly available from a public *Drosophila* stock center to the whole research community. This will facilitate and spread the use of our novel FALS-24B-hSOD1^{G93A} model for research on mitochondrial dysfunction in FALS.

Restricted expression of hSOD1^{G93A} has been performed and reported before using transgenic mice models (M. Wong and Martin 2010). The authors found that expression of hSOD1^{G93A} in muscle fibers triggers degeneration of motor neurones in a pre-synaptic manner consistent with the dying-back hypothesis in ALS. Major pathological hallmarks following muscle restricted expression of this FALS mutant were found in the axons of α-MNs that showed higher amount of dysfunctional mitochondria and protein fibrillar inclusions (M. Wong and Martin 2010). These findings clearly state that mitochondrial dysfunction and aggregation of fibrillar proteins are concomitant factors in ALS that need to be explored in convergent approaches as we propose in this thesis. Finally, recent research results imply that the affectation of mitochondria precedes the apparition of fibrillar proteins in MNs, a fact that seems supported by our results as we will discuss in the next paragraphs of this global discussion.

7. C-terminals and protein aggregation in FALS motoneurones

Formation of aggregates in MNs and other neurones during neurodegenerative diseases fascinates scientists as these features have been considered for a long time the unique traces of the neurodegenerative process. These were considered as the culprits that sustain degeneration of neurones in many aspects. However, recent novel research approaches consider the formation of aggregates and aggresomes as a protective response in MNs (Arrasate et al. 2004). Although aggregates can be considered as proteins with prionic properties that causes other proteins to become dysfunctional in ALS and spread their toxic properties to affect essential cellular organelles (Lee and Kim 2015). The responses of the cell tend to be the same with all the dysfunctional proteins during the neurodegenerative process. MNs attempt to confine these culprits to aggregates along the whole MNs from the axon terminals to the dendrites with higher burden of fibrillations in the soma.

In FALS murine models expressing hSOD1^{G93A}, it has been shown how MNs become highly susceptible to imbalances on excitability homeostasis (Piotrkiewicz and Hausmanowa-Petrusewicz 2011). It has therefore been indicated that mutant SOD1 interacts in MNs with calcium transport molecules via affectation of the mitochondria which leads to low endoplasmic reticulum load of calcium and high cytosolic load of calcium promoting hypoexcitability in the affected α-MNs (Rizzuto et al. 2012). In this context, C-boutons are the unique terminals that survive progression of ALS in the affected MNs. Thus, it has been proposed that these terminals could play an essential role on MNs excitability in this disease (Pullen and Athanasiou 2009). Whether the role of C-boutons is protective is still matter of discussion. However, it has been shown how the increase in MNs excitability reduces the FALS hallmarks in vulnerable motor neurones of hSOD1^{G93A} mice (Saxena et al. 2013). The authors mainly found that higher excitability even at pre-symptomatic stage of these mice (P60)

prevented accumulation of mis-folded SOD1 and also promoted healthy mitochondria in vulnerable α-MNs. The link between C-boutons and mitochondria in the aggregation of misfolded proteins in ALS has not been explored yet. Even so, this thesis illustrates for the first time, the link between mitochondria affectation, protein aggregation and clearance via essential mitochondrial proteins as we will discuss in the next paragraph. Further research needs to be performed to address the involvement of C-terminals in protein aggregation in FALS, role in which the protein NRG-1 might play an important role, especially in the activation of signalling pathways between C-boutons and α-MNs with important repercussion for vulnerable MNs in FALS.

8. Our discovery of novel pathways of protein misfolding and clearance in FALS

An implication of mitochondria on aggregation of dysfunctional proteins in ALS was unclear. It was pointed, as we discussed in the above paragraphs that mitochondria via the calcium signalling pathways may play an essential role in the toxic effects of ALS mutant SOD1 isoforms. Other implications between mitochondria and aggregation in ALS still remain unknown. In this thesis, we confirm that mutant hSOD1^{G93A} translocates to mitochondria at higher rates than normal hSOD1. This was already justified as this cytosolic enzyme could translocate to mitochondria to help to reduce ROS effects in a dynamic way (Vehviläinen, Koistinaho, and Gundars 2014; Ahtoniemi et al. 2008). Whether mutant ALS SOD1 mutants follow the same circuit to access the mitochondria is still unclear, ALS mutants seem to accumulate in the intermembrane space mitochondria in α-MNs. According to our results, hSOD1^{G93A} after translocation into mitochondria we have shown its interaction with PINK1 and promotes its co-aggregation in the cytoplasm of the cells. Interaction between PINK-1 and

hSOD1^{G93A} activates the translocation of the NFκB to the nucleus what promotes formation of aggregates in the cell via impairment of the proteasome. The link between the proteasome and NFκB has been clearly established in this thesis and the ability of this nuclear factor to impair the proteasome in presence of hSOD1^{G93A} seems out of discussion. These findings can have profound implications on the proteasome dysfunction in neurodegenerative diseases as the link between NFκB and the proteasome in other neurodegenerative diseases needs also to be elucidated. Our results also add functional knowledge to the roles of mitochondria in the neurodegenerative process. Our findings regarding PINK1 levels in MNs has been validated '*in vivo*' in the hSOD1^{G93A} transgenic mice. Nonetheless, the link between NFκB and the proteasome is currently lacking further validation *in vivo*. We consider this as priority element to study in ALS, since the relationship between PINK1 and the proteasome via activation of NFκB holds promise to reveal conclusive information on the mechanisms that promote proteasome dysfunction and rescue in ALS. Thismatter has been considered a great mystery in ALS from its very initial apparition.

9. Final considerations

Degeneration of MNs in ALS is complex and involves several pathways and mechanisms that currently scientists are unable to localize in a sequential manner. However, considering this complexity, the role of mitochondria seems central. ALS mutants translocate to mitochondria and from this translocation promote degeneration of motor neurones. We discovered that this translocation results in the impairment of the proteasome and accumulation of dysfunctional proteins in cells. However, the extent of this fact seems wider, whichwe consider requires extensive research. Mitochondria also control the excitatory level in MNs through calcium homeostasis. It also seems that imbalances in this

pathway start even at the pre-symptomatic stages of this disease in MNs and may promote the changes that occur in C-boutons. The role of synaptic terminals and most particularly, C-boutons in this process is unclear and any association with mitochondria in its changes is lacking. However, we hypothesize that this may be revealed in further research. Currently, we have found that the presence of the neurotrophic factor NRG-1 in C-boutons changes in accordance to alterations previously described for C-terminals in FALS. These include when NRG-1 signal enlarges according to the SSC enlargement that occurs in FALS. and vulnerable MNs at symptomatic stages ,when degeneration of other MN terminals has already occurred. With this thesis, therefore, we have provided knowledge on previously unknown mechanisms of neurodegeneration in FALS. Through our research, we have contributed to the further understanding of some already-known processes with regard to the terminal synaptic affectation in MNs.Also, we have discovered novel and unknown pathogenic mechanisms as the link between mitochondria and proteasome dysfunction by the effect of $hSOD1^{G93A}$. Additionally, we have contributed novel and improved methodology designed and intended to overcome important technical challenges that currently hinder further exploration of ALS pathogenic mechanisms. We have developed the PROSPR method to isolate extracellular vesicles that of which we hope will provide future understanding on the roles of NRG-1 in FALS. We also created a new *Drosophila* model to study and perform therapeutic screenings able to rescue the effects of $hSOD1^{G93A}$ in mitochondria with the discovery of new promising therapeutic compounds and further genetic screenings. Taken together, our contributions reported in this thesis help to better categorize the complexity that promotes degeneration of motor neurones in ALS. It is thus considered as the basic step to develop ways and treatments to reverse the dramatic degenerative imprint in this motor neurone disease.

10. References

Ahtoniemi, Toni, Merja Jaronen, Velta Keksa-Goldsteine, Gundars Goldsteins, and Jari Koistinaho. 2008. “Mutant SOD1 from Spinal Cord of G93A Rats Is Destabilized and Binds to Inner Mitochondrial Membrane.” Neurobiology of Disease 32 (3): 479–85. doi:10.1016/j.nbd.2008.08.010. http://www.ncbi.nlm.nih.gov/pubmed/18817872.

Andersen, P. M. (2000). "Genetic factors in the early diagnosis of ALS." Amyotroph Lateral Scler Other Motor Neuron Disord 1 Suppl 1: S31-42.

Al-Saif, Amr, Futwan Al-Mohanna, and Saeed Bohlega. 2011. “A Mutation in Sigma-1 Receptor Causes Juvenile Amyotrophic Lateral Sclerosis.” Annals of Neurology 70 (6): 913–19. doi:10.1002/ana.22534. http://www.ncbi.nlm.nih.gov/pubmed/21842496.

Arrasate, Montserrat, Siddhartha Mitra, Erik S Schweitzer, Mark R Segal, and Steven Finkbeiner. 2004. “Inclusion Body Formation Reduces Levels of Mutant Huntingtin and the Risk of Neuronal Death.” Nature 431 (7010): 805–10. doi:10.1038/nature02998. http://www.ncbi.nlm.nih.gov/pubmed/15483602.

Basso, Manuela, Silvia Pozzi, Massimo Tortarolo, Fabio Fiordaliso, Cinzia Bisighini, Laura Pasetto, Gabriella Spaltro, et al. 2013. “Mutant Copper-Zinc Superoxide Dismutase (SOD1) Induces Protein Secretion Pathway Alterations and Exosome Release in Astrocytes: Implications for Disease Spreading and Motor Neuron Pathology in Amyotrophic Lateral Sclerosis.” The Journal of Biological Chemistry 288 (22): 15699–711. doi:10.1074/jbc.M112.425066. http://www.pubmedcentral.nih.gov/articlerender.fcgi?artid=3668729&tool=pmcentrez&rendertype=abstract.

Calvo, Margarita, Ning Zhu, Christoforos Tsantoulas, Zhenzhong Ma, John Grist, Jeffrey A Loeb, and David L H Bennett. 2010. “Neuregulin-ErbB Signaling Promotes Microglial Proliferation and Chemotaxis Contributing to Microgliosis and Pain after Peripheral Nerve Injury.” The Journal of Neuroscience: The Official Journal of the Society for Neuroscience 30 (15): 5437–50. doi:10.1523/JNEUROSCI.5169-09.2010. http://www.pubmedcentral.nih.gov/articlerender.fcgi?artid=2862659&tool=pmcentrez&rendertype=abstract.

Cozzolino, Mauro, and Maria Teresa Carrì. 2012. “Mitochondrial Dysfunction in ALS.” Progress in Neurobiology 97 (2): 54–66. doi:10.1016/j.pneurobio.

2011.06.003. http://www.sciencedirect.com/science/article/pii/S0301008211000918.

Dadon-Nachum, Michal, Eldad Melamed, and Daniel Offen. 2011. “The ‘Dying-Back’ Phenomenon of Motor Neurones in ALS.” Journal of Molecular Neuroscience: MN 43 (3): 470–77. doi:10.1007/s12031-010-9467-1. http://www.ncbi.nlm.nih.gov/pubmed/21057983.

Dimayuga, Filomena O, Qunxing Ding, Jeffrey N Keller, Mark A Marchionni, Kim B Seroogy, and Annadora J Bruce-Keller. 2003. “The Neuregulin GGF2 Attenuates Free Radical Release from Activated Microglial Cells.” Journal of Neuroimmunology 136 (1-2): 67–74. http://www.ncbi.nlm.nih.gov/pubmed/12620644.

Falls, D. 2003. “Neuregulins: Functions, Forms, and Signaling Strategies.” Experimental Cell Research 284 (1): 14–30. doi:10.1016/S0014-4827(02)00102-7. http://www.sciencedirect.com/science/article/pii/S0014482702001027.

Frank, Eric. 2009. “A New Class of Spinal Interneurones: The Origin and Function of C Boutons Is Solved.” Neuron 64 (5): 593–95. doi:10.1016/j.neuron.2009.11.030. http://www.ncbi.nlm.nih.gov/pubmed/20005814.

Gerecke, K M, J M Wyss, I Karavanova, A Buonanno, and S L Carroll. 2001. “ErbB Transmembrane Tyrosine Kinase Receptors Are Differentially Expressed throughout the Adult Rat Central Nervous System.” The Journal of Comparative Neurology 433 (1): 86–100. http://www.ncbi.nlm.nih.gov/pubmed/11283951.

Grad, Leslie I, Justin J Yerbury, Bradley J Turner, William C Guest, Edward Pokrishevsky, Megan A O’Neill, Anat Yanai, et al. 2014. “Intercellular Propagated Misfolding of Wild-Type Cu/Zn Superoxide Dismutase Occurs via Exosome-Dependent and -Independent Mechanisms.” Proceedings of the National Academy of Sciences of the United States of America 111 (9): 3620–25. doi:10.1073/pnas.1312245111. http://www.pnas.org/content/111/9/3620.long.

Henriques, A., S. Kastner, E. Chatzikonstantinou, C. Pitzer, C. Plaas, F. Kirsch, O. Wafzig, K. Carola, R. Spoelgen, J.-L. Gonzalez De Aguilar, N. Gretz and A. Schneider (2015). "Gene expression changes in spinal motoneurones of the SOD1G93A transgenic model for ALS after treatment with G-CSF." Frontiers in Cellular Neuroscience 8.

Higgins, Cynthia M J, Cheolwha Jung, and Zuoshang Xu. 2003. "ALS-Associated Mutant SOD1G93A Causes Mitochondrial Vacuolation by Expansion of the Intermembrane Space and by Involvement of SOD1 Aggregation and Peroxisomes." BMC Neuroscience 4 (July): 16. doi: 10.1186/1471-2202-4-16. http://www.pubmedcentral.nih.gov/articlerender.fcgi?artid=169170&tool=pmcentrez&rendertype=abstract.

Issa, Amine N, Wen-Zhi Zhan, Gary C Sieck, and Carlos B Mantilla. 2010. "Neuregulin-1 at Synapses on Phrenic Motoneurones." The Journal of Comparative Neurology 518 (20): 4213–25. doi:10.1002/cne.22449. http://www.pubmedcentral.nih.gov/articlerender.fcgi?artid=2948240&tool=pmcentrez&rendertype=abstract.

Kanning, Kevin C, Artem Kaplan, and Christopher E Henderson. 2010. "Motor Neuron Diversity in Development and Disease." Annual Review of Neuroscience 33 (January): 409–40. doi:10.1146/annurev.neuro.051508.135722. http://www.ncbi.nlm.nih.gov/pubmed/20367447.

Kettenmann, Helmut, Frank Kirchhoff, and Alexei Verkhratsky. 2013. "Microglia: New Roles for the Synaptic Stripper." Neuron 77 (1): 10–18. doi:10.1016/j.neuron.2012.12.023. http://www.sciencedirect.com/science/article/pii/S0896627312011622.

Lachenal, Gaelle, Karin Pernet-Gallay, Mathilde Chivet, Fiona J Hemming, Agnès Belly, Gilles Bodon, Béatrice Blot, Georg Haase, Yves Goldberg, and Rémy Sadoul. 2011. "Release of Exosomes from Differentiated Neurones and Its Regulation by Synaptic Glutamatergic Activity." Molecular and Cellular Neurosciences 46 (2): 409–18. doi:10.1016/j.mcn.2010.11.004. http://www.ncbi.nlm.nih.gov/pubmed/21111824.

Lee, Shynrye, and Hyung-Jun Kim. 2015. "Prion-like Mechanism in Amyotrophic Lateral Sclerosis: Are Protein Aggregates the Key?" Experimental Neurobiology 24 (1): 1–7. doi:10.5607/en.2015.24.1.1. http://www.pubmedcentral.nih.gov/articlerender.fcgi?artid=4363329&tool=pmcentrez&rendertype=abstract.

Li, W, P A Ochalski, S Brimijoin, L M Jordan, and J I Nagy. 1995. "C-Terminals on Motoneurones: Electron Microscope Localization of Cholinergic Markers in Adult Rats and Antibody-Induced Depletion in Neonates." Neuroscience 65 (3): 879–91. http://www.ncbi.nlm.nih.gov/pubmed/7609885.

Lin, Jin, Jing Li, Bo Huang, Jing Liu, Xin Chen, Xi-Min Chen, Yan-Mei Xu, Lin-Feng Huang, and Xiao-Zhong Wang. 2015. "Exosomes: Novel Biomarkers for Clinical Diagnosis." TheScientificWorldJournal 2015 (January): 657086.

doi:10.1155/2015/657086. http://www.pubmedcentral.nih.gov/articlerender.fcgi?artid=4322857&tool=pmcentrez&rendertype=abstract.

Mavlyutov, T A, M L Epstein, Y I Verbny, M S Huerta, I Zaitoun, L Ziskind-Conhaim, and A E Ruoho. 2013. “Lack of Sigma-1 Receptor Exacerbates ALS Progression in Mice.” Neuroscience 240 (June): 129–34. doi:10.1016/j.neuroscience.2013.02.035. http://www.pubmedcentral.nih.gov/articlerender.fcgi?artid=3665351&tool=pmcentrez&rendertype=abstract.

McGuire, Sean E, Gregg Roman, and Ronald L Davis. 2004. “Gene Expression Systems in Drosophila: A Synthesis of Time and Space.” Trends in Genetics: TIG 20 (8): 384–91. doi:10.1016/j.tig.2004.06.012. http://www.ncbi.nlm.nih.gov/pubmed/15262411.

Moran, Linda B, and Manuel B Graeber. 2004. “The Facial Nerve Axotomy Model.” Brain Research. Brain Research Reviews 44 (2-3): 154–78. doi:10.1016/j.brainresrev.2003.11.004. http://www.ncbi.nlm.nih.gov/pubmed/15003391.

Pandey, Udai Bhan, and Charles D Nichols. 2011. “Human Disease Models in Drosophila Melanogaster and the Role of the Fly in Therapeutic Drug Discovery.” Pharmacological Reviews 63 (2): 411–36. doi:10.1124/pr.110.003293. http://www.pubmedcentral.nih.gov/articlerender.fcgi?artid=3082451&tool=pmcentrez&rendertype=abstract.

Pasinelli, Piera, Mary Elizabeth Belford, Niall Lennon, Brian J Bacskai, Bradley T Hyman, Davide Trotti, and Robert H Brown. 2004. “Amyotrophic Lateral Sclerosis-Associated SOD1 Mutant Proteins Bind and Aggregate with Bcl-2 in Spinal Cord Mitochondria.” Neuron 43 (1): 19–30. doi:10.1016/j.neuron.2004.06.021. http://www.scopus.com/inward/record.url?eid=2-s2.0-3242703300&partnerID=tZOtx3y1.

Pickles, Sarah, and Christine Vande Velde. 2012. “Misfolded SOD1 and ALS: Zeroing in on Mitochondria.” Amyotrophic Lateral Sclerosis: Official Publication of the World Federation of Neurology Research Group on Motor Neuron Diseases 13 (4): 333–40. doi:10.3109/17482968.2012.648645. http://www.ncbi.nlm.nih.gov/pubmed/22471903.

Piotrkiewicz, Maria, and Irena Hausmanowa-Petrusewicz. 2011. “Motoneuron Afterhyperpolarisation Duration in Amyotrophic Lateral Sclerosis.” The Journal of Physiology 589 (Pt 11): 2745–54. doi:10.1113/jphysiol.2011.204891. http://www.pubmedcentral.nih.gov/articlerender.fcgi?artid=3112552&tool=pmcentrez&rendertype=abstract.

Pullen, A H. 1992. “Presynaptic Terminal Loss from Alpha-Motoneurones Following the Retrograde Axonal Transport of Diphtheria Toxin.” Acta Neuropathologica 83 (5): 488–98. http://www.ncbi.nlm.nih.gov/pubmed/1377857.

Pullen, A H, and D Athanasiou. 2009. “Increase in Presynaptic Territory of C-Terminals on Lumbar Motoneurones of G93A SOD1 Mice during Disease Progression.” The European Journal of Neuroscience 29 (3): 551–61. doi:10.1111/j.1460-9568.2008.06602.x. http://www.ncbi.nlm.nih.gov/pubmed/19187267.

Rizzuto, Rosario, Diego De Stefani, Anna Raffaello, and Cristina Mammucari. 2012. “Mitochondria as Sensors and Regulators of Calcium Signalling.” Nature Reviews. Molecular Cell Biology 13 (9): 566–78. doi:10.1038/nrm3412. http://www.ncbi.nlm.nih.gov/pubmed/22850819.

Rothstein, Jeffrey D. 2009. “Current Hypotheses for the Underlying Biology of Amyotrophic Lateral Sclerosis.” Annals of Neurology 65 Suppl 1 (January): S3–9. doi:10.1002/ana.21543. http://www.ncbi.nlm.nih.gov/pubmed/19191304.

Saxena, Smita, and Pico Caroni. 2011. “Selective Neuronal Vulnerability in Neurodegenerative Diseases: From Stressor Thresholds to Degeneration.” Neuron 71 (1): 35–48. doi:10.1016/j.neuron.2011.06.031. http://www.ncbi.nlm.nih.gov/pubmed/21745636.

Saxena, Smita, Francesco Roselli, Katyayani Singh, Kerstin Leptien, Jean-Pierre Julien, Francois Gros-Louis, and Pico Caroni. 2013. “Neuroprotection through Excitability and mTOR Required in ALS Motoneurones to Delay Disease and Extend Survival.” Neuron 80 (1): 80–96. doi:10.1016/j.neuron.2013.07.027. http://www.sciencedirect.com/science/article/pii/S089662731300651X.

Song, Fei, Pohung Chiang, Jiajing Wang, John Ravits, and Jeffrey A Loeb. 2012. “Aberrant Neuregulin 1 Signaling in Amyotrophic Lateral Sclerosis.” Journal of Neuropathology and Experimental Neurology 71 (2): 104–15. doi:10.1097/NEN.0b013e3182423c43. http://www.pubmedcentral.nih.gov/articlerender.fcgi?artid=3270561&tool=pmcentrez&rendertype=abstract.

Tan, Wenzhi, Piera Pasinelli, and Davide Trotti. 2014. “Role of Mitochondria in Mutant SOD1 Linked Amyotrophic Lateral Sclerosis.” Biochimica et Biophysica Acta 1842 (8): 1295–1301. doi:10.1016/j.bbadis.2014.02.009. http://www.ncbi.nlm.nih.gov/pubmed/24568860.

Van Deun, Jan, Pieter Mestdagh, Raija Sormunen, Veronique Cocquyt, Karim Vermaelen, Jo Vandesompele, Marc Bracke, Olivier De Wever, and An Hendrix. 2014. “The Impact of Disparate Isolation Methods for Extracellular Vesicles on Downstream RNA Profiling.” Journal of Extracellular Vesicles 3 (January). doi:10.3402/jev.v3.24858. http://www.pubmedcentral.nih.gov/articlerender.fcgi?artid=4169610&tool=pmcentrez&rendertype=abstract.

Vehviläinen, Piia, Jari Koistinaho, and Goldsteins Gundars. 2014. “Mechanisms of Mutant SOD1 Induced Mitochondrial Toxicity in Amyotrophic Lateral Sclerosis.” Frontiers in Cellular Neuroscience 8 (January): 126. doi: 10.3389/fncel.2014.00126. http://www.pubmedcentral.nih.gov/articlerender.fcgi?artid=4023018&tool=pmcentrez&rendertype=abstract.

Vinsant, Sharon, Carol Mansfield, Ramon Jimenez-Moreno, Victoria Del Gaizo Moore, Masaaki Yoshikawa, Thomas G Hampton, David Prevette, James Caress, Ronald W Oppenheim, and Carol Milligan. 2013. “Characterization of Early Pathogenesis in the SOD1(G93A) Mouse Model of ALS: Part II, Results and Discussion.” Brain and Behavior 3 (4): 431–57. doi:10.1002/brb3.142. http://www.pubmedcentral.nih.gov/articlerender.fcgi?artid=3869683&tool=pmcentrez&rendertype=abstract.

Vinsant, S., C. Mansfield, R. Jimenez-Moreno, V. Del Gaizo Moore, M. Yoshikawa, T. G. Hampton, D. Prevette, J. Caress, R. W. Oppenheim and C. Milligan (2013)."Characterization of early pathogenesis in the SOD1(G93A) mouse model of ALS: part I, background and methods." Brain Behav 3(4): 335-350.

Wen, D, E Peles, R Cupples, S V Suggs, S S Bacus, Y Luo, G Trail, S Hu, S M Silbiger, and R B Levy. 1992. “Neu Differentiation Factor: A Transmembrane Glycoprotein Containing an EGF Domain and an Immunoglobulin Homology Unit.” Cell 69 (3): 559–72. http://www.ncbi.nlm.nih.gov/pubmed/1349853.

Wong, Margaret, and Lee J Martin. 2010. “Skeletal Muscle-Restricted Expression of Human SOD1 Causes Motor Neuron Degeneration in Transgenic Mice.” Human Molecular Genetics 19 (11): 2284–2302. doi: 10.1093/hmg/ddq106. http://www.pubmedcentral.nih.gov/articlerender.fcgi?artid=2865380&tool=pmcentrez&rendertype=abstract.

Wong, P C, C A Pardo, D R Borchelt, M K Lee, N G Copeland, N A Jenkins, S S Sisodia, D W Cleveland, and D L Price. 1995. “An Adverse Property of a Familial ALS-Linked SOD1 Mutation Causes Motor Neuron Disease Characterized by Vacuolar Degeneration of Mitochondria.” Neuron 14 (6): 1105–16. http://www.ncbi.nlm.nih.gov/pubmed/7605627.

Xiang, Y, T Liu, H Yang, F Gao, H Xiang, A Manyande, Y Tian, and X Tian. 2015. "NRG1-ErbB Signalling Promotes Microglia Activation Contributing to Incision-Induced Mechanical Allodynia." European Journal of Pain (London, England) 19 (5): 686–94. doi:10.1002/ejp.590. http://www.ncbi.nlm.nih.gov/pubmed/25159022.